



Université  
de Toulouse

# THÈSE

En vue de l'obtention du

## DOCTORAT DE L'UNIVERSITÉ DE TOULOUSE

**Délivré par :**

Institut National Polytechnique de Toulouse (INP Toulouse)

**Discipline ou spécialité :**

Génie des Procédés et de l'Environnement

---

**Présentée et soutenue par :**

Mme CHING SHYA LEE

le mardi 27 septembre 2016

**Titre :**

STUDY OF GLYCEROL ELECTROCHEMICAL CONVERSION INTO  
ADDED-VALUE COMPOUNDS

---

**Ecole doctorale :**

Mécanique, Energétique, Génie civil, Procédés (MEGeP)

**Unité de recherche :**

Laboratoire de Génie Chimique (L.G.C.)

**Directeur(s) de Thèse :**

M. PATRICK COGNET

MME YOLANDE LUCCHESI

**Rapporteurs :**

M. CHRISTOPHE COUTANCEAU, UNIVERSITE DE POITIERS

M. PEDRO ROQUERO TEJEDA, UNIVERSITE NATIONALE AUTONOME DE MEXICO

**Membre(s) du jury :**

M. CHRISTOPHE COUTANCEAU, UNIVERSITE DE POITIERS, Président

M. MAXIME FERAILLE, CENTRE UNIVERSITAIRE FRANCO-MALAISIE, Membre

Mme ROZITA YUSOFF, UNIVERSITY OF MALAYA, Membre

M. MOHAMED KHEIREDDINE AROUA, UNIVERSITY OF MALAYA, Membre

M. PATRICK COGNET, INP TOULOUSE, Membre

## ABSTRACT

The price of crude glycerol has significantly decreased worldwide because of its oversupply. Many chemical and biological processes have been proposed to transform glycerol into numerous added-value products, such as glycolic acid, 1,3-propanediol (1,3-PDO), 1,2-propanediol (1,2-PDO), glyceric acid, and lactic acid. However, these processes suffer several drawbacks, including high production cost. Therefore, in this study, a simple and robust electrochemical synthesis was developed to convert glycerol into various added-value compounds.

This study reports for the first time the use of Amberlyst-15 as a reaction medium and redox catalyst for electrochemical conversion of glycerol. In the first part, the electrochemical performance of Amberlyst-15 over platinum (Pt) electrode was compared with that of conventional acidic ( $\text{H}_2\text{SO}_4$ ) and alkaline (NaOH) media. Other parameters such as reaction temperature [room temperature (27 °C) to 80 °C] and applied current (1.0 A to 3.0 A) were also examined. Under the optimized experimental condition, this novel electrocatalytic method successfully converted glycerol into glycolic acid after 8 h of electrolysis, with a yield of 45% and selectivity of 65%, as well as to glyceric acid after 3 h of electrolysis, with a yield of 27% and selectivity of 38%.

In the second part of this study, two types of cathode electrodes, namely, activated carbon composite (ACC) and carbon black diamond (CBD) electrodes, were used in electrochemical conversion of glycerol. To the best of our knowledge, electrochemical studies of glycerol conversion using these electrodes have not been reported yet. Glycerol was also successfully reduced to lactic acid, 1,2-PDO, and 1,3-PDO, in addition to oxidation compounds (e.g. glycolic acid). Three operating parameters, namely, catalyst amount (6.4% to 12.8% w/v), reaction temperature [room temperature

(27 °C) to 80 °C], and applied current (1.0 A to 3.0 A), were tested. In the presence of 9.6% w/v Amberlyst-15 at 2.0 A and 80 °C, the selectivity of glycolic acid can reach 72% and 68% (with yield of 66% and 58%) for ACC and CBD electrodes, respectively. Lactic acid was obtained as the second largest compound, with selectivity of 16% and yield of 15% for the ACC electrode and 27% selectivity and 21% yield for the CBD electrode.

Finally, electro-oxidation and electroreduction of glycerol were performed in a two-compartment cell separated by a cation exchange membrane (Nafion 117). This study only focused on the electroreduction region. Three cathode electrodes (Pt, ACC, and CBD) were evaluated under the following conditions: 2.0 A, 80 °C, and 9.6% w/v Amberlyst-15. ACC demonstrated excellent performance in the electroreduction study and successfully reduced glycerol to 1,2-PDO, with a high selectivity of 85%. The selectivity of 1,2-PDO on Pt and CBD was 61% and 68%, respectively. Acetol and diethylene glycol were also obtained. The reaction mechanisms underlying the formation of these products are then proposed.

## RÉSUMÉ

Au cours des dernières années, la production excédentaire et sans cesse croissante de bioglycérol a provoqué une chute spectaculaire de son prix. Au cours des dernières années, un grand nombre de processus chimiques et biologiques ont été élaborés pour transformer le bioglycérol en divers produits à haute valeur ajoutée, tels que la dihydroxyacétone, l'acide glycolique, le 1,3-propanediol (1,3-PDO), 1,2-propanediol (1,2-PDO), l'acide glycérique, l'acide lactique, le carbonate de glycérol etc. Malheureusement, ces procédés souffrent de nombreux inconvénients comme par exemple, un coût élevé de production. Par conséquent, dans cette étude, une synthèse simple et robuste, basée sur un processus électrochimique a été introduite afin de convertir le bioglycérol en une grande variété de composés à haute valeur ajoutée.

Cette étude rapporte pour la première fois l'utilisation de la résine Amberlyst-15 comme milieu réactionnel et comme catalyseur d'oxydo-réduction pour la conversion électrochimique du glycérol. La performance électrochimique du système composé par la résine Amberlyst-15 et l'électrode au platine (Pt), a été comparée à celle utilisant un milieu électrolytique conventionnel acide ( $H_2SO_4$ ) ou alcalin (NaOH). D'autres paramètres tels que la température de réaction (température ambiante à 80 °C) et l'intensité du courant appliqué (1,0 A à 3,0 A) ont également été examinés. Dans les conditions expérimentales optimales, ce nouveau procédé électrocatalytique permet de convertir le glycérol, soit en acide glycolique, avec un rendement de 45% et une sélectivité élevée de 65%, soit en acide glycérique, avec un rendement de 27% et une sélectivité de 38%.

D'autre part, deux autres électrodes ont été préparées et testées dans la réaction de transformation du glycérol : une électrode au charbon actif (ACC) et une électrode composite au noir de carbone et diamant CBD). A notre connaissance, il n'existe pas

dans la littérature d'étude de transformation électrochimique du glycérol utilisant ce type d'électrodes. Dans ce travail, nous avons montré que le glycérol peut être oxydé en divers composés d'oxydation mais peut également être réduit avec succès en acide lactique, 1,2-PDO et 1,3-PDO. Trois paramètres de fonctionnement, tels que la quantité de catalyseur (6.4 - 12.8% w/v), la température de réaction [température ambiante (27 °C) à 80 °C] et l'intensité du courant appliqué (1,0 A à 3,0 A), ont été testés. L'étude a révélé que, pour une quantité de catalyseur 9.6% w/v Amberlyst-15, un courant de 2,0 A et une température de 80 °C, la sélectivité en acide glycolique peut atteindre jusqu'à 72% et 68% (avec un rendement de 66% et 58%) en utilisant respectivement l'électrode ACC et l'électrode CBD. L'acide lactique a aussi été obtenu avec une sélectivité de 16% et un rendement de 15% en utilisant l'électrode ACC et une sélectivité de 27% pour un rendement de 21% dans le cas de l'électrode CBD.

Enfin, l'électro-oxydation et l'électro-réduction du glycérol a été effectuée dans une cellule à deux compartiments séparés par une membrane échangeuse de cations (Nafion 117). L'étude s'est focalisée sur l'électro-réduction. Trois cathodes (Pt, ACC et CBD) ont été évaluées dans les conditions suivantes : 2.0 A, 80 °C et 9.6% w/v Amberlyst-15. Les trois électrodes ont permis de réduire le glycérol en 1,2-PDO. Nous avons obtenu une sélectivité de 61% avec l'électrode au Pt et une sélectivité de 68% avec l'électrode CBD. En fait, c'est l'électrode ACC qui a démontré les meilleures performances puisqu'elle a permis de réduire le glycérol en 1,2-PDO avec une sélectivité élevée de 85%. Enfin, la réaction conduit aussi à la formation d'acétol et de diéthylèneglycol. Les mécanismes de formation des différents produits obtenus à partir de chaque réaction sont proposés.

## ACKNOWLEDGEMENTS

First of all, I would like to thank my thesis adviser, Professor Kheireddine, for offering me an opportunity to work with an excellent team from the University of Toulouse in France. As a supervisor and thesis adviser, he has always given me support and encouragement in my career as well as in my study. He always stands by me and gives me motivation anytime I needed it. Without his encouragement, I would not have surpassed all obstacles I encountered and reached this stage. I deeply appreciate his thoughtfulness and open-mindedness.

I would also like to thank my thesis adviser from the University of Toulouse, Professor Patrick. I started this project with limited knowledge. I tend to limit my thinking and lack confidence. However, he has given me many ideas and guidance to think out of the box and move to a better direction.

I would like to thank another thesis adviser from the University of Toulouse, Dr. Yolande. I am so thankful to have this opportunity to meet one of the most awesome people in my life. She is not only a thesis adviser but also a life coach. I am a pessimistic person and used to think the worst before the good, but she always give me positive energies and encouragement to move forward.

I am also grateful to my co-supervisor in University of Malaya, Professor Wan Ashri and former colleagues in this team, namely, Professor Paul-Louis, Dr. Olivier, and Mrs. Laure, as well as Dr. Maxime from the French Embassy in Malaysia. Their valuable advice and assistance have lead this research to even better direction.

I would like to thank the Center for Separation Science and Technology at University of Malaya, the Laboratoire de Génie Chimique at Campus INP-ENSIACET, and Campus Université Paul Sabatier for all their support. I am also grateful for the financial

support provided by the High Impact Research Grant (HIR Grant No: HIR/MOHE/ENG/59) and the Postgraduate Research Grant (PPP Grant No: PG006-2012B) from the University of Malaya and French Embassy (Malaysia).

Special thanks to my colleague Mr. Al-Ajeel. He is a kind hearted and helpful friend who is always willing to share his knowledge to everyone. He has guide me to think in a right direction and has given me many ideas through his working experience.

To all my friends, especially Norhaya, Wei Tze, Su Sin, Gina, Liesah, Mei Yee, Joyce, and Siew Moy, who accompany me through both good and bad times, I am so grateful to have all of you in my life and for helping me to accomplish this thesis.

Last but not the least, to my family, the most important people in my life, my dearest father, Lee Ah See; mother, Loh Poh Chee; and my sister, Lee Ching Huey, I especially want to say thank you for your unconditional support since the first day I started my degree. I could not have succeeded in my endeavor without your kind understanding and encouragement. Thank you for everything you have done for me. I love you!

## TABLE OF CONTENTS

Abstract .....	i
Résumé .....	iii
Acknowledgements .....	v
Table of Contents .....	vii
List of Figures .....	x
List of Tables .....	xvi
List of schemes .....	xviii
List of Symbols and Abbreviations .....	xix
List of Appendices .....	xxi
<b>CHAPTER 1: INTRODUCTION .....</b>	<b>1</b>
1.1 General .....	1
1.2 Scope of research .....	3
1.3 Problem statement .....	3
1.4 Research objectives .....	4
1.5 Thesis structure .....	5
<b>CHAPTER 2: LITERATURE REVIEW .....</b>	<b>7</b>
2.1 Introduction .....	7
2.2 Glycerol and its sustainable applications .....	7
2.3 Added-value compounds available from glycerol .....	10
2.3.1 General overview .....	10
2.3.2 Propanediols .....	12
2.3.3 Glycolic and glyceric acids .....	17
2.3.4 Lactic acid .....	20



2.3.5	Shortcomings of existing conversion methods.....	25
2.4	Electrochemical conversion of glycerol .....	26
2.4.1	Electrocatalytic behavior study .....	27
2.4.2	Electrochemical fuel cell .....	29
2.4.3	Electrochemical study in galvanostatic mode .....	30
2.5	Redox catalyst in organic electrosynthesis .....	33
2.5.1	Amberlyst-15 .....	34
2.5.2	Amberlyst-15 as a solid acid catalyst in glycerol conversion .....	36
2.6	Activated carbon electrode .....	37
2.7	Diamond electrode.....	39
2.8	Separations and purifications.....	42
2.9	Outlook and conclusion .....	46
<b>CHAPTER 3: METHODOLOGY .....</b>		<b>47</b>
3.1	Introduction.....	47
3.2	Electrochemical study in a one-pot reactor .....	48
3.2.1	Electrode preparation.....	48
3.2.1.1	Preparation of ACC and CBD electrodes.....	48
3.2.1.2	Scanning electron microscopy analysis (SEM).....	48
3.2.1.3	Measurement of active surface areas.....	49
3.2.1.4	Electrochemical measurement.....	49
3.2.2	Screening of reaction medium.....	50
3.2.2.1	Electrochemical measurement.....	50
3.2.2.2	Bulk electrochemical study .....	50
3.2.3	Evaluation of cathode materials and optimization study.....	52
3.3	Electrochemical study in a two-compartment reactor .....	52
3.4	Product characterization and quantification .....	53

3.4.1	Standard calibration.....	54
3.4.2	Sample analysis .....	58
<b>CHAPTER 4: RESULTS AND DISCUSSION .....</b>		<b>60</b>
4.1	Introduction.....	60
4.2	Electrochemical valorization of glycerol over Pt electrode.....	60
4.2.1	Cyclic voltammetry analysis .....	60
4.2.2	Bulk electrochemical synthesis .....	62
4.2.2.1	Effect of reaction medium.....	63
4.2.2.2	Effect of electric current.....	68
4.2.2.3	Effect of reaction temperature.....	72
4.2.2.4	Reaction mechanism .....	79
4.3	Evaluation of cathode material .....	82
4.3.1	SEM Analysis.....	82
4.3.5	Reaction mechanism.....	95
4.4	Optimization study on the ACC cathode electrode .....	99
4.6.2	Electro-oxidation of glycerol.....	130
<b>CHAPTER 5: CONCLUSION AND RECOMMENDATION FOR FUTURE RESEARCH.....</b>		<b>136</b>
5.1	Conclusion.....	136
5.2	Suggestions for future studies.....	138
	References.....	139
	List of Publications and Papers Presented .....	158
	Appendices.....	159

## LIST OF FIGURES

Figure 2.1: Chemical structure of Amberlyst-15 (Pal <i>et al.</i> , 2012).....	35
Figure 2.2. Cyclic voltammetry curves of platinum and diamond electrode in 0.2 M H <sub>2</sub> SO <sub>4</sub> , $v = 0.1 \text{ Vs}^{-1}$ (Kraft, 2007).....	40
Figure 2.3. Effect of pH on the rejection of anion species on charged membrane (Childress <i>et al.</i> , 2000).....	43
Figure 2.4. Working principle of a single-stage electro-deionization technique for lactate ion separation (Boontawan <i>et al.</i> , 2011). ....	44
Figure 2.5. Schematic represents the electro-dialysis process for concentrate organic acids or organic salts. MX: organic acid or salt; Z: neutral substances or low concentration of inorganic salts (Huang <i>et al.</i> , 2007).....	45
Figure 3.1: Electrochemical set-up (one-pot reactor). ....	51
Figure 3.2: Electrochemical set-up (two-compartment reactor). ....	53
Figure 3.3: Glycerol calibration curve. ....	57
Figure 4.1: CV curves of Amberlyst-15 (potential scan range: $- 1.80$ to $+ 0.80 \text{ V}$ ), NaOH (potential scan range: $-1.10$ to $+ 0.90 \text{ V}$ ) and H <sub>2</sub> SO <sub>4</sub> (potential scan range: $- 0.30$ to $+ 1.30 \text{ V}$ ), without glycerol on Pt at a scan rate of $0.1 \text{ Vs}^{-1}$ .....	61
Figure 4.2: CV curves of Amberlyst-15 blank solution and amberlyst-15 with glycerol solution on Pt at a scan rate of $0.1 \text{ Vs}^{-1}$ in potential window range of $- 1.80$ to $+ 1.50 \text{ V}$ . ....	62
Figure 4.3: Glycerol conversion from the electrochemical study on Pt electrode in the presence of Amberlyst-15, H <sub>2</sub> SO <sub>4</sub> and NaOH media, at room temperature ( $27 \text{ }^\circ\text{C}$ ) and $1.0 \text{ A}$ constant current. ....	64
Figure 4.4: First-order kinetics model of the electrochemical conversion of glycerol in the presence of Amberlyst-15, H <sub>2</sub> SO <sub>4</sub> , and NaOH media on Pt electrode at room temperature ( $27 \text{ }^\circ\text{C}$ ) and $1.0 \text{ A}$ constant current. ....	65
Figure 4.5: Product distribution from the electrochemical conversion of glycerol (a) in the presence of Amberlyst-15, (b) H <sub>2</sub> SO <sub>4</sub> , and (c) in NaOH on Pt electrode at room temperature ( $27 \text{ }^\circ\text{C}$ ) and $1.0 \text{ A}$ constant current. ....	66
Figure 4.6: Maximum yield of glycolic and glyceric acids obtained from the electrochemical conversion of glycerol (a) in the presence of Amberlyst-15, (b) H <sub>2</sub> SO <sub>4</sub> , and (c) NaOH on Pt electrode at room temperature ( $27 \text{ }^\circ\text{C}$ ) and $1.0 \text{ A}$ constant current. ....	67

Figure 4.7: Glycerol conversion from the electrochemical study on Pt electrode in the presence of Amberlyst-15 at room temperature (27 °C) and constant currents of 1.0, 2.0, and 3.0 A. ....	70
Figure 4.8: First-order kinetic model of the electrochemical conversion of glycerol in the presence of Amberlyst-15 on Pt electrode at room temperature (27 °C) and constant currents of 1.0, 2.0, and 3.0 A. ....	70
Figure 4.9: Product distribution from the electrochemical conversion of glycerol in the presence of Amberlyst-15 on Pt electrode at room temperature (27 °C) and constant currents of (a) 1.0, (b) 2.0, and (c) 3.0 A. ....	71
Figure 4.10: Maximum yield of glycolic and glyceric acids obtained from the electrochemical conversion of glycerol in the presence of Amberlyst-15 on Pt electrode at room temperature (27 °C) and constant currents of (a) 1.0, (b) 2.0, and (c) 3.0 A. ....	72
Figure 4.11: Glycerol conversion from the electrochemical study on Pt electrode in the presence of Amberlyst-15 at 1.0 A constant current at room temperature (27 °C), 50 °C, and 80 °C. ....	73
Figure 4.12: First-order kinetic model of the electrochemical conversion of glycerol in the presence of Amberlyst-15 on Pt electrode at 1.0 A constant current at room temperature (27 °C), 50 °C, and 80 °C. ....	74
Figure 4.13: Product distribution from the electrochemical conversion of glycerol in the presence of Amberlyst-15 on Pt electrode at 1.0 A constant current at (a) room temperature (27 °C), (b) 50 °C, and (c) 80 °C. ....	75
Figure 4.14: Maximum yield of glycolic and glyceric acids obtained from the electrochemical conversion of glycerol in the presence of Amberlyst-15 at 1.0 A constant current at (a) room temperature, 27 °C (RT), (b) 50 °C and (c) 80 °C. ....	76
Figure 4.15: GC chromatogram from the electrochemical conversion of glycerol in the presence of Amberlyst-15 on Pt electrode at 80 °C and 1.0 A constant current. ....	79
Figure 4.16: SEM images of (a) virgin ACC electrode and (b) ACC electrode after the electrochemical reaction. ....	83
Figure 4.17: SEM-EDX spectrum for virgin ACC electrode. ....	83
Figure 4.18: SEM-EDX spectrum for ACC electrode after the electrochemical reaction. ....	83
Figure 4.19: SEM images of (a) virgin CBD electrode and (b) CBD electrode after the electrochemical reaction. ....	84
Figure 4.20: SEM-EDX spectrum for virgin CBD electrode. ....	85

Figure 4.21: SEM-EDX spectrum for CBD electrode after the electrochemical reaction. ....	85
Figure 4.22: Cottrell current plot for ACC electrode with surface area 0.45 cm <sup>2</sup> . ....	86
Figure 4.23: Cottrell current plot for CBD electrode with surface area 0.45 cm <sup>2</sup> . ....	87
Figure 4.24: CV curves of Amberlyst-15 blank solution and Amberlyst-15 with glycerol solution on ACC electrode at scan range from – 3.00 to + 3.50 V versus Ag/AgCl, with potential scan rate of 0.02 Vs <sup>-1</sup> . ....	88
Figure 4.25: CV curves of Amberlyst-15 blank solution and Amberlyst-15 with glycerol solution on CBD electrode at scan range from – 3.00 to + 3.50 V versus Ag/AgCl, with potential scan rate of 0.02 Vs <sup>-1</sup> . ....	89
Figure 4.26: Glycerol conversion from the electrochemical study on (a) Pt, (b) ACC and (c) CBD cathode electrodes in the presence of Amberlyst-15 at 80 °C and 1.0 A constant current. ....	90
Figure 4.27: First-order kinetic model of the electrochemical conversion of glycerol in the presence of Amberlyst-15 on (a) Pt, (b) ACC, and (c) CBD cathode electrodes at 80 °C and 1.0 A constant current. ....	90
Figure 4.28: GC chromatogram of the products obtained from the electrochemical conversion of glycerol in the presence of Amberlyst-15 on (a) ACC and (b) CBD cathode electrodes at 80 °C and 1.0 A constant current. ....	91
Figure 4.29: Product distribution from the electrochemical conversion of glycerol in the presence of Amberlyst-15 on (a) Pt, (b) ACC, and (c) CBD cathode electrodes at 80 °C and 1.0 A constant current. ....	94
Figure 4.30: Glycerol conversion from the electrochemical study on ACC cathode electrode at 80 °C, 2.0 A constant current and in the presence of Amberlyst-15 varied from 6.4% w/v to 12.8% w/v. ....	101
Figure 4.31: First-order kinetic model of the electrochemical conversion of glycerol in the presence of Amberlyst-15 varied from 6.4 to 12.8% w/v on ACC cathode electrode at 80 °C and 2.0 A constant current. ....	101
Figure 4.32: Product distribution from the electrochemical conversion of glycerol in the presence of Amberlyst-15 at (a) 6.4% w/v, (b) 9.6% w/v, and (c) 12.8% w/v on ACC cathode electrode at 80 °C and 2.0 A constant current. ....	102
Figure 4.33: Maximum yield of glycolic and lactic acids obtained from the electrochemical conversion of glycerol in the presence of 6.4% w/v, 9.6% w/v, and 12.8% w/v Amberlyst-15 on ACC cathode electrode at 80 °C and 2.0 A constant current. ....	103

Figure 4.34: Glycerol conversion from the electrochemical study on ACC cathode electrode in the presence of 9.6% w/v Amberlyst-15 at 2.0 A constant current at room temperature (27 °C), 50 °C, and 80 °C. ....	104
Figure 4.35: First-order kinetic model of the electrochemical conversion of glycerol in the presence of 9.6% w/v Amberlyst-15 on ACC cathode electrode at 2.0 A constant current at room temperature (27 °C), 50 °C, and 80 °C.....	105
Figure 4.36: Maximum yield of glycolic and lactic acids obtained from the electrochemical conversion of glycerol in the presence of 9.6% w/v Amberlyst-15 on ACC cathode electrode at 2.0 A constant current at (a) room temperature, 27 °C (RT), (b) 50 °C, and (c) 80 °C. ....	105
Figure 4.37: Product distribution from the electrochemical conversion of glycerol in the presence of 9.6% w/v Amberlyst-15 on ACC cathode electrode at 2.0 A constant current at (a) room temperature (27 °C), (b) 50 °C, and (c) 80 °C. ....	106
Figure 4.38: Glycerol conversion from the electrochemical study on ACC cathode electrode in the presence of 9.6% w/v Amberlyst-15 at 80 °C and constant currents of 1.0, 2.0, and 3.0 A. ....	108
Figure 4.39: First-order kinetic model of the electrochemical conversion of glycerol in the presence of 9.6% w/v Amberlyst-15 on ACC cathode electrode at 80 °C and constant currents of 1.0, 2.0, and 3.0 A. ....	108
Figure 4.40: Product distribution from the electrochemical conversion of glycerol in the presence of 9.6% w/v Amberlyst-15 on ACC cathode electrode at 80 °C and constant currents of (a) 1.0, (b) 2.0, and (c) 3.0 A. ....	109
Figure 4.41: Maximum yield of glycolic and lactic acids obtained from the electrochemical conversion of glycerol in the presence of 9.6% w/v Amberlyst-15 on ACC cathode electrode at 80 °C and constant currents of 1.0, 2.0, and 3.0 A. ....	110
Figure 4.42: Glycerol conversion from the electrochemical study on CBD cathode electrode at 80 °C, 2.0 A constant current and in the presence of Amberlyst-15 varied from 6.4% w/v to 12.8% w/v. ....	113
Figure 4.43: First-order kinetic model of the electrochemical conversion of glycerol in the presence of Amberlyst-15 varied from 6.4% w/v to 12.8% w/v on the CBD cathode electrode at 80 °C and 2.0 A constant current.....	114
Figure 4.44: Maximum yield of glycolic and lactic acids obtained from the electrochemical conversion of glycerol in the presence of 6.4% w/v, 9.6% w/v and 12.8% w/v Amberlyst-15 on CBD cathode electrodes, at 80 °C and 2.0 A constant current. ....	114

Figure 4.45: Product distribution from the electrochemical conversion of glycerol in the presence of Amberlyst-15 at (a) 6.4% w/v, (b) 9.6% w/v, and (c) 12.8% w/v on CBD cathode electrodes at 80 °C and 2.0 A constant current.....	115
Figure 4.46: Glycerol conversion from the electrochemical study on CBD cathode electrode in the presence of 9.6 % w/v Amberlyst-15 at 2.0 A constant current, at room temperature (27 °C), 50 °C and 80 °C. ....	117
Figure 4.47: First-order kinetic model of the electrochemical conversion of glycerol in the presence of 9.6% w/v Amberlyst-15 on CBD cathode electrode at 2.0 A constant current at room temperature (27 °C), 50 °C, and 80 °C.....	117
Figure 4.48: Product distribution from the electrochemical conversion of glycerol in the presence of 9.6% w/v Amberlyst-15 on CBD cathode electrode at 2.0 A constant current at (a) room temperature (27 °C), (b) 50 °C, and (c) 80 °C. ....	118
Figure 4.49: Maximum yield of glycolic and lactic acids obtained from the electrochemical conversion of glycerol in the presence of 9.6% w/v Amberlyst-15 on CBD cathode electrode at 2.0 A constant current at room temperature, 27 °C (RT), 50 °C, and 80 °C. ....	119
Figure 4.50: Glycerol conversion from the electrochemical study on CBD cathode electrode in the presence of 9.6% w/v Amberlyst-15 at 80 °C and constant currents of 1.0, 2.0, and 3.0 A. ....	120
Figure 4.51: First-order kinetic model of the electrochemical conversion of glycerol in the presence of 9.6% w/v Amberlyst-15 on CBD cathode electrode at 80 °C at constant currents of 1.0, 2.0, and 3.0 A.....	121
Figure 4.52: Product distribution from the electrochemical conversion of glycerol in the presence of 9.6% w/v Amberlyst-15 on CBD cathode electrode at 80 °C and constant currents of (a) 1.0, (b) 2.0, and (c) 3.0 A. ....	122
Figure 4.53: Maximum yield of glycolic and lactic acids obtained from the electrochemical conversion of glycerol in the presence of 9.6% w/v Amberlyst-15 on CBD cathode electrode at 80 °C and constant currents of 1.0, 2.0, and 3.0 A. ....	123
Figure 4.54: Glycerol conversion from the electroreduction study of glycerol in the presence of 9.6% w/v Amberlyst-15 at 2.0 A constant current and 80 °C on Pt, ACC, and CBD cathode electrodes. ....	125
Figure 4.55: First-order kinetic model of the electroreduction of glycerol in the presence of 9.6% w/v Amberlyst-15 at 2.0 A constant current and 80 °C on Pt, ACC, and CBD cathode electrodes. ....	125

Figure 4.56: The GC-MS chromatogram of the products obtained from the electroreduction of glycerol in the presence of Amberlyst-15 on Pt, ACC or CBD cathode electrodes, at 80 °C and at 2.0 A constant current.....	126
Figure 4.57: Product distribution from the electroreduction of glycerol in the presence of 9.6% w/v Amberlyst-15 at 2.0 A and 80 °C on (a) Pt, (b) ACC, and (c) CBD cathode electrodes.....	127
Figure 4.58: Glycerol conversion from the electro-oxidation study of glycerol in the presence of 9.6% w/v amberlyst-15 at 2.0 A constant current and 80 °C on Pt anode electrode versus Pt, ACC, and CBD cathode electrode. ....	131
Figure 4.59: First-order kinetic model of the electro-oxidation of glycerol in the presence of 9.6% w/v Amberlyst-15 at 2.0 A constant current and 80 °C on Pt anode electrode versus Pt, ACC, and CBD cathode electrodes.....	131
Figure 4.60: Product distribution from the electro-oxidation of glycerol in the presence of 9.6% w/v Amberlyst-15 at 2.0 A constant current and 80 °C on Pt anode electrode versus (a) Pt, (b) ACC, and (c) CBD cathode electrodes.....	133
Figure 4.61: GC chromatogram of the products obtained from the electro-oxidation of glycerol in the presence of Amberlyst-15 on Pt anode electrodes at 80 °C and 2.0 A constant current. ....	134



## LIST OF TABLES

Table 2.1: Chemical content in crude glycerol and purified glycerol (Hazimah <i>et al.</i> , 2003). .....	9
Table 2.2: Grades and usage of commercial purified glycerol (Kenkel <i>et al.</i> , 2008). .....	9
Table 2.3: List of added-value compounds derived from glycerol (Datta <i>et al.</i> , 2006; Koivistoinen <i>et al.</i> , 2013; Lee <i>et al.</i> , 2015; Liu <i>et al.</i> , 2012; Pandhare <i>et al.</i> , 2016; Kishimoto, 2008). .....	11
Table 2.4: Physical properties of 1,2-Propanediol and 1,3-Propanediol (Sigma_Aldrich). .....	12
Table 2.5: Literature data on the selectivity and yield of 1,2-propanediol, and glycerol conversion obtained by catalytic and biofermentation methods. ....	14
Table 2.6: Literature data on the yield of 1,3-propanediol obtained from glycerol by biofermentation approach. ....	16
Table 2.7: Literature data on the selectivity and yield of 1,3-propanediol, and glycerol conversion obtained by catalytic approach. ....	18
Table 2.8: Literature data on the selectivity and yield of glyceric and glycolic acids, and glycerol conversion obtained by catalytic approach. ....	21
Table 2.9: Physical properties of lactic acid (Sigma_Aldrich). ....	22
Table 2.10: Literature data on the selectivity and yield of lactic acid, and glycerol conversion obtained by catalytic approach. ....	24
Table 2.11: Literature data on the selectivity and yield of glycolic and glyceric acids, and glycerol conversion obtained by electrochemical approach. ....	32
Table 2.12: Physical properties of Amberlyst-15 (Pal <i>et al.</i> , 2012). ....	35
Table 2.13: List of the common noble metals used for catalyst preparation with their current price and CAS reference number, compare with commercial activated carbon (Sigma_Aldrich). ....	39
Table 3.1. List of chemicals and reagents used. ....	47
Table 3.2: Gas chromatography-mass spectroscopy analysis conditions. ....	54
Table 3.3: Gas chromatography analysis conditions. ....	54

Table 3.4: List of chemical standards and their physical properties (Sigma_Aldrich) as well as retention time in GC-MS and GC-FID analysis. ....	55
Table 3.5: The glycerol solution preparation for standard calibration curve. ....	57
Table 4.1: Electrochemical conversion of glycerol in the presence of Amberlyst-15 over Pt electrode; the yield and selectivity for glycolic and glyceric acids are given at the maximum level. ....	63
Table 4.2: Comparison between data from Saila <i>et al.</i> , 2015 and the present study. ....	78
Table 4.3: Active surface areas for ACC and CBD electrodes estimated from Cottrell current plot. ....	86
Table 4.4: Electrochemical conversion of glycerol in the presence of Amberlyst-15 over Pt, ACC and CBD cathode electrodes; the yield and selectivity for glycolic, glyceric and lactic acids at the maximum level. ....	93
Table 4.5: Electrochemical conversion of glycerol in the presence of Amberlyst-15 over ACC cathode electrode; the yield and selectivity for glycolic and lactic acids at the maximum level. ....	99
Table 4.6: Electrochemical conversion of glycerol in the presence of Amberlyst-15 over CBD cathode electrode; the yield and selectivity for glycolic and lactic acids at the maximum level. ....	112
Table 4.7: Electroreduction of glycerol over Pt, ACC and CBD cathode electrodes: yields and selectivities for 1,2-propanediol, acetol and diethylene glycol obtained after 8 h reaction time. ....	128
Table 4.8: Electro-oxidation of glycerol over Pt anode electrode versus Pt, ACC, and CBD cathode electrode: maximum yield and selectivity for glyceric and glycolic acids. ....	132

## LIST OF SCHEMES

Scheme 2.1: Transesterification of triglycerides with methanol.....	8
Scheme 2.2: Conversion of glycerol to added-value chemicals (Zhou <i>et al.</i> , 2008). ....	10
Scheme 2.3: Glycerol electro-oxidation pathway in acidic medium (Roquet <i>et al.</i> , 1994). .....	27
Scheme 2.4: General principle of redox catalyst (Francke <i>et al.</i> , 2014).....	33
Scheme 4.1. Catalyzed oxidation of glyceraldehyde and acetol to glyceric as well as glycolic acids by Amberlyst-15 .....	68
Scheme 4.2: Proposed reaction mechanism of electrochemical conversion of glycerol in the presence of Amberlyst-15 on the Pt electrode. ....	81
Scheme 4.3: Electroreduction of pyruvic acid on the porous ACC cathode electrode...	96
Scheme 4.4: Proposed reaction mechanism of the electrochemical conversion of glycerol in the Amberlyst-15 medium on ACC cathode electrode and Pt anode electrode. ....	97
Scheme 4.5: Proposed reaction mechanism of the electrochemical conversion of glycerol in the Amberlyst-15 medium on CBD cathode electrode and Pt anode electrode. ....	98
Scheme 4.6: Proposed reaction mechanism for electroreduction of glycerol.....	128
Scheme 4.7: Proposed reaction mechanism for the electro-oxidation of glycerol.....	135

## LIST OF SYMBOLS AND ABBREVIATIONS

### ABBREVIATIONS

ACC	:	Activated carbon composite
BP	:	Boiling point
CBD	:	Carbon black diamond
CE	:	Counter electrode
CV	:	Cyclic voltammetry
DEG	:	Diethylene glycol
DHA		Dihydroxyacetone
EDX	:	Energy Dispersive X-ray analyzer
EG		Ethylene glycol
FCC	:	Food Chemical Codex
FTIR	:	Fourier Transform Infrared Spectroscopy
GC-FID	:	Gas Chromatography flame ionization detector
GC-MS	:	Gas Chromatography Mass Spectroscopy
h	:	hour
MW	:	Molecular weight
PBI	:	Polybenzimidazole
PDO	:	Propanediol
PEM	:	Proton exchange membrane
PGA	:	Polyglycolic acid
PTT	:	Polytrimethylene terephthalate
PTFE	:	Polytetrafluoroethylene
RT	:	Room temperature
SEM	:	Scanning Electron Microscopy

SS	:	Stainless steel
TEG	:	Tetraethylene glycol
TEMPO	:	2,2,6,6-tetramethylpiperidiny1-N-oxyl
USP	:	United States Pharmacopeia
WE	:	Working electrode

## SYMBOLS

Symbol	Meaning	Unit
A	: Active surface area	cm <sup>2</sup>
C <sub>o</sub>	: Initial concentration of the reducible analyte	mol/cm <sup>3</sup>
D	: Diffusion coefficient	cm <sup>2</sup> /s
F	: Faraday constant	C/mol
I	: Current	A
k	: Rate constant	h <sup>-1</sup>
n	: Number of electron	-
t	: Time	s or h
T	: Temperature	°C
R <sub>t</sub>	: Retention time	min

## LIST OF APPENDICES

Appendix 1: GC mass spectra for compounds obtained from the electrolysis .....	159
Appendix 2: GC chromatograms for the standards.....	164
Appendix 3: Standards calibration curve .....	168
Appendix 4: Calculation for active surface area of an electrode by chronoamperometry analysis.....	177

## CHAPTER 1: INTRODUCTION

### 1.1 General

Crude glycerol is the major byproduct of transesterification of vegetable oils during manufacturing of biodiesel for modern fuel or fuel components. Crude glycerol is approximately 10% wt of the total biodiesel products (Cardona *et al.*, 2007; Heming, 2012). With the rapid growth of the biodiesel industry, the production of crude glycerol has also significantly increased. The current market value of glycerol is at its minimum point because of oversupply. Therefore, it is necessary to develop alternative applications for glycerol. To date, many works have focused on transforming glycerol into various high added-value chemicals, such as glyceric acid, glycolic acid, 1,3-propanediol, 1,2-propanediol, acrolein, dihydroxyacetone, and lactic acid (Bagheri *et al.*, 2015; Pagliaro *et al.*, 2007; Simões *et al.*, 2012).

Previous works demonstrated that several chemical and biological processes can be used to convert glycerol into various added-value compounds; these processes include selective oxidation, etherification, hydrogenolysis, catalytic reforming, dehydration, and enzymatic fermentation (Bagheri *et al.*, 2015; Pagliaro *et al.*, 2007). However, these processes may suffer from some drawbacks; for instance, high pressure and high temperature are required during chemical processes, thereby rendering the production as economically impractical. Furthermore, organic solvents commonly used in catalysis may negatively affect the environment. Whereas, in biological pathways, expensive and complicated procedures are usually employed during cultivation of bacteria (Kurosaka *et al.*, 2008; Lee *et al.*, 2015). In the past few years, inexpensive electrochemical techniques have been intensively studied to replace existing methods for glycerol conversion.

Electrochemical method is relatively simple and robust in terms of structure and operation. This method is environment friendly because chemical reagents are substituted by electrons. Previous studies reported the electro-oxidation of glycerol by investigating the electrocatalytic behavior and electrochemical fuel cells. Electro-oxidation of glycerol produces glyceraldehyde, glycolic acid, oxalic acid, formic acid, and other oxidation compounds. The selectivity toward the production of these compounds significantly depends on the pH of the reaction medium and the type of electrode materials (Avramov-Ivic *et al.*, 1993; Avramov-Ivić *et al.*, 1991; Roquet *et al.*, 1994; Yildiz *et al.*, 1994).

Currently, electrochemical conversion of glycerol is mostly performed in alkaline media. The effects of electrode materials, such as gold, platinum, palladium, and nickel, have been investigated. Although a wide range of compounds, including glycerate, oxalate, glycolate, tartronate, carbamate, and formate, have been detected, lack of product selectivity is apparent (Kwon *et al.*, 2014; Oliveira *et al.*, 2014). An excess of caustic solution may also cause corrosion of the electrochemical reactor during the actual production (Carrettin *et al.*, 2003).

Limited information is available regarding the electrochemical oxidation of glycerol in acidic media. Although researchers reported successful electro-oxidation of glycerol in acidic media, their works only focused on the electrochemical behavior study based on the effects of the electrode material and electrode potential; bulk electrochemical study in galvanostatic mode has been rarely discussed in the literature (Kwon *et al.*, 2011; Roquet *et al.*, 1994). To the best of our knowledge, only Kongjao *et al.* (2011) reported the bulk electrochemical conversion of glycerol in galvanostatic mode; in this study, glycerol was electrolyzed in sulfuric acid solution ( $\text{H}_2\text{SO}_4$ ) over platinum electrode in a one-pot electrochemical cell. Glycerol was converted into ethylene glycol,



acrolein, 1,3-propanediol, glycidol, and 1,2-propanediol; however, the mineral acid ( $\text{H}_2\text{SO}_4$ ) used is toxic and corrosive, which may negatively affect the environment (Kongjao *et al.*, 2011).

## **1.2 Scope of research**

In this work, a novel method was adopted to convert glycerol through electrochemical method over a solid acid catalyst (Amberlyst-15) on three types of electrodes: platinum (Pt), activated carbon composite (ACC), and carbon black diamond (CBD) composite electrodes. To the best of our knowledge, this work is the first to report the use of ACC and CBD electrodes as well as Amberlyst-15 in electrochemical study of glycerol. The comprehensive electrochemical study of glycerol focused on both electro-oxidation and electroreduction processes. The effects of reaction temperature, electric current, and amount of catalyst were also investigated. The reaction mechanisms underlying glycerol conversion are then proposed.

## **1.3 Problem statement**

In previous studies, the electrochemical conversion of glycerol is mainly based on direct electrolysis without adding a redox catalyst (Fashedemi *et al.*, 2015; Holade *et al.*, 2013; Qi *et al.*, 2014; Zhang *et al.*, 2014). In the presence of a redox catalyst, the kinetic inhibition of electron transfer between the electrode and electrolyte can be eliminated, resulting in increased product yield or totally different selectivity. In addition, the use of redox catalyst can help to avoid over-oxidation or reduction of the substrate as well as electrode passivation (Francke *et al.*, 2014). Few researchers reported the addition of oxidizing agents, such as 2,2,6,6-tetramethylpiperidiny1-N-oxyl (TEMPO), hydrogen peroxide ( $\text{H}_2\text{O}_2$ ), and manganese (IV) oxide ( $\text{MnO}_2$ ), for electrochemical studies of glycerol (Prieto *et al.*, 2013a; Prieto *et al.*, 2014; Saila *et al.*, 2015). However, homogeneous catalysts are relatively expensive, and a complicated

distillation process is generally required during recovery (Farnetti *et al.*, 2009; Thornton *et al.*, 2002). In this regard, a cheap and green heterogeneous catalyst is introduced in the present study. The solid acid catalyst (Amberlyst-15) was used in bulk electrochemical study of glycerol, to convert glycerol into various added-value compounds. Compared with the toxic and corrosive mineral acids or caustic solution (Zhou *et al.*, 2012), Amberlyst-15 is safer to use because of its environmentally benign characteristic. Furthermore, Amberlyst-15 can be readily removed from the reaction medium and can be regenerated and reused several times (Pal *et al.*, 2012). The macro-reticular pore structure of Amberlyst-15 allows the liquid reactants to penetrate through the pores, thereby permitting them to react with hydrogen ion sites located throughout the beads. Although Amberlyst-15 has been widely studied in chemical catalytic synthesis, to the best of our knowledge, the electrochemical behavior and organic electrosynthesis in the presence of Amberlyst-15 have not been reported. In addition, this solid acid is tested for the first time as a redox catalyst for electrochemical study or conversion of glycerol. The electroreduction of glycerol was studied by evaluating the electrode material in the cathodic region to provide a wide range of added-value compounds with improved yield and selectivity.

#### **1.4 Research objectives**

The objectives of this research are:

- a) To determine the effects of process parameters on the electrochemical conversion of glycerol in the presence of Amberlyst-15 on Pt electrode in a one-pot electrochemical cell.
- b) To compare the electrocatalytic conversion of glycerol on novel ACC and CBD cathode electrodes with that on conventional Pt electrode.

- c) To optimize the electrochemical conversion of glycerol on ACC and CBD cathode electrodes.
- d) To develop and evaluate the performance of a two-compartments electrochemical cell.

## **1.5 Thesis structure**

This thesis is divided into five chapters arranged in the following sequences: introduction, literature review, methodology, results and discussion, and conclusion.

The introductory chapter briefly highlights recent issues encountered during glycerol conversion through chemical and biological pathways. This chapter also presents studies on electrochemical conversion of glycerol and its corresponding challenges. The research aims and objectives of this study are also described.

The literature review chapter comprehensively evaluates existing methods, including chemical, biological, or electrochemical pathways, for converting glycerol into various added-value compounds.

The research methodology chapter demonstrates the detailed method and experimental set-up for electrochemical processing of glycerol with Amberlyst-15 over Pt, ACC, and CBD electrodes. This section also illustrates analytical techniques used to characterize the electrodes and products.

The results and discussion chapter presents variations in added-value compounds obtained through electrolysis of glycerol with Amberlyst-15 on Pt, ACC, and CBD electrodes. Glycerol conversion and yield for each compound are also discussed in detail. Additionally, the reaction mechanisms for each electrochemical study are proposed.

Finally, the conclusion chapter summarizes all research outputs and suggests further works for future research.

## CHAPTER 2: LITERATURE REVIEW

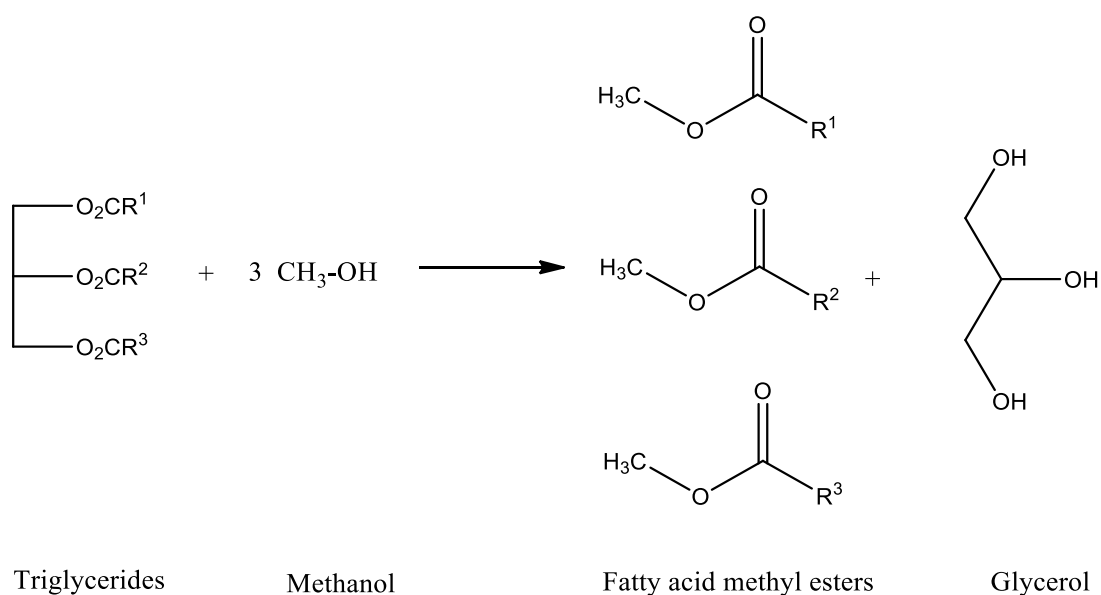
### 2.1 Introduction

This chapter presents an overview of the current market of glycerol and its applications. Glycerol-derived added-value compounds including 1,2-propanediol, 1,3-propanediol, glyceric acid, glycolic acid, and lactic acid are reviewed in detail in terms of their uses, market value, and production process. The electrochemical conversion of glycerol is also elucidated. Finally, a detailed explanation on the redox catalyst, activated carbon electrode, and diamond electrode in the electrochemistry study is presented.

### 2.2 Glycerol and its sustainable applications

To date, the utilization of biomass as a renewable feedstock for biofuel production has received significant attention because of the environmental issues and decreasing supply of fossil fuel (Bozell, 2010). The amount of biofuel produced is expected to reach 60 billion gallons worldwide in 2020 (Brown, 2012). As such, biodiesel has been considered an alternative option to replace conventional fossil fuel.

Biodiesel is produced by transesterification of vegetable oils, such as rapeseed, sunflower, palm, and soybean oils, with methanol. In this process, glycerol is obtained as a byproduct amounting to approximately 10% wt of the total biodiesel produced. Scheme 2.1 shows that 1 mole of glycerol is obtained when 3 moles of fatty acid methyl esters are produced.



**Scheme 2.1:** Transesterification of triglycerides with methanol.

Generally, glycerol produced through biodiesel production can be classified according to its purity into crude glycerol (with 60% to 80% purity) and pure or refined glycerol (with 99.1% to 99.8% purity) (Table 2.1). The use of crude glycerol in cosmetic, pharmaceutical, and food industries is unsustainable because of high contamination from methanol solvent (14% to 50%). Glycerol is typically purified or refined to purity above 99% for commercial use. The grades of the purified glycerol and its applications are summarized in Table 2.2. Removing excess methanol requires high processing cost; as such, glycerol purification is not economically viable for small or medium industries. The high market price of purified glycerol is significantly attributed to additional costs from refinery processes, such as distillation, chemical treatment, extraction, ion exchange, decantation, adsorption, and crystallization. The price of purified glycerol worldwide is around USD \$1.10/kg to \$3.30/kg, which is 10 or more times higher than that of crude glycerol (USD \$0.04/kg to \$0.33/kg).

**Table 2.1:** Chemical content in crude glycerol and purified glycerol (Hazimah *et al.*, 2003).

Parameter	Crude glycerol	Purified glycerol
Glycerol content (%)	60 - 80	99.1 - 99.8
Moisture contents (%)	1.5 - 6.5	0.11 - 0.8
Ash (%)	1.5 - 2.5	0.054
Soap (%)	3.0 - 5.0	0.56
Acidity (pH)	0.70 - 1.30	0.10 - 0.16
Chloride (ppm)	ND	1.0
Colour (APHA)	Dark	34 - 45

**Table 2.2:** Grades and usage of commercial purified glycerol (Kenkel *et al.*, 2008).

Grade	Type of glycerol	Usage
Grade – I	Technical grade ~ 99.5 %	Intermediate compound for various chemicals however not applied to food or drug formulation
Grade – II	*USP grade 96-99.5 %	Food products, pharmaceuticals and cosmetics
Grade – III	Kosher or USP/**FCC grade 99.5 – 99.7%	Kosher foods and drinks

\*USP - United States Pharmacopeia

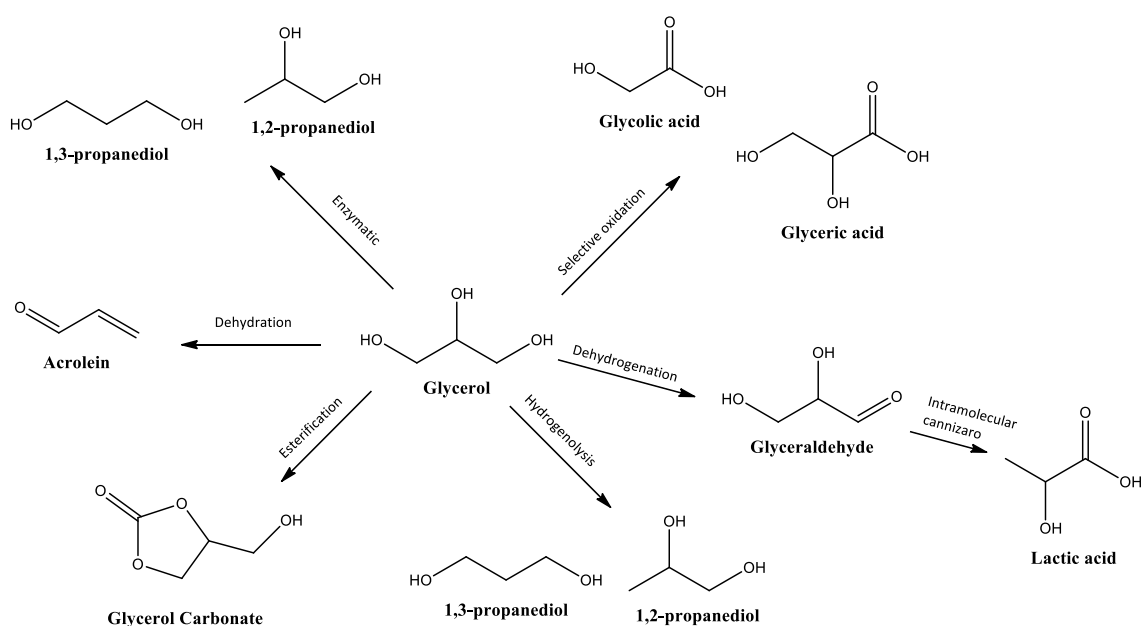
\*\* FCC – Food Chemical Codex

The rapid growth of global biodiesel production in recent years has resulted in drastic surplus of crude glycerol, whose cost has declined significantly (Yang *et al.*, 2012). According to a previous report, the trading price for crude glycerol in Southeast Asia was as low as USD \$0.30/kg in 2015 (Ng, 2015). Therefore, researchers must discover alternative uses for glycerol.

## 2.3 Added-value compounds available from glycerol

### 2.3.1 General overview

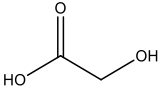
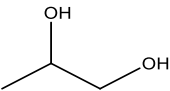
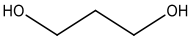
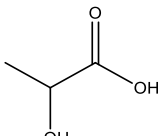
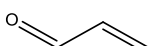
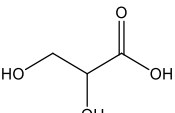
Crude glycerol has attracted substantial attention as renewable feedstock for synthesis of various added-value compounds, such as acrolein (Bagheri *et al.*, 2015), glyceric acid (Prieto *et al.*, 2013b), and lactic acid (Bagheri *et al.*, 2015; Lux *et al.*, 2010). Table 2.3 summarizes some of the valuable compounds derived from glycerol. Researchers have focused on synthesis through the catalytic pathway, such as selective oxidation, dehydration, esterification, and hydrogenolysis, or through bioproduction with bacterial strains (Scheme 2.2) (Bagheri *et al.*, 2015; Kusunoki *et al.*, 2005; Menzel *et al.*, 1997).



**Scheme 2.2:** Conversion of glycerol to added-value chemicals (Zhou *et al.*, 2008).



**Table 2.3:** List of added-value compounds derived from glycerol (Datta *et al.*, 2006; Koivistoinen *et al.*, 2013; Lee *et al.*, 2015; Liu *et al.*, 2012; Pandhare *et al.*, 2016; Kishimoto, 2008).

Name	Molecular structure	Selling Price (USD \$)	Applications	Current Industrial Processes
Glycolic acid		611/kg	<ul style="list-style-type: none"> <li>Chemical peels performed by a dermatologist, skin care products</li> </ul>	<ul style="list-style-type: none"> <li>Chemically produced from formaldehyde and CO</li> <li>Bioproduction from lignocellulosic, ethylene glycol (oxidation), glycolonitrile (hydrolyzation)</li> </ul>
1,2-propanediol (propylene glycol)		117/kg	<ul style="list-style-type: none"> <li>Functional fluids (antifreeze, deicing, cosmetics, liquid detergent etc)</li> </ul>	<ul style="list-style-type: none"> <li>Hydration of propylene glycol through chlorohydrine and hydroperoxide process</li> <li>Hydrogenolysis of glycerol</li> <li>Biofermentation from glycerol</li> </ul>
1,3-propanediol		215/kg	<ul style="list-style-type: none"> <li>Copolymer to produce polymer (textile fibers exhibiting chemical resistance)</li> </ul>	<ul style="list-style-type: none"> <li>Hydration of acrolein</li> <li>Hydroformylation of ethylene oxide</li> <li>Enzymatic transformation of glycerol</li> <li>Selective deoxygenation or hydrogenolysis of glycerol</li> </ul>
Lactic acid		132/kg	<ul style="list-style-type: none"> <li>Food acidulant, feedstock for food emulsifying agent, acidulant for leather and textile industry</li> <li>Platforms chemicals for polymers</li> </ul>	<ul style="list-style-type: none"> <li>Carbohydrate or sugar fermentation</li> <li>Chemical synthesis via lactonitrile route</li> <li>Double electrodialysis of dextrose</li> </ul>
Acrolein		500/kg	<ul style="list-style-type: none"> <li>Intermediate compounds to produce acrylic acid, esters, glutaraldehyde, methionine, polyurethane and polyester resins.</li> </ul>	<ul style="list-style-type: none"> <li>Partial oxidation of propylene</li> <li>Glycerol dehydration</li> </ul>
Glyceric acid		400/g	<ul style="list-style-type: none"> <li>Intermediate compounds to produce tartronic or mesoxalic acids</li> </ul>	<ul style="list-style-type: none"> <li>Bioproduction from glycerol by bacteria strain: Methylobacterium, Arthrobacter and Pseudonocardia</li> </ul>

### 2.3.2 Propanediols

Propanediols, such as 1,2-propanediol (1,2-PDO) or 1,3-propanediol (1,3-PDO), have gained significant research interest because of their high commercial values.

1,2-PDO, which is also known as propylene glycol, is a colorless, odorless, clear, and viscous liquid with slightly sweet taste. The physical properties of 1,2-PDO are listed in Table 2.4. This compound is widely used to produce unsaturated polyester resins, polymers, and functional fluids, such as antifreeze or deicing agents, cosmetics, and foods (Maris *et al.*, 2007). The global market of 1,2-PDO is driven by its major applications, particularly in the manufacture of unsaturated polyester resins. The leading consumers of 1,2-PDO include North America, China, and Germany because of the growing demand for unsaturated polyester resins in these countries. The global market price of 1,2-PDO is expected to increase up to USD \$4.2 billion/kt by 2019 (Future\_Market\_Insights, 2016; Markets\_and\_Markets, 2016b). Generally, 1,2-PDO is commercially produced from propylene oxide with water through hydroperoxide or chlorohydrin process (Yadav *et al.*, 2012). 1,2-PDO has been extensively produced from glycerol through catalytic hydrogenolysis or via the enzymatic pathway.

**Table 2.4:** Physical properties of 1,2-Propanediol and 1,3-Propanediol (Sigma\_Aldrich).

Physical properties	1,2-Propanediol	1,3-Propanediol
Chemical formula	C <sub>3</sub> H <sub>8</sub> O <sub>2</sub>	C <sub>3</sub> H <sub>8</sub> O <sub>2</sub>
Molar mass	76.10 gmol <sup>-1</sup>	76.10 gmol <sup>-1</sup>
Density	1.036 g/cm <sup>3</sup>	1.053 g/cm <sup>3</sup>
Boiling Point	187 °C	214 °C

Previous studies demonstrated the effectiveness of various catalyst systems in glycerol hydrogenolysis; these systems combine noble metals, including ruthenium, palladium, rhodium, and platinum, with other transition metals, such as zinc, chromium, and copper, with silica, zeolite, aluminum oxide, or activated carbon supports (Rode *et al.*, 2010). Kusunoki and his co-workers reported that the Ru/C catalyst converted 79% glycerol to 1,2-PDO, with selectivity of 82%, under the reaction condition of 120 °C and 4 MPa H<sub>2</sub> pressure for 10 h in the presence of Amberlyst-15. However, Ru alone could effectively enhance the byproduct reaction by cracking glycerol into smaller compounds, such as ethylene glycol, ethanol, methanol, and methane (Kusunoki *et al.*, 2005). Maris *et al.* indicated that hydrogenolysis on Pt or bimetallic Pt/Ru supported on C resulted in high selectivity for lactate under basic medium (Maris *et al.*, 2007). Copper-based solid catalysts, such as Cu/ZnO (Wang *et al.*, 2014), Cu/MgO (Pandhare *et al.*, 2016; Yuan *et al.*, 2010), Cu/Cr(Ba) (Rode *et al.*, 2010), Ru-Cu/ZrO<sub>2</sub> (Liu *et al.*, 2012), and Cu<sub>a</sub>/Mg<sub>x</sub>Al<sub>y</sub>O<sub>z</sub> (Xia *et al.*, 2013) are also effective catalysts for selective glycerol hydrogenolysis. The reaction conditions, type of catalyst, glycerol conversion, and selectivity for 1,2-PDO are summarized in Table 2.5.

Fermentation with bacterial strains is another well-developed method for glycerol conversion. Glycerol can be converted into 1,2-PDO by *Escherichia coli*, with 21.3% (w/w) yield (Jung *et al.*, 2008). 1,2-PDO can also be produced by metabolically engineered *Saccharomyces cerevisiae* strains with glycerol, with 2.19 g/L yield (Jung *et al.*, 2011).

**Table 2.5:** Literature data on the selectivity and yield of 1,2-propanediol, and glycerol conversion obtained by catalytic and biofermentation methods.

Catalyst/ Bacteria strain	T (°C)	P H <sub>2</sub> (MPa)	Time (h)	Glycerol conversion (%)	1,2-PDO		Ref.
					Y (%)	S (%)	
Rh <sub>0.02</sub> Cu <sub>0.4</sub> /Mg <sub>5</sub> <sub>6</sub> Al <sub>1.98</sub> O <sub>8.57</sub>	180	2.0	10	91	-	98.7	(Xia <i>et al.</i> , 2012)
Ru/SiO <sub>2</sub>	240	8.0	5	21.7	-	60.5	(Vasiliado u <i>et al.</i> , 2011)
CuO	200	Ambient	180 g <sub>cat</sub> min/mol	100	-	60	(Dieuzeide <i>et al.</i> , 2016)
Cu <sub>0.4</sub> /Mg <sub>6.28</sub> Al <sub>1.3</sub> <sub>2</sub> O <sub>8.26</sub>	210	3.0 (N <sub>2</sub> )	10	95.1	-	92.2	(Xia <i>et al.</i> , 2013)
Cu/MgO	220	0.75	14	100	-	95.5	(Pandhare <i>et al.</i> , 2016)
Cu-Al mixed oxides	220	7.0	24	74.3	58.6	78.9	(Valencia <i>et al.</i> , 2015)
Cu/MgO	210	4.5	12	96.6	-	92.6	(Pandhare <i>et al.</i> , 2016)
Ru-Cu	180	8.0	24	100	-	78.5	(Liu <i>et al.</i> , 2012)
CuO/MgO	180	3.0	20	72.0	-	97.6	(Yuan <i>et al.</i> , 2010)
Pt impregnated NaY zeolite	230	4.2	15	85.4	-	64.0	(D'Hondt <i>et al.</i> , 2008)
Cu-Cr(Ba)	220	5.2	<u>Batch:</u> 5 <u>Continuous:</u> 800	34 65	-	84 >90	(Rode <i>et al.</i> , 2010)
Cu/Al <sub>2</sub> O <sub>3</sub>	205	2.0	23	88.7	-	94.3	(Wołosiak- Hnat <i>et al.</i> , 2013)
Escherichia coli	37	-	72	78.0	21.3	-	(Clomburg <i>et al.</i> , 2011)

Note:

T: reaction temperature; P H<sub>2</sub>: hydrogen pressure

Y: yield; S: selectivity

As shown in Table 2.4, the physical properties of 1,3-PDO are similar to those of 1,2-PDO, which is also a colorless and viscous liquid miscible with water. 1,3-PDO is an important chemical intermediate in the manufacture of polyethers, polyurethanes, polyesters, biocides, and heterocyclic compounds. 1,3-PDO is widely used in food, cosmetic, and pharmaceutical industries (Biebl *et al.*, 1999; Katrlík *et al.*, 2007; Menzel *et al.*, 1997; Saxena *et al.*, 2009). In particular, 1,3-PDO is used to manufacture

polytrimethylene terephthalate (PTT) as fiber for carpets (Biebl *et al.*, 1999; Liu *et al.*, 2007; Zhang *et al.*, 2007). The rapid growth of 1,3-PDO production worldwide is related to the increasing market demand of PTT. The price of 1,3-PDO is estimated to increase from USD \$310.5 million/kt in 2014 to USD \$621.2 million/kt in 2020 (Markets\_and\_Markets, 2016a). 1,3-PDO is commercially produced by hydration of acrolein, hydroformylation of ethylene oxide, or enzymatic transformation of glycerol (Pagliaro *et al.*, 2007). Currently, many processes have been developed to produce 1,3-PDO from glycerol through the chemical catalytic pathway by selective deoxygenation or hydrogenolysis (Kraus, 2008).

In the enzymatic process, 1,3-PDO is mainly produced through fermentation with anaerobic bacteria or micro-aerobic fermentation (Chen *et al.*, 2003; Liu *et al.*, 2007; Yang *et al.*, 2007). Fermentation is usually performed with bacterial strains, such as *Clostridium butyricum*, *C. acetbutyricum*, *C. Pasteurianum*, *C. beijerinckii*, and *C. diolis* (Biebl *et al.*, 2002; Dabrock *et al.*, 1992; Forsberg, 1987; Heyndrickx *et al.*, 1991; Matsumoto *et al.*, 2007). According to Metsoviti *et al.* (2012), *Clostridium sp.* can breakdown glycerol under anaerobic conditions to produce up to 11.3 g/L 1,3-PDO. Myszka *et al.* (2012) obtained 16.98 g/L 1,3-PDO through fermentation with *C. bifermentans*; however, byproducts such as ethanol, lactic acid, formic acid, and acetic acid were also generated. Table 2.6 summarizes the fermentation results of 1,3-PDO production from glycerol.

**Table 2.6:** Literature data on the yield of 1,3-propanediol obtained from glycerol by biofermentation approach.

Type of Species	Type of Families	By-product	Process	Product (Concentration / Yield)	Ref.
<i>Halanaerobium saccharolyticum</i> (Strain: D6643 <sup>T</sup> )	Halanaerobiaceae	Acetate	Batch	0.61-0.63 mol/mol	(Kivistö <i>et al.</i> , 2012)
<i>Clostridium butyricum</i> (AKR102a)	Clostridiaceae	Acetic acid Butyric acid	Fed-Batch	93.7 g/L	(Wilkens <i>et al.</i> , 2012)
<i>Clostridium butyricum</i> (AKR102a)	Clostridiaceae	Acetic acid Butyric acid	Fed-Batch	76.2 g/L	(Wilkens <i>et al.</i> , 2012)
<i>Clostridium butyricum</i> (NRRLB-23495)	Clostridiaceae	Acetic acid Lactic acid Butyric acid	Batch	11.3 g/L	(Metsovi ti <i>et al.</i> , 2012)
<i>Citrobacter freundii</i> (FMCC-B294 (VK-19))	Enterobacteriaceae	Acetic acid Lactic acid Formic acid	Batch	10.1 g/L	(Metsovi ti <i>et al.</i> , 2012)
<i>Klebsiella oxytoca</i> (FMCC-197)	Enterobacteriaceae	Ethanol 2,3-butanediol	Batch	3.8 g/L	(Metsovi ti <i>et al.</i> , 2012)
<i>C. freundii</i>	Enterobacteriaceae	Lactic acid Acetic acid	Batch	25.36 g/L	(Anand <i>et al.</i> , 2012; Saxena <i>et al.</i> , 2009)
<i>C. freundii</i>	Enterobacteriaceae	Lactic acid Acetic acid	Batch	23.40 g/L	(Anand <i>et al.</i> , 2012; Saxena <i>et al.</i> , 2009)
<i>C. freundii</i>	Enterobacteriaceae	Lactic acid Acetic acid	Batch	21.42 g/L	(Anand <i>et al.</i> , 2012; Saxena <i>et al.</i> , 2009)
<i>C. freundii</i>	Enterobacteriaceae	Lactic acid Acetic acid	Batch	25.63 g/L	(Anand <i>et al.</i> , 2012; Saxena <i>et al.</i> , 2009)

Several well-known chemical conversion processes for producing 1,3-PDO from glycerol are based on homogeneous and heterogeneous catalytic hydrogenolysis. In 1985, the Celanese Corporation filed a patent for homogeneous catalytic hydrogenolysis of glycerol. The reaction was developed over homogeneous rhodium complex catalyst under 32 MPa syngas pressure at 473 K in the presence of 1-methyl-pyrrolidinone and tungstic acid as promoters. The yield of 1,3-PDO was 21.0% (Che, 1985). To overcome the separation problem of catalysts in homogeneous processes, many studies attempted to conduct hydrogenolysis on glycerol over heterogeneous catalysts. Chaminand *et al.* (2004) performed glycerol conversion at 453 K under 80 bar H<sub>2</sub> in the presence of a catalyst (Cu, Pd, or Rh) supported on zinc oxide, carbon, or aluminum oxide in solvents such as water, dioxane, or sulfolane. The addition of tungstic acid (H<sub>2</sub>WO<sub>4</sub>), which acts as an additive, can improve the selectivity toward 1,3-PDO. Kusunoki *et al.* (2005) carried out a reaction in the presence of cation exchange resin (Amberlyst-15) over a metal catalyst (Ru) supported on activated carbon under mild reaction conditions (120 °C, 4 MPa H<sub>2</sub>). However, the Ru/C catalyst promoted the production of 1,2-PDO. Table 2.7 summarizes the results of research on catalytic glycerol hydrogenolysis.

### 2.3.3 Glycolic and glyceric acids

Glycolic and glyceric acids are hydroxyl acids containing alcohol and carboxyl functional groups; as such, glycolic acid is widely used as an anti-oxidizing agent or chemical peeling product in the cosmetic industry. Glycolic acid is also used as a platform molecule for biopolymers. This compound can be polymerized into polyglycolic acid (PGA), which is a valuable material for food packaging (Robertson, 2016). Considering its increasing demand in the cosmetic industry, the global market of glycolic acid has increased and is expected to reach USD \$277.8 million by 2020 (Grand\_View\_Research, 2016). Glyceric acid has no significant commercial

applications at present. However, this acid can function as an important intermediate for further oxidation to tartronic acid or mesoxalic acid (Katryniok *et al.*, 2011).

**Table 2.7:** Literature data on the selectivity and yield of 1,3-propanediol, and glycerol conversion obtained by catalytic approach.

Catalyst	Reaction conditions	Selectivity of 1,3-PDO (%)	Conversion of Glycerol (%)	Yield of 1,3-PDO (%)	Reference
Rh-complex catalyst	Patented	-	-	21.0	(Che, 1985)
Pd-complex catalyst	Patented	30.8	-	-	(Drent <i>et al.</i> , 1998)
Ru-complex catalyst complex [ $\{Cp^*Ru(CO)_2\}_2Cu-H]^+OTf^-$ ( $Cp^* = \eta^5-C_5Me_5$ ; $OTf = OSO_2CF_3$ )	T: 110 °C P $H_2$ : 5.2MPa Time: 30h	-	-	-	(Schlaf <i>et al.</i> , 2001)
Rh/C+ $H_2WO_4$	T: 180 °C P $H_2$ : 80 bar Time: 48h	12	32	4	(Chaminand <i>et al.</i> , 2004)
Ru/C+Amberlyst 15	T: 393 K P $H_2$ : 4 MPa Time: 10h	1.2	33.1	-	(Kusunoki <i>et al.</i> , 2005)
Cu- $H_4SiW_{12}O_{40}/SiO_2$	T: 210 °C P vapour: 0.54MPa	32.1	83.4	-	(Huang <i>et al.</i> , 2009)
Rh-ReOx/ $SiO_2$	T: 393 K P $H_2$ : 8.0 MPa Time: 5h	13	78	10.1	(Shinmi <i>et al.</i> , 2010)
Ir-ReO <sub>x</sub> / $SiO_2$ (Re/Ir = 2)	T: 393 K P $H_2$ : 8 MPa	38	67± 3	81	(Amada <i>et al.</i> , 2011; Shinmi <i>et al.</i> , 2010)
Pt/ $WO_3/ZrO_2$	T: 443 K P $H_2$ : 8.0 MPa Time: 18h	28	86	24.2	(Kurosaka <i>et al.</i> , 2008)
Pt/ $WO_3/ZrO_2$	T: 130 °C P $H_2$ : 4.0 MPa Time: 24h	45.6	70.2	32	(Qin <i>et al.</i> , 2010)
Pt/ $WO_3/TiO_2$	T: 453 K P $H_2$ : 5.5 MPa Time: 12h	50.5	15.3	-	(Gong <i>et al.</i> , 2010)
Pt- $H_4SiW_{12}O_{40}/SiO_2$	T: 200 °C P $H_2$ : 6.0 MPa Time: 24h	38.7	81.2	-	(Zhu <i>et al.</i> , 2012)
Pt-sulfated $ZrO_2$	T:170 °C P $H_2$ : 7.3 MPa Time: 24h	-	66.5	55.6	(Oh <i>et al.</i> , 2011)
Pt-LiHSiW/ $ZrO_2$	T: 180 °C P $H_2$ : 5.0 MPa	53.6	43.5	-	(Zhu <i>et al.</i> , 2013)

Note: T: Temperature, P: Pressure



Glycolic acid is commercially produced from formaldehyde and carbon monoxide by using petrochemicals as feedstock (Koivistoinen *et al.*, 2013). However, the use of glycerol as feedstock is more sustainable than that of petrochemicals. Glycolic and glyceric acids can be produced through selective oxidation of glycerol (Zhou *et al.*, 2008). The product selectivity is strongly dependent on the catalyst structure, particularly type of metal used, particle size of the metal, and pore size of the support. In addition, reaction conditions, including pH of the medium, reaction temperature, and mole ratio of substrate to metal significantly affect the product selectivity (Bagheri *et al.*, 2015; Katryniok *et al.*, 2011; Wang *et al.*, 2015).

Pt, Pd, and Au are the most common metallic catalysts used for selective oxidation (Bagheri *et al.*, 2015). In the study of Garcia *et al.* (1995), the major product obtained from glycerol oxidation on Pd/C and Pt/C is glyceric acid, with selectivity of 70% and 55%, respectively. Carretin *et al.* (2003) studied a gold-based catalyst at low pressure (1 bar) in the absence of NaOH; the catalyst is totally inactive under this condition. When NaOH was introduced and the pressure was increased to 3 bar O<sub>2</sub>, the selectivity to glyceric acid reached as high as 100%.

Platinum metals yield high selectivity for oxidation of primary alcohol (Mallat *et al.*, 1994; Vinke *et al.*, 1992). However, these metals are easily deactivated by acid products or intermediates from the reaction mixture (Zope *et al.*, 2011). This inhibition can be addressed by incorporating other p-electron metals, such as Pb and Bi, or other support materials, including carbon, graphite, or activated carbon. Adjusting the ratio of the supporting material to the metal can alter the mean particle size of the latter. Increasing the particle size to 3.7 nm improves the selectivity to glyceric acid, whereas reducing the particle size to 2.7 nm enhances the selectivity to glycolic acid (Demirel-Gülen *et al.*, 2005; Gil *et al.*, 2014).

Although base media (e.g., NaOH) can increase the activity of a metal and reduce the formation of byproducts (Carrettin *et al.*, 2003), when glycerate sodium salt is obtained as the main product, additional processes, such as neutralization and acidification, are required to recover free glyceric acid (Wang *et al.*, 2015). Zhang *et al.* (2014) and Wang *et al.* (2015) performed selective oxidation in a base-free medium with a heterogeneous catalyst. The selectivity of glyceric acid on Pt-supported S-graphite carbon nanofibers (Pt/S-CNFs) reached 90% (Zhang *et al.*, 2015). In a study on Pt-supported mesoporous carbon nitride (Pt/MCN), increasing the nitrite content would increase the glycolic selectivity from 6.3% to 12.1% (Wang *et al.*, 2015). The reaction temperature can also influence the product selectivity. Increasing the reaction temperature from 50 °C to 70 °C can reduce the glyceric acid selectivity from 67% to 55% (Dimitratos *et al.*, 2006). Table 2.8 shows the results of catalytic oxidation of glycerol for producing glyceric and glycolic acids.

#### **2.3.4 Lactic acid**

Lactic acid is a hydroxyl acid with IUPAC name of 2-hydroxypropanoic acid. Lactic acid is a white, water-soluble solid or clear liquid, whose physical appearance is dependent on its chiral form. Table 2.9 shows the physical properties of lactic acid. Lactic acid was traditionally used as food acidulant or chemical source to produce an emulsifier. Lactic acid was also used as acidulant for leather tanning and textile industries. Currently, lactic acid exhibits wide applications in pharmaceutical and cosmetic industries. Lactic acid is also used as a platform molecule to produce polylactic acid, which is a biodegradable polymer (Datta *et al.*, 2006; Ghaffar *et al.*, 2014; Research\_and\_Markets, 2015). Given its increasing demand for pharmaceutical and personal care industries, the global market of lactic acid has grown significantly and its market price could reach USD \$3.82 billion by 2020 (Research\_and\_Markets, 2015).

**Table 2.8:** Literature data on the selectivity and yield of glyceric and glycolic acids, and glycerol conversion obtained by catalytic approach.

Catalyst	Reaction conditions	Glycerol conversion (%)	Glyceric acid		Glycolic acid		Ref.
			Y (%)	S (%)	Y (%)	S (%)	
<b><u>Glyceric acid:</u></b>							
Pd/C	T: 333K pH: 11 P: atm Time: 8 h	100	-	70 (4 h)	-	-	(Garcia <i>et al.</i> , 1995)
Au/C	T: 60 °C NaOH medium	48.3	32.3	93.1	-	-	(Carretti <i>n et al.</i> , 2003)
Pt/C	P Air: 1 bar Time: 21 h	89.0	41	100	-	-	
Au/AC	T: 60 °C NaOH medium	56	-	100	-	-	
Au/C	P O <sub>2</sub> : 3 bar Time: 21 h	54	-	100	-	-	
<b><u>Glyceric acid and glycolic acid:</u></b>							
Au/C (1% CB)	T: 60 °C NaOH medium	100	-	75	-	40	(Demirel-Gülen <i>et al.</i> , 2005)
Au/C (5% CB)	P O <sub>2</sub> : 10 bar Time: 3 h	100	-	40	-	36	
Au/C	T: 50 °C NaOH medium	90	-	81.2	-	17.0	(Dimitratos <i>et al.</i> , 2006)
Pd/C	P O <sub>2</sub> : 3 atm	90	-	79.4	-	5.6	
Pt	T: 60 °C NaOH medium	40	-	62	-	22	(Rodrigues <i>et al.</i> , 2013)
Pt/C	P O <sub>2</sub> : 3 bar Time: 3 h	81	-	67	-	19	
Au/C		61	-	44	-	18	
Pt/C-Au/C		98	-	47	-	20	
Pt/S-CNFs	T: 60 °C P O <sub>2</sub> : 0.4 MPa Time: 6 h	89.9	-	83.2	-	8.9	(Zhang <i>et al.</i> , 2015)
Au/PUF (295 nm)	T: 333 K NaOH medium	30	-	12	-	76	(Gil <i>et al.</i> , 2014)
Au/PUF (236 nm)		30	-	18	-	74	
Au/PUF (111 nm)		30	-	42	-	50	
Au/PUF (138 nm)	P O <sub>2</sub> : 5 bar Time: 1 h	30	-	38	-	55	
Pt/MCN	T: 60 °C P O <sub>2</sub> : 0.3 MPa Time: 4 h	88.5	-	35.9	-	12.1	(Wang <i>et al.</i> , 2015)
N amount: 3.3 g N amount: 2.7 g		63.1	-	58.5	-	6.3	

Note: T: Temperature, P: Pressure, atm: atmospheric, Y: Yield, S: Selectivity

**Table 2.9:** Physical properties of lactic acid (Sigma\_Aldrich).

Physical properties	Lactic acid
Chemical formula	$C_3H_6O_3$
Molar mass	90.08 $gmol^{-1}$
Melting point	L: 53 °C D: 53 °C D/L: 16.8 °C
Boiling Point	122 °C

Lactic acid is commercially manufactured through carbohydrate fermentation (Datta *et al.*, 2006). However, this method presents disadvantages, such as poor productivity, time-consuming process, and complicated purification (Castillo Martinez *et al.*, 2013; Purushothaman *et al.*, 2014). An alternative chemoselective method is therefore applied to convert biomass, such as sugar or cellulose, into lactic acid (Clippel *et al.*, 2012; Dusselier *et al.*, 2013; Holm *et al.*, 2010). This chemical process employs glycerol as substitute feedstock. The chemical conversion of lactic acid from glycerol has been investigated through different pathways, including selective oxidation, hydrogenolysis, and hydrothermal processes.

Kishida *et al.* (2005) efficiently produced lactic acid through hydrothermal conversion of glycerol with NaOH at 300 °C. Shen *et al.* (2009) studied the effects of alkali metal hydroxides and earth metal hydroxides on the hydrothermal reaction. Alkali metal hydroxides, such as KOH, NaOH, and LiOH, exerted better effects on the catalysis of hydrothermal reactions than alkaline-earth metal hydroxides. The use of KOH or NaOH as alkaline catalyst elicited a high yield of 90% at 573 K (Shen *et al.*, 2009). However, the process requires severe reaction conditions, such as high

temperature, pressure, and alkalinity; hence, a specific reactor must be developed for upscale production to avoid high corrosiveness and other relevant issues (Arcanjo *et al.*, 2016).

Chemical conversion of lactic acid from glycerol with heterogeneous catalysts has been explored through oxidation and reduction. Maris *et al.* (2007) investigated the hydrogenolysis of glycerol over carbon-supported Pt and Ru catalysts in the presence of promoters such as NaOH and CaO. These promoters increased the glycerol hydrogenolysis rate but were difficult to separate from the reaction medium (Maris *et al.*, 2007). Feng *et al.* (2014) improved the process by preparing few types of basic-oxide supported Ru catalysts (Ru/CeO<sub>2</sub>, Ru/MgO, and Ru/La<sub>2</sub>O<sub>3</sub>), which contain both metal and base sites. However, in the improved process, the lactic acid selectivity was relatively low and the reduction process favored the production of 1,2-propanediol (Feng *et al.*, 2014).

Considering the low product yield and selectivity in hydrogenolysis, researchers have focused on selective oxidation, which is performed over bimetallic Au-Pt catalysts incorporated with various supportors, such as TiO<sub>2</sub> and CeO<sub>2</sub>, in alkaline aqueous solution; this process exhibited high lactic acid selectivity (Kumar *et al.*, 2008; Lakshmanan *et al.*, 2013; Purushothaman *et al.*, 2014). Arcanjo *et al.* (2016) and Zhang *et al.* (2016) investigated Pt- and Pd-supported over activated carbon catalysts in alkaline media. The product selectivity on Pt and Pd was lower than that on Au-based catalysts (Arcanjo *et al.*, 2016; Zhang *et al.*, 2016). Table 2.10 presents the yield and selectivity of lactic acid produced through hydrothermal process, hydrogenolysis, and selective oxidation of glycerol.

**Table 2.10:** Literature data on the selectivity and yield of lactic acid, and glycerol conversion obtained by catalytic approach.

Catalyst	Reaction conditions	Glycerol conversion (%)	Lactic acid		Ref.
			Y (%)	S (%)	
Pt/C (NaOH)	T: 473 K P H <sub>2</sub> : 40 bar Time: 5 h	20 92 (5 h)	-	0.62 0.48	(Maris <i>et al.</i> , 2007)
Ru/C (NaOH)		20 100 (5 h)	-	0.47 0.34	
Pt/C (CaO)		30 100 (5 h)	-	0.58 0.58	
Ru/C (CaO)		20 85 (5 h)	-	0.54 0.48	
Alkaline metal-hydroxide	T: 300 °C Time: 1.5 h				(Shen <i>et al.</i> , 2009)
KOH		> 90	90.0	-	
NaOH		> 90	87.1	-	
LiOH		> 90	81.2	-	
Au-Pt/TiO <sub>2</sub>	T: 363 K P: atm NaOH medium	30	-	85.6	(Shen <i>et al.</i> , 2010)
Ir-based catalyst	T: 160 °C P N <sub>2</sub> : atm Time: 15 h KOH medium	34.8	-	> 95	(Sharninghausen <i>et al.</i> , 2014)
Au-Pt/nCeO <sub>2</sub>	T: 373 K P O <sub>2</sub> : 5 bar Time: 30 min NaOH medium	99	-	80	(Purushothaman <i>et al.</i> , 2014)
Au/CeO <sub>2</sub>	T: 90 °C P O <sub>2</sub> : atm NaOH medium	98	-	83	(Lakshmanan <i>et al.</i> , 2013)
Ru/La <sub>2</sub> O <sub>3</sub>	T: 180 °C P H <sub>2</sub> : 5 MPa	31.5	-	8.5	(Feng <i>et al.</i> , 2014)
Ru/MgO	Time: 10 h	60.4	-	21.3	
Ru/CeO <sub>2</sub>		85.2	-	3.1	
Pt/C	T: 90 °C P O <sub>2</sub> : atm Time: 6 h LiOH medium	100	-	69.3	(Zhang <i>et al.</i> , 2016)
Pd/C	T: 230 °C P O <sub>2</sub> : atm	99	-	68	(Arcanjo <i>et al.</i> , 2016)
Pt/C	Time: 3 h NaOH medium	99	-	74	

Note: T: Temperature, P: Pressure, atm: atmospheric, Y: Yield, S: Selectivity

### 2.3.5 Shortcomings of existing conversion methods

Existing chemical and biological methods for glycerol conversion exhibit several limitations. In hydrogenolysis of 1,3-propanediol from glycerol, the reaction should be performed in polar aprotic solvents, such as sulfolane, 1-methyl-pyrrolidinone, and 1,3-dimethyl-2-imidazolidinone (Ania *et al.*, 2007; Chaminand *et al.*, 2004; Che, 1985; Drent *et al.*, 1998; Schlaf *et al.*, 2001). However, organic solvents negatively affect the environment. Furthermore, in selective oxidation, reactions are usually conducted under high-temperature and -pressure conditions; thus, the cost of production is high because of high energy usage. Hazardous risks also increase because several explosions may occur from over-pressurization of the reactor or sudden increase in temperature during the reaction (Dasari *et al.*, 2005; Kusunoki *et al.*, 2005; Neher *et al.*, 1995; Ott *et al.*, 2006). A strong alkaline medium may also cause severe corrosion of the reactor (Arcanjo *et al.*, 2016).

Biological conversion employs expensive equipment and complicated cultivation procedures. Various byproducts, such as butyrate, ethanol, acetate, and lactate, are produced during fermentation for production of 1,2-PDO and 1,3-PDO. These byproducts can inhibit the process and reduce the yield of 1,2-PDO and 1,3-PDO (Clomburg *et al.*, 2011; Kivistö *et al.*, 2012). According to Zeng *et al.* (2002), glycerol can act as a substrate inhibitor for fermentation and bacteria cannot function at glycerol concentrations above 17%.

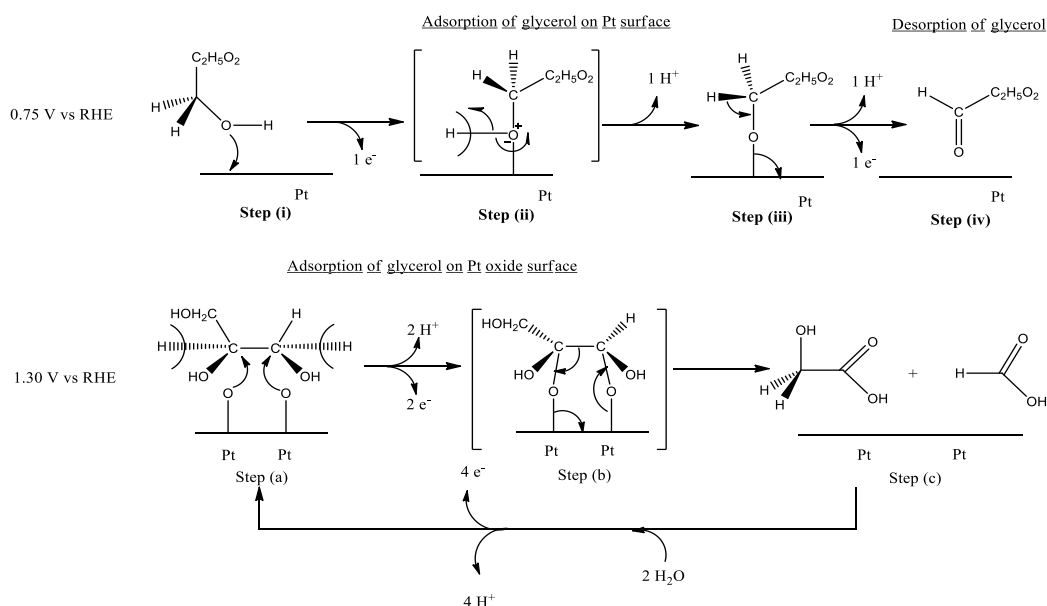
To overcome the shortcomings of existing methods, researchers aim to develop alternative techniques for glycerol conversion. Electrochemical methods are a feasible technique used to convert glycerol into various added-value compounds.

## 2.4 Electrochemical conversion of glycerol

Electrochemical conversion of glycerol has been widely studied because of its simplicity and robustness in terms of structure and operation. This method uses electrons, instead of chemical reagents, and is therefore considered environment friendly. Electrolysis is driven at ambient pressure and temperature and consumes less energy compared with chemical methods. In addition, electricity used in the system can be replaced by renewable resources, such as solar energy (Okada, 2013; Simões *et al.*, 2012).

Roquet *et al.* (1994) studied the electro-oxidation behavior of glycerol on platinum electrodes. The selectivity toward the production of oxidized chemicals, such as glyceraldehyde, glycolic acid, oxalic acid, and formic acid, significantly depends on the applied potential and pH of the reaction medium. Generally, electrochemical conversion of glycerol involves the following steps: adsorption of OH species from glycerol on the electrode surface [Step (i)], electronic charge transfer [Step (ii)], interaction between oxygenated species on the electrode surface with the glycerol molecule [Step (iii)], and breaking of inter-atomic bonds and desorption of the reaction product [Step (iv)] (Roquet *et al.*, 1994). As shown in Scheme 2.3, at 0.75 V versus RHE at pH 1.0, the adsorbed OH of glycerol would interact with Pt; as such, glycerol is oxidized into glyceraldehyde (product yield of 96%). At 1.30 V versus RHE, glycerol interacts with oxides formed on the surface of Pt (Pt-O) [step (a)], causing C-C bond cleavage [step (b)] and formation of glycolic and formic acids (product yield of 51%) [step (c)].





**Scheme 2.3:** Glycerol electro-oxidation pathway in acidic medium (Roquet *et al.*, 1994).

### 2.4.1 Electrocatalytic behavior study

In previous studies on alcohol electro-oxidation, monometallic Pt, Pd, and Au were proposed as excellent electrode materials. Pt is considered the only material that can initiate oxidation in acidic media. Conversely, Pd and Au perform more stable in alkaline media (Bełtowska-Brzezinska *et al.*, 1997; Kim *et al.*, 2008a). In the electrochemical behavior study of Simões *et al.* (2010), the polarization curves of Pt/C, Pd/C, and Au/C were recorded through in situ FTIR analysis in 0.1 M glycerol with 1.0 M NaOH. Results indicated that oxidation for Pt/C started at 0.35 V, and that for Pd/C and Au/C shifted to higher potential at 0.5 V. In situ FTIR spectra reflected that Pt/C and Pd/C oxidized glycerol into dihydroxyacetone. However, Au/C converted glycerol into glyceric acid, which was further oxidized into glycolic acid and formic acid. Kwon *et al.* (2011) reported the production of reaction intermediates such as glyceraldehyde and dihydroxyacetone (Fordham *et al.*) over Pt in 0.1 M glycerol and 0.1 M NaOH. Glyceric acid was the main product on Au in the alkaline medium and was further oxidized into glycolic acid and formic acid. In other studies, the oxidant MnO<sub>2</sub> was added to the glycerol solution in alkaline media. Chronoamperometry experiment was

performed on the Pt anode electrode, and central composite design (CCD) was applied in the study. These reactions led to the formation of glyceraldehyde, glyceric acid, glycolic acid, and tartronic acid (Prieto *et al.*, 2013a, 2013b; Prieto *et al.*, 2014). The effects of pH and glycerol concentration on electro-oxidation have also been investigated. Gomes and Martins *et al.* (2013) found that electro-oxidation of glycerol on Pt in acidic media is strongly influenced by glycerol concentration. At high glycerol concentrations, the electrode surface was covered by glycerol residues, which affect the formation of oxides on the Pt surface and delay oxidation. Similarly, the support actively participated in the electro-oxidation reaction over Au supported on glassy carbon in 0.1 M glycerol at different pH values (Gomes and Gasparotto *et al.*, 2013).

The catalytic activity of electrodes can be improved by modifying their surface or alloying them with foreign metals (Kokoh *et al.*, 1993; Rousseau *et al.*, 2006). In a previous study, carbon-supported PdPt and PdAu alloys were prepared by substituting 50% of Pt and Au with a cheaper electrode material, namely, Pd. CV scan for Pd<sub>0.5</sub>Au<sub>0.5</sub>/C was performed in 0.1 M glycerol with 1.0 M NaOH. The polarization curve indicated that both alloy catalysts displayed higher activity than the monometallic catalysts (Simões *et al.*, 2010). Addition of co-catalysts, such as Ni and Bi, to the electrode catalyst could also improve glycerol electro-oxidation (Bianchini *et al.*, 2009; Kadirgan *et al.*, 1982, 1983; Kumar *et al.*, 2008; Singh *et al.*, 2009). Kwon *et al.* (2014) performed electro-oxidation of glycerol into DHA by modifying Pt/C with Bi and conducted CV scanning in 0.1 M glycerol with 0.5 M H<sub>2</sub>SO<sub>4</sub>; results indicated 100% selectivity to DHA. In a similar study conducted by Simões *et al.*, low amount of Bi was deposited on the surface of Pt/C and Pd/C. This modification enhanced the glycerol electro-oxidation activity by adjusting the ratio of Pt, Pd, and Bi; hence, Pd<sub>0.45</sub>Pt<sub>0.45</sub>Bi<sub>0.1</sub>/C successfully replaced the expensive Pt into half and performed better than that of the Pd/C or Pt/C electrode (Simões *et al.*, 2011). Zalineeva *et al.* (2014) also

synthesized a self-supported Pd<sub>4</sub>Bi catalyst, which features high surface area (75–100 m<sup>2</sup>g<sup>-1</sup>) and a porous nanostructure; the fabricated electrode acts as a catalyst (or a nanoreactor). The confinement of intermediates and reactants inside the pores confer the unique behavior of Pd<sub>4</sub>Bi in terms of selectivity for glycerol electro-oxidation. Holade *et al.* (2013) investigated glycerol electro-oxidation on PtNi and PtAg supported on carbon in alkaline media. Glycolate and glycerate ions were the major oxidized compounds. The reaction kinetics improved by combining less expensive non-noble metals (Ni and Ag) with Pt. Furthermore, Kwon *et al.* (2014) continued working on modification of the Pt/C electrode by reversible/irreversible addition of adatoms, including Sb, Pb, Sn, and In. The modified electrode can enhance the oxidation peak current density, thereby oxidizing glycerol into DHA with 100% selectivity at low onset potentials. Overall, the electro-oxidation activity is strongly dependent on catalytic materials used for the electrode; hence, modification of the electrode can generally improve the glycerol electro-oxidation activity.

#### 2.4.2 Electrochemical fuel cell

The feasibility of cogenerating energy and valuable chemicals through electro-oxidation of glycerol in fuel cells has been widely studied. Simões *et al.* (2010, 2012) were the first to discuss the electrochemical oxidation of glycerol for cogenerating energy with other added-value chemicals. Similarly, Zhu *et al.* (2012) used Pt/C as anode catalyst and Fe-Cu-N<sub>4</sub>/C as cathode catalyst; results indicated that glycerol electro-oxidation demonstrated very high selectivity toward glyceric and tartronic acids. In the same year, Zhang *et al.* (2012b) used Au/C as anode catalyst and Fe-based catalyst as cathode in the anion-exchange membrane fuel cells; Au/C favored oxidation and produced chemicals such as tartronic acid, mesoxalic acid, and oxalic acid. In the continuation of their study, the anode potential was fine-tuned from 0.35 V to 0.65 V. The tests indicated that the selectivity shifted from tartronate to mexolate ions (Zhang *et*

*al.*, 2014). Paula *et al.* (2014) studied the electrochemical reformation of glycerol in alkaline-doped polybenzimidazole (PBI) proton-exchange membrane (PEM) fuel cell for hydrogen production with PtRu/C as anode catalyst and Pt/C as cathode catalyst. At high current density ( $0.80 \text{ Acm}^{-2}$ ) and intermediate temperature ( $60 \text{ }^\circ\text{C}$ ), the reaction achieved the optimal hydrogen production and tartronate ion was the most abundant oxidized chemical obtained. In the study by Qi *et al.* (2014a), the electrocatalytic reaction of glycerol was performed in an anion exchange membrane fuel cell with Au/C as anode catalyst exhibiting for cogenerating electricity. The anode potential was tuned below  $0.45 \text{ V}$  to induce selective oxidation to tartronate ion.

Current research directions mainly focus on electro-oxidation of glycerol either in the electrochemical behavior study or fuel cell study. However, relevant information about electrochemical conversion of glycerol in the cathodic and anodic regions remains limited. Bulk electrosynthesis under galvanostatic condition is an alternative scheme used to convert glycerol into a wide range of added-value compounds, including oxidation and reduction compounds (Kongjao *et al.*, 2011).

#### **2.4.3 Electrochemical study in galvanostatic mode**

A group of researchers from Thailand, Kongjao *et al.*, (2011), started to work on bulk electrochemical conversion of glycerol in a one-pot electrochemical cell in galvanostatic mode. This study is a novel attempt to investigate glycerol reformation in the anode and cathode regions. In their first published work in 2011, electrochemical conversion of glycerol was performed in  $\text{H}_2\text{SO}_4$  solution with Pt as cathode and anode electrode. A list of chemicals, including propanediol, glycidol, and 2-propenol, exhibited potential for converting glycerol into a wide variety of added-value compounds.

The effects of initial solution pH (1, 7, and 11) on glycerol conversion and product distribution have been investigated by Hunsom *et al.*, 2013. The highest glycerol conversion rate was obtained at pH 1 ( $2.95 \times 10^{-3} \text{ min}^{-1}$ ), followed by pH 11 ( $7.95 \times 10^{-4} \text{ min}^{-1}$ ) and pH 7 ( $9.20 \times 10^{-4} \text{ min}^{-1}$ ). Under strong acidic conditions, a broad range of chemicals, including glycidol, acetol, 1,2-propanediol, 1,3-propanediol, and ethylene glycol, with product yields of 24.0, 13.4, 32.2, 3.8, and 12.0 mole C%, respectively, were obtained after 19 h of electrolysis.

Operation variables, such as cathode materials [platinum (Pt), titanium-coated ruthenium oxide (Ti/RuO<sub>2</sub>), and stainless steel (SS)] and current density, significantly affect glycerol conversion and product distribution. Pt showed 100% glycerol conversion after 17 h of the reaction, and Ti/RuO<sub>2</sub> and SS converted 42.5% and 22.5% glycerol, respectively. Glycidol is the major compound obtained after 24 h of the reaction, with corresponding yields of 48% and 14% over Pt and Ti/RuO<sub>2</sub> cathode electrodes, respectively. Other chemicals such as acrolein, acetol, 1,3-propanediol, and 1,2-propanediol were produced as minor compounds. Glycerol conversion was promoted at high applied current density, but very high current density did not facilitate the formation of added-value compounds (Hunsom *et al.*, 2015). Table 2.11 summarizes the yield and selectivity for glyceric and glycolic acids reported in electrochemistry studies.

Product selectivity and yield are key challenges in electrosynthesis. Selectivity strongly depends on the reaction medium and electrode material used. Previous electrochemical studies were mostly based on direct conversion without using a mediator. In the presence of a redox catalyst, the kinetic inhibition of electron transfer between the electrode and electrolyte can be eliminated, thereby increasing the number of products with different selectivities. Saila *et al.* (2015) added oxidants [hydrogen

peroxide (H<sub>2</sub>O<sub>2</sub>), sodium persulfate (Na<sub>2</sub>S<sub>2</sub>O<sub>8</sub>), and TEMPO] into an electrochemical medium. The presence of different oxidizing agents influenced the reaction mechanism, generating different added-value compounds. However, these homogeneous catalysts are relatively expensive, and a complicated distillation process is usually involved during the recovery process (Farnetti *et al.*, 2009; Thornton *et al.*, 2002).

**Table 2.11:** Literature data on the selectivity and yield of glycolic and glyceric acids, and glycerol conversion obtained by electrochemical approach.

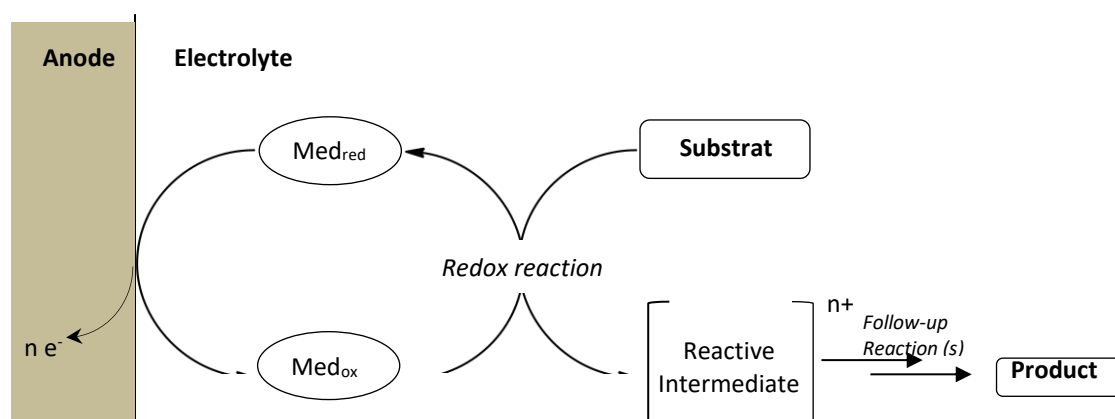
Electrode		Reaction Medium	Electrochemical study	Glycerol Conversion (%)	Glycolic acid		Glyceric acid		Ref
A (WE)	C (CE)				Y (%)	S (%)	Y (%)	S (%)	
Pt	Pt	H <sub>2</sub> SO <sub>4</sub>	Bulk Electrosynthesis	100 (14 h)	21 (24 h)	-	-	-	(Saila <i>et al.</i> , 2015)
		<u>Additional:</u> H <sub>2</sub> O <sub>2</sub>							
		Na <sub>2</sub> S <sub>2</sub> O <sub>8</sub>		100 (14 h)	5 (24 h)	-	-	-	
		TEMPO		100 (14 h)	14 (24 h)	-	-	-	
FeCO@Fe@Pd/MW-CNT-COOH **	Pt	KOH	Fuel cell	-	7 (4.6 h)	-	3 (4.6 h)	-	(Fashemi <i>et al.</i> , 2015)
Pt/MWCNT-COOH **	Pt	KOH	Fuel cell	-	14 (4.6 h)	-	14 (4.6 h)	-	(Fashemi <i>et al.</i> , 2015)
Pt	Pt	H <sub>2</sub> SO <sub>4</sub>	Bulk Electrosynthesis	100 (24 h)	-	-	-	-	(Hunsom <i>et al.</i> , 2015)
Ni/C	C	NaOH	Chronoamperometry	32.2 (4 h)	-	11.5 (4 h)	-	-	(Oliveira <i>et al.</i> , 2014)
FeCoNi/C	C	NaOH	Chronoamperometry	34.1 (4 h)	-	10.3 (4 h)	-	-	
Pt	Pt	MnO <sub>2</sub>	Chronoamperometry	100 (14 h)	4 (14 h)	-	11 (14 h)	-	(Prieto <i>et al.</i> , 2014)
PtRu/C	Pt/C	KOH	Fuel cell	-	9	-	30	-	(Paula <i>et al.</i> , 2014)
Pt	Pt	NaOH	Chronoamperometry	59 (14 h)	-	-	-	62 (14 h)	(Prieto <i>et al.</i> , 2013b)
Pd <sub>80</sub> Ni <sub>20</sub> /C	C	NaOH	Chronoamperometry	31.3 (4 h)	√	-	√	-	(Holade <i>et al.</i> , 2013)
Pt/C	Pt	KOH	Fuel cell	4.7 (2 h)	-	-	-	41 (2 h)	(Zhu <i>et al.</i> , 2012)
Au/C	Pt	KOH	Fuel cell	-	-	-	-	26 (2 h)	(Zhang <i>et al.</i> , 2012b)

Note:

A: Anode; C: Cathode; WE: working electrode; CE: counter electrode

## 2.5 Redox catalyst in organic electrosynthesis

Organic electrosynthesis is an environment-friendly method used to oxidize or reduce organic compounds; in this process, hazardous chemical reagents are substituted by electric current and the overall energy consumption is reduced (Frontana-Uribe *et al.*, 2010; Schäfer Hans *et al.*, 2007). During electrosynthesis, direct electrolysis occurs, in which electrons transfer on the electrode surface. However, the heterogeneous electron transfer between the electrode and substrate can be a kinetic inhibitor for this process. As such, the redox catalyst/mediator can be added into electro-organic synthesis to achieve indirect electrolysis, in which the redox catalyst initiates a pair of reversible redox reactions at the electrode, followed by catalytic chemical reaction between the substrate and redox catalyst (Francke *et al.*, 2014). The basic principle of indirect electrolysis is shown in Scheme 2.4. Therefore, the redox catalyst can prevent over-oxidation or over-reduction of the substrate. In addition, electrode passivation commonly caused by direct electrolysis can be avoided (Francke *et al.*, 2014).



**Scheme 2.4:** General principle of redox catalyst (Francke *et al.*, 2014).

A redox catalyst is a key component that effectively influences indirect electrosynthesis; hence, appropriate selection of a redox catalyst is essential. Generally, the redox potential of an effective redox catalyst must be lower than the potential of the

substrate being oxidized or higher than the reduction potential (Contentin *et al.*, 2012; Steckhan, 1986). The redox catalyst should also be inert to all processes apart from the electron transfer at the electrode. Moreover, the oxidized and reduced forms of the catalyst must be highly soluble in the electrolyte to ensure a homogeneous system (Francke *et al.*, 2014). However, homogeneous catalysts are difficult to recover from the reaction medium. The usual recovery method involves precipitation with continuous recovery processes, such as distillation of the reaction mixture, in which high energy is employed (Farnetti *et al.*, 2009). For example, TEMPO is the most frequently studied redox catalyst for alcohol oxidation (Semmelhack *et al.*, 1983). TEMPO is used for oxidation, and the expensive azeotropic distillation can be applied for recovery; separation is favorably achieved by selective adsorption onto hydrophobic resins, such as hydrophobized silica gel or amberlite (Thornton *et al.*, 2002). Furthermore, homogeneous catalysts are relatively more expensive than heterogeneous catalysts (Farnetti *et al.*, 2009). Thus, a cheap heterogeneous catalyst must be developed to overcome the complicated recovery process. The solid acid catalyst Amberlyst-15 can be used as redox catalyst and acidic medium for electrochemical conversion of glycerol.

### 2.5.1 Amberlyst-15

Amberlyst-15 is a macro-reticular polystyrene compound containing cation exchange resin and strong sulfonic acid group. The molecular structure of Amberlyst-15 is shown in Figure 2.1, and its physical properties are summarized in Table 2.12. With its mild and highly selective properties, Amberlyst-15 is widely used as a heterogeneous catalyst in various chemical organic reactions, such as acylation, alkylation, halogenation, esterification, and transesterification (Frija *et al.*, 2012; Pal *et al.*, 2012). The macro-reticular pore structure of Amberlyst-15 allows liquid or gaseous reactants to penetrate the pores, thereby permitting them to react with hydrogen ions located throughout the beads. In traditional organic synthesis, mineral acids, such as hydrofluoric acid, sulfuric



acid, and paratoluenesulfonic acid, were used as catalysts. However, these homogeneous acids are corrosive, toxic, and difficult to remove at the end of the reaction (Zhou *et al.*, 2012). These limitations can be overcome by using the heterogeneous acid Amberlyst-15. This catalyst is safe to use because of its environmentally benign characteristic. Furthermore, Amberlyst-15 can be readily removed from the reaction medium and can be regenerated or reused several times (Pal *et al.*, 2012).

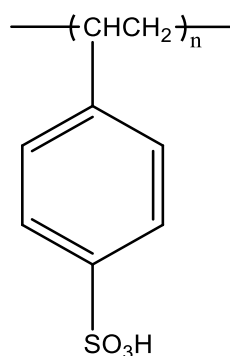


**Figure 2.1:** Chemical structure of Amberlyst-15 (Pal *et al.*, 2012).

**Table 2.12:** Physical properties of Amberlyst-15 (Pal *et al.*, 2012).

	Physical properties
Ionic form as shipped	Hydrogen
Colour	Brown-grey
Concentration of active sites	$\geq 1.7$ eq/L; $\geq 4.7$ eq/kg
Moisture holding capacity	52 to 57 % (H <sup>+</sup> form)
Shipping weight	770 g/L
Particle size	0.600 to 0.850 mm
Average pore diameter	300 Å
Total pore volume	0.40 mL/g
Maximum operating temperature	120 °C

### 2.5.2 Amberlyst-15 as a solid acid catalyst in glycerol conversion

Amberlyst-15 has been extensively studied for chemical catalytic conversion of glycerol. Amberlyst-15 is an effective heterogeneous catalyst for glycerol hydrogenolysis, dehydration, esterification, and etherification. Kusunoki *et al.* (2005) reported that glycerol can be hydrogenolyzed into 1,2-propanediol under a mild reaction condition (393 K and 4 MPa H<sub>2</sub>) over metal catalyst (Ru) supported on activated carbon in the presence of Amberlyst-15, compared with other metal-acid bifunctional catalysts, such as tungstic acid (H<sub>2</sub>WO<sub>4</sub>) and liquid acid (H<sub>2</sub>SO<sub>4</sub>). Ru/C + Amberlyst showed higher activity in glycerol hydrogenolysis than Ru/C + H<sub>2</sub>SO<sub>4</sub>, indicating that the solid acid catalyst was more effective for the reaction (Kusunoki *et al.*, 2005).

Amberlyst-15 is also broadly used in glycerol esterification study. Rezayat *et al.* (2009) conducted continuous esterification of glycerol with acetic acid and supercritical carbon dioxide in the presence of Amberlyst-15. Up to 100% selectivity for triacetin was achieved after 2 h of reaction under the following conditions: 24 molar ratio of acetic acid to glycerol, 200 bar pressure, and 110 °C reaction temperature. Considering that high molar ratio of acetic acid to glycerol is inapplicable to industrial processes because of difficulty in separation, Zhou *et al.* (2012) attempted to investigate the influence of molar ratio of acetic acid to glycerol and the reaction temperature on the product distribution of glycerol esterification over Amberlyst-15. The optimum yield was achieved at acetic acid to glycerol molar ratio of 9:1 and temperature of 110 °C after 2 h of reaction, with glycerol conversion of 97% and total yield of diacetin and triacetin of 90% (Zhou *et al.*, 2012).

Glycerol etherification with tert-butyl alcohol can be performed over Amberlyst-15. Few studies investigated the effects of the concentration and type of catalyst. Frusteri *et al.* (2009) reported that glycerol ether formation increased with increasing catalyst

dosage. Klepáčová *et al.* and Pico *et al.* studied the performance of different types of Amberlyst on product distribution and glycerol conversion during etherification. In both studies, Amberlyst-15 showed the optimal performance relative to its high acidity and improved textural properties with high apparent surface area ( $44 \text{ m}^2\text{g}^{-1}$ ) and pore volume ( $0.34 \text{ cm}^3\text{g}^{-1}$ ). Pico *et al.* also characterized the catalyst before and after the reaction. The results indicated that Amberlyst-15 can be reused, and this catalyst only exhibited slight decrease in acidity and textural properties (Klepáčová *et al.*, 2005; Pico *et al.*, 2013).

Amberlyst-15 has been comprehensively studied in catalytic glycerol conversion. With its acidity and porous structure properties, Amberlyst-15 can serve as redox catalyst in electrochemical conversion of glycerol. Once a redox catalyst has been initially assessed, other parameters that can significantly influence the product selectivity and yield must also be determined; these parameters include type of supporting electrolytes and working electrodes.

## **2.6 Activated carbon electrode**

Activated carbon with high specific surface area ( $1000 \text{ m}^2/\text{g}$ ) can be produced from readily available biomass precursors, such as coal, coke, saw dust, peat, wood char, seed hulls, and palm kernel shell (Elmouwahidi *et al.*, 2012; Foo *et al.*, 2011, 2013; He *et al.*, 2013; Kalderis *et al.*, 2008; Lee *et al.*, 2013; Omar *et al.*, 2003). The pore structure and pore size distribution of activated carbon are highly dependent on the nature of feedstock (Gergova *et al.*, 1994). Pore size can be categorized into three major groups: micropore ( $< 2 \text{ nm}$ ), mesopore ( $2\text{--}50 \text{ nm}$ ), and macropore ( $> 50 \text{ nm}$ ) (Everett, 1972). For example, coconut-shell-based activated carbon consists of pores less than  $1 \text{ nm}$ , and wood-based activated carbon contains macropores and mesopores (McDougall, 1991). Characteristics, such as pore volume of activated carbon, can be varied by adjusting the

activation period and processes, including chemical activation or physical activation (Daud *et al.*, 2004). The activated carbon is produced in a two-stage process, comprising carbonization and activation. Carbonization occurs at low temperatures (400 °C to 850 °C) in the absence of oxygen. Physical activation is performed with steam or carbon dioxide, whereas chemical activation is conducted with zinc chloride and phosphoric acid (Rodríguez–Reinoso *et al.*, 1992).

Activated carbon is widely used as an electrode for electro-oxidation of glycerol, electroreduction of oxygen, electrochemical fuel cell, and electro-sorption in wastewater treatment (Bambagioni *et al.*, 2009; Card *et al.*, 1990; Kwon *et al.*, 2012; Qu, 2007; Xu *et al.*, 2000; Zou *et al.*, 2008). However, most studies reported that activated carbon cannot perform alone as electrode and should be functionalized with polymer (Murayama *et al.*, 2011; Qu, 2007) or used as supporter to incorporate with noble metals, such as Pt, Pd, Rh, and Au (Bambagioni *et al.*, 2009; Linares *et al.*, 2014). Sharma and Pollet (2012) reported that a good support for an electrocatalyst should feature the following characteristics: large surface area, mesoporous structure, corrosion resistance, high electrical conductivity, easy recovery, and good catalyst–support interaction (Sharma *et al.*, 2012).

Electrochemical performance can be enhanced using a mesoporous carbon composite supporter. The large surface area and pore size of the carbon supporter can improve ion transportation and electrolyte accessibility (Tang *et al.*, 2013). The porous structure can hold or trap the reaction intermediate, thereby controlling the product selectivity (Qi *et al.*, 2014b; Zhang *et al.*, 2014). The diffusion limit of substrates increases with decreasing pore size (McMorn *et al.*, 1999). Hence, mesoporous and macroporous structures provide high contribution to substrate diffusion in electrochemical study. In addition, the carbon material can improve the electrochemical stability. The chemically

inert surface of carbon renders the electrocatalyst as susceptible to deactivation and aggregation during electrolysis (Bo *et al.*, 2013; Tang *et al.*, 2013).

The price of the electrode material must be inexpensive to compete effectively with existing electrocatalysts. Ajeel *et al.* (2015) introduced the ACC electrode for the first time to study phenol degradation. The electrode was prepared by mixing 20% carbon black nanopowder with 80% activated carbon powder. The electrolysis process achieved removal efficiency for 2-chlorophenol as high as 82.5% (Ajeel *et al.*, 2015a). Carbon black nanopowder was added during the preparation to increase the conductivity of the electrode (Ajeel *et al.*, 2015c). The ACC electrode is relatively cheaper than noble metal catalysts (Pt, Pd, Rh, and Au), and the price of each material per gram is displayed in Table 2.13 (Sigma\_Aldrich). Activated carbon is a cheap and green material that possesses high surface area and porous structure; hence, this compound can effectively function as supporter or electrode alone in electrochemistry studies.

**Table 2.13:** List of the common noble metals used for catalyst preparation with their current price and CAS reference number, compare with commercial activated carbon (Sigma\_Aldrich).

Type of material	CAS Number	% Purity	Price (USD \$/g)
Platinum*	7440-06-4	99	2015.00
Palladium*	7440-05-3	99	1260.00
Rhodium*	7440-16-6	99	506.00
Gold*	7440-57-5	99	347.00
Activated carbon**	7440-44-0	99	0.11

\*In the form of nanopowder

\*\*In the form of powder

## 2.7 Diamond electrode

Diamond exhibits special properties, such as high thermal conductivity ( $2600 \text{ W m}^{-1} \text{ K}^{-1}$ ), high hardness ( $1 \times 10^4 \text{ kg mm}^{-2}$ ), and high charge carrier mobility (electron mobility:  $2200 \text{ cm}^2 \text{ V}^{-1} \text{ s}^{-1}$ , hole mobility:  $1600 \text{ cm}^2 \text{ V}^{-1} \text{ s}^{-1}$ ). Diamond is an excellent

electrical insulator because of its large bandgap (5.5 eV). Hence, diamond cannot be used as an electrode material alone. However, diamond can be conductive by doping it with certain elements. Boron is the most commonly studied dopant for diamond. The doped diamond electrode can act as a semimetal at high doping levels and as an extrinsic semiconductor at low doping levels (Kraft, 2007).

Kraft (2007) investigated the electrochemical behavior of doped diamond electrode in 0.2 M H<sub>2</sub>SO<sub>4</sub> by using cyclic voltammetry (CV). The doped diamond electrode was compared with platinum electrode in the region between oxygen and hydrogen evolution. From the CV curves in Figure 2.2, the doped diamond electrode shows wide potential window and high oxygen and hydrogen evolution overpotential (Kraft, 2007). This striking feature distinguishes the doped diamond electrode from common electrode materials, such as Pt, Au, or mixed metal electrodes (Alfaro *et al.*, 2006; Panizza *et al.*, 2005). The high oxygen evolution overpotential can also increase the production of anodic OH radicals in aqueous solutions. The OH radicals are used for electrochemical study in wastewater treatment (Farrell *et al.*, 2005; Honda *et al.*, 2005; Marselli *et al.*, 2003).

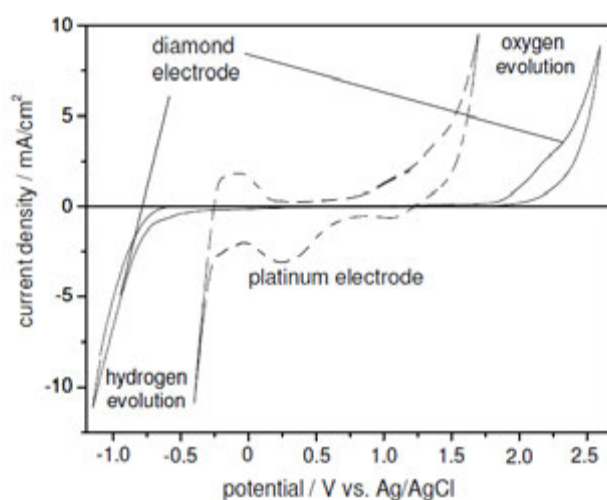


**Figure 2.2.** Cyclic voltammograms of platinum and diamond electrode in 0.2 M H<sub>2</sub>SO<sub>4</sub>,  $v = 0.1 \text{ Vs}^{-1}$  (Kraft, 2007).

The doped diamond electrode demonstrates high electrochemical stability under severe conditions (Alfaro *et al.*, 2006; Panizza *et al.*, 2005). Panizza *et al.* (2003) did not find any loss of diamond material during electrolysis in 1 M H<sub>2</sub>SO<sub>4</sub> with current density of 1 A/cm<sup>2</sup> at 40 °C. This finding can be a major advantage of the doped diamond electrode over other conventional electrode materials.

Diamond electrode is chemically, mechanically, and thermally more stable than most of the existing electrodes and thus provides great benefits to electro-organic synthesis. Diamond electrode can regenerate the oxidative mediator, which benefits indirect oxidation reaction (Puetter *et al.*, 2002). In addition to indirect electrolysis study, diamond electrode exerts great effects on direct electrolysis, such as in anodic conversion of 2,-dimethylphenol to 2,2'-biphenol, methoxylation of p-tert-butyltoluene, and electrochemical cleavage of 1,2-diphenylethanes (Fardel *et al.*, 2006; Griesbach *et al.*, 2005; Malkowsky *et al.*, 2006).

Despite their remarkable electrochemical properties, doped diamond electrodes present limitations in terms of mechanical properties for film deposition on silicon and titanium substrate as well as high preparation costs for film deposition on tantalum, tungsten, and niobium substrates (Panizza *et al.*, 2005). In addition, the surface area of doped diamond electrode is restricted by the size of chemical vapor deposition chamber. Therefore, Lee *et al.* (2011) introduced a diamond composite electrode for the first time to remove microorganisms in wastewater treatment. This electrode exerts no limitation on shape or dimension, and the preparation cost is reasonable (Lee *et al.*, 2011). Carbon black is blended with diamond nanopowder during electrode preparation to increase the conductivity of the electrode. Ajeel *et al.* (2015) reported that increase in carbon black percentage will increase the conductivity but decrease the potential window of the diamond composite electrode. These findings indicated that diamond electrode with 5%

carbon black exhibit similar potential window to high-quality boron-doped diamond electrodes, within the range of 3 V to 4 V (Ajeel *et al.*, 2015a, 2015b, 2015c; Ajeel *et al.*, 2016). The diamond composite electrode is cheap and exhibits excellent electrochemical properties and thus can replace the doped diamond electrode in organic electrosynthesis.

## **2.8 Separations and purifications**

Carboxylic acids and polyols are common chemicals produced from the electrochemical conversion of glycerol. Purification and separation is an important step in downstream operation to recover these valuable compounds. The traditional separation methods include solvent extraction, crystallization, ion exchange, precipitation and acidification as well as adsorption. Nowadays, these methods become less popular because they hardly meet the modern green chemistry requirement (Anastas *et al.*, 1997). Solvent extraction would cause environment problem due to the use of hazardous solvents. Ion exchange is unfavourable because usually large amount of base, acid and water are needed to restore the ion-exchange resins. As for crystallization, the yield obtained are relatively low (Huang *et al.*, 2007).

Membrane technologies have attracted significant interests in recent years. Nano-filtration, electro-deionisation and electro-dialysis are the common separation methods that have been widely studied. In commercial nano-filtration process, the separation efficacy highly depends on the charge effect of membrane. The charge relies on the pH of the solution and its isoelectric point. Nano-filtration membranes normally charged negatively in neutral or alkaline condition and charged positively at low pH (Tanninen *et al.*, 2002). When the nano-filtration membrane is negatively charged, organic acids in their dissociated form are more effectively rejected, meanwhile uncharged solutes can permeate through the membrane, thus the carboxylic acids can be separated from other



solutes in the reaction mixtures. In this case, the pH of the organic electrolyte containing carboxylic acids must be set at the pH higher than their pKa value, so that the acids exist in dissociated form (Xu, 2005). Figure 2.3 shows the effect of pH of feed solution to the anion rejection on the charged membrane (Childress *et al.*, 2000). In a study by González *et al.* (2007), the lactic acid was recovered from fermentation broth by nano-filtration membranes in the treatment of ionic solution. Two polyamide nano-filtration membranes were used. The pH of the feed solution affects both lactate rejection and permeate flux. The highest lactate rejection was 91 % in the pH range of 2.7-6 (González *et al.*, 2008).

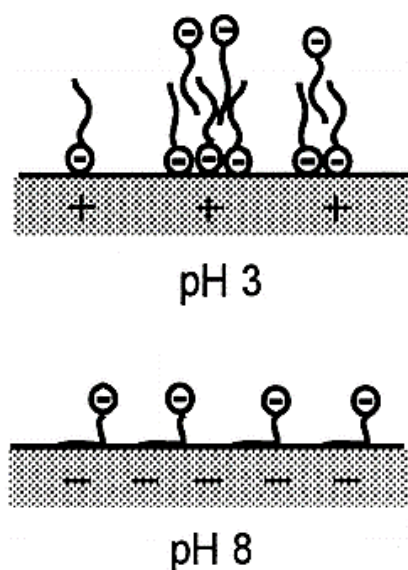


**Figure 2.3.** Effect of pH on the rejection of anion species on charged membrane (Childress *et al.*, 2000).

Electro-deionization (EDI) is a combination process of electrolysis and membrane technology. It comprises of ion exchange resins and ion exchange membrane sandwiched between the cathode and anode electrodes as shown in Figure 2.4

(Boontawan *et al.*, 2011). The operating cost of EDI process is lower than the conventional ion exchange process, as the ion exchange resins can be regenerated by the DC electric field (Huang *et al.*, 2007). Boontawan *et al.* (2011) studied on an EDI system to recover lactic acid from the fermentation broth, by setting-up a combination of cation (Neosepta CM-1) and anion (Neosepta AM-1) exchange membranes with cation exchange resin that comprised of Purolite strong acid. Platinum and stainless were used for anode and cathode, respectively. The highest lactate concentration in the receiving solution was 185 g/L.

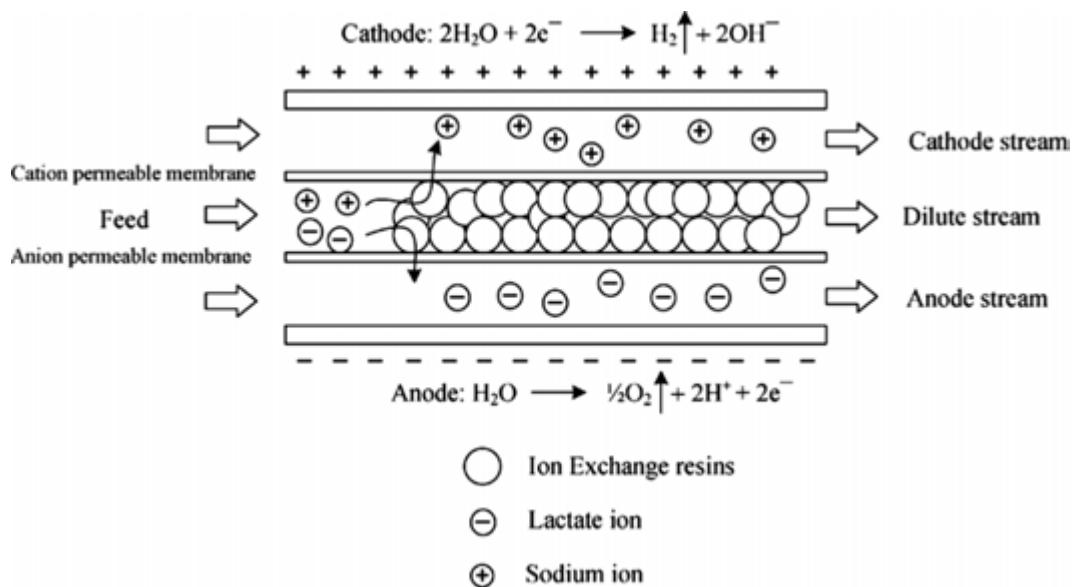


**Figure 2.4.** Working principle of a single-stage electro-deionization technique for lactate ion separation (Boontawan *et al.*, 2011).

Electro-dialysis is another kind of separation method with combination of membrane technology and electrolysis process. The operating manual is relatively similar to the electro-deionization. The system consists of a cation-selective membrane, an anion-selective membrane and two-compartments as shown in Figure 2.5, but ion exchange resins are not used here (Huang *et al.*, 2007). From the previous reported literatures, it

was used for recovery of pyruvate (Zelić *et al.*, 2005), glycine (Elisseeva *et al.*, 2002), formic acid (Luo *et al.*, 2002), lactate (Boniardi *et al.*, 1996; Danner *et al.*, 2000; Hábová *et al.*, 2004; Madzingaidzo *et al.*, 2002) and propionate (Fidaleo *et al.*, 2006). Moon *et al.* (1998) carried out a batch electro-dialysis process to separate a mixture of acetic, formic, lactic and succinic acids. The author observed that the parameters such as molar concentration of feeding solution, molecular weight of acids, charge on ionic species, degree of ionization and ionic equivalent conductivity can affect the separation selectivity (Moon *et al.*, 1998).

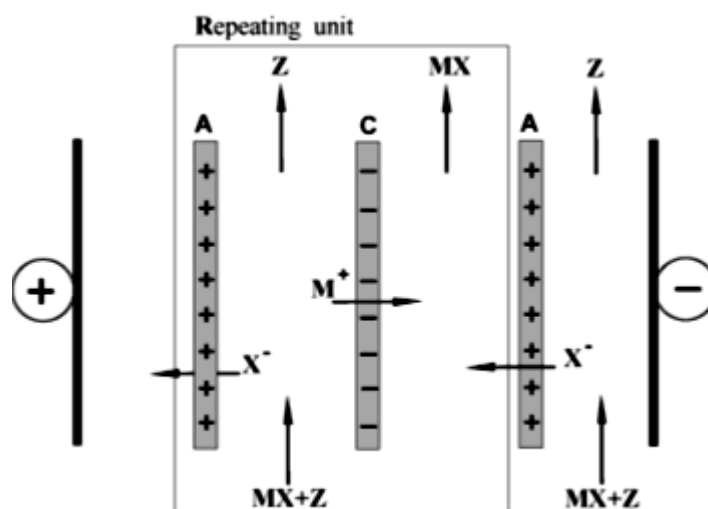


**Figure 2.5.** Schematic represents the electro-dialysis process for concentrate organic acids or organic salts. MX: organic acid or salt; Z: neutral substances or low concentration of inorganic salts (Huang *et al.*, 2007).

A few separation methods have been reviewed in this section. Due to that different physical properties of different organic acids and polyols, there is no specific method which is suitable for all. Usually several methods have to be combined to removing the major impurities (by primary purification such as membrane filtration, electro-dialysis, electro-deionization etc.) and further separation for the compounds with close physical

properties (by secondary purification such as direct distillation or esterified the organic acids follow-by distillation).

## **2.9 Outlook and conclusion**

As described in this chapter, glycerol is a useful feedstock for production of various added-value compounds for food, pharmaceutical, polymer, household, and cosmetic industries. Current catalytic and enzymatic processes used to convert glycerol into valuable compounds are illustrated in previous sections, and the limitations of these methods are highlighted. Electrochemical conversion of glycerol is also demonstrated in detail. Product selectivity and yield remain as the main challenges in glycerol conversion. By introducing the application of redox catalysts, possible enhancement of this additive in electrochemical synthesis will be illustrated in detail in Chapter 4. Glycerol electrochemical synthesis is expected to improve when using a cheap and porous electrode.

## CHAPTER 3: METHODOLOGY

### 3.1 Introduction

Generally, in this study, the electrochemical processes were divided into two main sections. Firstly, the electrochemical studies were conducted in a one-pot electrochemical cell. In this section, the reaction medium was first screened out by running the reaction in the presence of Amberlyst-15, H<sub>2</sub>SO<sub>4</sub> and NaOH with Pt as working electrode. Later, two new electrodes (ACC and CBD) were prepared as cathode materials and compared with that conventional Pt electrode. Reaction parameters such as catalyst amount, applied electric current and reaction temperature were studied in order to obtain the optimum reaction conditions. In the second section, the electrochemical studies were carried out in a two-compartment system and three cathode materials (Pt, ACC and CBD) were tested in the cathodic region. The chemicals and reagents that used in this study are listed in Table 3.1.

**Table 3.1.** List of chemicals and reagents used

<b>Chemicals or reagents</b>	<b>Purity</b>	<b>Manufacturer</b>
Acetaldehyde	99.5%, GC grade	Acros Organic, Belgium
Acetol	>90%, GC grade	Acros Organic, Belgium
Activated carbon powder	99.5%, AR grade	Sigma Aldrich, Malaysia
Amberlyst-15	100%, AR grade	Acros Organics, France
Carbon black powder	99%, AR grade	Alfa-Chemicals, Malaysia
Diethylene glycol	99% GC grade	Fluka, Germany
1,4-Dioxane	99.8%, GC grade	Sigma Aldrich, Germany
Ethanol	>99.8%, GC grade	Merck, Malaysia
Ethyl acetate	99.5%, GC grade	Acros Organics, Germany
Glyceraldehyde	>90%, GC grade	Sigma Aldrich, Germany
Glycerol	>99%, AR grade	Merck, Malaysia
Glycidol	96%, GC grade	Acros Organics, Belgium
Nanodiamond powder	98.3%, AR grade	Sigma Aldrich, Malaysia
1,2-Propanediol	99%, GC grade	Acros Organics, Belgium
1,3-Propanediol	99%, GC grade	Acros Organics, Belgium
Sodium sulphate	99+%, AR grade	Acros Organics, Malaysia
Sulfuric acid	98%, AR grade	Merck, Malaysia
Sodium hydroxide	≥97.0%, AR grade	Fisher Scientific, Malaysia
Tetraethylene glycol	99%, GC grade	Sigma Aldrich, Germany

## **3.2 Electrochemical study in a one-pot reactor**

### **3.2.1 Electrode preparation**

#### **3.2.1.1 Preparation of ACC and CBD electrodes**

ACC electrode (with surface area of 4.5 cm<sup>2</sup>) was prepared by mixing 80% wt activated carbon (99.5% purity, average particle size of 100 μm, and specific surface area of 950 m<sup>2</sup>/g; Sigma Aldrich) and 20% wt carbon black (99% purity, average particle size of 13 nm, and specific surface area of 550 m<sup>2</sup>/g; Alfa-chemicals, Malaysia) to a total weight of 1.0 g.

CBD electrodes (with surface areas of 2.3 and 9.8 cm<sup>2</sup>) were prepared by blending 20% wt carbon black and 80% wt nanodiamond powder (98.3% purity, average particle sizes of 3–10 nm, and specific surface area of 200 m<sup>2</sup>/g to 400 m<sup>2</sup>/g; Sigma Aldrich, Malaysia).

The pre-mixed powder was added into a mixture containing 20% v/v polytetrafluoroethylene and 80% v/v 1,3-propanediol to obtain a powder-to-liquid ratio of 1:2. The slurry was pressed neatly and oven dried in accordance with the following heating program: 100 °C (2 h), 180 °C (1 h), 250 °C (1 h), and finally 350 °C for 30 min to allow complete sintering of the powder and increase the electrode hardness (Ajeel *et al.*, 2015a).

#### **3.2.1.2 Scanning electron microscopy analysis (SEM)**

The morphological appearances of the ACC and CBD electrodes, before and after the reaction, were studied by scanning electron microscope (SEM) (Hitachi SU-8000, Japan) equipped with an energy-dispersive X-ray (EDX) analyzer. The element content in the electrode was determined by EDX.

### 3.2.1.3 Measurement of active surface areas

Active surface areas of ACC and CBD electrodes (with surface area of 0.45 cm<sup>2</sup>) were measured by chronoamperometry analysis in 0.005 M ferrocyanide solution (K<sub>4</sub>Fe(CN)<sub>6</sub>) containing 0.1 M KH<sub>2</sub>PO<sub>4</sub>. The test was performed by an Autolab Potentiostat from Metrohm (Model PGSTAT101). The active surface areas of the ACC and CBD electrodes were obtained using the famous Cottrell equation:

$$I = \frac{nFAD^{1/2}C_0}{\pi^{1/2}t^{1/2}} \quad \text{Eq. 3.1}$$

where  $I$  is the current (A),  $n$  is the number of electrons,  $A$  is the active surface areas of the electrode (cm<sup>2</sup>),  $D$  is the diffusion coefficient ( $6.20 \times 10^{-6}$  cm<sup>2</sup>/s),  $C_0$  is the bulk concentration of K<sub>4</sub>Fe(CN)<sub>6</sub> (mol/cm<sup>3</sup>),  $F$  is the Faraday constant 96487 (C/mol), and  $t$  is the reaction time (s) (Ajeel *et al.*, 2015a).

### 3.2.1.4 Electrochemical measurement

The electrochemical behavior of ACC and CBD electrodes in aqueous glycerol solution was studied using a Potentiostat in an electrochemical cell with a total capacity of 100 mL. The solution was prepared from pure glycerol stock (>99% purity, Merck, Malaysia) with an initial concentration of 0.15 M. About 3.0 g of Amberlyst-15 (weight total capacity (H): > 4.70 eq/ Kg, Acros Organics, France) was dispersed in aqueous solution containing 0.15 M glycerol and 0.10 M Na<sub>2</sub>SO<sub>4</sub> (99+% purity, Acros Organics, Malaysia). ACC and CBD electrodes (with surface area of 0.45 cm<sup>2</sup>) were used as working electrodes, and Pt and Ag/AgCl were used as counter and reference electrodes, respectively. The system was agitated with a magnetic stirrer at a constant rate of 400 rpm. Cyclic voltammetry (CV) was scanned within -3.00 V to +3.50 V with a scan rate 0.02 V s<sup>-1</sup>.

### **3.2.2 Screening of reaction medium**

#### **3.2.2.1 Electrochemical measurement**

The possible electrochemical performance of three blank solutions, namely, Amberlyst-15, H<sub>2</sub>SO<sub>4</sub>, and NaOH, were compared through CV analysis. Blank solutions were prepared as follows: (i) 3.0 g of Amberlyst-15 was dispersed into 100 mL of distilled water; (ii) 50 mL of 0.15 M H<sub>2</sub>SO<sub>4</sub> (98% purity, Merck, Malaysia) was mixed with 50 mL of distilled water; and (iii) 50 mL of 0.30 M NaOH ( $\geq$  97.0% purity, Fisher Scientific, Malaysia) was added to 50 mL of distilled water. Second, the electrochemical behavior of 3.0 g of Amberlyst-15 in the presence of 0.15 M glycerol aqueous solution was studied.

CV experiments were conducted using a Potentiostat (Autolab Metrohm, model PGSTAT101) in an electrochemical cell with a total capacity of 100 mL. The system was agitated with a magnetic stirrer at a constant rate of 400 rpm. CV test was conducted using a Pt planar (total surface area of 0.20 cm<sup>2</sup>) as the working electrode. Pt wire and Ag/AgCl were used as counter and reference electrodes, respectively. The scan potential range of each system was varied.

#### **3.2.2.2 Bulk electrochemical study**

Laboratory-scale electrochemical conversion of glycerol was conducted in a one-pot electrochemical cell (total capacity: 100 mL) at room temperature (27 °C) for 8 h. The temperature of the electrochemical cell was controlled by a laboratory chiller. The reaction set-up is shown in Figure 3.1. The system was supplied with a constant current of 1.0 A and agitated with a magnetic stirrer at a constant rate of 800 rpm. Three solution systems were prepared as follows: (i) 3.0 g of Amberlyst-15 was dispersed into 100 mL of 0.15 M glycerol aqueous solution, (ii) 50 mL of 0.15 M H<sub>2</sub>SO<sub>4</sub> was mixed



with 50 mL of 0.30 M glycerol aqueous solution, and (iii) 50 mL of 0.30 M NaOH was mixed with 50 mL of 0.30 M glycerol aqueous solution.

The electrochemical performance of glycerol in the presence of Amberlyst-15 was compared with the conventional method in H<sub>2</sub>SO<sub>4</sub> or NaOH medium. Platinum (Pt) with surface areas of 33 and 22 cm<sup>2</sup> was used as cathode and anode electrodes, respectively. The effects of applied current (1.0, 2.0, and 3.0 A) and reaction temperature [room temperature (27 °C), 50 °C, and 80 °C] were studied. A control reaction of Amberlyst-15 in glycerol aqueous solution was carried out at 80 °C in the absence of electricity.

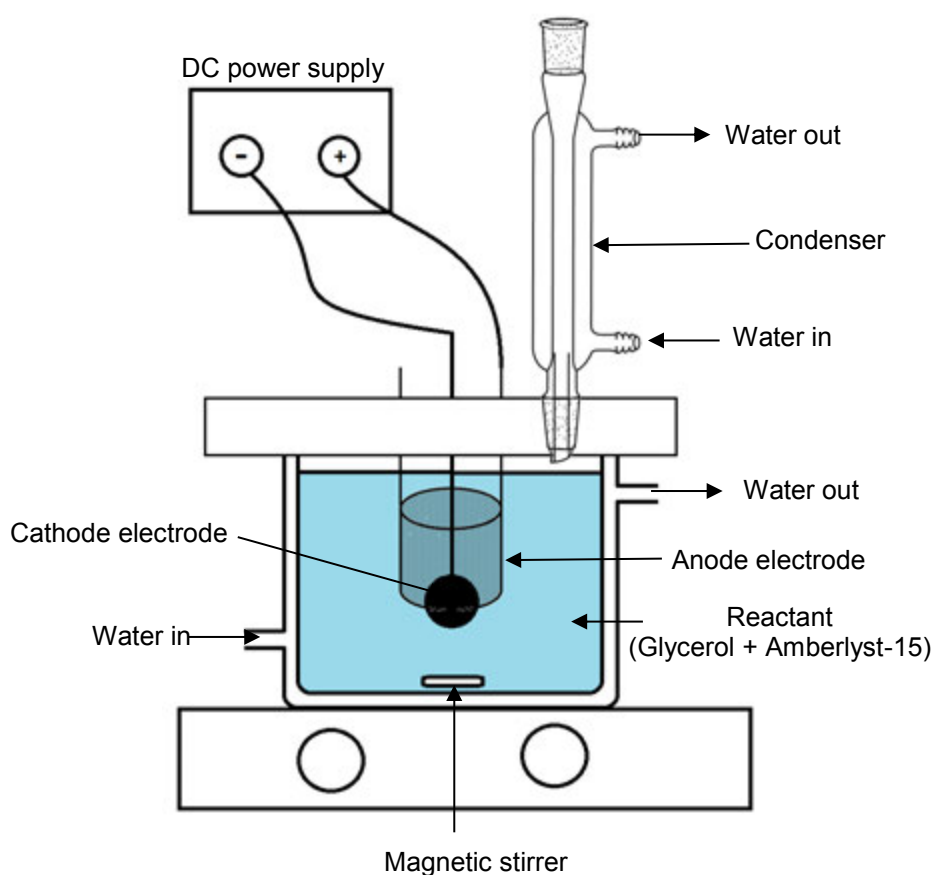


**Figure 3.1:** Electrochemical set-up (one-pot reactor).

### 3.2.3 Evaluation of cathode materials and optimization study

Two types of cathode materials were evaluated. Electrochemical experiments were performed over ACC and CBD cathode electrodes, with surface areas of 4.5 and 2.3 cm<sup>2</sup>, respectively. The first attempts were carried out at the optimum condition obtained from the preliminary study (applied current of 1.0 A and reaction temperature of 80°C) in a one-pot reactor.

Optimization studies were conducted for both electrodes (ACC and CBD, with respective active surface areas of 69.4 and 61.1 cm<sup>2</sup>). The effect of catalyst amount (6.4, 9.6, and 12.8% w/w), applied current (1.0, 2.0, and 3.0 A), and reaction temperature [room temperature (27 °C), 50 °C, and 80 °C] were studied in the bulk electrochemical study. The solutions were prepared by dispersing 6.4 g of Amberlyst-15 and 1.5 g of Na<sub>2</sub>SO<sub>4</sub> in 0.30 M glycerol solution (total volume of 100 mL).

### 3.3 Electrochemical study in a two-compartment reactor

Electrochemical study was performed in a two-compartment reactor separated by a cation exchange membrane, Nafion-117 (Figure 3.2). The membrane contains persulfonated polytetrafluoroethylene (PTFE)-based polymer with high chemical and thermal stability. The membrane also contains a sulfonic acid group, which can transfer proton from one compartment to another but does not allow electrons to cross over (Fang *et al.*, 2010).

Each compartment was filled with 250 mL of 0.30 M glycerol solution. Briefly, 24.0 g of Amberlyst-15 and 10.0 g of Na<sub>2</sub>SO<sub>4</sub> were dispersed into the entire glycerol solution. Pt (surface area of 22 cm<sup>2</sup>) was used as anode electrode. The three types of cathode materials evaluated include Pt (surface area of 33.0 cm<sup>2</sup>), ACC (surface area of 14.1 cm<sup>2</sup>), and CBD (surface area of 14.1 cm<sup>2</sup>). Constant current (2.0 A) was supplied to the system, and the reaction temperature was controlled at 80 °C for 8 h.

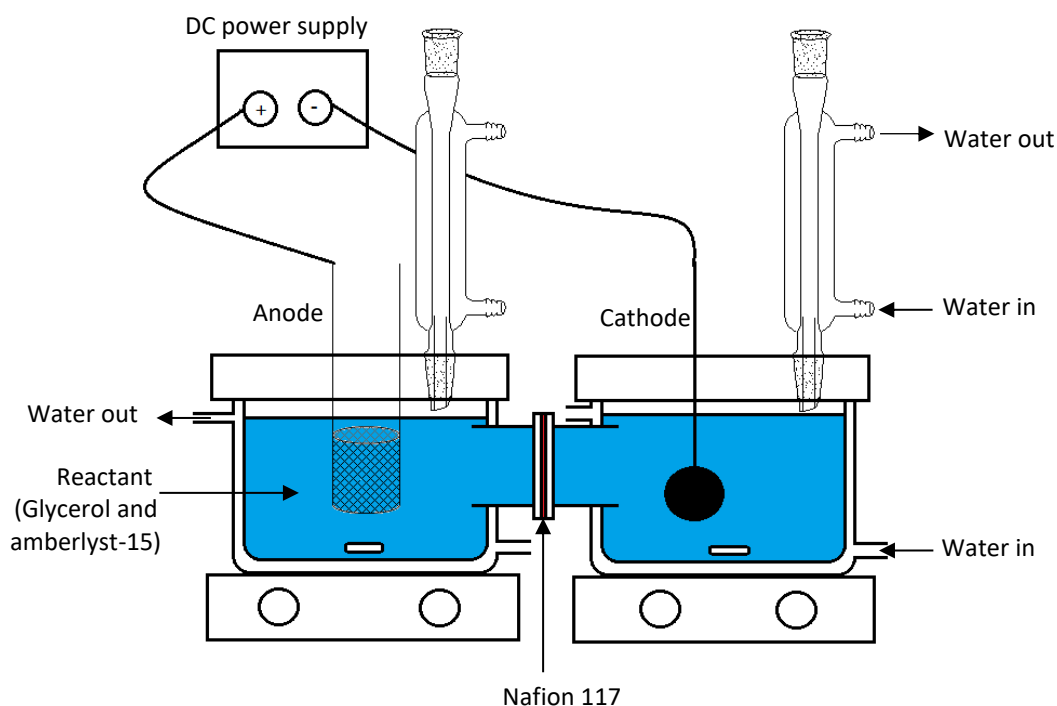


**Figure 3.2:** Electrochemical set-up (two-compartment reactor).

### 3.4 Product characterization and quantification

Chemical compounds were characterized by gas chromatography–mass spectroscopy (GC-MS) (Agilent, Model 7890). Compounds were separated using a ZB-Wax (Phenomenex, United States) capillary column (30 m × 0.25 mm × 0.25 μm) with high-purity helium (> 99.99%) as a carrier gas at constant flow rate of 2.0 mL min<sup>-1</sup>. The initial oven temperature was set at 45 °C, held for 5 min, and then increased at 10 °C min<sup>-1</sup> to a final temperature of 240 °C, which was maintained for 5 min. The injection volume was 1 μL. The GC-MS analysis condition is shown in Table 3.2. The results obtained were compared with the chemical standards and MS library (Agilent, ChemStation software). The retention time ( $R_t$ ) of each compound is shown in Table 3.4, and the MS spectra are displayed in Appendix 1.

Samples obtained from electrochemical studies were quantified using a gas chromatography (GC) equipment (Model 6890, Agilent) connected with a flame ionization detector (FID) attached with the same capillary column. The analysis was

performed under the same condition as GC-MS analysis (Table 3.3). The retention time ( $R_t$ ) of each compound is shown in Table 3.4, and the GC chromatograms for the standards are presented in Appendix 2.

**Table 3.2:** Gas chromatography-mass spectroscopy analysis conditions.

Column	ZB-Wax (30m × 0.25mm × 0.25 μm)
Detector	MS
Carrier Gas	He
Injector Temperature	240 °C
Flow Rate	2.0 mL/min
Injection volume	1 μL
Oven Temperature	45 °C (5 min) → 10 °C/min → 240 °C (5 min)
Ionization	Electron impact (70 eV)

**Table 3.3:** Gas chromatography analysis conditions.

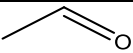
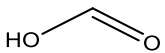
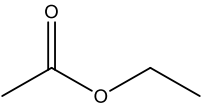
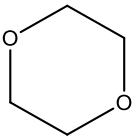
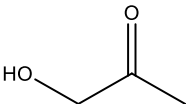
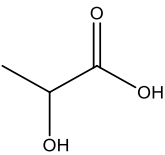
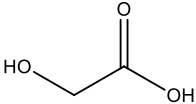
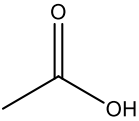
Column	ZB-Wax (30m × 0.25mm × 0.25 μm)
Detector	FID
Carrier Gas	He
Injector Temperature	240 °C
Detector	240 °C
Flow Rate	2.0 mL/min
Injection volume	1 μL
Oven Temperature	45 °C (5 min) → 10 °C/min → 240 °C (5 min)

### 3.4.1 Standard calibration

An eight-level glycerol calibration curve was prepared for glycerol concentrations ranging from 0.05 mg/mL to 2.00 mg/mL with 2.00 mg/mL tetraethylene glycol (TEG) as internal standard. About 1000 μL of 20.00 mg/mL TEG was added into various volumes (50–1000 μL) of 10.00 mg/ml glycerol solution. The solutions were added with ethanol (> 99.8%, GC grade, Merck Malaysia) in a 10 ml volumetric flask. The amount

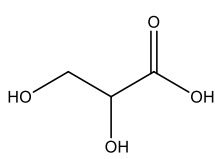
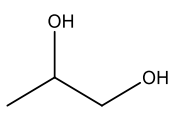
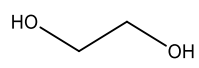
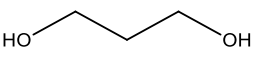
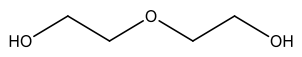
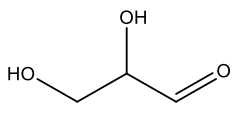
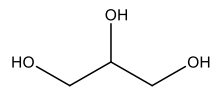
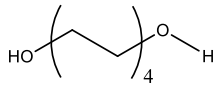
of glycerol standards used for calibrations, area of the standard, and area of the internal standard are summarized in Table 3.5. The glycerol calibration curve is shown in Figure 3.3.

**Table 3.4:** List of chemical standards and their physical properties (Sigma\_Aldrich) as well as retention time in GC-MS and GC-FID analysis.

Chemical	Molecular structure	MW (g/mole)	BP (°C)	R <sub>t</sub> GC-MS (min)	R <sub>t</sub> GC-FID (min)
Acetaldehyde		44.05	20.2	1.26	1.52
Formic acid		46.03	100.8	1.57	1.89
Ethyl acetate		88.11	77.1	1.88	2.20
1,4-dioxane		88.11	101.1	4.16	5.36
Acetol		74.08	145	9.61	10.31
Lactic acid		90.08	122	10.40	10.94
Glycolic acid		76.05	75	11.56	12.06
Acetic acid		60.05	118	12.04	12.26

Note: MW: molecular weight      R<sub>t</sub>: retention time      BP: Boiling point

**Table 3.4 continued:** List of chemical standards and their physical properties (Sigma\_Aldrich) as well as retention time in GC-MS and GC-FID analysis.

Chemical	Molecular structure	MW (g/mole)	BP (°C)	R <sub>t</sub> GC-MS (min)	R <sub>t</sub> GC-FID (min)
Glyceric acid		106.08	100	12.18	12.54
1,2-Propanediol		76.10	188.2	13.87	14.42
Ethylene glycol		62.07	197.3	14.27	14.60
1,3-Propanediol		76.10	211	16.12	16.60
Diethylene glycol		106.12	244	18.06	18.61
Glyceraldehyde		90.08	127	21.07	19.76
Glycerol		92.08	290	21.32	21.84
Tetraethylene glycol		194.23	313	24.59	25.00

Note: MW: molecular weight      R<sub>t</sub>: retention time      BP: Boiling point

**Table 3.5:** The glycerol solution preparation for standard calibration curve.

<b>Preparation of mother solution:</b>						
Amount of glycerol standard (mg) : 249.82						
Volumetric flask (mL) : 25						
<b>Mother solution (mg/mL)</b>	<b>Volume taken from mother solution (µL)</b>	<b>Actual concentration (mg/mL) **</b>	<b>Theoretical concentration (mg/mL)</b>	<b>Area of glycerol (GC)</b>	<b>Area of TEG (GC)</b>	<b>Area glycerol/ Area TEG</b>
9.9928 ± 0.0058	50	0.0500	0.05	18.49	757	0.0244
9.9928 ± 0.0058	75	0.0749	0.075	23.59	756	0.0312
9.9928 ± 0.0058	100	0.0999	0.1	34.48	693	0.0498
9.9928 ± 0.0058	500	0.4996	0.5	186.35	778	0.2395
9.9928 ± 0.0058	750	0.7495	0.75	234.2	654	0.3581
9.9928 ± 0.0058	1000	0.9993	1	327.1	550	0.5947
9.9928 ± 0.0058	1500	1.4989	1.5	569.49	665	0.8564
9.9928 ± 0.0058	2000	1.9986	2	752.07	722	1.0416

Note: \*\*Dilution in 10 mL

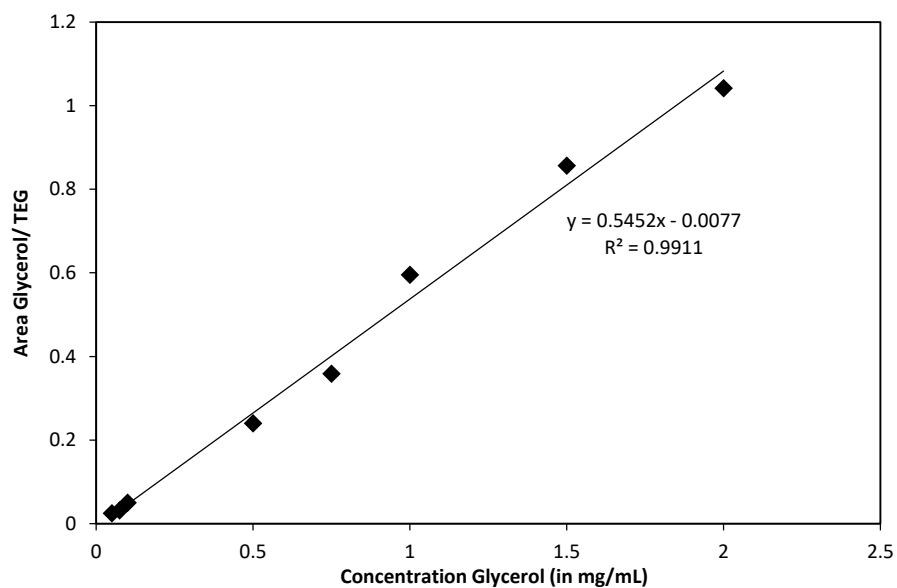


**Figure 3.3:** Glycerol calibration curve.

Three-level concentrations calibration curves for other chemical standards, such as 1,2-PDO, 1,3-PDO, lactic acid, acetol, diethylene glycol (DEG), ethyl acetate, acetic acid, acetaldehyde, and ethylene glycol, were prepared within 0.10–1.00 mg/mL. Glycolic and glyceric acids, which are grouped under hydroxyl carboxylic acid as lactic acid, were quantified using the calibration curve as lactic acid. Triplicate injections were carried out to improve the accuracy of the standard curves. The standard calibration curves are shown in Appendix 3.

### 3.4.2 Sample analysis

Samples were prepared in the same manner. Briefly, 1000  $\mu$ L of the sample was spiked with 1000  $\mu$ L of 20.00 mg/mL TEG and added with ethanol to reach a total volume of 10 mL. Glycerol conversion, yield, and selectivity were calculated based on Equations 3.2, 3.3, and 3.4, respectively.

$$\text{Glycerol conversion (\%)} = \frac{\text{Amount of glycerol converted (in mole C)}}{\text{Total amount of glycerol in reactant (in mole C)}} \times 100 \% \quad \text{Eq. 3.2}$$

$$\text{Product yield (\%)} = \frac{\text{Amount of product (in mole C)}}{\text{Total amount of glycerol in reactant (in mole C)}} \times 100 \% \quad \text{Eq. 3.3}$$

$$\text{Product selectivity (\%)} = \frac{\text{Amount of product (in mole C)}}{\text{Sum of all products (in mole C) in liquid phase}} \times 100 \quad \text{Eq. 3.4}$$

In accordance with the study of Hunsom *et al.* (2013), the kinetics of glycerol conversion was calculated using a macro-kinetics model based on the first-order rate



kinetics in a mathematical software (Statistica). The following formula was applied to obtain the first-order kinetic model, and the graph is displayed in concentration versus time.

$$C = C_o e^{-kt} \quad \text{Eq. 3.5}$$

Where  $C$  = glycerol concentration of that time ( $\text{mol}/\text{dm}^3$ ),  $C_o$  = initial glycerol concentration ( $\text{mol}/\text{dm}^3$ ),  $k$  = kinetic rate constant ( $\text{h}^{-1}$ ),  $t$  = time (h)

## CHAPTER 4: RESULTS AND DISCUSSION

### 4.1 Introduction

This chapter is divided into five sections. Electrochemical valorization of glycerol in the presence of Amberlyst-15 over the Pt electrode in a one-pot electrochemical cell is first studied. The effects of reaction medium, electric current, and reaction temperature on product yield and selectivity are discussed. Afterward, the effects of two novel cathode electrodes (ACC and CBD electrodes) on the type of added-value compounds obtained are assessed. In the third and fourth sections, the effects of catalyst amount, reaction temperature, and electric current on the electrolysis over ACC and CBD electrodes are discussed in detail. Finally, the results of the electrochemical valorization of glycerol in the two-compartment cell are presented. The reaction mechanisms leading to the formation of the added-value compounds are also proposed.

### 4.2 Electrochemical valorization of glycerol over Pt electrode

#### 4.2.1 Cyclic voltammetry analysis

Figure 4.1 shows the CV curves of the blank solutions, namely, (i) Amberlyst-15 (in water), (ii) H<sub>2</sub>SO<sub>4</sub> aqueous solution, and (iii) NaOH aqueous solution. The potential scan range of each solution is stated in the figure caption. The CV curves of NaOH and H<sub>2</sub>SO<sub>4</sub> aqueous solutions present a nearly straight line without visible redox peaks. In the CV curve of Amberlyst-15 (in water solution), a pair of symmetrical redox peaks was observed at the electrode potential of  $-0.80$  V (peak a) and  $+0.04$  V (peak b). The appearance of this pair of redox peaks could be attributed to the oxidation and reduction of Amberlyst-15 in the electrolyte system.

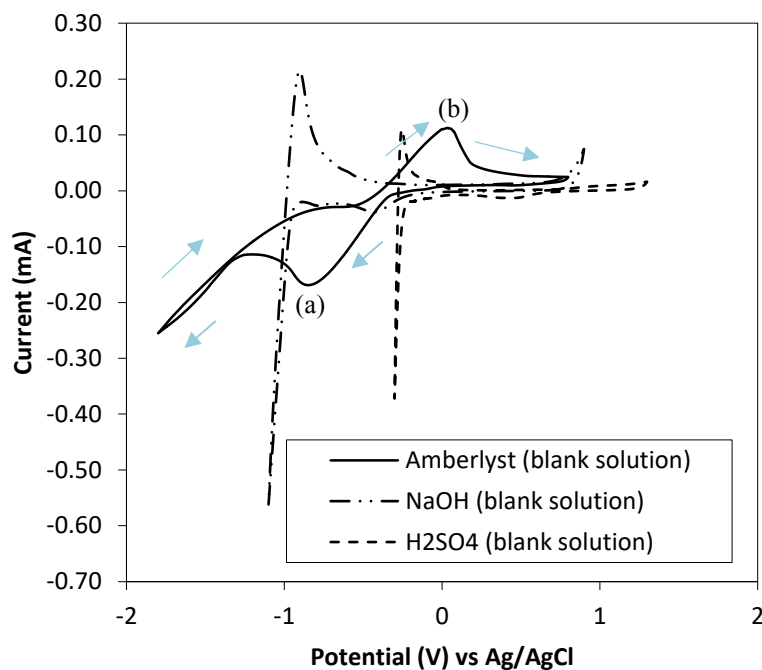


**Figure 4.1:** CV curves of Amberlyst-15 (potential scan range:  $-1.80$  to  $+0.80$  V), NaOH (potential scan range:  $-1.10$  to  $+0.90$  V) and  $\text{H}_2\text{SO}_4$  (potential scan range:  $-0.30$  to  $+1.30$  V), without glycerol on Pt at a scan rate of  $0.1 \text{ Vs}^{-1}$ .

Figure 4.2 shows the CV curves for Amberlyst-15 in the presence and absence of glycerol aqueous solution. Scanning was performed from  $-1.80$  to  $+1.50$  V at a scan rate of  $0.1 \text{ Vs}^{-1}$  over the Pt electrode. In the presence of glycerol, the first oxidation peak (peak A) was observed at the electrode potential of  $+0.56$  V during the anodic scan. This peak is attributed to direct oxidation of glycerol. The shoulder peak (peak B) near the oxygen evolution region is also due to glycerol oxidation. During the backward scan, a cathodic peak (peak C) was observed at the potential of  $+0.33$  V, which corresponds to the reduction of Pt oxide. Another oxidation peak (peak D) was observed at the electrode potential of  $+0.26$  V; this peak is related to incompletely oxidized carbonaceous species, such as formates, which are chemically adsorbed on the electrode surface (Fashedemi *et al.*, 2015).

When backward scanning was performed, a sharp reduction peak (peak E) was observed at the electrode potential at  $-0.90$  V. Compared with the CV curve for Amberlyst-15 blank solution in Figure 4.1, this peak exhibits similar potential to the reduction behavior of Amberlyst-15 (peak a). In the presence of glycerol, the peak current density of peak E increased compared with that of the blank solution (dash-dotted line); this result explains the indirect reaction that re-occurred between Amberlyst-15 and glycerol in the electrolysis system (Francke *et al.*, 2014).

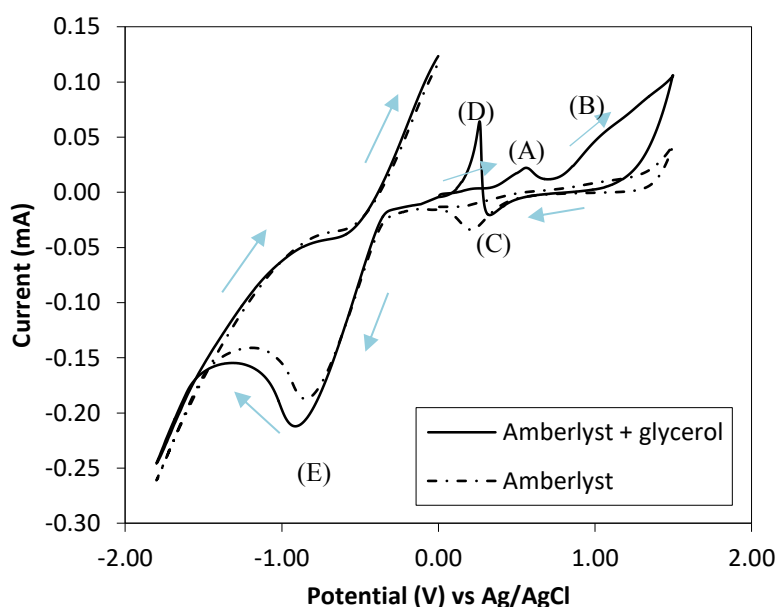


**Figure 4.2:** CV curves of Amberlyst-15 blank solution and amberlyst-15 with glycerol solution on Pt at a scan rate of  $0.1 \text{ Vs}^{-1}$  in potential window range of  $-1.80$  to  $+1.50$  V.

#### 4.2.2 Bulk electrochemical synthesis

Pt electrode was used in the first part of this study because most studies evolved from the first study on glycerol electro-oxidation conducted by Roquet *et al.* (1994). In the present study, glycerol was successfully converted into glycolic acid, glyceric acid, acetol, acetaldehyde, glyceraldehyde, formic acid, and ethylene glycol by using Amberlyst-15 as reaction medium. However, only glycolic and glyceric acids were considered in this section because these compounds exhibit considerably high market

value and are widely used in pharmaceutical, cosmetic, and food industries (Bagheri *et al.*, 2015). The maximum yield and selectivity from each trial are summarized in Table 4.1. The selectivity toward each compound highly depends on the reaction conditions.

**Table 4.1:** Electrochemical conversion of glycerol in the presence of Amberlyst-15 over Pt electrode; the yield and selectivity for glycolic and glyceric acids are given at the maximum level.

Electrode	Electrolyte/ Acid	I (A)	T (°C)	Glycerol Conversion*		Yield (Y) & Selectivity (S) (%, in mole C)			
				%	k	Glycolic acid		Glyceric acid	
						Y	S	Y	S
Pt	Amberlyst-15	1.0	RT	80.0	0.119 h <sup>-1</sup> (6h)	19.1 (6h)	41.8 (6h)	20.5 (6h)	45.0 (6h)
Pt	H <sub>2</sub> SO <sub>4</sub>	1.0	RT	59.6	0.121 h <sup>-1</sup>	3.9 (8h)	43.4 (8h)	3.8 (8h)	42.3 (8h)
Pt	NaOH	1.0	RT	45.4	0.068 h <sup>-1</sup>	Nil	Nil	2.4 (6h)	85.5 (6h)
Pt	Amberlyst-15	2.0	RT	96.3	0.678 h <sup>-1</sup>	18.6 (5h)	19.1 (5h)	11.4 (5h)	11.7 (5h)
Pt	Amberlyst-15	3.0	RT	99.4	0.649 h <sup>-1</sup>	2.6 (3h)	62.4 (3h)	3.0 (2h)	61.9 (2h)
Pt	Amberlyst-15	1.0	50	96.5	0.385 h <sup>-1</sup>	21.4 (8h)	33.3 (8h)	23.2 (5h)	53.4 (5h)
Pt	Amberlyst-15	1.0	80	97.2	0.370 h <sup>-1</sup>	44.7 (6h)	64.7 (6h)	27.2 (3h)	38.2 (3h)
-	Amberlyst-15	-	80	28.6	0.001 Mh <sup>-1</sup>	Nil	Nil	Nil	Nil

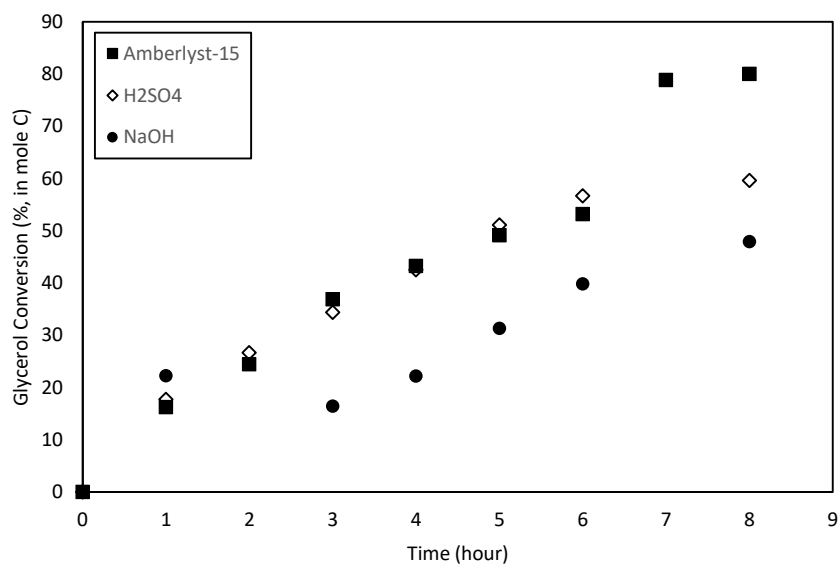
Note: RT: room temperature, 27 °C; I: current; T: reaction temperature; k = rate constant  
 [Glycerol]: 0.15 M; [H<sub>2</sub>SO<sub>4</sub>]: 0.075 M; [NaOH]: 0.15 M  
 \*After 8 h of reaction time. Total reaction time: 8 h  
 Nil: zero value

#### 4.2.2.1 Effect of reaction medium

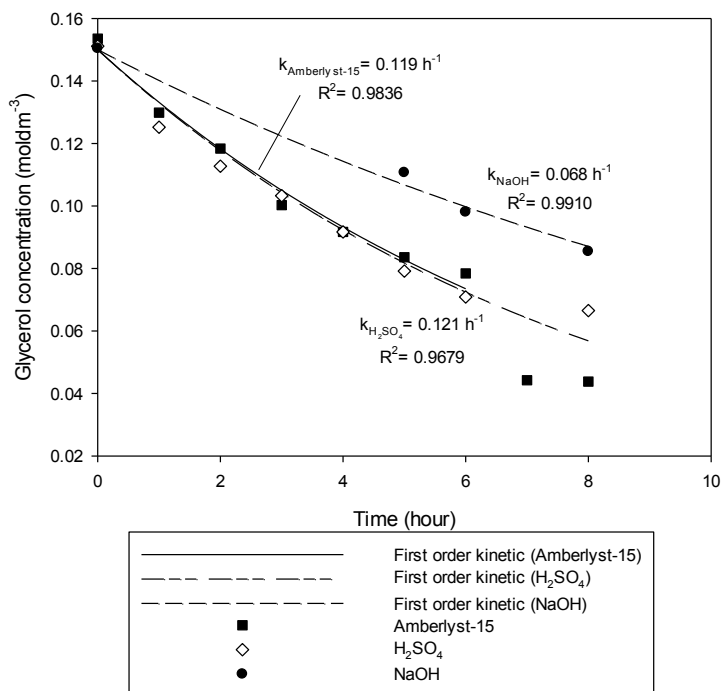
Electrochemical conversion of glycerol was conducted in the presence of Amberlyst-15. The reaction was also performed using conventional acidic (H<sub>2</sub>SO<sub>4</sub>) and alkaline (NaOH) media for comparison.

Figure 4.3 shows glycerol conversion in the presence of Amberlyst-15, H<sub>2</sub>SO<sub>4</sub>, and NaOH. The glycerol conversion rate of Amberlyst-15 reached 80% after 8 h of electrolysis, and those of H<sub>2</sub>SO<sub>4</sub> and NaOH reached 59.6% and 45.4%, respectively. According to Hunsom *et al.* (2013), glycerol conversion undergoes the first-order

kinetics. The kinetics of glycerol conversion was then calculated by employing a first-order kinetic rate model [Equation (4) in Section 3.4.2], and the graphs are displayed in Figure 4.4. The rate constant ( $k$ ) in Amberlyst-15 and  $H_2SO_4$  solutions (0.119 and 0.121  $h^{-1}$ , respectively) is higher than that in NaOH solution (0.068  $h^{-1}$ ).



**Figure 4.3:** Glycerol conversion from the electrochemical study on Pt electrode in the presence of Amberlyst-15,  $H_2SO_4$  and NaOH media, at room temperature (27 °C) and 1.0 A constant current.



**Figure 4.4:** First-order kinetics model of the electrochemical conversion of glycerol in the presence of Amberlyst-15, H<sub>2</sub>SO<sub>4</sub>, and NaOH media on Pt electrode at room temperature (27 °C) and 1.0 A constant current.

According to the product distribution graphs shown in Figure 4.5, Amberlyst-15 exhibited the highest yield and selectivity for glycolic (yield: 19.1%, selectivity: 41.8%) and glyceric acids (yield: 20.5%, selectivity: 45.0%) after 6 h of the reaction. The yield started to decrease after this point and favored other compounds, such as formic acid and DEG. Glycolic and glyceric acids were the major compounds obtained; other compounds, such as acetaldehyde, formic acid, acetol, and ethylene glycol, were also produced. In H<sub>2</sub>SO<sub>4</sub> medium, glycolic and glyceric acids were generated after 4 h of electrolysis. The maximum yield and selectivity were achieved after 8 h, with 3.9% and 3.8% yields for glycolic and glyceric acids, respectively. In NaOH medium, only 2.4% of glyceric acid was obtained after 6 h of the reaction. The yields for other products, such as acetol and ethylene glycol, were less than 1%. According to Roquet *et al.* (1994), dissociative oxidation compounds, such as formic and glycolic acids, are rarely

detected in alkaline media. Referring to the bar chart shown in Figure 4.6, Amberlyst-15 obviously showed higher product yield than H<sub>2</sub>SO<sub>4</sub> and NaOH.

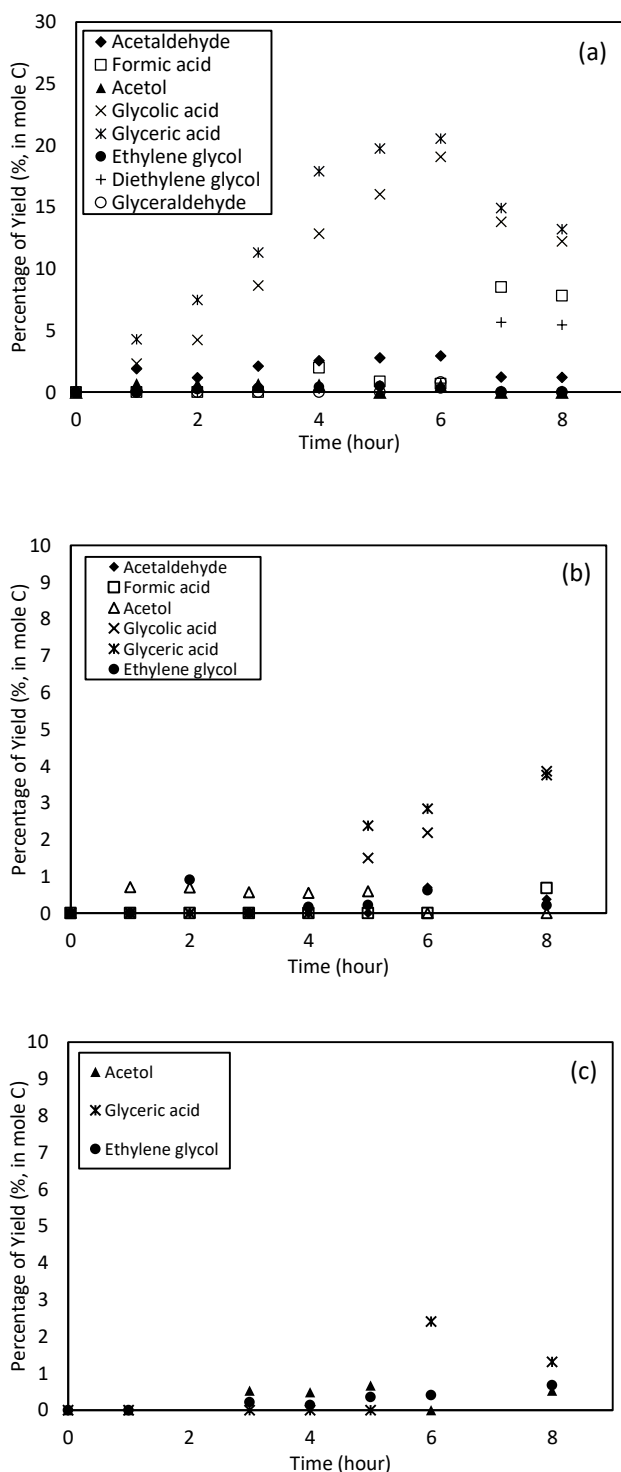


**Figure 4.5:** Product distribution from the electrochemical conversion of glycerol (a) in the presence of Amberlyst-15, (b) H<sub>2</sub>SO<sub>4</sub>, and (c) in NaOH on Pt electrode at room temperature (27 °C) and 1.0 A constant current.



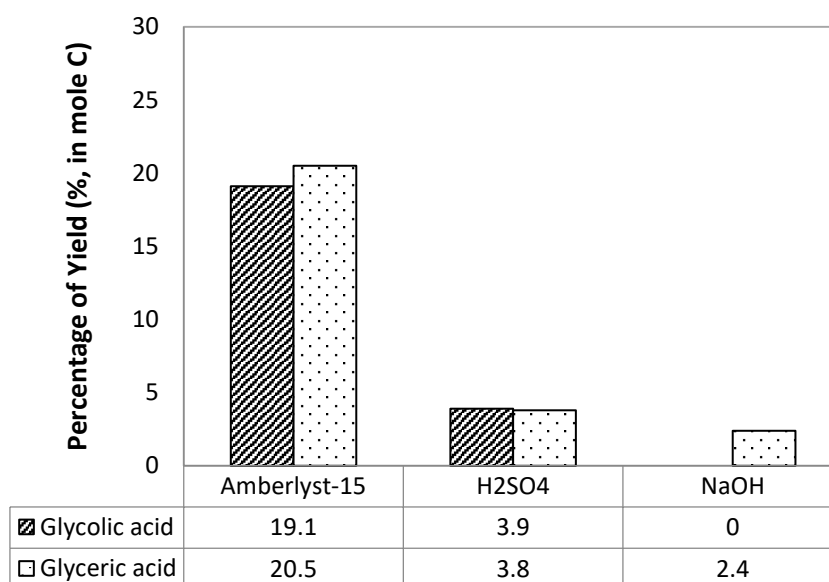
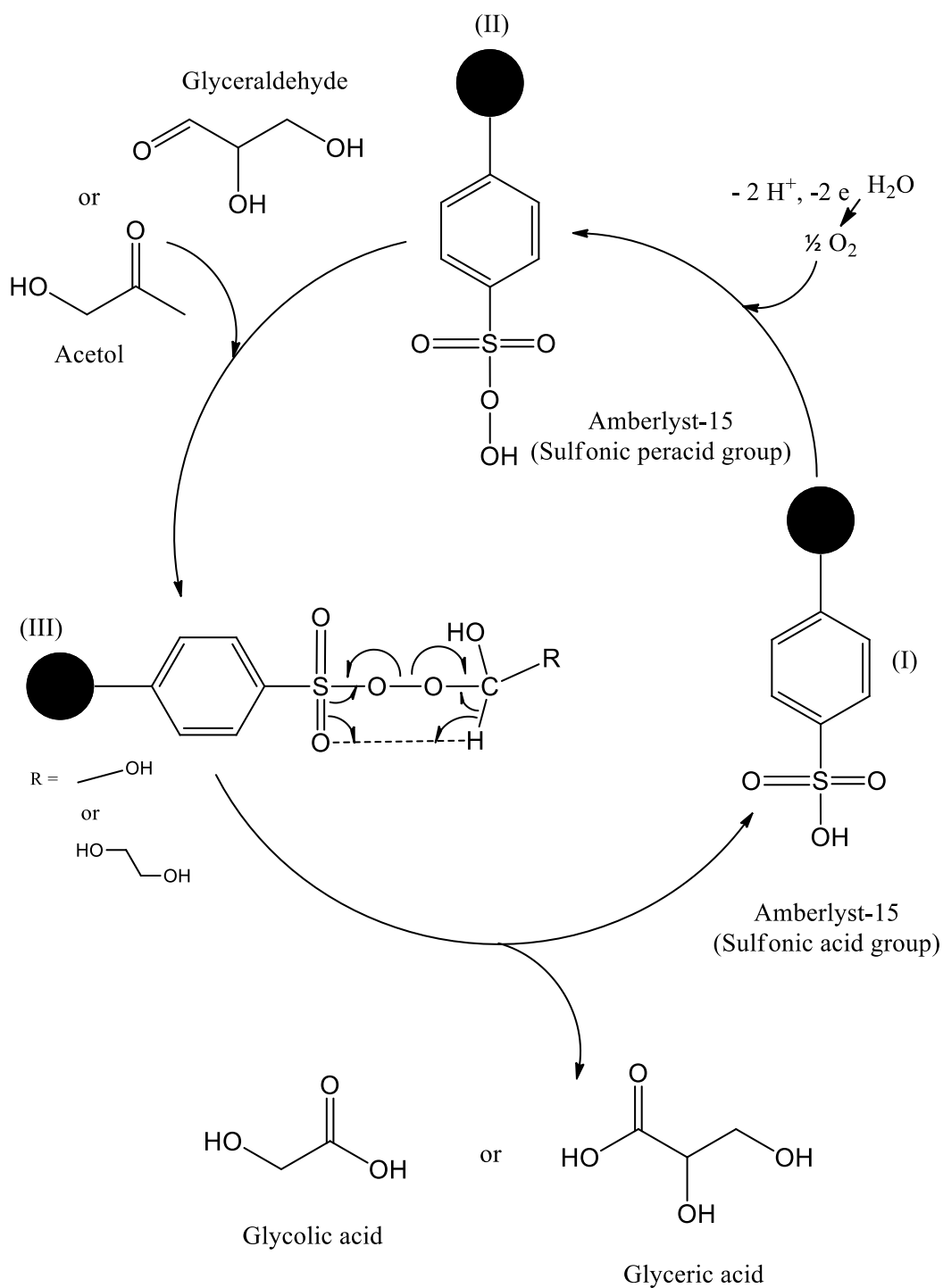


**Figure 4.6:** Maximum yield of glycolic and glyceric acids obtained from the electrochemical conversion of glycerol (a) in the presence of Amberlyst-15, (b) H<sub>2</sub>SO<sub>4</sub>, and (c) NaOH on Pt electrode at room temperature (27 °C) and 1.0 A constant current.

The CV curve in Figure 4.1 shows that Amberlyst-15 may function as redox catalyst in organic electrosynthesis. Its catalytic behavior may have an added advantage to the chemical catalytic pathway. According to Yang *et al.* (2013), Amberlyst-15 has a great catalytic activity on the oxidation of aldehyde to carboxylic acid. Scheme 4.1 shows that sulfonic acid group on Amberlyst-15 (I) may possible to react with O<sub>2</sub> from the water electrolysis in anodic region, thus forms an intermediate sulfonic peracid group (II). The intermediate sulfonic peracid may continue to react with glyceraldehyde or acetol (III) to produce glyceric and glycolic acids, respectively. In the present study, Amberlyst-15 provided an additional indirect electro-oxidation pathway, in addition to the direct electro-oxidation pathway, which is commonly found in H<sub>2</sub>SO<sub>4</sub> or NaOH (Roquet *et al.*, 1994).



**Scheme 4.1.** Catalyzed oxidation of glyceraldehyde and acetol to glyceric as well as glycolic acids by Amberlyst-15

#### 4.2.2.2 Effect of electric current

In this study, three different electric currents, namely, 1.0, 2.0, and 3.0 A, were tested and selected based on the study of Kongjao *et al.* (2011). In their study, electrochemical

conversion of glycerol was conducted in galvanostatic mode at electric current of 4.5 A over Pt electrode with surface area of 66.49 cm<sup>2</sup>; the applied current density was 0.06 Acm<sup>-2</sup> (Kongjao *et al.*, 2011). When this current density was applied as central, the current density was expanded to one level lower and one level upper, viz. 0.03, 0.06, and 0.09 Acm<sup>-2</sup>, which correspond to 1.0, 2.0, and 3.0 A, respectively, on the Pt electrode with surface area of 33 cm<sup>2</sup>.

The glycerol conversion and kinetic rate models at different electric currents (1.0, 2.0, and 3.0 A) are summarized in Figures 4.7 and 4.8, respectively. Electrolysis at 1.0 A fitted the first-order kinetic model within the first 6 h of the reaction. According to Faraday's law, increasing the electric current can directly increase the level of glycerol conversion (Prentice, 1991). The glycerol conversion was almost completed after 8 h of the reaction at high electric currents. The glycerol conversion rates were about 96% and 99% at electric currents of 2.0 and 3.0 A, respectively. The rate constant also increased from 0.119 h<sup>-1</sup> (1.0 A) to 0.678 h<sup>-1</sup> (2.0 A) and to 0.649 h<sup>-1</sup> (3.0 A). However, these high glycerol conversion and kinetic rates only correspond to small amount of product yield; hence, glycerol might have been converted into other volatile side products, such as CO<sub>2</sub>, which could not be detected in the liquid phase of the system.

Product distribution and yields are shown in Figure 4.9. When the electric current increased, glyceric and glycolic acid yields decreased. At high currents (2.0 and 3.0 A), the reactions were considerably vigorous and facilitated the decomposition of glycerol into small compounds, such as formic acid and CO<sub>2</sub> (Ishiyama *et al.*, 2013). Therefore, low electric current (1.0 A) was preferred for production of glyceric and glycolic acids. The maximum yields of glyceric and glycolic acids obtained under an electric current of 1.0 A were 20.5% and 19.1%, respectively. The maximum yields of glyceric and glycolic acids at different electric currents are summarized in Figure 4.10.

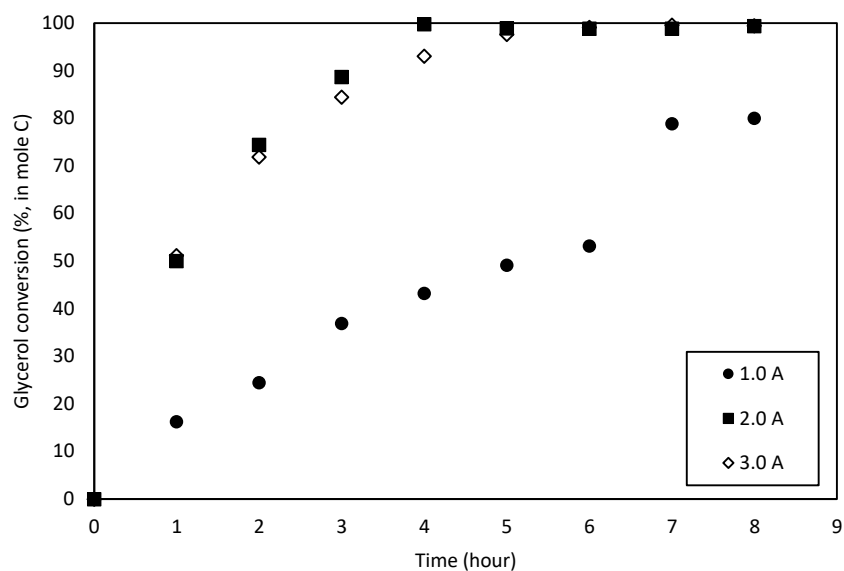


**Figure 4.7:** Glycerol conversion from the electrochemical study on Pt electrode in the presence of Amberlyst-15 at room temperature (27 °C) and constant currents of 1.0, 2.0, and 3.0 A.

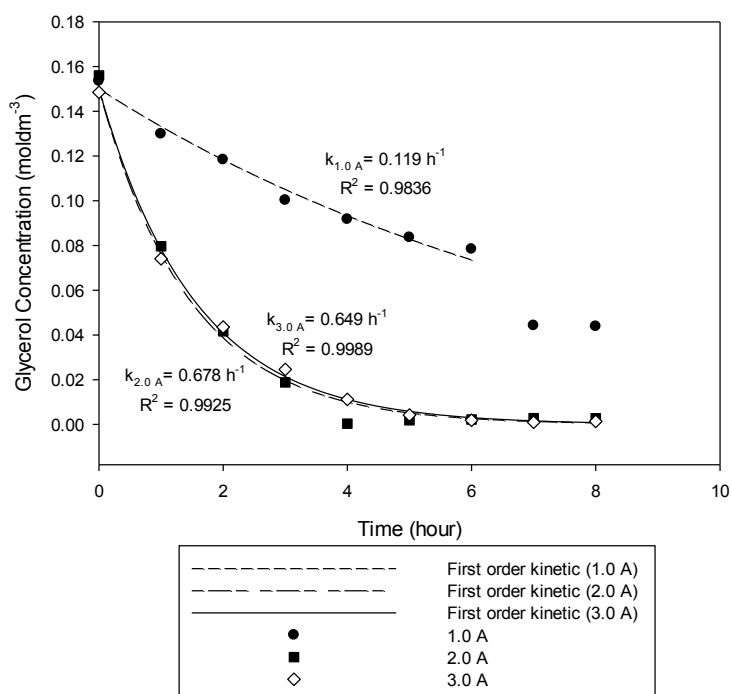


**Figure 4.8:** First-order kinetic model of the electrochemical conversion of glycerol in the presence of Amberlyst-15 on Pt electrode at room temperature (27 °C) and constant currents of 1.0, 2.0, and 3.0 A.

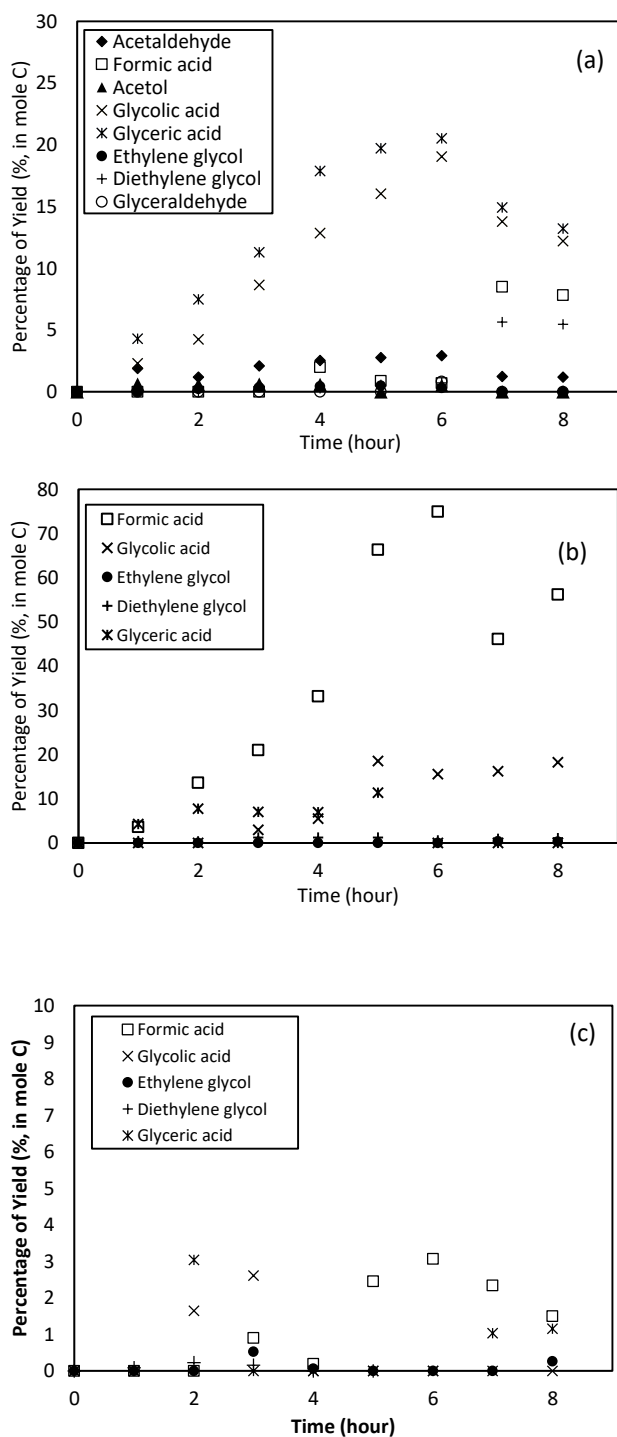


**Figure 4.9:** Product distribution from the electrochemical conversion of glycerol in the presence of Amberlyst-15 on Pt electrode at room temperature (27 °C) and constant currents of (a) 1.0, (b) 2.0, and (c) 3.0 A.

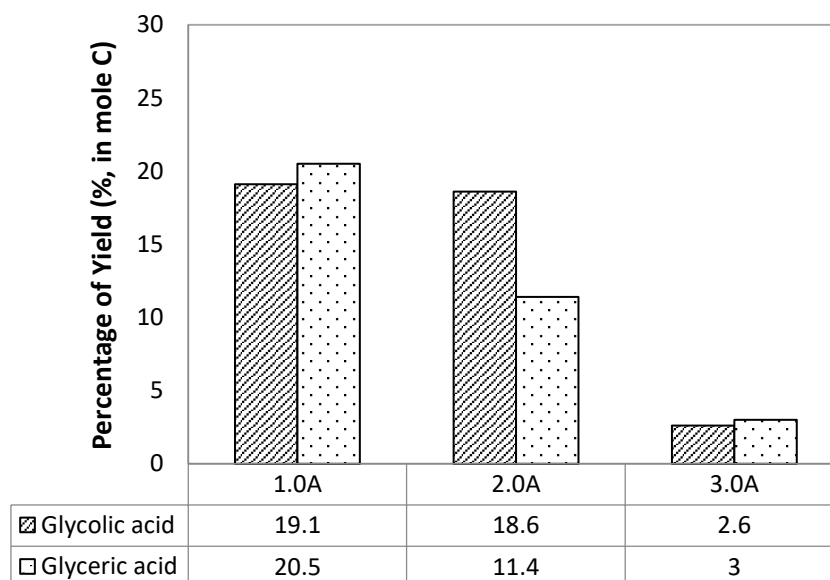


**Figure 4.10:** Maximum yield of glycolic and glyceric acids obtained from the electrochemical conversion of glycerol in the presence of Amberlyst-15 on Pt electrode at room temperature (27 °C) and constant currents of (a) 1.0, (b) 2.0, and (c) 3.0 A.

#### 4.2.2.3 Effect of reaction temperature

Glyceric and glycolic acids conversion were preferred at low electric currents; thus, the effect of reaction temperature was investigated at an applied current of 1.0 A. The reaction was carried out at three reaction temperatures, namely, room temperature (27 °C), 50 °C, and 80 °C. The glycerol conversion rates at these temperatures are summarized in Figure 4.11. Increasing the reaction temperature increased the glycerol conversion rate. About 96%–97% of glycerol was converted into added-value compounds after 8 h of the reaction at 50 °C and 80 °C. This result could be due to high temperature requirement for adsorption of the OH molecule on the Pt electrode surface for electrochemical process enhancement (Paula *et al.*, 2014; Zhang *et al.*, 2012a). According to the first-order kinetics rates displayed in Figure 4.12, high glycerol conversion rates were observed with increasing reaction temperature; these rates were 0.119, 0.385, and 0.370 h<sup>-1</sup> at room temperature (27 °C), 50 °C, and 80 °C, respectively.

A control reaction was carried out under the same reaction temperature (80 °C) in the absence of electricity. The glycerol conversion rate was rather low at about 28.6% after 8 h of the reaction. In this case, the reaction kinetics fitted to the zero-order kinetic order, given that  $k = 0.001 \text{ Mh}^{-1}$  (Table 4.1 in Section 4.2.2). This observation highlights that the reaction without electricity is not affected by glycerol concentration. This control run showed that electric current is the main factor that initiates the reaction, and the reaction temperature displays an added advantage to glycerol conversion.

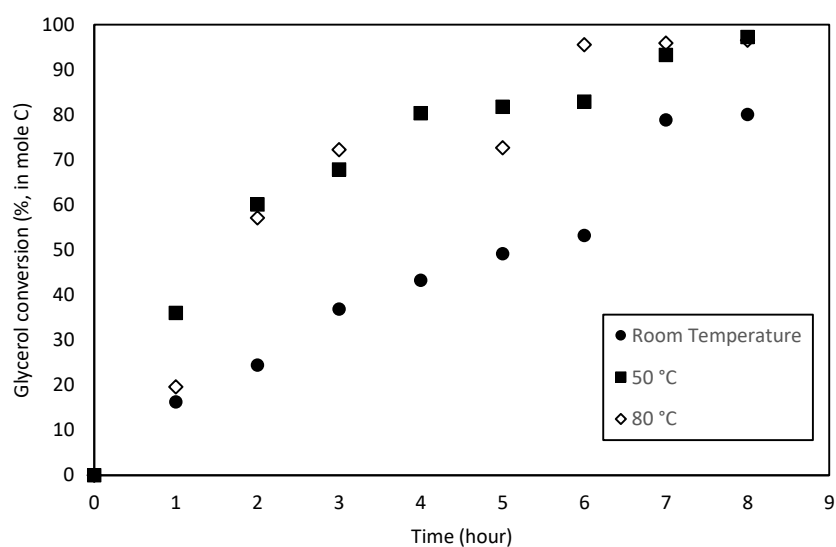


**Figure 4.11:** Glycerol conversion from the electrochemical study on Pt electrode in the presence of Amberlyst-15 at 1.0 A constant current at room temperature (27 °C), 50 °C, and 80 °C.

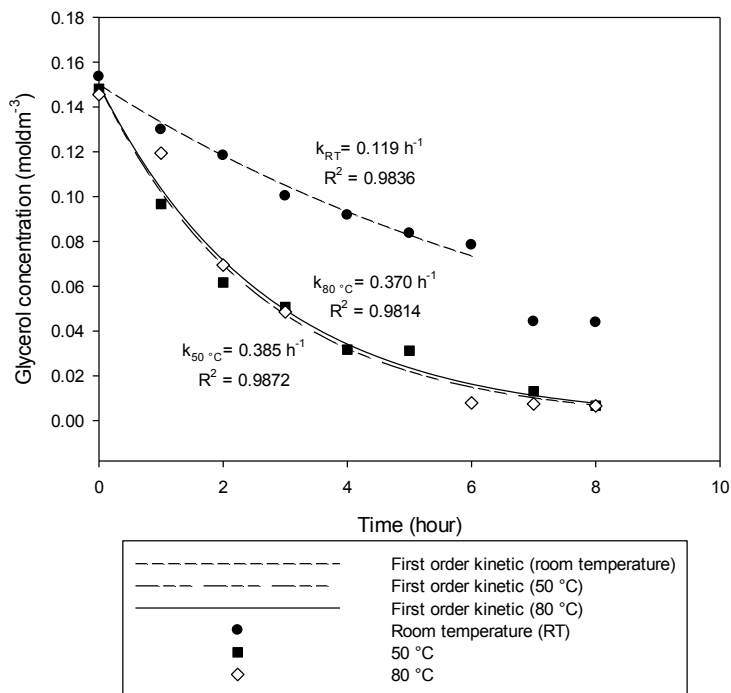


**Figure 4.12:** First-order kinetic model of the electrochemical conversion of glycerol in the presence of Amberlyst-15 on Pt electrode at 1.0 A constant current at room temperature (27 °C), 50 °C, and 80 °C.

With respect to the product distributions and yields in Figure 4.13, the maximum yield of glyceric acid was achieved after 3-5 h of electrolysis at high temperatures (50 °C and 80 °C) and decreased thereafter. The glycolic acid yield continuously increased up to 8 h (at 50 °C) and 6 h (at 80 °C). Generally, the yields of glycolic and glyceric acids increased by increasing the reaction temperature, which could be due to the large amount of energy available with increasing temperature. In addition, the increased reaction temperature could favor OH adsorption on the electrode surface. The presence of the submonolayer-adsorbed OH can reduce the barrier for both C–H and O–H bond dissociations, thereby enhancing the oxidation behavior of glycerol (Beden *et al.*, 1987; Paula *et al.*, 2014; Zhang *et al.*, 2012a; Zope *et al.*, 2010).



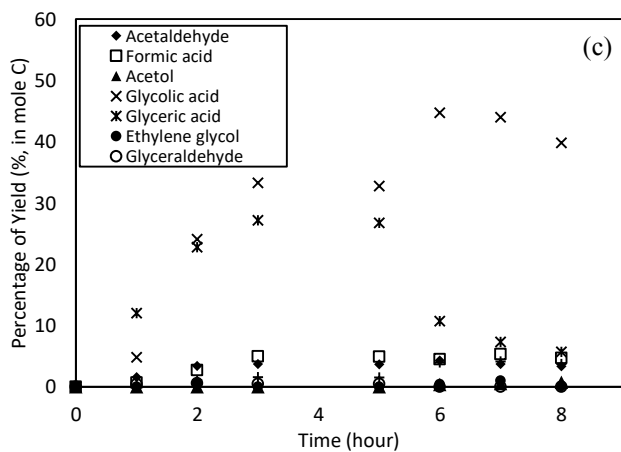
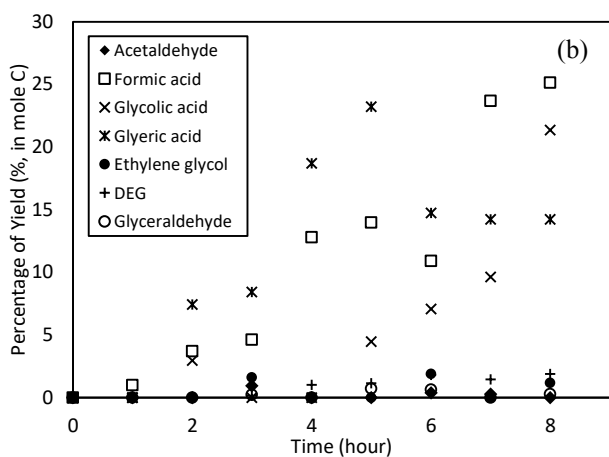
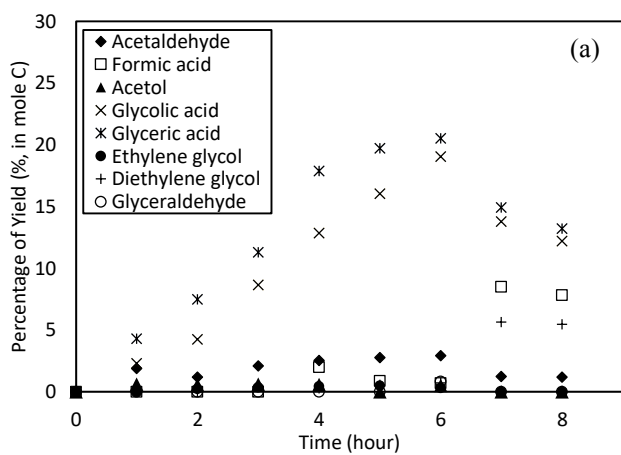


**Figure 4.13:** Product distribution from the electrochemical conversion of glycerol in the presence of Amberlyst-15 on Pt electrode at 1.0 A constant current at (a) room temperature (27 °C), (b) 50 °C, and (c) 80 °C.

At 50 °C, 23.2% of glyceric acid was produced after 5 h of the reaction and 21.4% of glycolic acid was formed after 8 h. High glyceric acid yield was obtained at 80 °C, with 27.2% yield and 38.2% selectivity after 3 h of electrolysis. Glycolic acid reached the maximum amount after 5–6 h of the reaction, with yield of 44.7% and selectivity of 64.7%. Consequently, the optimum product yield and selectivity were achieved at 80 °C and 1.0 A. The bar chart in Figure 4.14 shows that high yields of glycolic and glyceric acids were obtained at 80 °C.

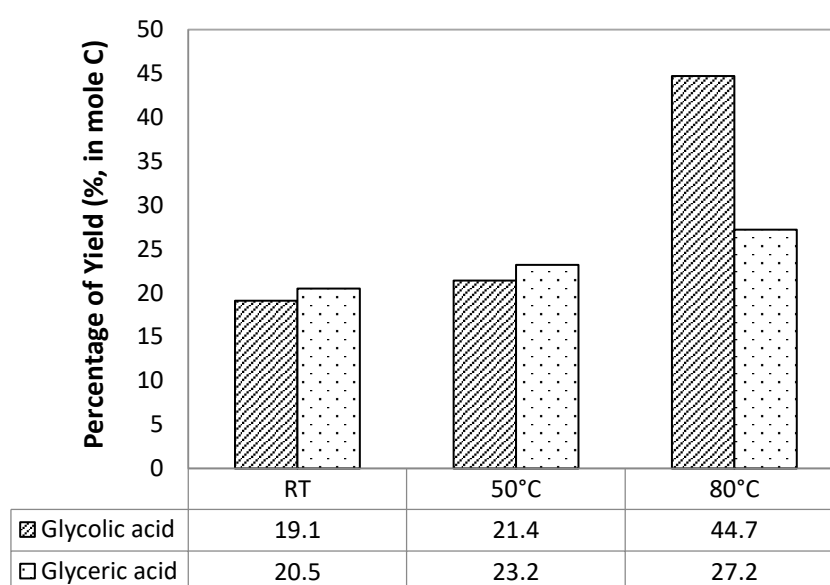


**Figure 4.14:** Maximum yield of glycolic and glyceric acids obtained from the electrochemical conversion of glycerol in the presence of Amberlyst-15 at 1.0 A constant current at (a) room temperature, 27 °C (RT), (b) 50 °C and (c) 80 °C.

A comprehensive literature review on the electrochemical conversion of glycerol into added-value compounds was conducted. Table 2.11 in Section 2.4.3 summarizes the selectivity and yield of glycolic and glyceric acids from the electrochemical study. Compared with the literature studies, higher yields and selectivities were achieved in this present study.

To date, bulk electrochemical synthesis of glycerol was only reported by Kongjao *et al.* (2011) and his research team (Hunsom *et al.*, 2013, 2015; Saila *et al.*, 2015). In one of their studies, oxidants, such as H<sub>2</sub>O<sub>2</sub>, sodium persulfate (Na<sub>2</sub>S<sub>2</sub>O<sub>8</sub>), and TEMPO, were added into the electrochemical medium. The presence of different oxidizing agents can affect the reaction mechanism, generating different added-value compounds (Saila *et al.*, 2015).

Table 4.2 summarizes the results attained from the present study and that of Saila *et al.* (2015) under close reaction conditions such as at room temperature (27 °C) and ambient pressure. In the present study, the reaction was carried out for 8 h, whereas Saila *et al.* (2015) performed the experiment for 24 h. In the present study, the maximum yield was obtained at 6 h. The glycerol conversion and total yield at this time point are relatively higher than those reported by Saila *et al.* (2015). A wide range of added-value compounds, such as acetol, ethylene glycol, glycolic acid, acetaldehyde, formic acid, glyceric acid, and glyceraldehyde, was also obtained. The major compounds included glycolic and glyceric acids, with yields of 19.1% and 20.5%, respectively. Although glycolic acid was successfully obtained by Saila *et al.* (2015), with corresponding yields of 21%, 5%, and 14% in the presence of H<sub>2</sub>O<sub>2</sub>, Na<sub>2</sub>S<sub>2</sub>O<sub>8</sub>, and TEMPO, respectively, the prolonged reaction period, that is, 24 h of electrolysis, is impractical and not cost effective. Moreover, Saila *et al.* (2015) mainly obtained 1,3-dihydroxyacetone (55%) after 24 h in the presence of TEMPO.

According to the results obtained in both studies, Amberlyst-15 exhibits advantages in electrochemical conversion of glycerol. Amberlyst-15 can act as redox catalyst during electrolysis, thereby increasing the glycerol conversion rate and product yield within only 6 h of the reaction. Furthermore, this catalyst is cheaper than TEMPO and safe to use because of its environment-friendly property.

**Table 4.2:** Comparison between data from Saila *et al.*, 2015 and the present study.

	<b>Study from Saila <i>et al.</i>, 2015</b>			<b>This study</b>
Reaction Medium, pH	H <sub>2</sub> SO <sub>4</sub> , pH = 1			Amberlyst-15, pH = 1.3
Advantages and disadvantages of the reaction medium	Toxic and corrosive			<ul style="list-style-type: none"> <li>• Environmental friendly, safe to use</li> <li>• Work as a redox catalyst to enhance the reaction process</li> </ul>
Feedstock	Crude glycerol			Pure Glycerol
Electrode material	Pt			Pt
Reaction temperature (°C)	Room temperature (27 °C)			Room temperature (27 °C)
Pressure	Ambient pressure			Ambient pressure
<b>Oxidizing agent</b>	<b><u>H<sub>2</sub>O<sub>2</sub></u></b>	<b><u>Na<sub>2</sub>S<sub>2</sub>O<sub>8</sub></u></b>	<b><u>TEMPO</u></b>	No oxidizing agent added
<b><u>After 6 hours:</u></b>				
Glycerol conversion	~ 28 %	~ 15 %	~ 15 %	52 %
<b><u>Yield:</u></b>				
Glycidol	~ 10 %	~ 20 %	~ 3 %	-
Acetol	-	-	~ 3 %	0.5 %
1,2-Propanediol	-	-	-	-
Ethylene glycol	-	-	-	0.3 %
Glycolic acid	-	-	-	19.1 %
1,3-dihydroxyacetone	-	-	-	-
Acetaldehyde	-	-	-	2.9 %
Formic acid	-	-	-	0.7 %
Glyceric acid	-	-	-	20.5 %
Diethylene glycol	-	-	-	0.7 %
Glyceraldehyde	-	-	-	0.8 %
<b>Total yield</b>	10 %	20 %	6 %	45.6 %
<b><u>After 24 hours:</u></b>				
Glycerol conversion	100 %	100 %	100 %	The reaction stop at 8-hour.
<b><u>Yield:</u></b>				
Glycidol	~ 22 %	~ 25 %	~ 15 %	The maximum glycerol conversion was 80 %.
Acetol	-	-	~ 5 %	
1,2-Propanediol	-	-	~ 3 %	
Ethylene glycol	~ 18 %	~ 60 %	~ 8%	
Glycolic acid	~ 21 %	~ 5 %	~ 14%	
1,3-dihydroxyacetone	-	-	~ 55 %	
<b>Total yield</b>	61 %	90 %	100 %	

#### 4.2.2.4 Reaction mechanism

The GC-FID chromatogram of the reaction mixtures is shown in Figure 4.15. The GC chromatogram shows that glycerol, in addition to glycolic and glyceric acids, was converted into other added-value compounds, such as acetaldehyde, acetol, and ethylene glycol. The chemical structures of each compound were further characterized via GC-MS analysis, and their MS spectra are shown in Appendix 1.

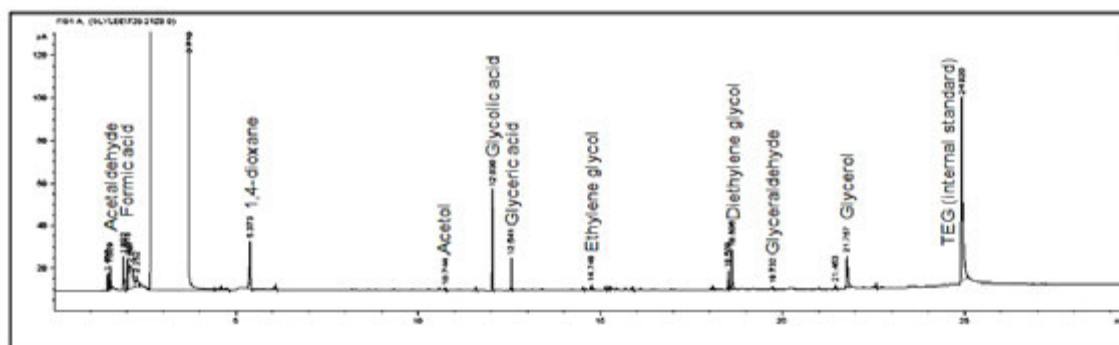


**Figure 4.15:** GC chromatogram from the electrochemical conversion of glycerol in the presence of Amberlyst-15 on Pt electrode at 80 °C and 1.0 A constant current.

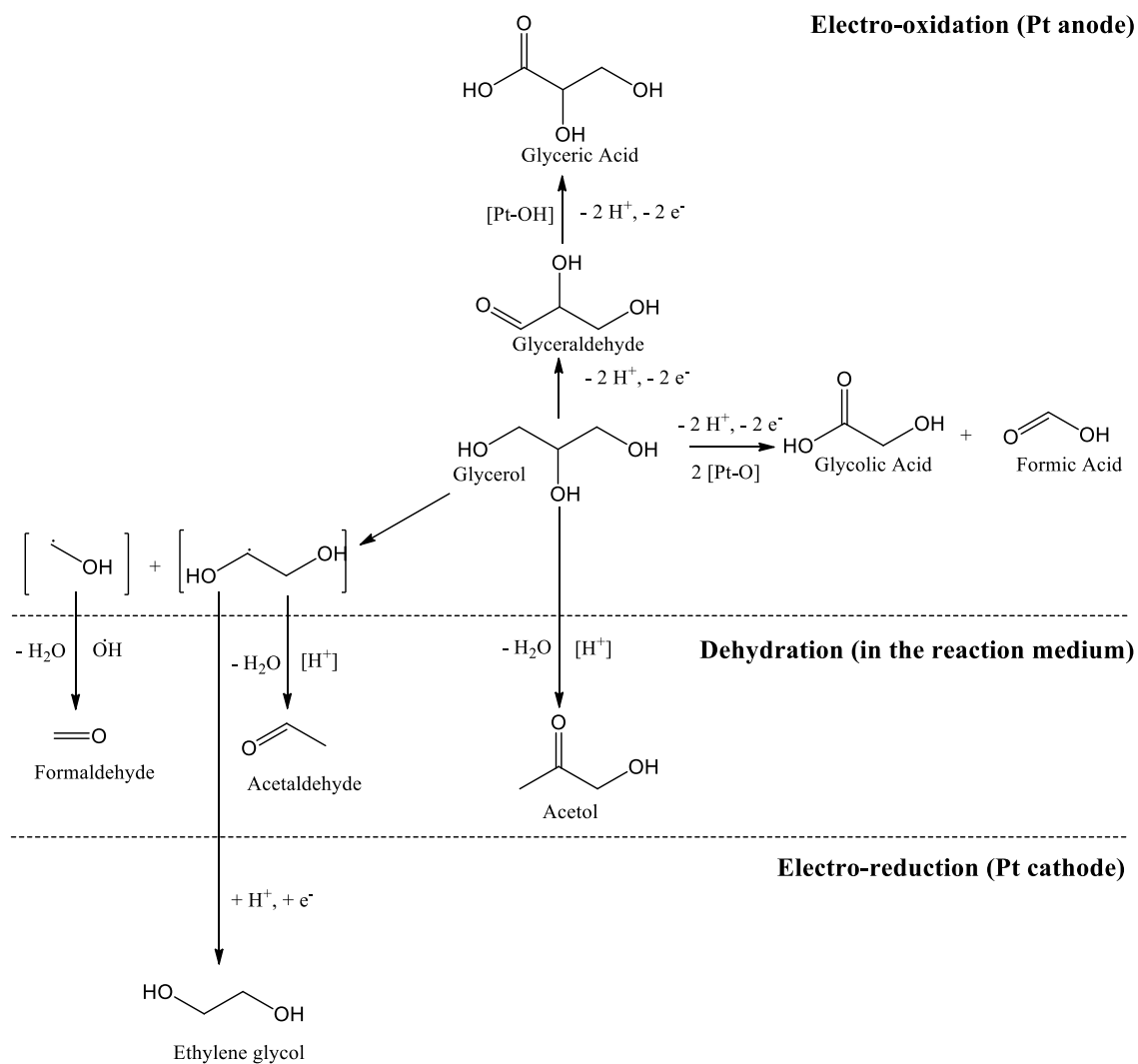
A general reaction pathway (Scheme 4.2) for electrolysis on Pt cathode electrode is proposed based on chemical compounds identified through GC-FID and GC-MS analyses. Dispersion of Amberlyst-15 in water generates hydronium ions ( $\text{H}_3\text{O}^+$ ) (Pal *et al.*, 2012). Roquet *et al.* (1994) reported that the following equilibrium can occur on the Pt electrode in acidic media:



The adsorbed OH species on the Pt surface interact and oxidize glycerol into glycerinaldehyde, which can be further oxidized into glyceric acid. Glycerol can also interact directly with the adsorbed OH on the surface of Pt to form glyceric acid. When

the reaction time is increased, stable oxides are formed on the Pt electrode surface. These oxygen molecules can interact with glycerol molecules and induce C–C bond cleavage, which leads to the formation of glycolic and formic acids (Roquet *et al.*, 1994). Furthermore, an indirect electro-oxidation pathway, which has been described in Scheme 4.1 (Section 4.2.2.1), may occur in this reaction route. Acetaldehyde and ethylene glycol are most likely obtained through oxidative cleavage of the C<sub>α</sub>–C<sub>β</sub> bond of glycerol with the hydroxyl radical (OH<sup>•</sup>) generated by adsorption of the water molecule on the electrode surface, followed by dehydration and reduction. Two free radical compounds, corresponding to C<sub>α</sub> alcohol-free radical and C<sub>β</sub> ethylene-free radical, are formed from C–C bond cleavage. The ethylene-free radical is either further dehydrated to acetaldehyde or reduced to ethylene glycol (Kongjao *et al.*, 2011; Saila *et al.*, 2015). Acetol can be obtained through dehydration by eliminating the water molecule from glycerol (Ishiyama *et al.*, 2013).

Electrochemical study of glycerol was performed in the presence of Amberlyst-15 over the Pt electrode. This novel electrochemical method successfully converted glycerol mainly into glycolic and glyceric acids. Other compounds, such as acetol, acetaldehyde, formic acid, ethylene glycol, and glyceraldehyde, were also obtained. At high reaction temperatures (80 °C) and low electric currents (1.0 A), the reaction exhibited the most remarkable glycerol conversion rate and product yield. Hence, Amberlyst-15 showed an added advantage, that is, it may work as redox catalyst during electrosynthesis. In the present study, high conversion rates were associated with glycerol decomposition into non-valuable products, such as formic acid and CO<sub>2</sub> gas.



**Scheme 4.2:** Proposed reaction mechanism of electrochemical conversion of glycerol in the presence of Amberlyst-15 on the Pt electrode.

### 4.3 Evaluation of cathode material

#### 4.3.1 SEM Analysis

SEM was used to investigate the morphology of ACC and CBD electrodes before (virgin) and after the electrochemical reaction. The scans were performed at high magnification ( $\times 50,000$  times) with image resolution of  $1.00\ \mu\text{m}$ . The SEM image [Figure 4.16(a)] shows that the virgin ACC electrode exhibits high porosity, with average pore sizes ranging from 90 nm to 170 nm. The elements present in the electrode were determined using SEM-EDX, and the spectrum is shown in Figure 4.17. The virgin ACC electrode contains three elements, namely, carbon (C), fluorine (F), and oxygen (O). C is the major element in the virgin ACC electrode, with nominal value of 75% wt, and F and O could be the elements from the binder and solvent (polytetrafluoroethylene and isopropyl alcohol) used in the electrode preparation.

The SEM image for the ACC electrode after the electrochemical reaction is shown in Figure 4.16(b). The pore sizes of this electrode evidently decreased, with average sizes ranging from 40 nm to 90 nm. This phenomenon can be explained by SEM-EDX test. The SEM-EDX spectrum in Figure 4.18 shows that sodium (Na) and sulfur (S), in addition to C, F, and O, were two other extra elements observed on the electrode surface, with corresponding nominal value of 8% wt and 10% wt. These two elements could have originated from  $\text{Na}_2\text{SO}_4$  and Amberlyst-15. Thus, the pore surface of the electrode could be covered by these compounds, subsequently reducing the pore sizes.



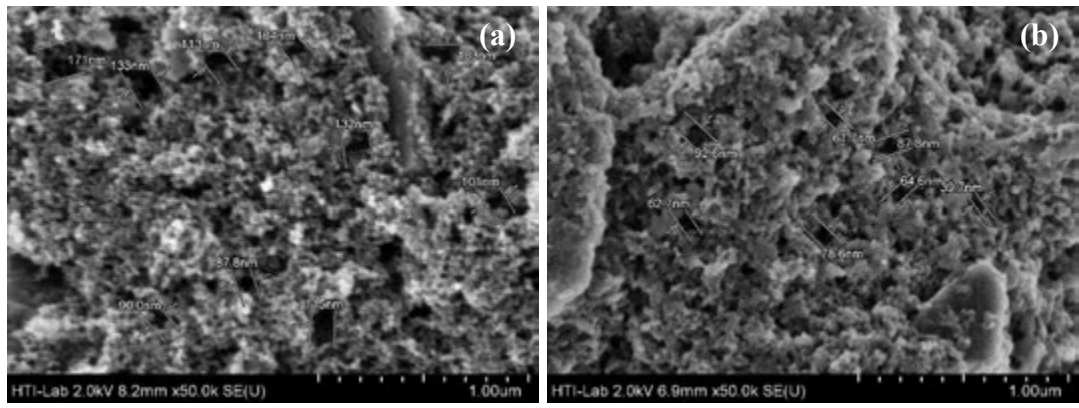


**Figure 4.16:** SEM images of (a) virgin ACC electrode and (b) ACC electrode after the electrochemical reaction.

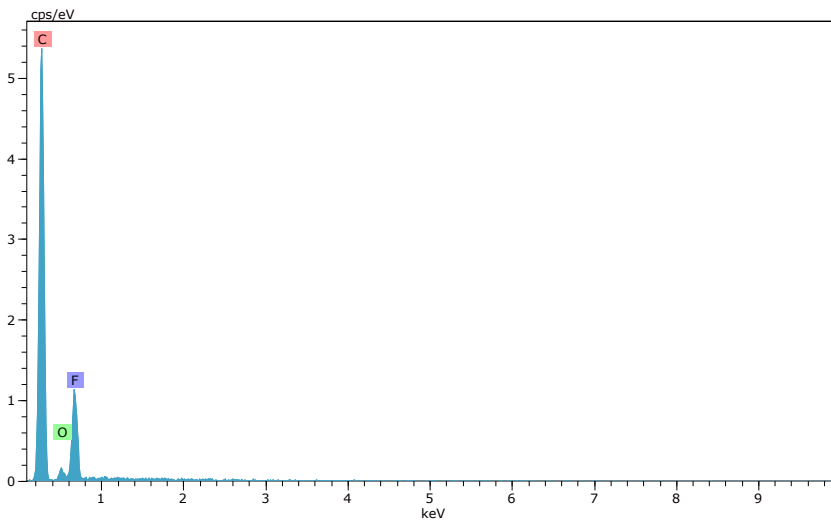


**Figure 4.17:** SEM-EDX spectrum for virgin ACC electrode.

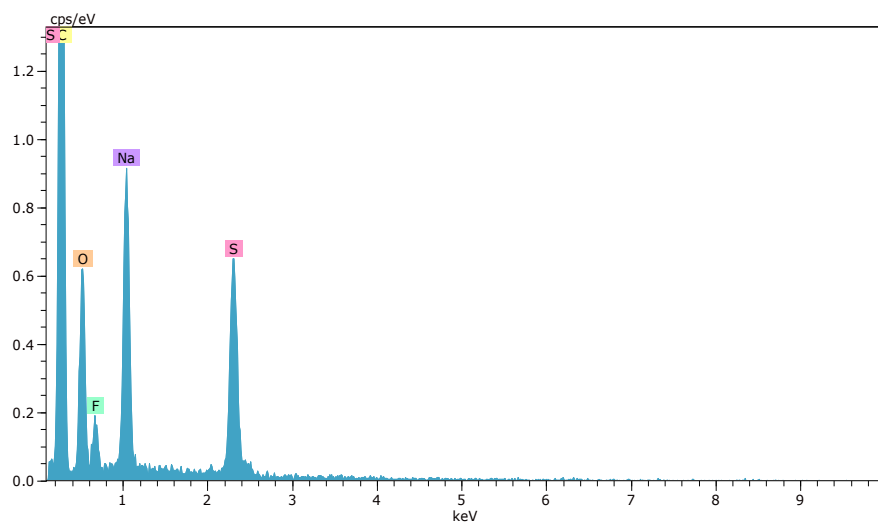


**Figure 4.18:** SEM-EDX spectrum for ACC electrode after the electrochemical reaction.

The SEM image of the virgin CBD electrode is shown in Figure 4.19(a). Pores were observed on the surface of CBD, but the pore sizes were relatively smaller (14–22 nm) and lower than those in the virgin ACC electrode (90–170 nm). The smooth surface could be due to the crystalline structure of nanodiamond. In Figure 4.20, the SEM-EDX spectrum shows that the virgin CBD electrode contains three elements, namely, C, F, and O. C was the major element with nominal value of 92% wt. F and O could be the elements from the binder and solvent. The SEM image for the CBD electrode after the electrochemical reaction is shown in Figure 4.19(b). The CBD electrode showed better physical property than the ACC electrode; the pore sizes of the former remained unchanged after long period of usage, with average size ranging from 14 nm to 22 nm. The SEM-EDX spectrum in Figure 4.21 shows that trace elements, such as Na and S, which originated from the  $\text{Na}_2\text{SO}_4$  salt, were observed at low nominal value, 3% wt and 2% wt, respectively.

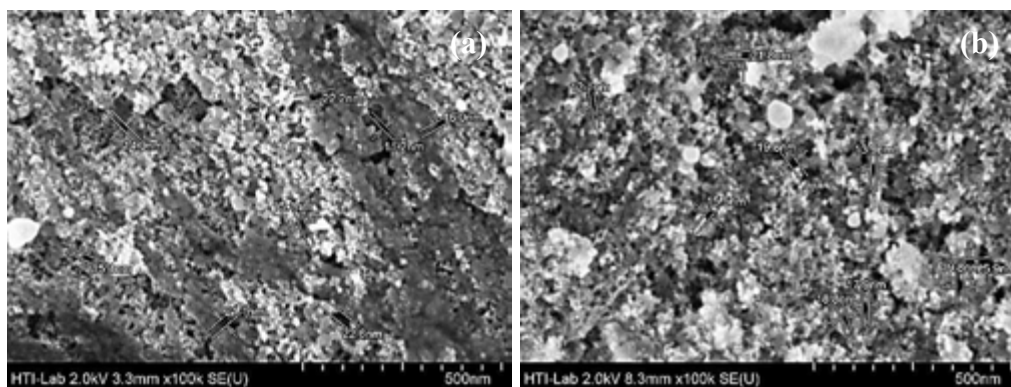


**Figure 4.19:** SEM images of (a) virgin CBD electrode and (b) CBD electrode after the electrochemical reaction.

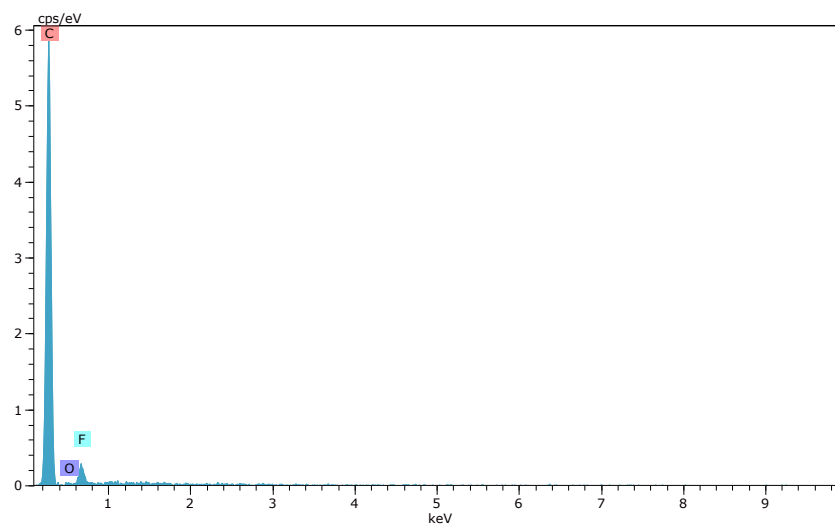


**Figure 4.20:** SEM-EDX spectrum for virgin CBD electrode.

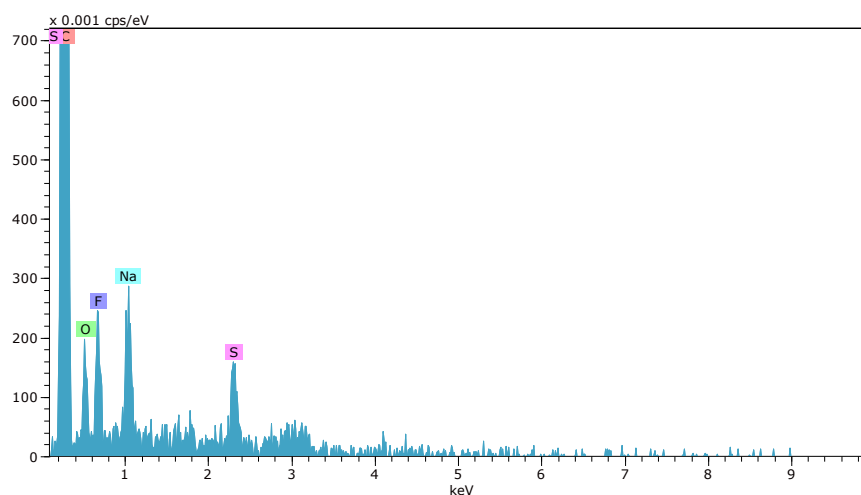


**Figure 4.21:** SEM-EDX spectrum for CBD electrode after the electrochemical reaction.

### 4.3.2 Measurement of active surface area

The Cottrell current plots for ACC and CBD electrodes are shown in Figures 4.22 and 4.23, respectively. The active surface areas were calculated based on the Cottrell plot, and the results are summarized in Table 4.3. The details of the calculation are presented in Appendix 4. The active surface areas for ACC and CBD electrodes were 7.22 and 2.80 cm<sup>2</sup>, respectively. With the same geometric area (0.45 cm<sup>2</sup>), the ACC

electrode presented higher active surface area than that of the CBD electrode. This observation could be due to the high specific surface area of activated carbon particles (950 m<sup>2</sup>/g) used in electrode preparation. The large surface area provided many active sites for the ACC electrode; the specific surface area for diamond nanopowder was within 200–400 m<sup>2</sup>/g. The large active surface area of these electrodes can improve ion transportation and electrolyte accessibility (Tang *et al.*, 2013). The porous structure can also hold or trap the reaction intermediate, thereby controlling product selectivity (Qi *et al.*, 2014b; Zhang *et al.*, 2014). In addition, the preparation cost for ACC and CBD electrodes is lower than that of the Pt electrode (Ajeel *et al.*, 2015a).

**Table 4.3:** Active surface areas for ACC and CBD electrodes estimated from Cottrell current plot.

Type of electrode	Surface areas (cm <sup>2</sup> )	Active surface areas (cm <sup>2</sup> )*
ACC	0.45	7.22
CBD	0.45	2.80

\*Note: Refer **Appendix 4** for the calculation of active surface areas

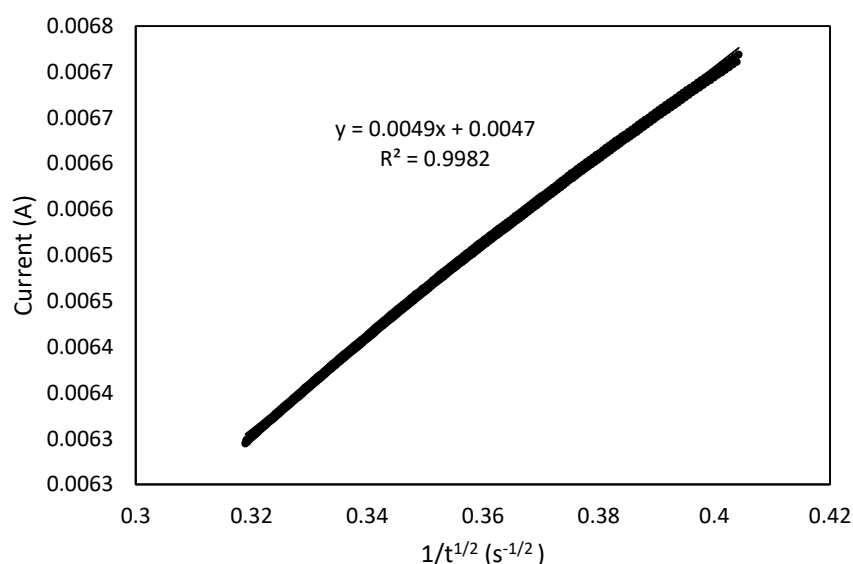


**Figure 4.22:** Cottrell current plot for ACC electrode with surface area 0.45 cm<sup>2</sup>.

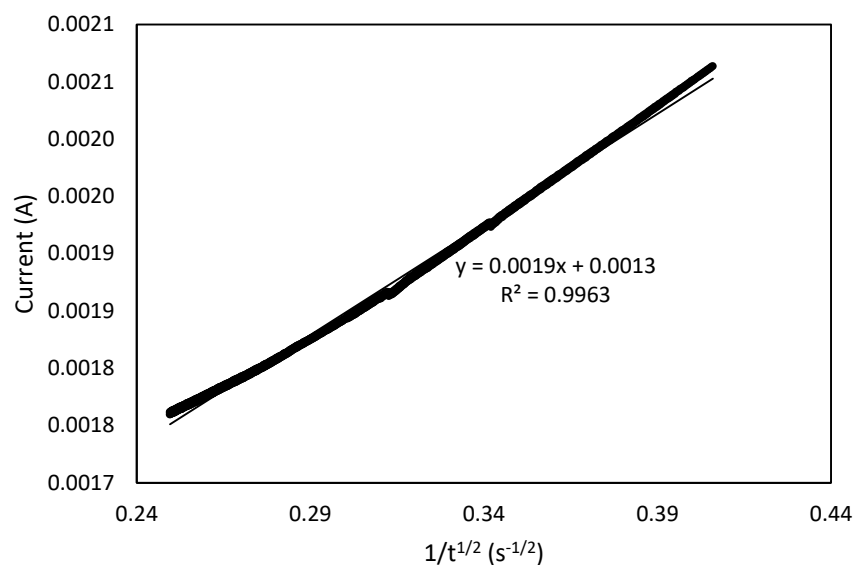


**Figure 4.23:** Cottrell current plot for CBD electrode with surface area 0.45 cm<sup>2</sup>.

### 4.3.3 CV analysis

Prior to the bulk electrochemical study, the electrochemical behavior of glycerol on ACC and CBD electrodes was examined through CV analysis in the presence of Amberlyst-15. Blank CVs without glycerol were also prepared on ACC and CBD electrodes. Scanning was performed from  $-3.00$  V to  $+3.50$  V at a scan rate of  $0.02$  Vs<sup>-1</sup>. Figure 4.24 shows the cyclic voltammogram of the ACC electrode. A pair of redox peaks was obtained at potential of  $+1.0$  (peak a) and  $-1.1$  V (peak b) in both aqueous solutions with and without glycerol. These peaks are attributed to the redox behavior of Amberlyst-15, as described in Section 4.2.1. Apart from the redox peaks of Amberlyst-15, no obvious cathodic or anodic peak was observed in the presence of glycerol. This result might be attributed to the lack of direct electron transfer on the ACC electrode with glycerol during electro-oxidation or -reduction. The electrochemical conversion of glycerol might have undergone an indirect process (Ajeel *et al.*, 2015a). Regardless of the absence of oxidation or reduction peaks for glycerol on the ACC electrode, the

cathodic current slightly increased for the glycerol solution; hence, glycerol electroreduction on the ACC electrode was favorable in the presence of Amberlyst-15.

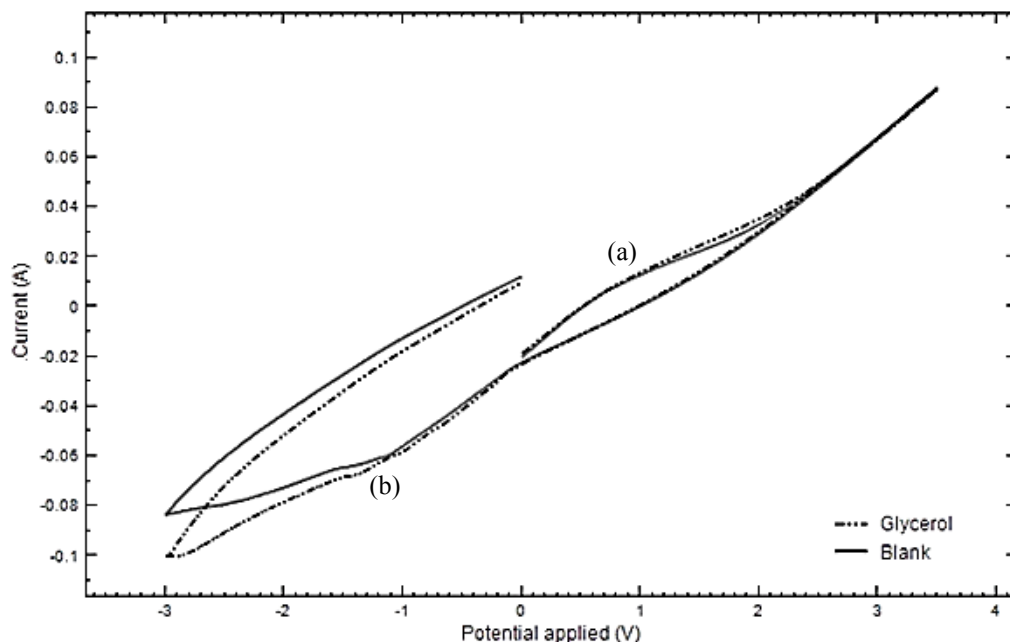


**Figure 4.24:** CV curves of Amberlyst-15 blank solution and Amberlyst-15 with glycerol solution on ACC electrode at scan range from  $-3.00$  to  $+3.50$  V versus Ag/AgCl, with potential scan rate of  $0.02$  Vs<sup>-1</sup>.

Figure 4.25 shows the electrochemical behavior in the presence of Amberlyst-15 with or without glycerol on the CBD electrode. In the blank solution CV curve, an oxidation slope was observed at the potential of  $+1.5$  V (peak a) and a reduction peak at  $-0.5$  V (peak b) versus Ag/AgCl. These oxidation and reduction peaks correspond to the redox behavior of Amberlyst-15. In the presence of glycerol, the same redox peaks were observed at the electrode potential of  $+1.5$  (peak a<sup>1</sup>) and  $-0.7$  V (peak b<sup>1</sup>). Similar to that on the ACC electrode, the electrochemical reaction on the CBD electrode is an indirect process because no additional peaks were observed other than the pair of the redox peaks and the current density increased in the presence of glycerol solution.

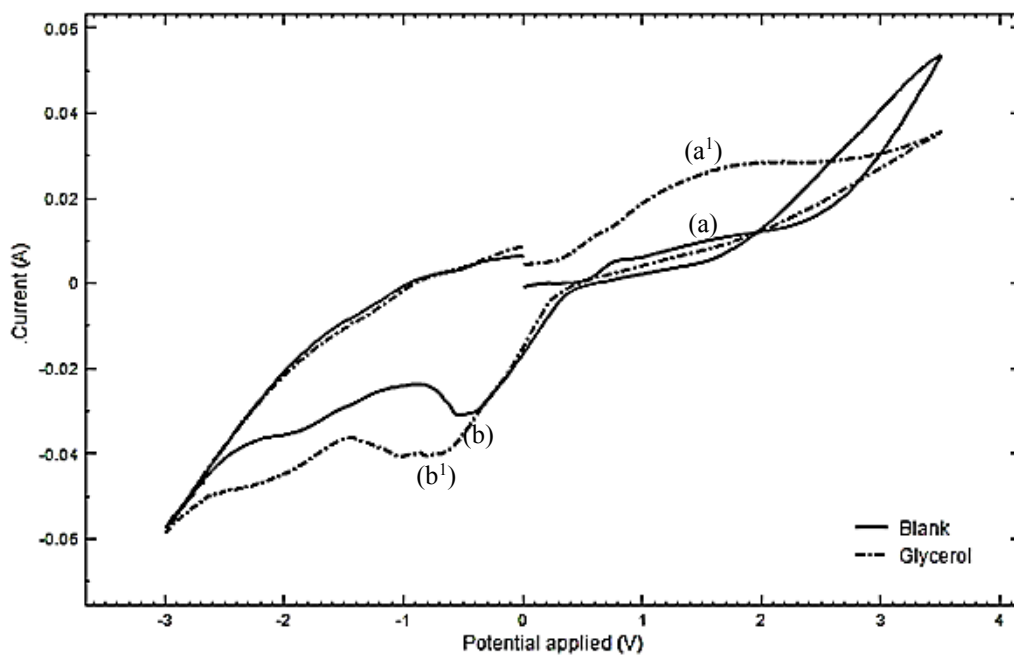


**Figure 4.25:** CV curves of Amberlyst-15 blank solution and Amberlyst-15 with glycerol solution on CBD electrode at scan range from  $-3.00$  to  $+3.50$  V versus Ag/AgCl, with potential scan rate of  $0.02$  Vs $^{-1}$ .

#### 4.3.4 Electrochemical conversion of glycerol over ACC and CBD cathode electrodes

The electrochemical conversion of glycerol was performed in the presence of Amberlyst-15 over ACC (active areas:  $69.4$  cm $^2$ ) and CBD (active areas:  $14.1$  cm $^2$ ) cathode electrodes. The first trials were carried out based on the optimum condition attained through the study on the Pt electrode (in Section 4.2.2). The glycerol conversions were above 95%, and the conversion rates were between  $0.550$  h $^{-1}$  to  $0.600$  h $^{-1}$  (Figures 4.26 and 4.27).

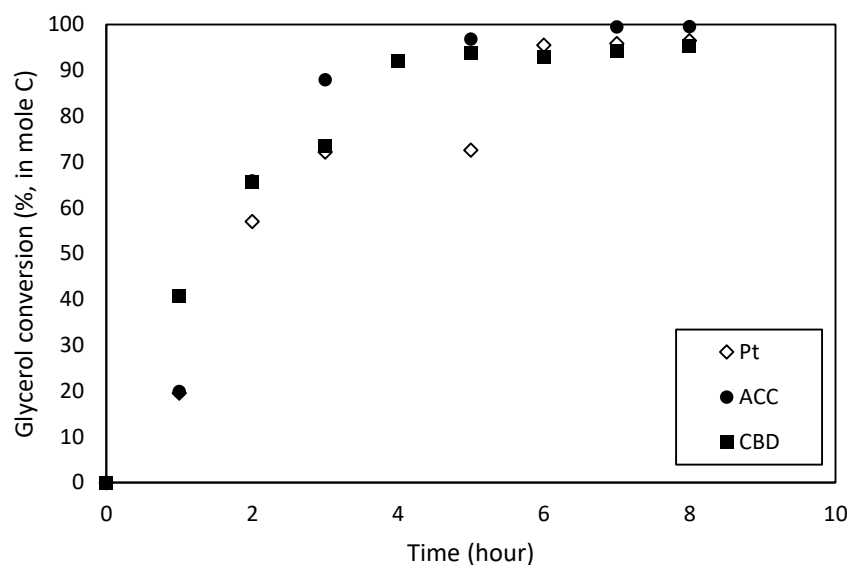


**Figure 4.26:** Glycerol conversion from the electrochemical study on (a) Pt, (b) ACC and (c) CBD cathode electrodes in the presence of Amberlyst-15 at 80 °C and 1.0 A constant current.

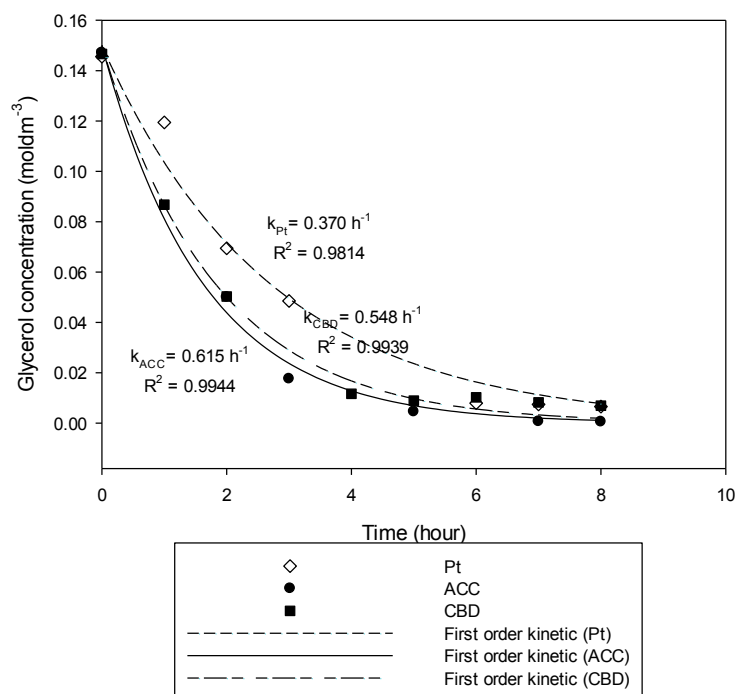


**Figure 4.27:** First-order kinetic model of the electrochemical conversion of glycerol in the presence of Amberlyst-15 on (a) Pt, (b) ACC, and (c) CBD cathode electrodes at 80 °C and 1.0 A constant current.



The compounds obtained on these two electrodes are shown in the GC chromatogram in Figures 4.28(a) and 4.28(b). The electrolysis reactions on ACC and CBD electrodes produced a larger variety of compounds than those on the Pt electrode (Figure 4.15 in Section 4.2.2.4). Glycolic and lactic acids were the major reaction products generated with the ACC cathode. In addition, acetaldehyde, acetol, glyceraldehyde, 1,2-PDO, 1,3-PDO, formic acid, acetic acid, and ethylene glycol were obtained. In the primary study on CBD cathode electrode, lactic acid was not observed in the reaction mixtures. The GC-MS spectra of each compound obtained in the reaction mixtures are shown in Appendix 1.

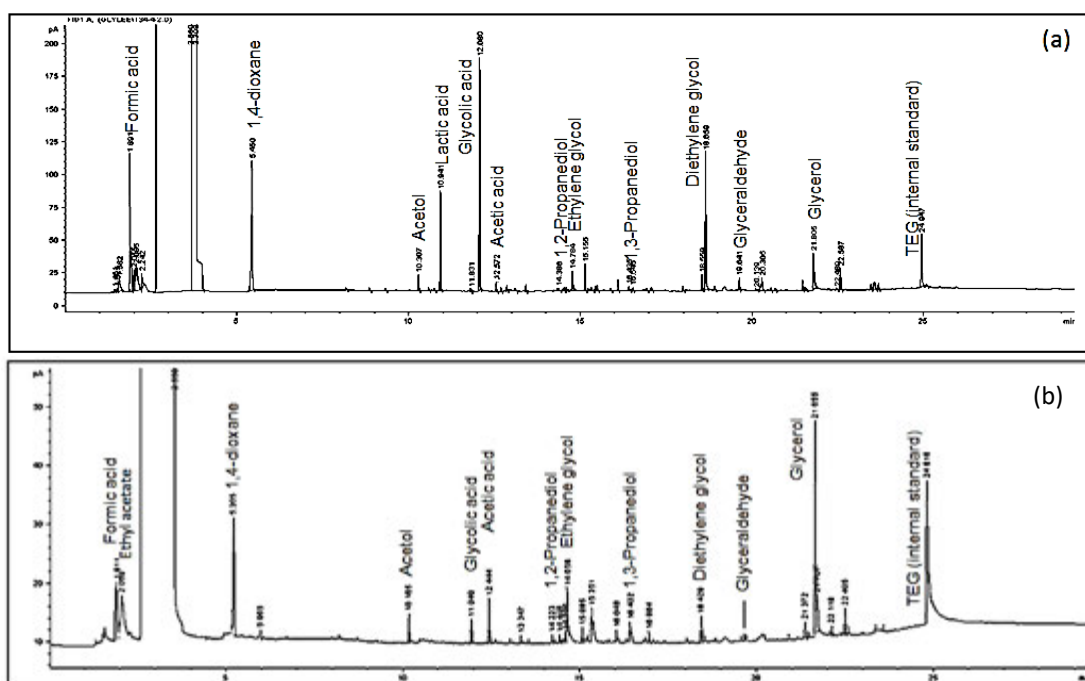


**Figure 4.28:** GC chromatogram of the products obtained from the electrochemical conversion of glycerol in the presence of Amberlyst-15 on (a) ACC and (b) CBD cathode electrodes at 80 °C and 1.0 A constant current.

The product distribution from the study on ACC cathode electrode is shown in Figure 4.29(b). Glycolic and lactic acids were the major compounds produced from the reaction, and the highest yield was obtained after 5 h, with corresponding values of 55.6% and 28.5%, respectively. The product selectivity for glycolic and lactic acids was 57.8% and 29.7%, respectively. Lactic acid exhibits significant usage in the food industry (Bagheri *et al.*, 2015). Similar to the study on the Pt cathode, C–C bond breaking of glycerol was favored at high reaction temperatures and produced a 2C compound (glycolic acid). Furthermore, reduction compounds, such as 1,2-PDO and 1,3-PDO, were produced on the ACC cathode electrode, in addition to the formation of acetaldehyde, acetol, ethylene glycerol, and glyceraldehyde. The concentrations of these compounds increased slowly and were only detected in trace amounts until 3 (1,3-PDO) and 6 h (1,2-PDO) of the reaction. Nevertheless, glyceric acid was not obtained on the ACC cathode electrode but was only found when both cathode and anode electrodes contained active metals, such as Pt. As presented in the earlier Section 4.2.2, glycolic and glyceric acids were the main compounds obtained through electrolysis on the Pt cathode electrode, with yields of 44.7% and 27.2%, respectively [Figure 4.29(a)]. The major compounds with the maximum yield and selectivity obtained through the studies on Pt, ACC, and CBD cathode electrodes are summarized in Table 4.4.

**Table 4.4:** Electrochemical conversion of glycerol in the presence of Amberlyst-15 over Pt, ACC and CBD cathode electrodes; the yield and selectivity for glycolic, glyceric and lactic acids at the maximum level.

Electrode		Electrolyte/Acid	I (A)	T (°C)	Glycerol conversion*		Yield (Y) & Selectivity (S) (% in mole C)					
<u>A</u>	<u>C</u>				%	k (h <sup>-1</sup> )	<u>Glycolic acid</u>		<u>Glyceric acid</u>		<u>Lactic acid</u>	
						Y	S	Y	S	Y	S	
Pt	Pt	Amberlyst-15	1.0	80	96.5	0.370	44.7 (6h)	46.8 (6h)	27.2 (5h)	37.6 (5h)	Nil	Nil
Pt	ACC	Amberlyst-15	1.0	80	99.6	0.615	55.6 (5h)	57.8 (5h)	Nil	Nil	28.5 (5h)	29.7 (5h)
Pt	CBD	Amberlyst-15	1.0	80	95.3	0.548	7.4 (4h)	24.3 (4h)	Nil	Nil	Nil	Nil

Note: \*After 8 h of reaction time. Total reaction time: 8 h  
A: Anode; C: Cathode; I: current; T: reaction temperature; k: rate constant  
Nil: zero value

According to the product distribution graph for the CBD electrode in Figure 4.29(c), glycolic acid was produced after 1 h of electrolysis and achieved the maximum level after 4 h, with 7.4% yield and 24.3% selectivity. Formic acid and ethyl acetate were two other major products generated, with yields of 6.4% and 6.0%, respectively. The product distribution using the CBD electrode is similar to that when using the ACC electrode. Acetic acid, ethylene glycol, 1,2-PDO, and 1,3-PDO were also obtained when using the CBD electrode.

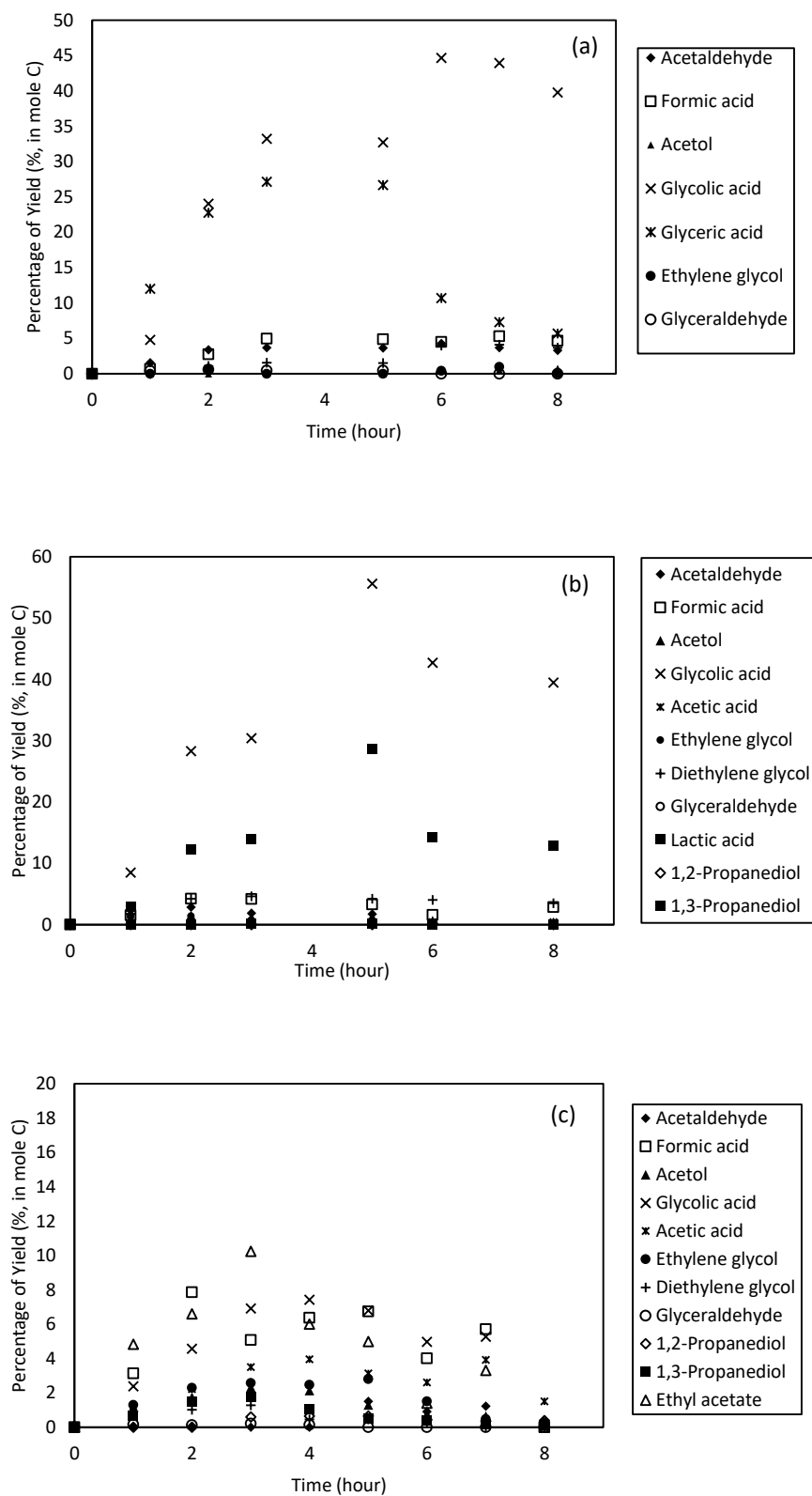
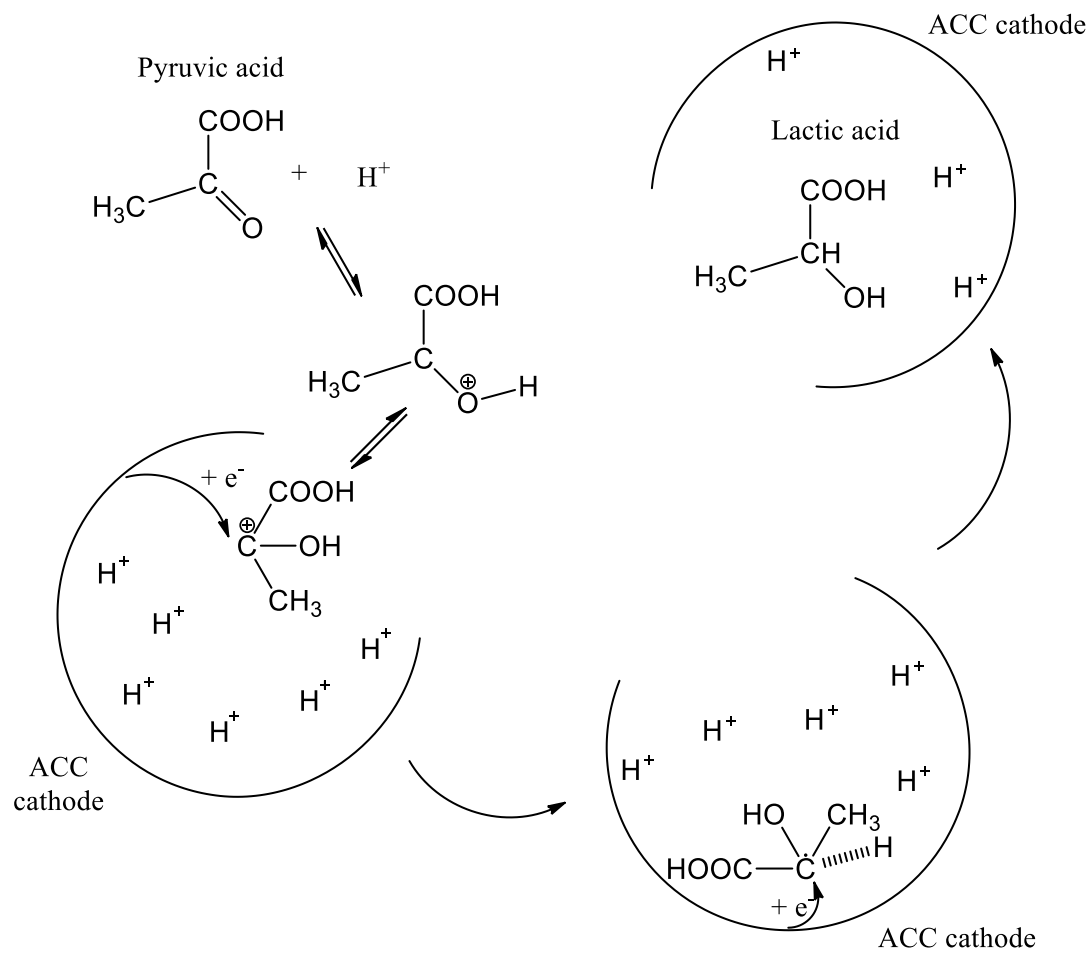


**Figure 4.29:** Product distribution from the electrochemical conversion of glycerol in the presence of Amberlyst-15 on (a) Pt, (b) ACC, and (c) CBD cathode electrodes at 80 °C and 1.0 A constant current.

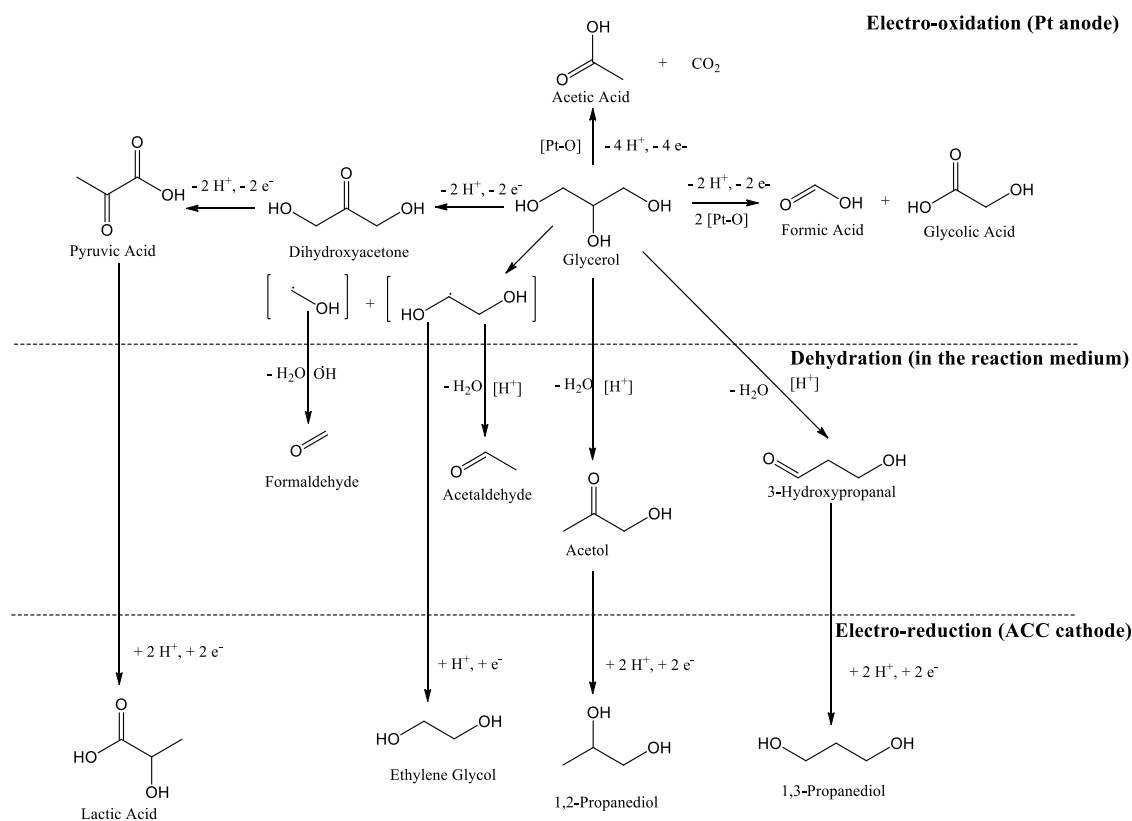
#### 4.3.5 Reaction mechanism

In the preliminary study on the Pt electrode, glycolic and glyceric acids were the major products generated. In the electrochemical study on the ACC electrode, lactic acid was obtained, instead of glyceric acid. According to Simões *et al.* (2012), selection of the reaction pathway (glyceraldehyde pathway or DHA pathway) is mainly controlled by few factors, such as applied potential, electrode material, and pH of the reaction medium. In the present work, although the same Pt anode material was used in both case studies, the reaction pathway involved in the electro-oxidation for these two studies were dissimilar because different cathode materials (Pt and ACC) were used.

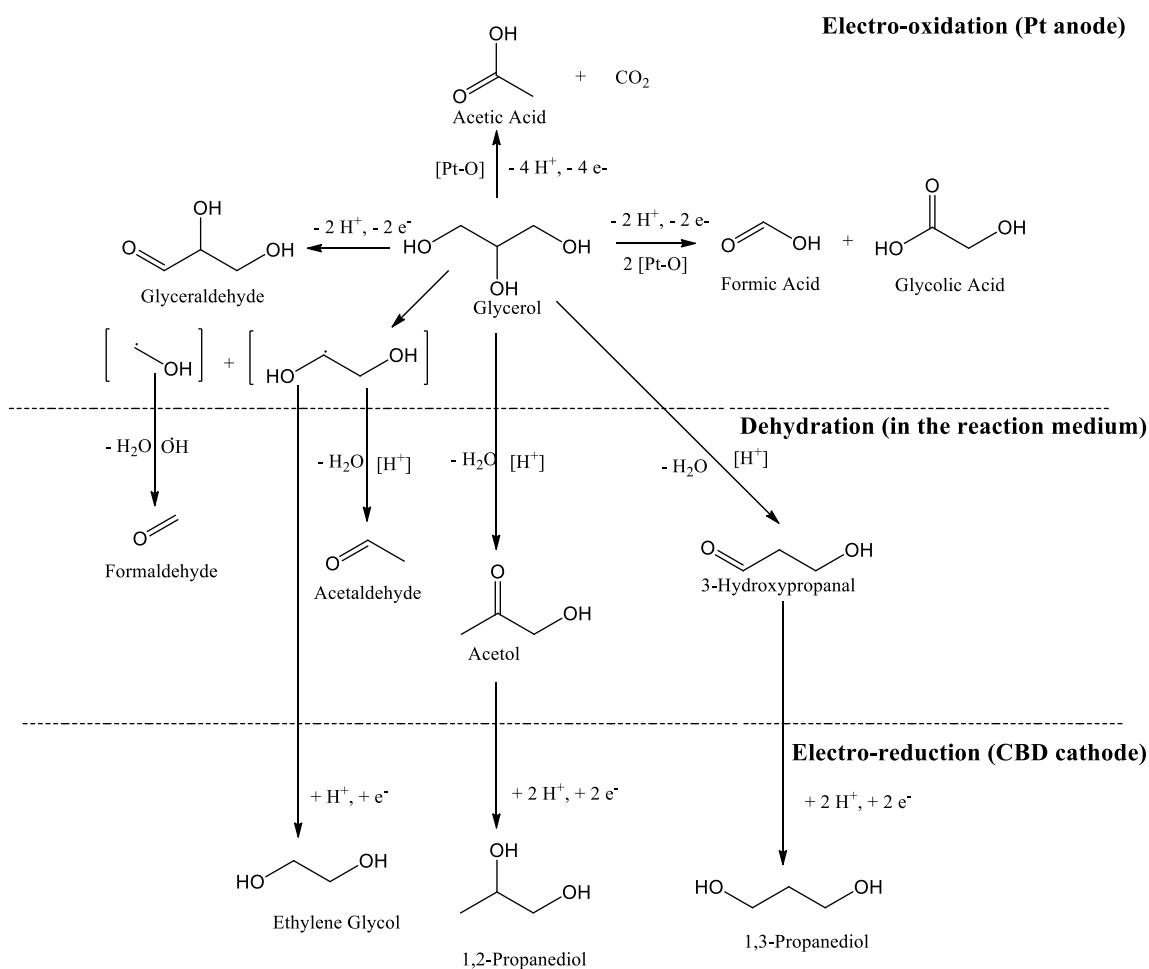
In this case, glycerol might have undergone the DHA pathway. Nevertheless, DHA compound could not be identified through the GC-MS analysis because it is unstable in acidic media due to the enolization reaction (Van de Vyver *et al.*, 2015). DHA continued to be oxidized into pyruvic acid. The reaction was carried out in a one-pot electrochemical cell; thus, pyruvic acid was immediately converted into lactic acid through the electroreduction pathway (Martin *et al.*, 2005, 2006), and pyruvic acid could not be identified. Acetic acid could be obtained from the over-oxidation of glycerol (Gomes and Martins, *et al.*, 2013). The porous surface of the ACC electrode could hold the reaction intermediates from dehydration and oxidation (e.g., pyruvic acid, acetol, and hydroxypropanal), thereby facilitating the electroreduction process (Qi *et al.*, 2014a) (Scheme 4.3). 1,2-PDO and 1,3-PDO were probably obtained from the reduction of acetol and hydroxypropanal, respectively (Hunsom *et al.*, 2015). Glycolic acid was formed through C–C bond cleavage of glycerol during oxidation at the anodic region. The reaction mechanism is proposed in Scheme 4.4. For the study on the CBD cathode electrode, glycerol underwent similar reaction pathway to that in the study with the ACC cathode electrode, except for lactic acid formation. The reaction mechanism is shown in Scheme 4.5.



**Scheme 4.3:** Electoreduction of pyruvic acid on the porous ACC cathode electrode.



**Scheme 4.4:** Proposed reaction mechanism of the electrochemical conversion of glycerol in the Amberlyst-15 medium on ACC cathode electrode and Pt anode electrode.



**Scheme 4.5:** Proposed reaction mechanism of the electrochemical conversion of glycerol in the Amberlyst-15 medium on CBD cathode electrode and Pt anode electrode.

According to the studies on ACC and CBD electrodes, the porous surface of these electrodes provided the possibility to reduce glycerol into 1,2-PDO and 1,3-PDO. The ACC electrode can also reduce pyruvic acid into lactic acid, which is used in the food industry and platform molecule for polymer. High active surface areas can improve the electrochemical performance. For example, ACC electrode produced higher amount of glycolic acid compared with CBD electrode, because the active surface areas of the ACC electrode are 2.5-fold higher than those of the CBD electrode with the same



geometric surface. Therefore, the active surface areas of ACC and CBD electrodes were standardized in the following optimization studies (as mentioned earlier in the methodology Section 3.2.3).

#### 4.4 Optimization study on the ACC cathode electrode

In this section, the effects of solid catalyst amount, applied electric current, and reaction temperature on the production of glycolic and lactic acids from the glycerol electrochemical study on the ACC cathode electrode were studied. The maximum product yield and selectivity obtained in each trial are summarized in Table 4.5. The results showed that glycerol conversion and product formation highly depended on reaction parameters applied. Under the reaction conditions (80 °C, electric current at 2.0 A, and 9.6% w/v solid acid catalyst), glycolic and lactic acids were successfully electrosynthesized from glycerol, with product yields of 66.1% and 14.8%, respectively.

**Table 4.5:** Electrochemical conversion of glycerol in the presence of Amberlyst-15 over ACC cathode electrode; the yield and selectivity for glycolic and lactic acids at the maximum level.

Elec-trode	Electrolyte/ Acid	I (A)	Amount of acid catalyst (% w/v)	T (°C)	Glycerol Conversion*		Yield (Y) & Selectivity (S) (%, in mole C)			
					%	k (h <sup>-1</sup> )	Lactic acid		Glycolic acid	
							Y	S	Y	S
ACC	Amberlyst-15	2.0	6.4	80	99.5	0.635	18.6 (6h)	20.7 (6h)	55.8 (6h)	62.1 (6h)
ACC	Amberlyst-15	2.0	9.6	80	99.3	0.724	14.8 (6h)	16.2 (6h)	66.1 (6h)	72.0 (6h)
ACC	Amberlyst-15	2.0	12.8	80	99.0	0.499	4.9 (5h)	10.1 (5h)	39.0 (5h)	79.9 (5h)
ACC	Amberlyst-15	2.0	9.6	RT	98.1	0.406	0.6 (7h)	3.5 (7h)	5.1 (7h)	30.9 (7h)
ACC	Amberlyst-15	2.0	9.6	50	92.6	0.402	3.6 (7h)	23.7 (7h)	8.0 (7h)	51.7 (7h)
ACC	Amberlyst-15	1.0	9.6	80	94.5	0.310	7.1 (8h)	31.2 (8h)	5.6 (8h)	24.6 (8h)
ACC	Amberlyst-15	3.0	9.6	80	99.3	0.685	25.9 (5h)	32.5 (5h)	34.8 (5h)	44.1 (5h)

Note: RT: Room temperature (27 °C); I: current; T: reaction temperature; k: rate constant  
[Glycerol]: 0.30 M

\*After 8 h of reaction time. Total reaction time: 8 h

Nil: zero value

ACC: Activated carbon composite electrode

#### 4.4.1 Effect of catalyst amount

The effect of catalyst concentration for Amberlyst-15 was studied in the electrochemical conversion of glycerol at 80 °C and electric current of 2.0 A for 8 h. The amount of Amberlyst-15 varied from 6.4% w/v to 12.8% w/v (Table 4.5). The glycerol conversions were above 99% (Figure 4.30), and the conversion rate increased slightly from 0.635 h<sup>-1</sup> to 0.724 h<sup>-1</sup> with increasing amount of Amberlyst-15 from 6.4% w/v to 9.6% w/v (Figure 4.31). However, when the amount of Amberlyst-15 was increased further to 12.8% w/v, the conversion rate slightly decreased. The yields for glycolic and lactic acids were also reduced. The decrease in catalytic activity of Amberlyst-15 could be due to the poisoning effect of the catalyst during the reaction. When the desired products compete with the reactant for chemisorption on the active sites, the reaction is self-inhibited. This self-inhibition effect can decrease the conversion rate (Bühler *et al.*, 2002; Farma *et al.*, 2013). In the present study, glycolic acid competed with glycerol for the active sites to be oxidized further into smaller compounds, such as CO<sub>2</sub>; consequently, the conversion rate and product yield decreased.

When increasing the amount of solid acid catalyst (Amberlyst-15) in the reaction medium, the product distributions varied (Figure 4.32). The maximum glycolic acid yield of 66.1% with selectivity of 72.0% was attained at 6 h by using 9.6% w/v Amberlyst-15. Nonetheless, lactic acid was favorably produced at low concentrations of Amberlyst-15 (6.4% w/v), with product yield of 18.6% after 6 h of electrolysis. No major improvement in the catalytic performance was observed with further increase in catalyst amount to 12.8% w/v. Moreover, the product yield reached the maximum value with 9.6% w/v Amberlyst-15 (Figure 4.33). This result indicated that 9.6% w/v Amberlyst-15 was sufficient to obtain the maximum glycerol conversion and product

yield; thus, in the following studies, the reaction was performed in the presence of 9.6% w/v Amberlyst-15.

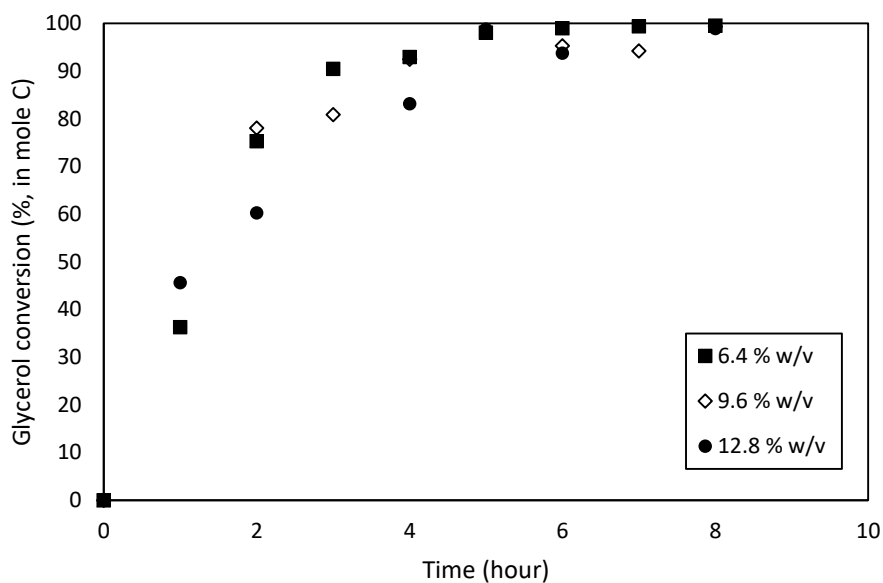


**Figure 4.30:** Glycerol conversion from the electrochemical study on ACC cathode electrode at 80 °C, 2.0 A constant current and in the presence of Amberlyst-15 varied from 6.4% w/v to 12.8% w/v.

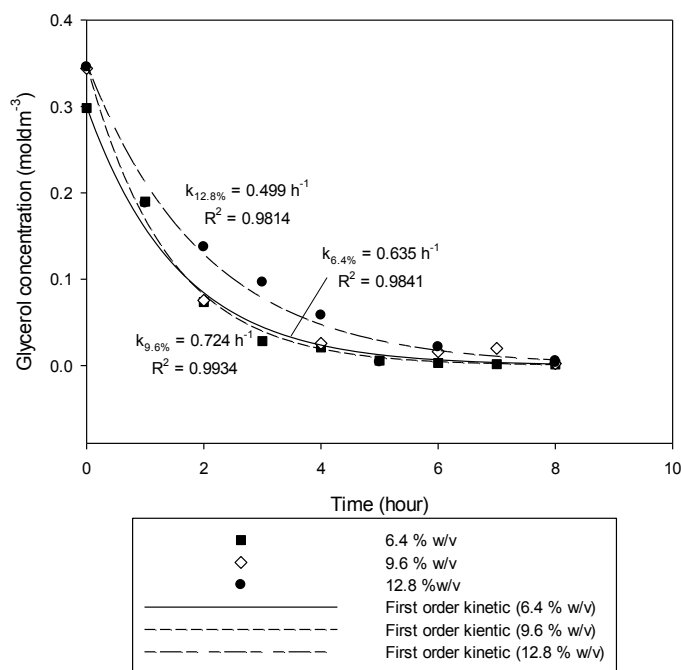


**Figure 4.31:** First-order kinetic model of the electrochemical conversion of glycerol in the presence of Amberlyst-15 varied from 6.4 to 12.8% w/v on ACC cathode electrode at 80 °C and 2.0 A constant current.

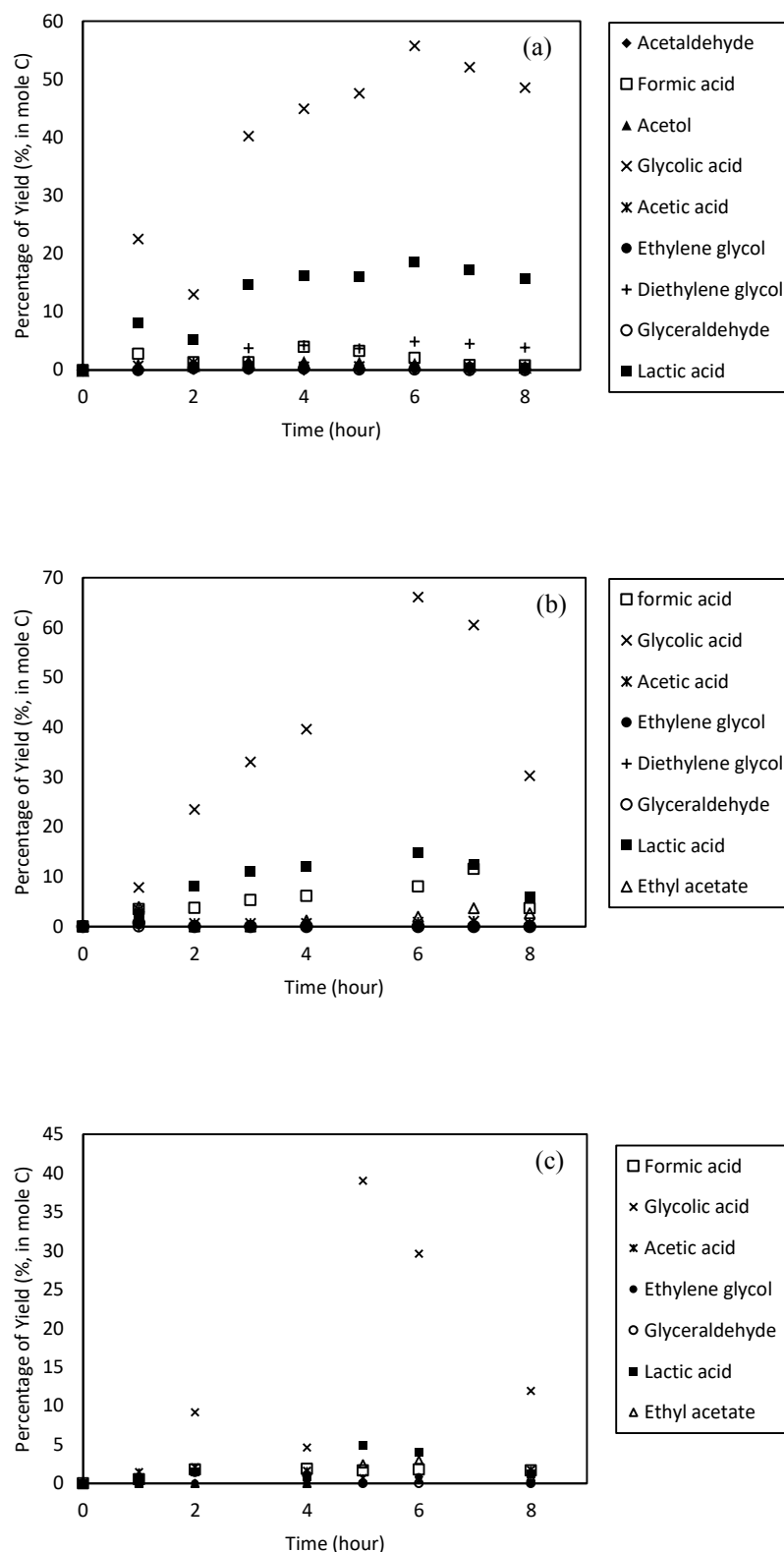


**Figure 4.32:** Product distribution from the electrochemical conversion of glycerol in the presence of Amberlyst-15 at (a) 6.4% w/v, (b) 9.6% w/v, and (c) 12.8% w/v on ACC cathode electrode at 80 °C and 2.0 A constant current.

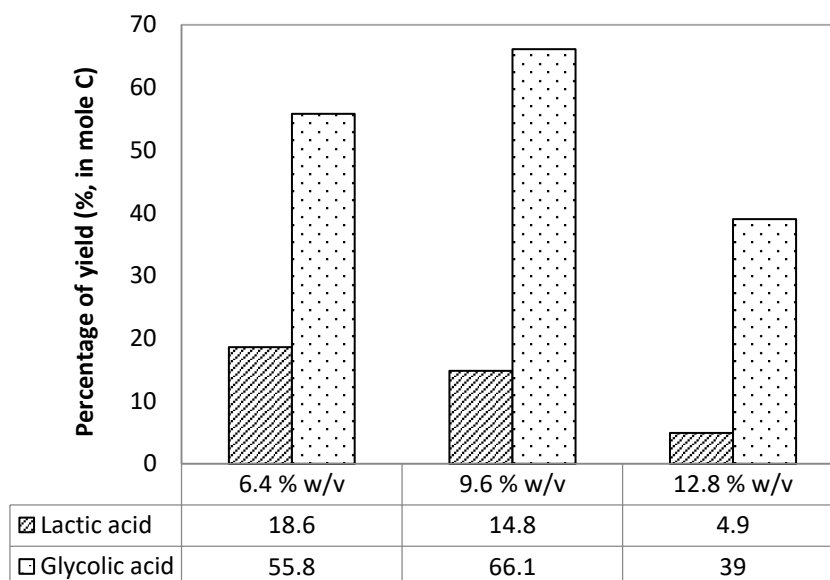


**Figure 4.33:** Maximum yield of glycolic and lactic acids obtained from the electrochemical conversion of glycerol in the presence of 6.4% w/v, 9.6% w/v, and 12.8% w/v Amberlyst-15 on ACC cathode electrode at 80 °C and 2.0 A constant current.

#### 4.4.2 Effect of reaction temperature

The effect of reaction temperature was studied from room temperature (27 °C) to 80 °C in the presence of 9.6% w/v Amberlyst-15 at 2.0 A for 8 h. The graph shown in Figure 4.34 indicates that glycerol conversions above these temperatures reached the maximum of 90%. At room temperature (27 °C) and 50 °C, the conversion rates were 0.406 and 0.402 h<sup>-1</sup>, respectively. The conversion rate slowly increased to 0.724 h<sup>-1</sup> with increasing reaction temperature (Figure 4.35).

The bar chart in Figure 4.36 illustrates that lactic acid yield increased from 0.6% to 14.8%, and the glycolic acid yield increased from 5.1% to 66.1% with increasing reaction temperature. At a high temperature of 80 °C, the formation of glycolic acid was faster than that of lactic acid, with 66.1% yield and 72.0% selectivity after 6 h of electrolysis. Similar to the preliminary study discussed in Section 4.2.2.3, at high temperatures, a large amount of energy was available to break the glycerol C–C bond,

thereby converting it to glycolic acid. At room temperature (27 °C) and 50 °C, the yield and selectivity for glycolic and lactic acids were low. The increase in temperature could favor OH adsorption on the electrode surface. The presence of this adsorbed OH submonolayer can reduce the barrier for both C–H and O–H bond dissociations and enhance the oxidation behavior (Beden *et al.*, 1987; Yang *et al.*, 2012; Zhang *et al.*, 2012a). The increase in the reaction temperature can also effectively reduce the thickness of the diffusion layer (Gupta *et al.*, 1984), thereby increasing the diffusion rate of the oxidized compounds (pyruvic acid) at the ACC cathode electrode; consequently, the reduction process was enhanced, leading to the formation of lactic acid. According to the product distribution graphs in Figure 4.37, formic and acetic acids were generally present in the three runs. Other compounds, such as ethylene glycol, DEG, acetaldehyde, glyceraldehyde, and ethyl acetate, were produced inconsistently. In this study, the formation of glycolic and lactic acids was pronounced at high temperatures, that is, 80 °C. Therefore, this temperature was applied in the following studies.

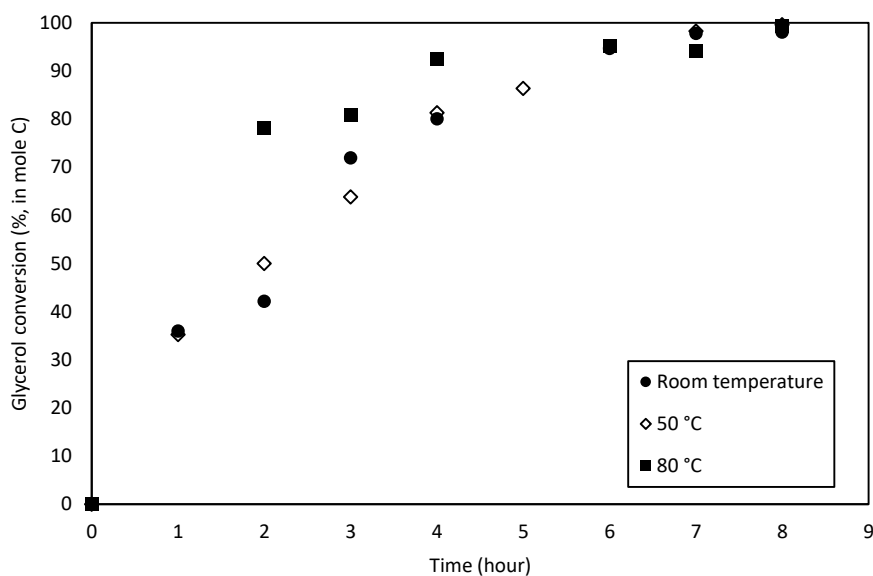


**Figure 4.34:** Glycerol conversion from the electrochemical study on ACC cathode electrode in the presence of 9.6% w/v Amberlyst-15 at 2.0 A constant current at room temperature (27 °C), 50 °C, and 80 °C.

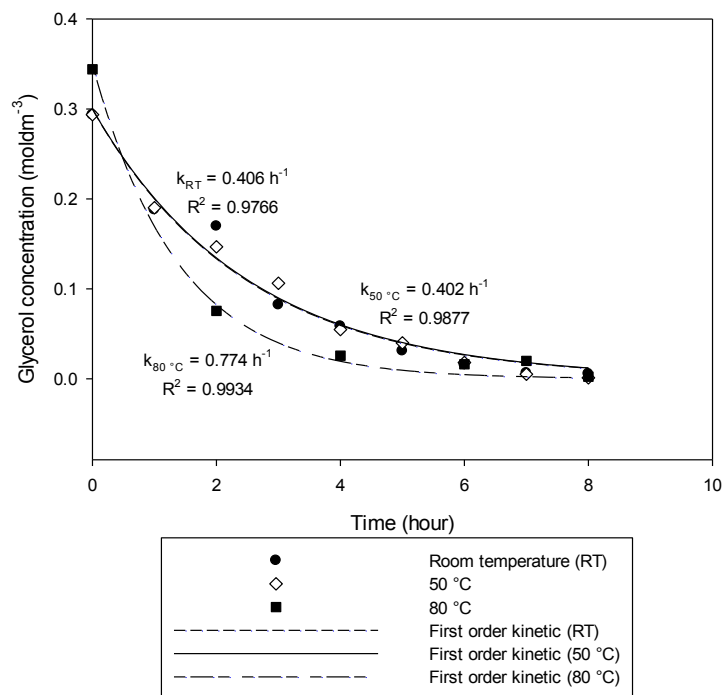


**Figure 4.35:** First-order kinetic model of the electrochemical conversion of glycerol in the presence of 9.6% w/v Amberlyst-15 on ACC cathode electrode at 2.0 A constant current at room temperature (27 °C), 50 °C, and 80 °C.

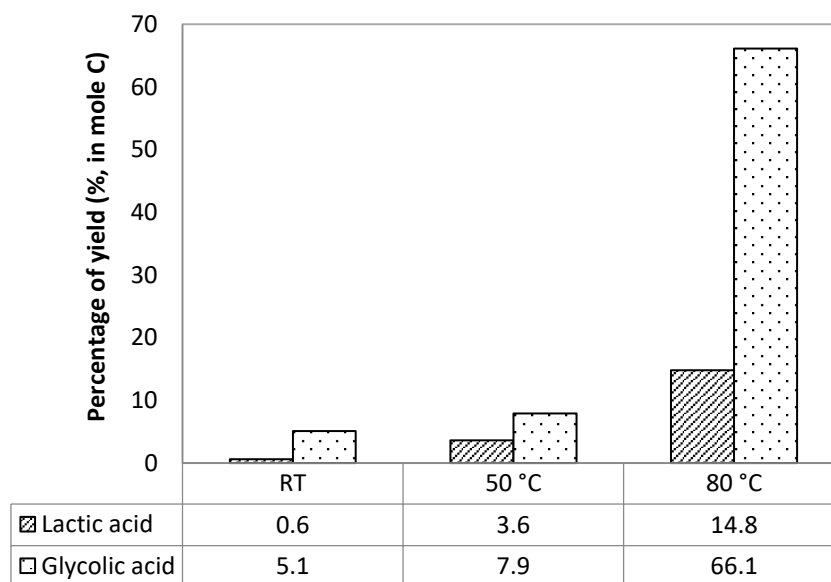


**Figure 4.36:** Maximum yield of glycolic and lactic acids obtained from the electrochemical conversion of glycerol in the presence of 9.6% w/v Amberlyst-15 on ACC cathode electrode at 2.0 A constant current at (a) room temperature, 27 °C (RT), (b) 50 °C, and (c) 80 °C.

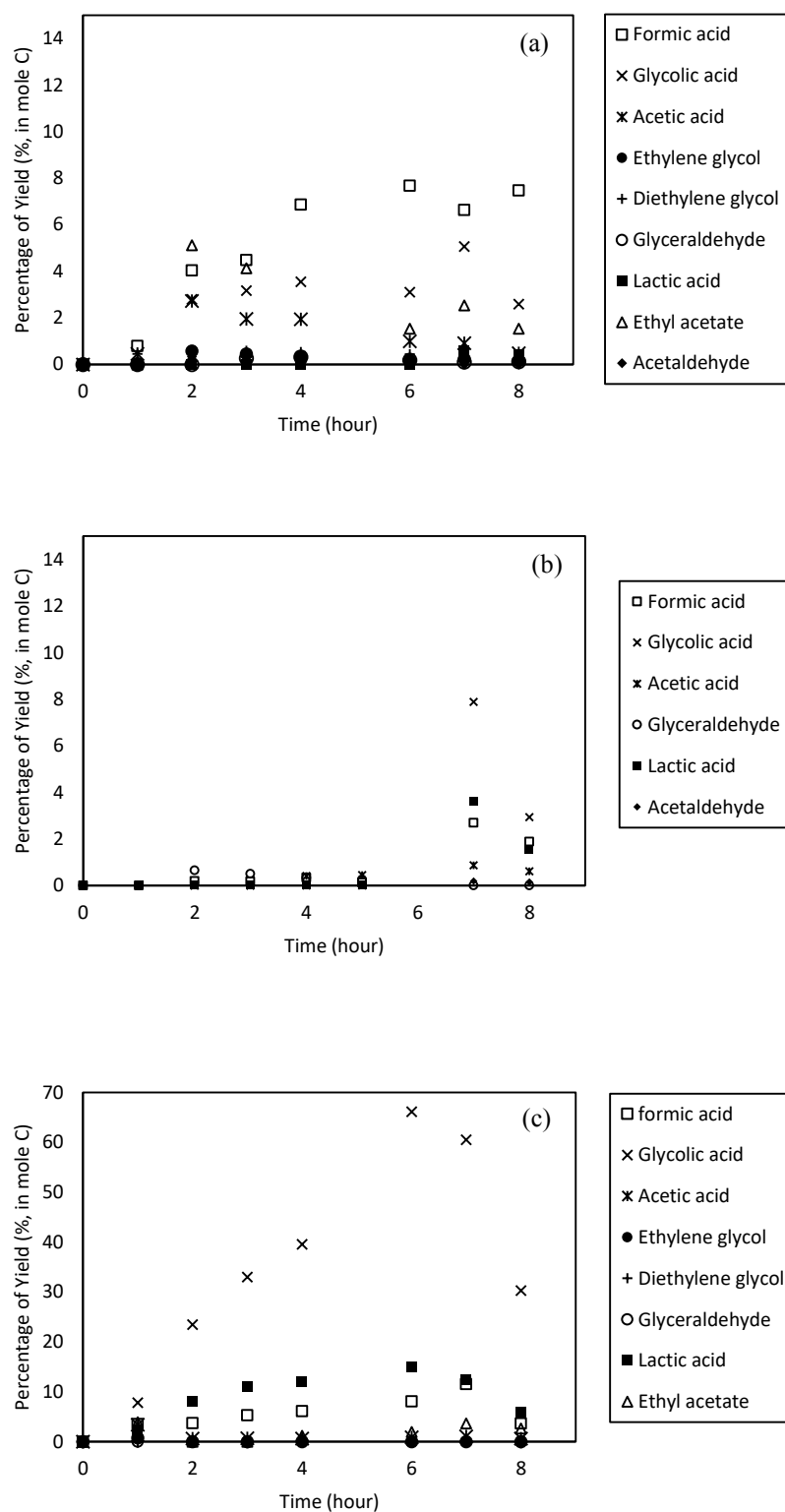


**Figure 4.37:** Product distribution from the electrochemical conversion of glycerol in the presence of 9.6% w/v Amberlyst-15 on ACC cathode electrode at 2.0 A constant current at (a) room temperature (27 °C), (b) 50 °C, and (c) 80 °C.



#### 4.4.3 Effect of electric current

The effect of electric current within 1.0–3.0 A was studied in the presence of 9.6% w/v Amberlyst-15 at 80 °C for 8 h (Table 4.5 in Section 4.4). The maximum glycerol conversion of 99% was attained after 5 h of reaction at an applied current of 3.0 A. The reaction under applied current of 2.0 A for 8 h also led to 99% of glycerol conversion; at lower electric current of 1.0 A, the maximum glycerol conversion of 94% was obtained after 8 h (Figure 4.38). In accordance with Faraday's Law, the glycerol conversion rate increased, which varied from 0.3 h<sup>-1</sup> to 0.7 h<sup>-1</sup>, as the applied current increased from 1.0 A to 3.0 A (Figure 4.39).

As shown in Figure 4.40, the product selectivity and yield were affected by the current supplied. At low current (1.0 A), the glycolic and lactic acids were produced gradually. The graph in Figure 4.40(a) shows that formic and lactic acids were growing at the similar production trend, whereas glycolic acid displayed a low production rate. On the basis of the product distribution graph, the yields of lactic and glycolic acids can possibly increase further after 8 h of electrolysis. At lower current, the reaction might require longer time for completion. The yield for glycolic and lactic acids increased from 5.6% to 66.1% and from 7.1 to 14.8%, respectively, with increasing electric current from 1.0 A to 2.0 A. Glycolic acid production was reduced to 34.8% when the electric current increased further to 3.0 A. This result indicated that high electric current would facilitate the decomposition of glycerol to gaseous compounds, such as CO<sub>2</sub> (Hunsom *et al.*, 2015). However, at high current, the reaction favored the reduction process to produce lactic acid, with maximum yield of 25.9% after 5 h of electrolysis. The maximum yields for glycolic and lactic acids under these three different electric currents are summarized in Figure 4.41.

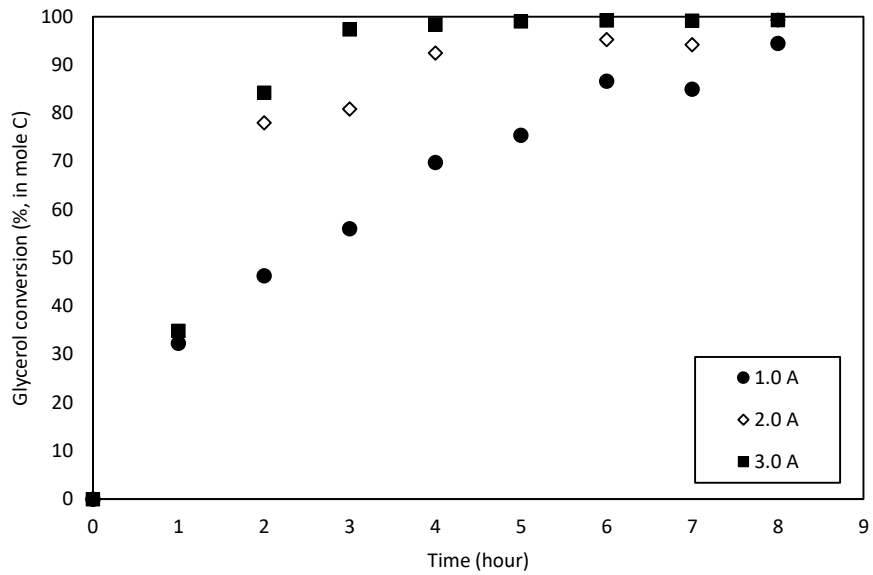


**Figure 4.38:** Glycerol conversion from the electrochemical study on ACC cathode electrode in the presence of 9.6% w/v Amberlyst-15 at 80 °C and constant currents of 1.0, 2.0, and 3.0 A.

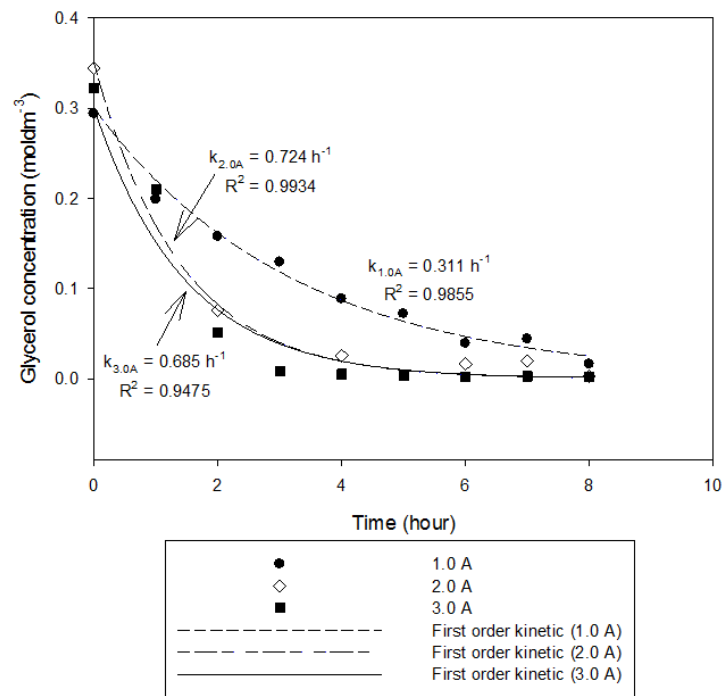


**Figure 4.39:** First-order kinetic model of the electrochemical conversion of glycerol in the presence of 9.6% w/v Amberlyst-15 on ACC cathode electrode at 80 °C and constant currents of 1.0, 2.0, and 3.0 A.

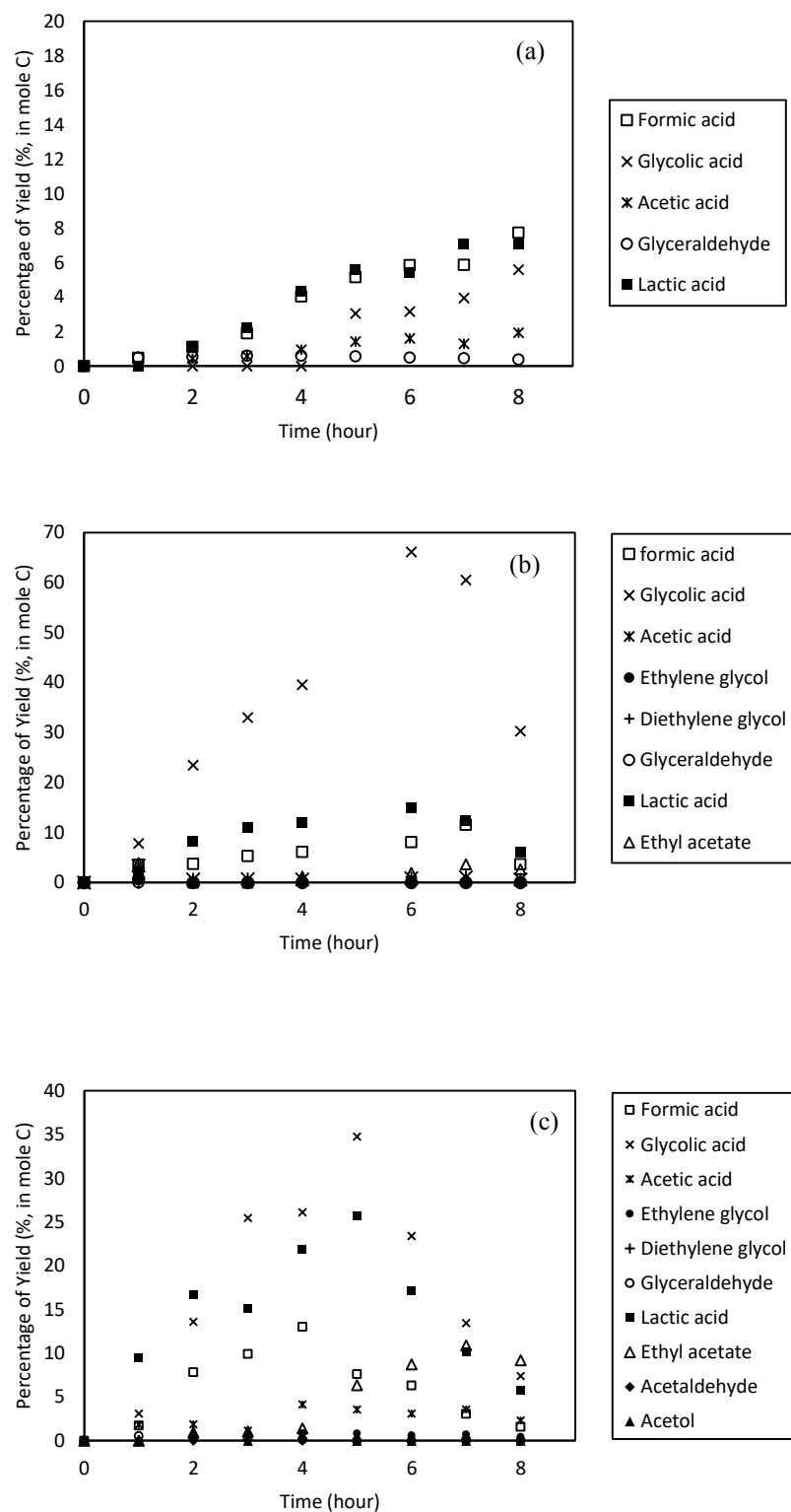


**Figure 4.40:** Product distribution from the electrochemical conversion of glycerol in the presence of 9.6% w/v Amberlyst-15 on ACC cathode electrode at 80 °C and constant currents of (a) 1.0, (b) 2.0, and (c) 3.0 A.

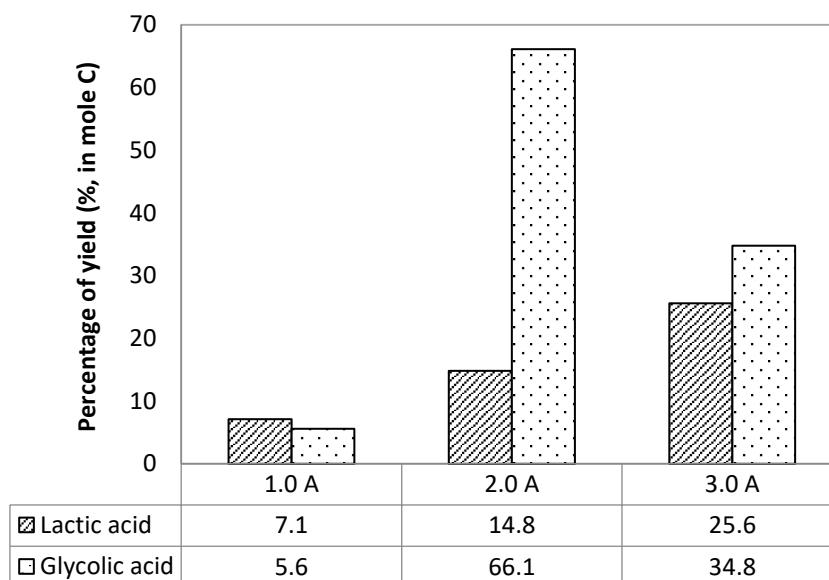


**Figure 4.41:** Maximum yield of glycolic and lactic acids obtained from the electrochemical conversion of glycerol in the presence of 9.6% w/v Amberlyst-15 on ACC cathode electrode at 80 °C and constant currents of 1.0, 2.0, and 3.0 A.

Overall, the maximum glycerol conversion (> 99%) was achieved at 80 °C and high electric current (2.0 A or 3.0 A) in the presence of 9.6% w/v Amberlyst-15. The product yield and selectivity varied according to the applied electric current. At 2.0 A, the highest yield (66.1%) and selectivity (72.0%) for glycolic acid were obtained after 6 h of the reaction. The highest selectivity (32.5%) and yield (25.9%) for lactic acid were attained when the applied current was increased to 3.0 A.

A thorough literature review on the conversion of glycolic acid from glycerol via catalytic pathway and electrochemical pathway was conducted. A summary from this review is given in Tables 2.8 (Section 2.3.3) and 2.11 (Section 2.4.3). Compared with the catalytic conversion, a similar or higher selectivity was achieved in our study under mild reaction conditions (low temperature and ambient pressure), which helps save production cost and energy. The glycolic acid yield and selectivity obtained in this study were relatively higher than those during electrochemical conversion. The presence of Amberlyst-15 as redox catalyst can hasten the reaction by improving the electron

transfer between the electrode and electrolyte (Francke *et al.*, 2014), thereby reducing the contact time of the products (from the reaction mixtures) with the electrode; consequently, the production of unfavorable byproducts, e.g., acetic acid, from over-oxidation was terminated.

Another comprehensive literature review on the lactic acid conversion from glycerol through catalytic method was conducted, as shown in Table 2.10 (Section 2.3.4). Although a lower lactic acid yield and selectivity was obtained in this study, the present electrocatalyst (ACC electrode) applied was relatively cheaper than the noble metal catalyst used in the chemical conversion (Arcanjo *et al.*, 2016; Zhang *et al.*, 2016). Product selectivity can be affected by the pore sizes (Qi *et al.*, 2014b; Zhang *et al.*, 2014); thus, the activated carbon and carbon black ratio should be fine-tuned to achieve a remarkable selectivity in our future study.

#### **4.5 Optimization study over CBD cathode electrode**

The influence of reaction parameters, e.g., amount of catalyst, reaction temperature, and electric current, on the electrochemical conversion of glycerol over CBD electrode was studied. Similar to the study on ACC electrode, CBD electrode also mainly converted glycerol into glycolic and lactic acids. The maximum yield and selectivity obtained for glycolic and lactic acids are summarized in Table 4.6. At 80 °C and electric current of 2.0 A, 9.6% w/v Amberlyst-15 showed the highest glycolic and lactic acid yields at 58.1 and 21.4%, respectively.

**Table 4.6:** Electrochemical conversion of glycerol in the presence of Amberlyst-15 over CBD cathode electrode; the yield and selectivity for glycolic and lactic acids at the maximum level.

Elec-trode	Electrolyte/ Acid	I (A)	Amount of acid catalyst (% w/v)	T (°C)	Glycerol Conversion*		Yield (Y) & Selectivity (S) (%, in mole C)			
					%	k (h <sup>-1</sup> )	Lactic acid		Glycolic acid	
							Y	S	Y	S
CBD	Amberlyst-15	2.0	6.4	80	98.1	0.606	13.9 (5h)	15.6 (5h)	47.4 (5h)	53.4 (5h)
CBD	Amberlyst-15	2.0	9.6	80	98.7	0.744	21.4 (4h)	27.0 (4h)	58.1 (6h)	67.9 (6h)
CBD	Amberlyst-15	2.0	12.8	80	97.4	0.552	19.5 (8h)	23.7 (8h)	46.7 (8h)	56.6 (8h)
CBD	Amberlyst-15	2.0	9.6	RT	87.4	0.233	2.4 (8h)	6.8 (8h)	22.7 (8h)	59.4 (8h)
CBD	Amberlyst-15	2.0	9.6	50	98.8	0.783	6.3 (4h)	6.9 (4h)	47.3 (4h)	52.1 (4h)
CBD	Amberlyst-15	1.0	9.6	80	88.7	0.523	7.8 (8h)	12.8 (8h)	42.1 (8h)	69.4 (8h)
CBD	Amberlyst-15	3.0	9.6	80	97.9	0.819	9.5 (6h)	22.8 (6h)	34.3 (4h)	58.8 (4h)

Note: RT: Room temperature (27 °C); I: current; T: reaction temperature; k: rate constant [Glycerol]: 0.30 M

\*After 8 h of reaction time. Total reaction time: 8 h

Nil: zero value

CBD: Carbon black diamond composite electrode

#### 4.5.1 Effect of catalyst amount

The effect of catalyst (Amberlyst-15) amount was studied on the electrochemical conversion of glycerol over the CBD electrode at 80 °C and electric current of 2.0 A. The catalyst amount was varied from 6.4% w/v to 12.8% w/v. In all cases, a maximum of 98% glycerol conversion was attained for 8 h of electrolysis (Figure 4.42). A slight increase in the glycerol conversion rate from 0.606 h<sup>-1</sup> to 0.744 h<sup>-1</sup> was observed when the amount of Amberlyst-15 increased from 6.4% w/v to 9.6% w/v. Nevertheless, conversion rate decreased to 0.552 h<sup>-1</sup> when the Amberlyst-15 amount further increased (Figure 4.43). This result indicated that the self-inhibition effect in the reaction caused the decrease in conversion rate because the glycolic acid competed with glycerol for the active sites during the electro-oxidation process; thus, its yield was also subsequently reduced from 58.1% to 46.7% because of the over-oxidation process (Figure 4.44).

The yield and selectivity for glycolic and lactic acids increased with the increase of Amberlyst-15 amount from 6.4% w/v to 9.6% w/v. The maximum yield for these acids was attained at 4 and 6 h for lactic acid (21.4%) and glycolic acid (58.1%), respectively, with 9.6% w/v Amberlyst-15. No major variation in the electrocatalytic performance was observed with further increase of the Amberlyst-15 amount to 12.8% w/v. The 9.6% w/v Amberlyst-15 was proven adequate to obtain the maximum glycerol conversion and desired product yields. Product distribution graphs for different catalyst concentrations are shown in Figure 4.45.

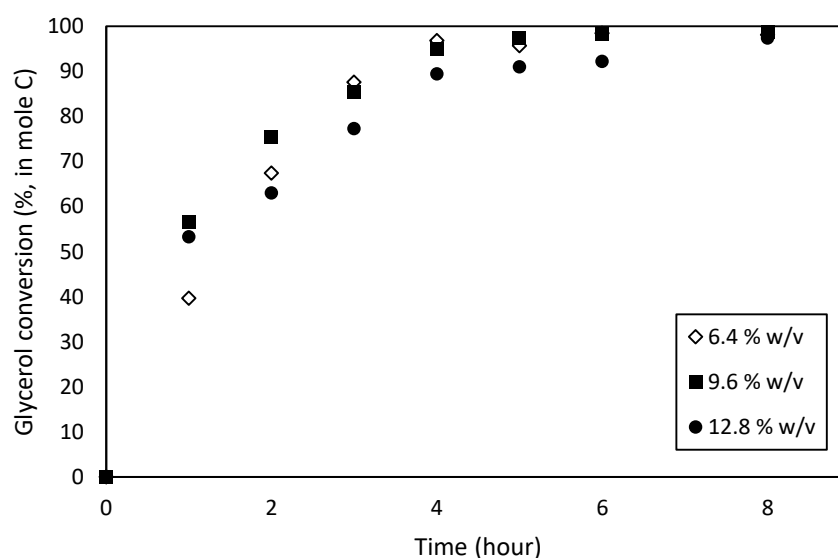


**Figure 4.42:** Glycerol conversion from the electrochemical study on CBD cathode electrode at 80 °C, 2.0 A constant current and in the presence of Amberlyst-15 varied from 6.4% w/v to 12.8% w/v.

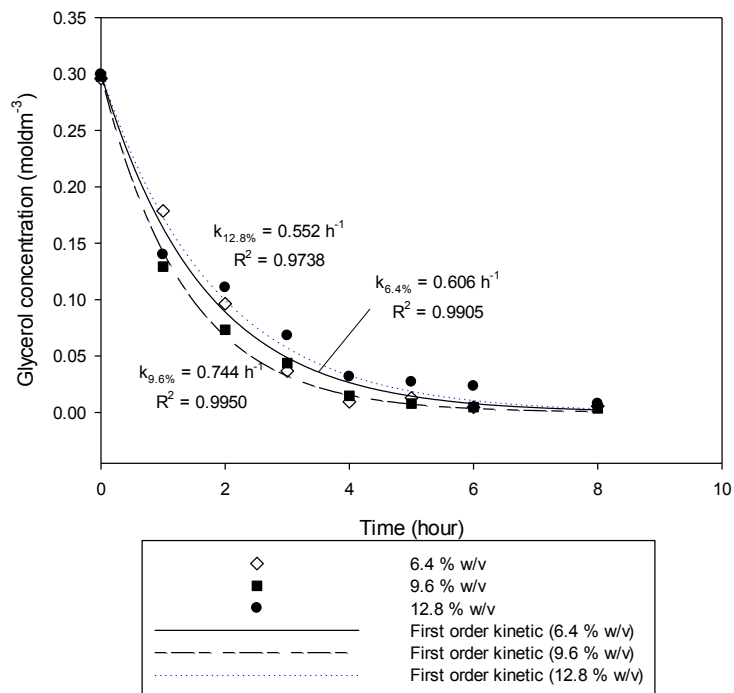


**Figure 4.43:** First-order kinetic model of the electrochemical conversion of glycerol in the presence of Amberlyst-15 varied from 6.4% w/v to 12.8% w/v on the CBD cathode electrode at 80 °C and 2.0 A constant current.

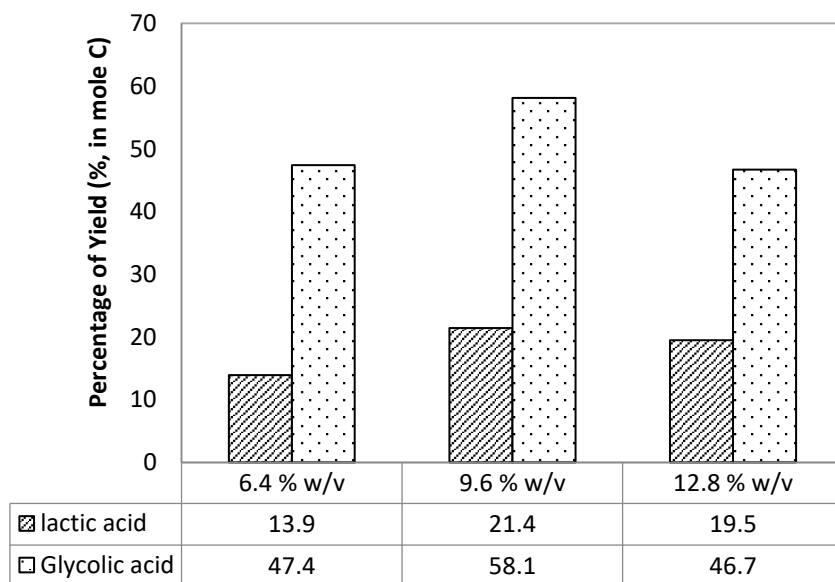


**Figure 4.44:** Maximum yield of glycolic and lactic acids obtained from the electrochemical conversion of glycerol in the presence of 6.4% w/v, 9.6% w/v and 12.8% w/v Amberlyst-15 on CBD cathode electrodes, at 80 °C and 2.0 A constant current.



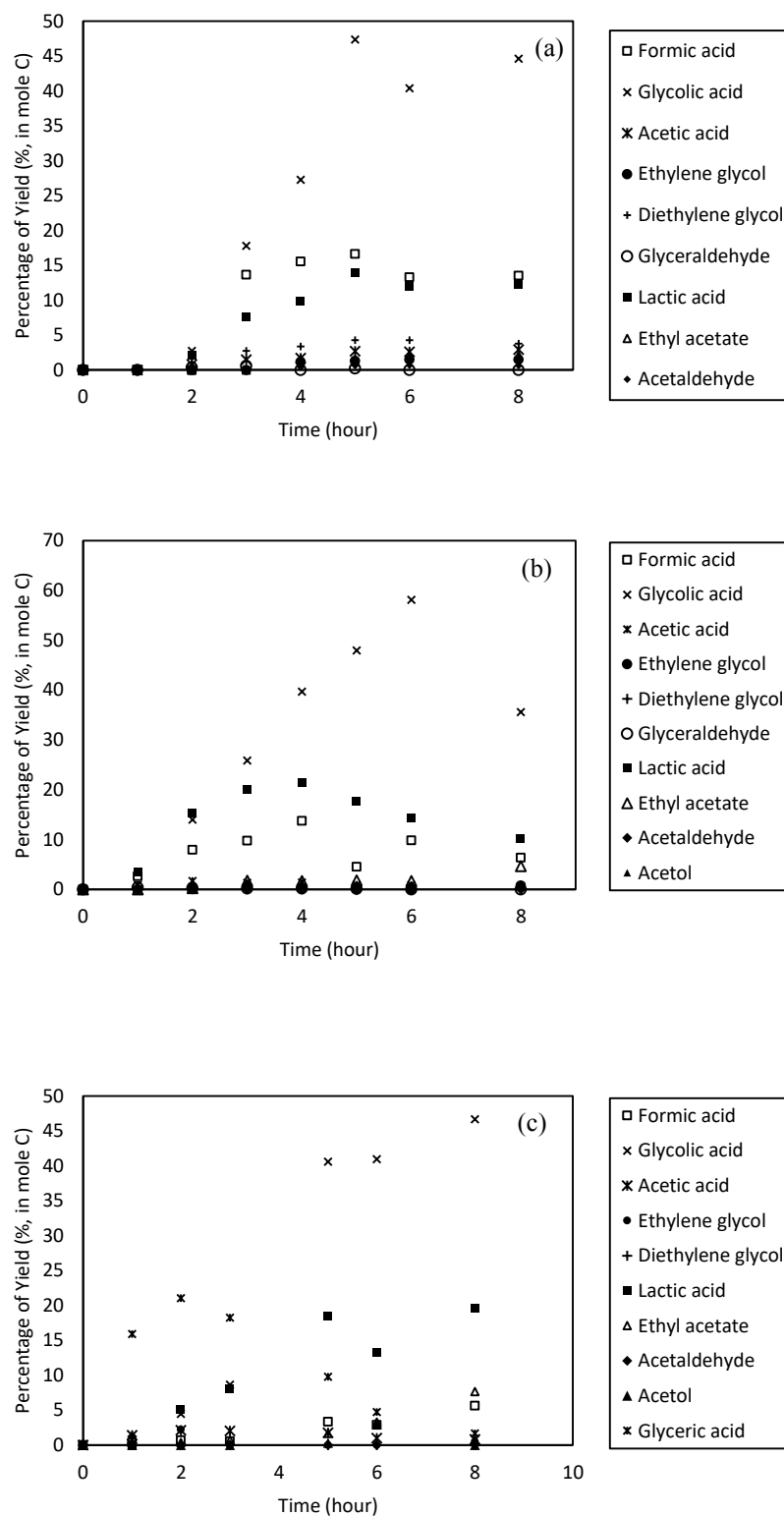


**Figure 4.45:** Product distribution from the electrochemical conversion of glycerol in the presence of Amberlyst-15 at (a) 6.4% w/v, (b) 9.6% w/v, and (c) 12.8% w/v on CBD cathode electrodes at 80 °C and 2.0 A constant current.

#### 4.5.2 Effect of reaction temperature

The effect of reaction temperature was studied from room temperature (27 °C) to 80 °C for 8 h, in the presence of 9.6% w/v Amberlyst-15 with applied current of 2.0 A (Table 4.6 in Section 4.5). Glycerol conversion increased with the increase of reaction temperature from room temperature (27 °C) to 50 °C and 80 °C. The maximum glycerol conversion (98%) was attained after 8 h of electrolysis at 50 °C and 80 °C (Figure 4.46). Assuming a first-order kinetic, Figure 4.47 shows that glycerol conversion rate also increased when the temperature increased from  $\sim 0.2 \text{ h}^{-1}$  [room temperature (27 °C)] to  $\sim 0.7 \text{ h}^{-1}$  (50 °C and 80 °C).

At low temperature, the formation of glycolic and lactic acids was the lowest than, compared with the yields obtained from the two other trials at high temperature. The maximum yield of glycolic acid obtained in this condition was 22.7% at 8 h. The product distribution graph in Figure 4.48 shows that the yield of ethyl acetate and formic acid increased gradually with reaction time. The lactic acid yield was rather low; only 2.4% was obtained after 8 h of electrolysis. When the reaction temperature increased to 50 °C, a fast rate for glycolic and formic acid production was observed, with a maximum yield of 47.3% and 30.8%, respectively, achieved at 4 h. The lactic acid yield slightly increased from 2.4% to 6.3% when the temperature increased from room temperature (27 °C) to 50 °C. At high temperature of 80 °C, the maximum glycolic acid yield was 58.1% at 6 h of electrolysis; this result indicated that oxidation is favorable under this condition because OH adsorption is likely to occur in high temperature, thereby reducing the barrier for both O–H and C–H bond dissociations of glycerol. Consequently, the catalytic behavior of the electrode for glycerol oxidation is enhanced (Beden *et al.*, 1987; Yang *et al.*, 2012). In addition, a temperature increase can decrease the diffusion layer thickness (Gupta *et al.*, 1984), which increases the diffusion rate of pyruvic acid (oxidation compound) to the cathode electrode and permits the

reduction of pyruvic acid to lactic acid. The bar chart in Figure 4.49 shows that the most suitable temperature for the electrochemical process is 80 °C, which yields maximum glycolic acid (58.1%) and lactic acid (21.4%) amounts.

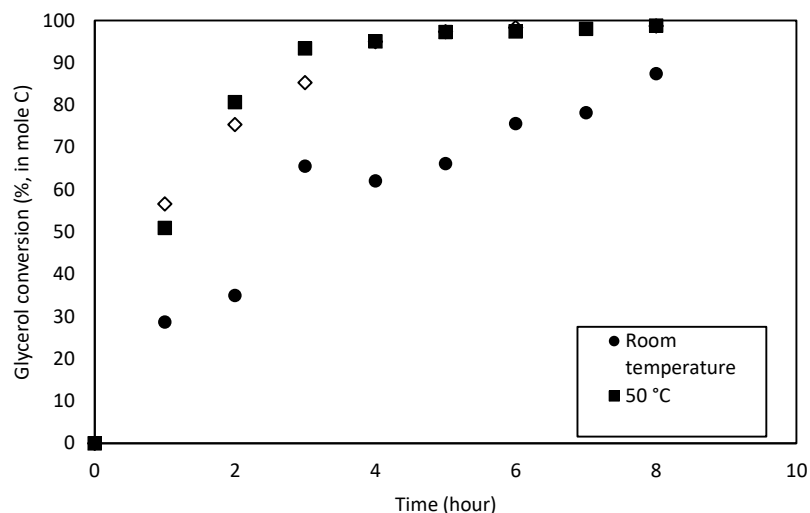


**Figure 4.46:** Glycerol conversion from the electrochemical study on CBD cathode electrode in the presence of 9.6 % w/v Amberlyst-15 at 2.0 A constant current, at room temperature (27 °C), 50 °C and 80 °C.

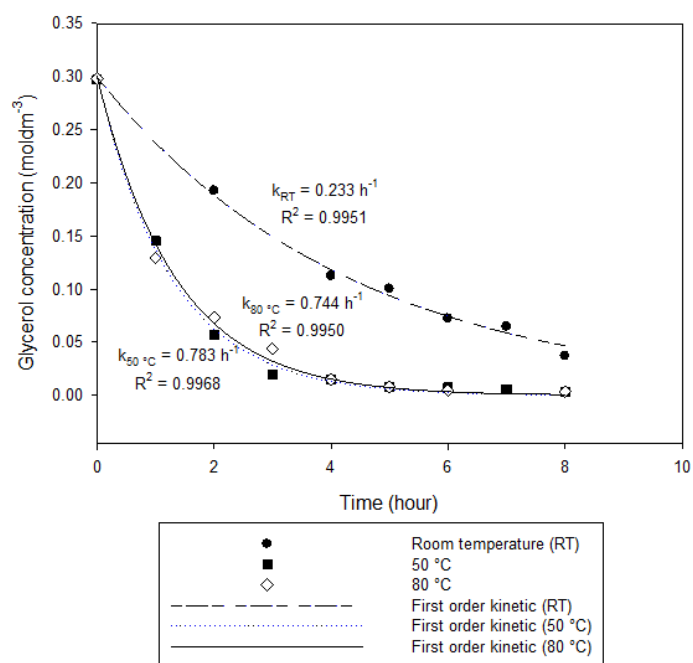


**Figure 4.47:** First-order kinetic model of the electrochemical conversion of glycerol in the presence of 9.6% w/v Amberlyst-15 on CBD cathode electrode at 2.0 A constant current at room temperature (27 °C), 50 °C, and 80 °C.

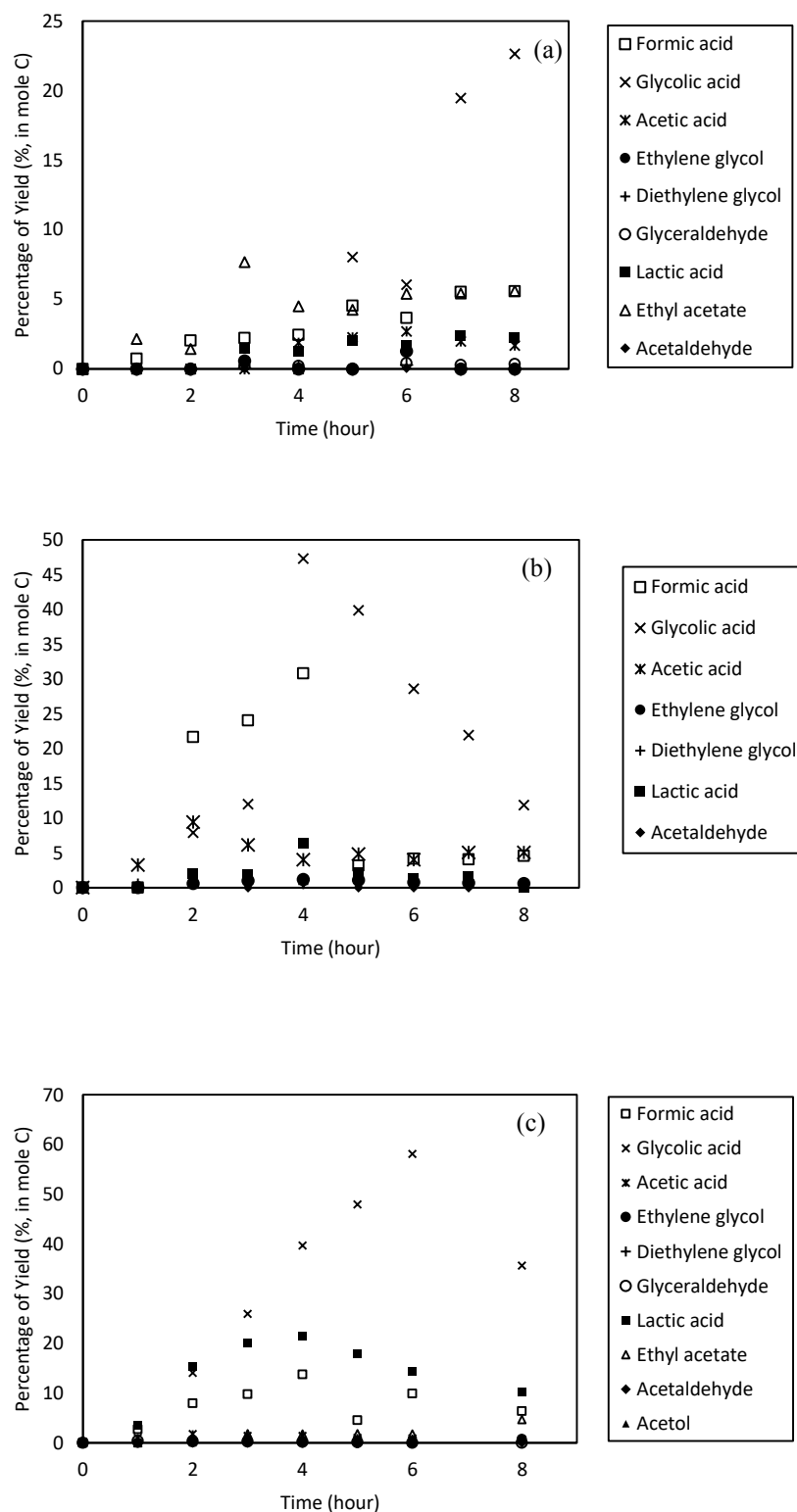


**Figure 4.48:** Product distribution from the electrochemical conversion of glycerol in the presence of 9.6% w/v Amberlyst-15 on CBD cathode electrode at 2.0 A constant current at (a) room temperature (27 °C), (b) 50 °C, and (c) 80 °C.

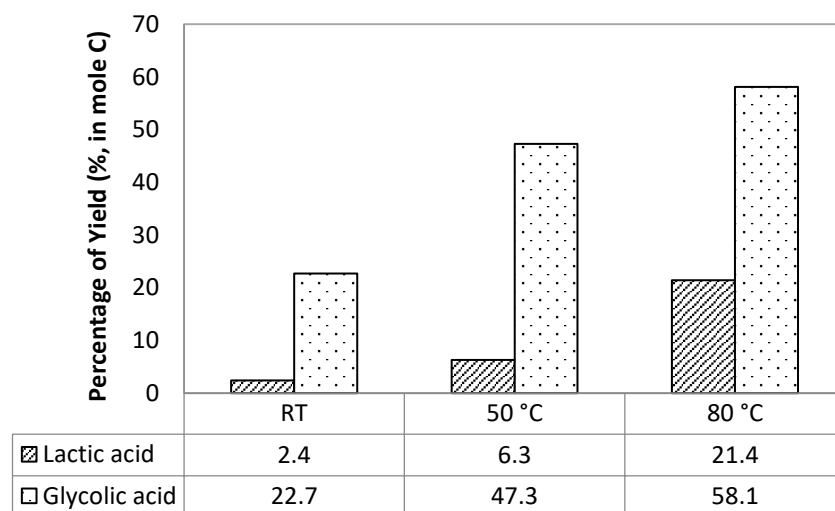


**Figure 4.49:** Maximum yield of glycolic and lactic acids obtained from the electrochemical conversion of glycerol in the presence of 9.6% w/v Amberlyst-15 on CBD cathode electrode at 2.0 A constant current at room temperature, 27 °C (RT), 50 °C, and 80 °C.

#### 4.5.3 Effect of electric current

When the optimum reaction temperature was determined, the effect of applied current in the range of 1.0–3.0 A on the glycerol conversion and desired product yield was studied in the presence of 9.6% w/v Amberlyst-15. The reaction parameters and experimental data are summarized in Table 4.6 (Section 4.5). As shown in Figure 4.50, the glycerol conversion increased with the increase of electric current from 88.7% (1.0 A) to about 98% (2.0 and 3.0 A) after 8 h. In agreement with Faraday’s Law, the glycerol conversion rate was increased from 0.523 h<sup>-1</sup> to 0.819 h<sup>-1</sup> with the increase in the electric current from 1.0 A to 3.0 A (Figure 4.51).

According to the product distribution graphs in Figure 4.52, at low electric current, the lactic and formic acids increased in parallel over time; their yields achieved the maximum after 8 h of electrolysis, with corresponding value of 7.8% and 9.0%. The glycolic acid production rate was relatively higher than that of lactic acid, and the

maximum yield attained was 42.1% at 8 h. Figure 4.52(a) shows that glycolic and lactic acid yields were likely to increase further after 8 h at low electric current. When the current increased to 2.0 A, the yield for glycolic and lactic acids subsequently increased and achieved the optimum yield of 58.1% and 21.4% at 6 h and 4 h, respectively. However, further increase in the electric current caused the decrease in the product yield of glycolic and lactic acids. The maximum yields were attained at 4 h, with 9.5% of lactic acid and at 6 h, with 34.3% of glycolic acid. This result was caused by that considerably high current would cause further decomposition of glycerol into CO<sub>2</sub> gas (Hunsom *et al.*, 2015). The bar chart in Figure 4.53 shows that glycolic and lactic acids were preferably produced using an applied current of 2.0 A.

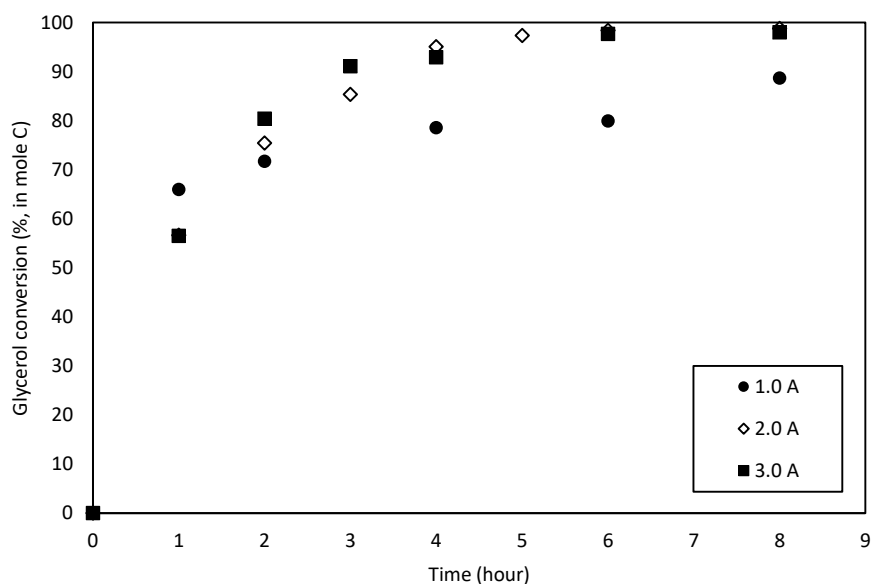


**Figure 4.50:** Glycerol conversion from the electrochemical study on CBD cathode electrode in the presence of 9.6% w/v Amberlyst-15 at 80 °C and constant currents of 1.0, 2.0, and 3.0 A.

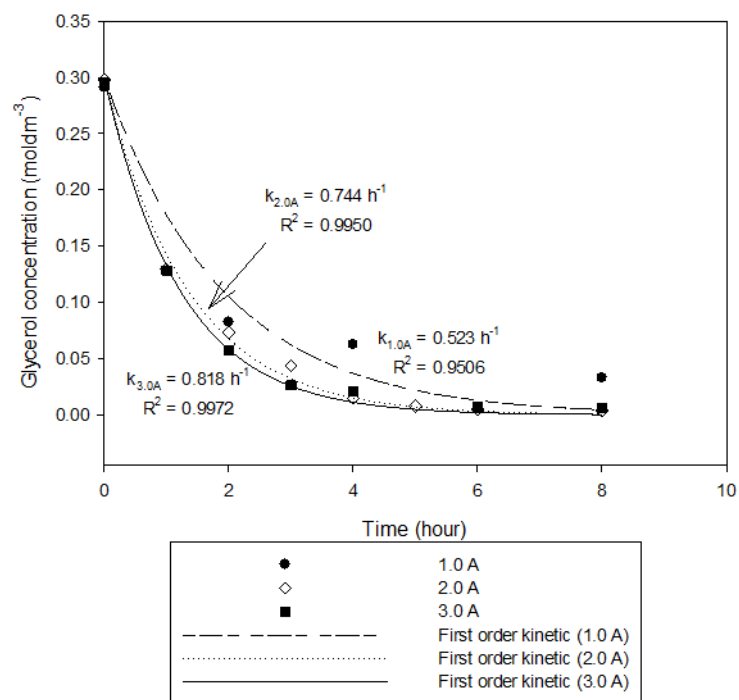


**Figure 4.51:** First-order kinetic model of the electrochemical conversion of glycerol in the presence of 9.6% w/v Amberlyst-15 on CBD cathode electrode at 80 °C at constant currents of 1.0, 2.0, and 3.0 A.

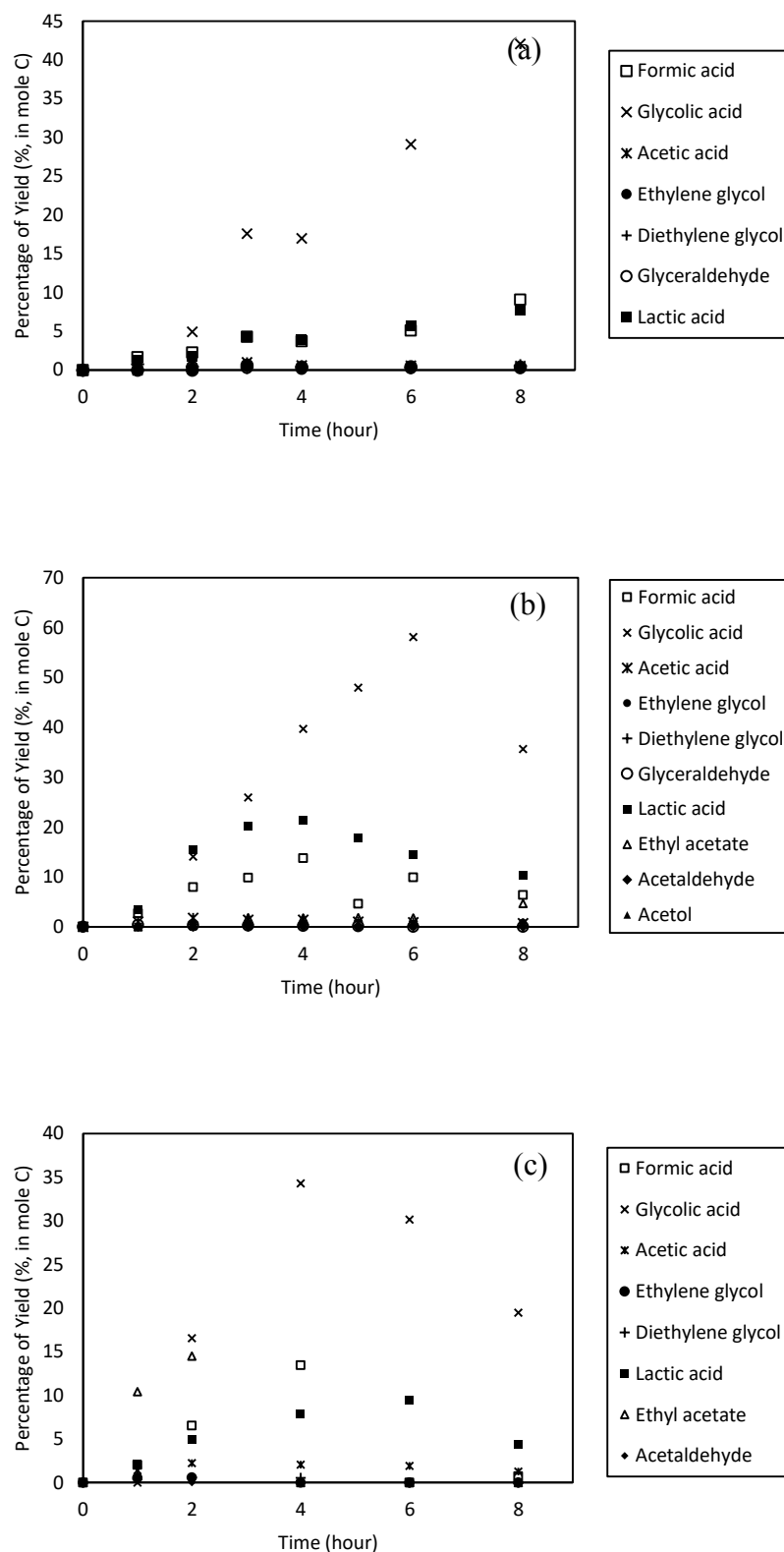


**Figure 4.52:** Product distribution from the electrochemical conversion of glycerol in the presence of 9.6% w/v Amberlyst-15 on CBD cathode electrode at 80 °C and constant currents of (a) 1.0, (b) 2.0, and (c) 3.0 A.



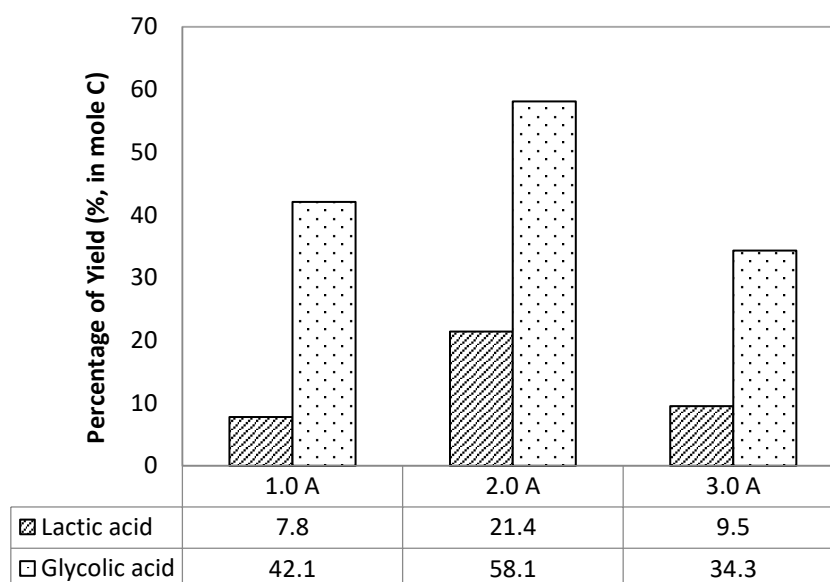


**Figure 4.53:** Maximum yield of glycolic and lactic acids obtained from the electrochemical conversion of glycerol in the presence of 9.6% w/v Amberlyst-15 on CBD cathode electrode at 80 °C and constant currents of 1.0, 2.0, and 3.0 A.

Earlier discussion on the effect of catalyst amount, reaction temperature, and applied electric current on the electrochemical conversion of glycerol on the CBD electrode showed that the optimum yields for glycolic and lactic acids at 80 °C and electric current of 2.0 A and in the presence of 9.6% w/v Amberlyst-15. The maximum glycerol conversion obtained under these conditions was 98%. The maximum glycolic acid yield of 58.1% was obtained at 6 h, with a selectivity of 67.9%. The optimum lactic acid yield was also attained under this reaction conditions at 4 h, with a yield of 21.4% and selectivity of 27.0%.

As mentioned in Section 3.2.3, optimization studies were performed on ACC and CBD electrodes with a similar active surface area (around 60 cm<sup>2</sup>). The active surface area for both electrodes was standardized; consequently, the glycolic and lactic acid yields obtained from both studies were equalized. Although similar yields were obtained, ACC electrode could show a higher investment value than CBD electrode in the future study because the raw material used for ACC electrode preparation is

cheaper. Activated carbon can be easily produced from the available biomass precursors, such as coal, coke, sawdust, peat, wood char, seed hull, and palm kernel shell.

#### **4.6 Electrochemical conversion of glycerol in a two-compartment reactor**

In this case study, the electrochemical conversion of glycerol was carried out in a two-compartment reactor. As mentioned in Section 3.3, three types of cathode materials were studied, namely Pt, ACC, and CBD. The electrosynthesis process was conducted in the presence of 9.6% w/v Amberlyst-15 at 80 °C and 2.0 A for 8 h. This study was mainly focused on the electroreduction of glycerol. Nevertheless, the electro-oxidation of glycerol was also studied on Pt electrode.

##### **4.6.1 Electroreduction of glycerol**

The evaluation of glycerol conversion over Pt, ACC, and CBD electrodes at the cathodic region is shown in Figure 4.54. Glycerol was converted to 67.2%, 73.8%, and 87.5% on Pt, ACC, and CBD electrodes, respectively. The first-order kinetic models for the reaction on Pt, ACC, and CBD are shown in Figure 4.55. In agreement with the study performed by Hunsom *et al.* (2013), the electrolysis on Pt cathode electrode can only fit the first-order kinetic model well at the first 2 h. The rate constants on Pt, ACC, and CBD are 0.191, 0.165, and 0.197 h<sup>-1</sup>, respectively.

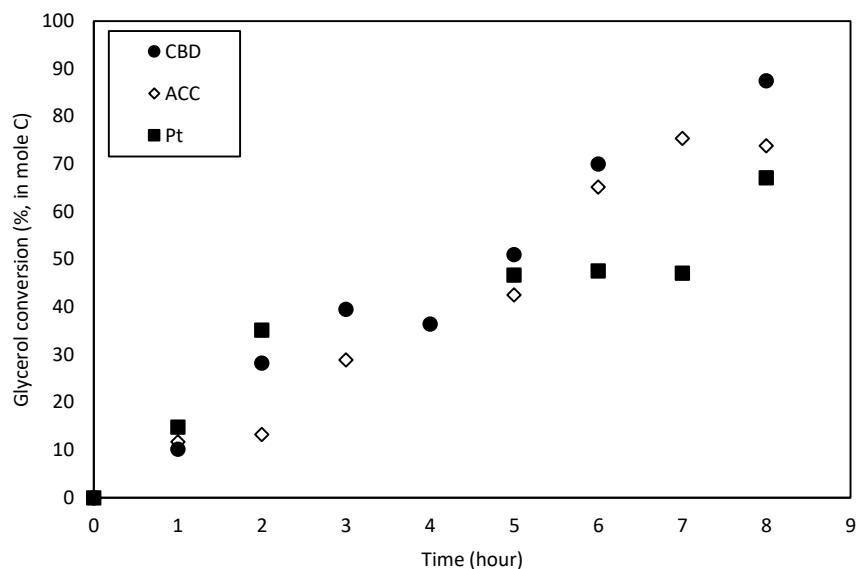


**Figure 4.54:** Glycerol conversion from the electroreduction study of glycerol in the presence of 9.6% w/v Amberlyst-15 at 2.0 A constant current and 80 °C on Pt, ACC, and CBD cathode electrodes.

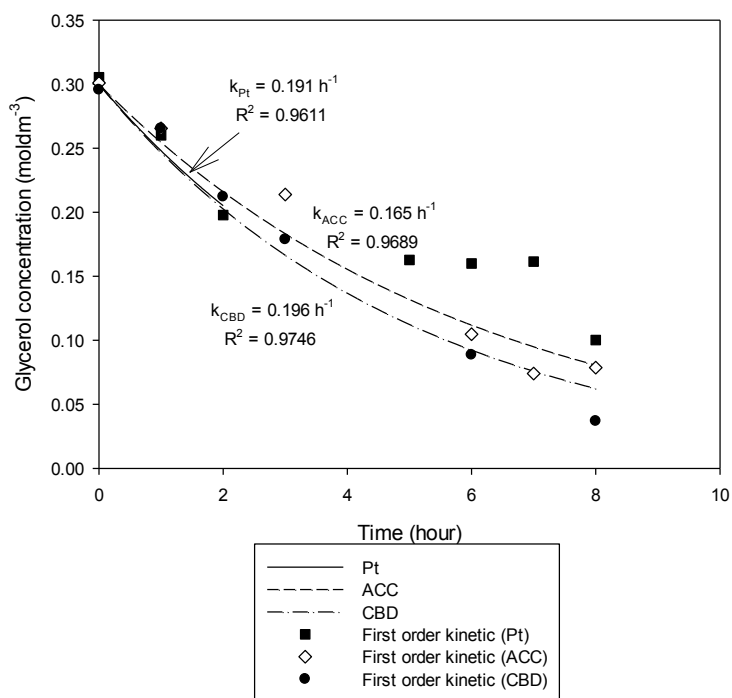


**Figure 4.55:** First-order kinetic model of the electroreduction of glycerol in the presence of 9.6% w/v Amberlyst-15 at 2.0 A constant current and 80 °C on Pt, ACC, and CBD cathode electrodes.

According to the GC-MS chromatogram in Figure 4.56, 1,2-PDO, acetol, and DEG were observed in the three experiments. In accordance with the glycerol conversion and conversion rate, the highest yield for 1,2-PDO (9.5%) was attained after 8 h of electrolysis over the CBD electrode, with a selectivity of 67.9%, as shown in Figure 4.57. Acetol and DEG were also obtained in the reaction mixture with corresponding yields of 2.3% and 2.1%, respectively. The highest product selectivity for 1,2-PDO (85.6%) was obtained on ACC electrode with maximum yield of 8.8% after 8 h. On the basis of the conversion rate and conversion value, the reduction process over Pt electrode was slower than on CBD and ACC electrodes with a maximum of 8.6% of 1,2-PDO and a selectivity of 60.9% after 8 h. The product yields and selectivities from the studies on Pt, ACC, and CBD electrodes are summarized in Table 4.7.

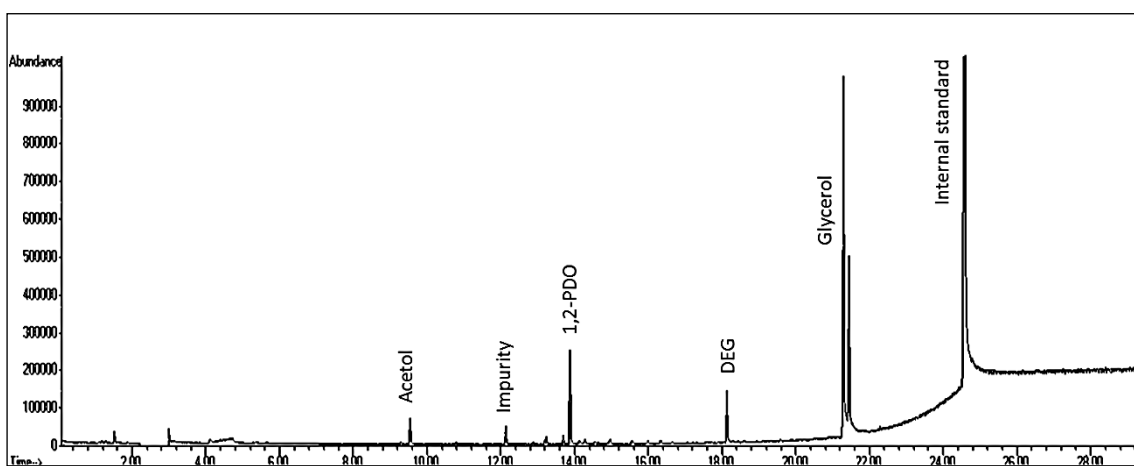


**Figure 4.56:** The GC-MS chromatogram of the products obtained from the electroreduction of glycerol in the presence of Amberlyst-15 on Pt, ACC or CBD cathode electrodes, at 80 °C and at 2.0 A constant current.

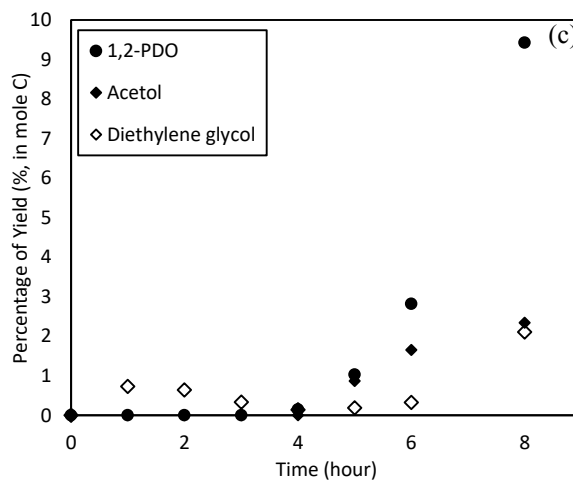
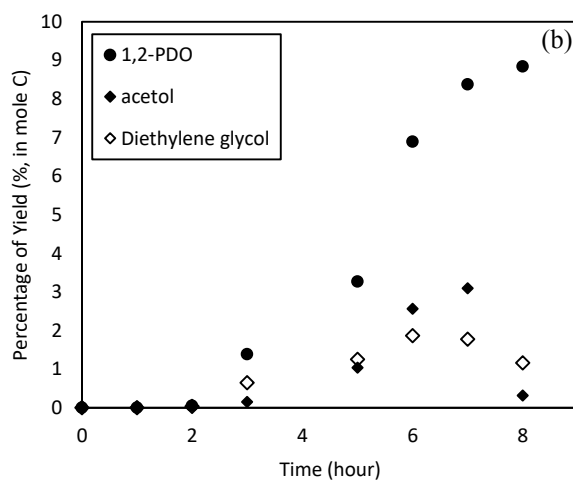
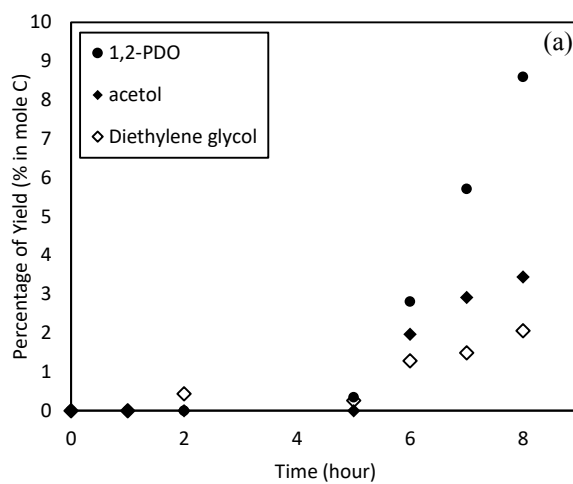


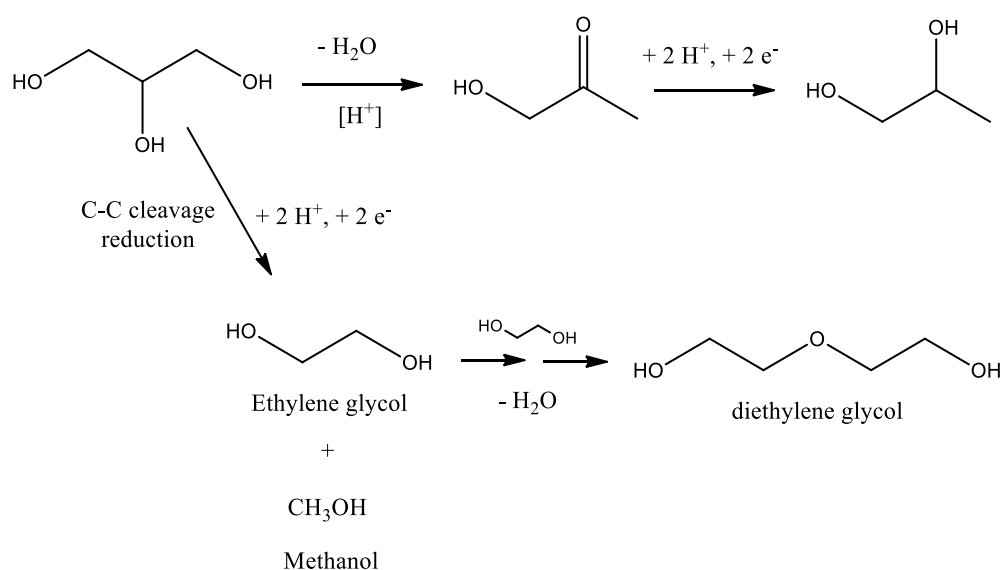
**Figure 4.57:** Product distribution from the electroreduction of glycerol in the presence of 9.6% w/v Amberlyst-15 at 2.0 A and 80 °C on (a) Pt, (b) ACC, and (c) CBD cathode electrodes.

**Table 4.7:** Electroreduction of glycerol over Pt, ACC and CBD cathode electrodes: yields and selectivities for 1,2-propanediol, acetol and diethylene glycol obtained after 8 h reaction time.

Electrode	Amberlyst-15 % (w/v)	I (A)	T (°C)	Glycerol conversion		Yield (Y) & Selectivity (S) (% in mole C)						
				%	k (h <sup>-1</sup> )	12-PDO		Acetol		DEG		
A	C					Y	S	Y	S	Y	S	
Pt	Pt	9.6	2.0	80	67.2	0.191 (2h)	8.6	60.9	3.4	24.4	2.1	14.7
Pt	ACC	9.6	2.0	80	73.8	0.165	8.8	85.6	0.3	3.1	1.2	11.3
Pt	CBD	9.6	2.0	80	87.5	0.197	9.5	67.9	2.3	16.9	2.1	15.1

Note: A: Anode; C: Cathode; I: current; T: reaction temperature; k: rate constant  
Total volume of each compartment: 0.25 L

In the presence of ion H<sup>+</sup> from Amberlyst-15, glycerol was first dehydrated into acetol by eliminating a water molecule from glycerol (Ishiyama *et al.*, 2013). In accordance with the catalytic hydrogenolysis pathway reported by Chaminand *et al.* and Huang *et al.*, acetol could be further reduced to 1,2-PDO over the surface of electrode (Chaminand *et al.*, 2004; Huang *et al.*, 2009). Ethylene glycol was produced through C–C bond cleavage during the reduction process (Nakagawa *et al.*, 2011). DEG can be formed through the coupling of ethylene glycol. The reaction mechanism is proposed in Scheme 4.6.



**Scheme 4.6:** Proposed reaction mechanism for electroreduction of glycerol.

In this study, the three electrodes (Pt, ACC, and CBD) successfully converted glycerol to 1,2-PDO. The ACC electrode showed an added advantage over Pt and CBD because of its high active surface area and low preparation cost. As described in Section 3.3, the ACC and CBD electrodes were prepared with the same geometrical surface area (14 cm<sup>2</sup>). The active surface areas of ACC and CBD electrodes (226.8 and 87.7 cm<sup>2</sup>, respectively) were calculated from the chronoamperometry analysis. The Pt electrode (surface area of 33.0 cm<sup>3</sup>) only showed 42.8 cm<sup>2</sup> of the active surface area. The high active surface area of ACC improved the electrocatalytic activity by increasing the ion transportation and electrolyte accessibility (Tang *et al.*, 2013). Although the 1,2-PDO yields obtained from these trials were relatively low, their selectivity was considered high, specifically for electroreduction, which was carried out on the ACC electrode; consequently, a selectivity of 86% was obtained.

On the basis of the research outcomes obtained from the previous literature (refer to Table 2.5 in Section 2.3.2), this study has led to a comparative or better selectivity for 1,2-PDO under milder conditions. Electrolysis was performed at ambient pressure and low reaction temperature (80 °C). Moreover, the maximum selectivity for 1,2-PDO was achieved after 8 h of electrolysis. Shortening the reaction time can reduce the contact time of glycerol with the electrocatalyst, thereby stopping the production of unfavorable byproducts. When glycerol reacts under high reaction temperature and pressure for long hours, the glycerol C–C bond breaks, which leads to further formation of small unwanted compounds, such as ethylene glycol (Rode *et al.*, 2010). The present study also showed that fewer compounds were formed during electrolysis than during the fermentation process.

In addition, the price of the electrode materials must be inexpensive to compete effectively with the current available catalyst and electrocatalyst. The ACC electrode is

relatively cheap compared with the noble metal catalyst (Pt, Pd, Rh, and Ru), as shown in Table 2.13 (Section 2.6). Furthermore, activated carbon can be easily obtained from the biomass feedstock, such as sawdust, seed hull, and palm kernel shell. In Malaysia, palm kernel shell is the main source for activated carbon because it is one of the largest agricultural wastes obtained from the oil palm industry (Abdullah *et al.*, 2011).

The previous published works reported the importance of the roles of pore size, pore volume, and active surface area of the electrode in the electrochemical processes. These findings demonstrated that pore volume and surface area can improve the diffusion limit and enhance the transportation rate of reactants and products by increasing the pore sizes (Bon Saint Côme *et al.*, 2011; Linares *et al.*, 2014; Qi *et al.*, 2014a; Zhang *et al.*, 2014). In the present study, the ACC electrode contained high pore volume with large active surface area (227 cm<sup>2</sup>) that can improve the process by holding or trapping the intermediate compound (e.g., acetol) for further reduction into 1,2-PDO (Zhang *et al.*, 2014).

#### 4.6.2 Electro-oxidation of glycerol

The electro-oxidation of glycerol was carried out on the Pt electrode. Although Pt electrode was used at the anodic region for all the three trials, the glycerol conversion and product distribution varied when different cathode electrodes were used. According to the graphs in Figure 4.58, a maximum of 100% glycerol conversion was achieved after 8 h for all the three experiments. In accordance with the study carried out by Hunsom *et al.* (2013), the trial on Pt anode versus Pt and CBD cathodes fitted the first-order kinetic model well at the first 5 and 3 h, respectively. When Pt electrode was used in both compartments, the first-order glycerol conversion rate constant was high, at 0.279 h<sup>-1</sup>. The conversion rate slightly decreased when ACC (0.182 h<sup>-1</sup>) and CBD (0.134 h<sup>-1</sup>) were used as cathode electrodes (Figure 4.59).



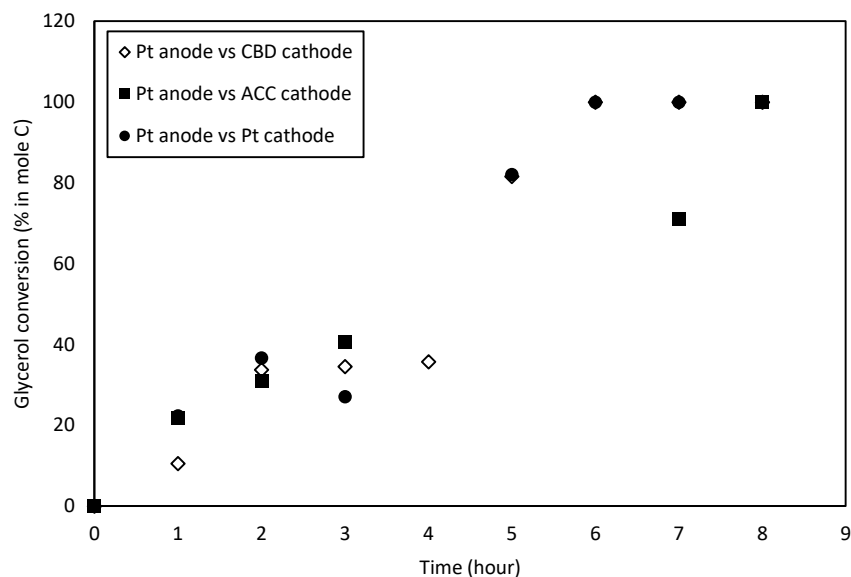


**Figure 4.58:** Glycerol conversion from the electro-oxidation study of glycerol in the presence of 9.6% w/v amberlyst-15 at 2.0 A constant current and 80 °C on Pt anode electrode versus Pt, ACC, and CBD cathode electrode.

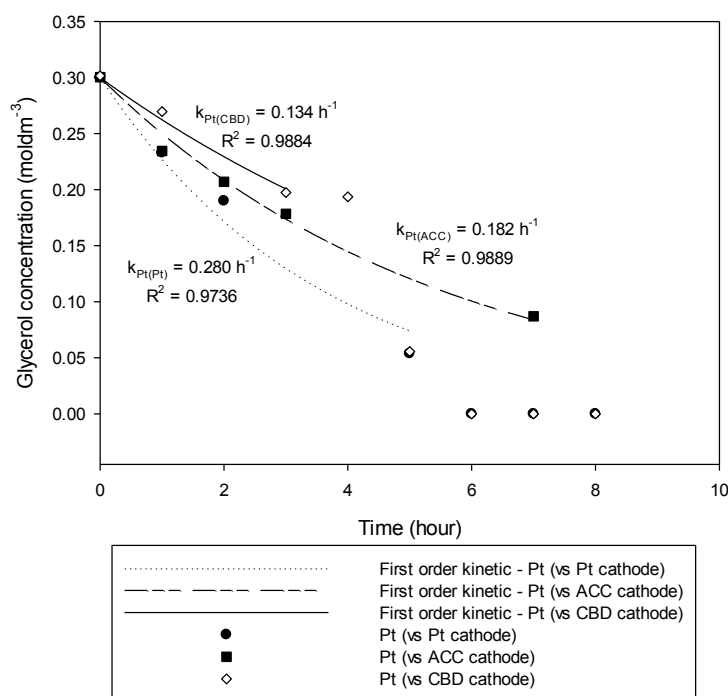


**Figure 4.59:** First-order kinetic model of the electro-oxidation of glycerol in the presence of 9.6% w/v Amberlyst-15 at 2.0 A constant current and 80 °C on Pt anode electrode versus Pt, ACC, and CBD cathode electrodes

The product distributions from these trials are shown in Figure 4.60. Generally, the electro-oxidation over Pt electrode produced glycolic and glyceric acids, regardless whether the cathode material was Pt, ACC, or CBD. However, the yield and distributions obtained varied when different cathode materials were used. Glycerol was oxidized to glycolic and glyceric acids on Pt anode (versus Pt cathode), with corresponding yields of 43.5% and 47.0% and selectivity of 44.8% and 48.3%, after 7 h of reaction, respectively. The glycolic and glyceric acid yields were reduced when ACC was used as the cathode electrode. The maximum product yield of 27.9% and 19.7% was obtained for glycolic and glyceric acids at 8 h, respectively. In the trial using CBD as cathode electrode, the Pt anode electrode oxidized the glycerol to only glyceric acid with maximum yield of 35.8% attained after 6 h of electrolysis. Glycolic acid was not observed in this trial, but ethyl acetate was obtained as the second major compound (20.9%) after 7 h of reaction. Ethyl acetate could be an acetic acid derivative because acetic acid reacted with ethanol during the GC injection. The maximum yield and selectivity for glycolic and glyceric acids for these three trials are summarized in Table 4.8. The electro-oxidation carried out on Pt anode versus Pt cathode electrode displayed the highest product yield and selectivity.

**Table 4.8:** Electro-oxidation of glycerol over Pt anode electrode versus Pt, ACC, and CBD cathode electrode: maximum yield and selectivity for glyceric and glycolic acids.

Electrode		Amberlyst-15 % (w/v)	I (A)	T (°C)	Glycerol conversion* % k (h <sup>-1</sup> )	Yield (Y) & Selectivity (S) (% in mole C)			
A	C					Glycolic acid		Glyceric acid	
						Y	S	Y	S
Pt	Pt	9.6	2.0	80	100 0.279 (5h)	43.5 (7h)	44.8 (7h)	47.0 (7h)	48.3 (7h)
Pt	ACC	9.6	2.0	80	100 0.182	27.9 (8h)	39.8 (8h)	19.7 (8h)	35.0 (8h)
Pt	CBD	9.6	2.0	80	100 0.134 (3h)	-	-	35.8 (6h)	67.1 (6h)

Note: A: Anode; C: Cathode; I: current; T: reaction temperature; k: rate constant  
 Total volume of each compartment: 0.25 L  
 \*After 8 h of reaction time

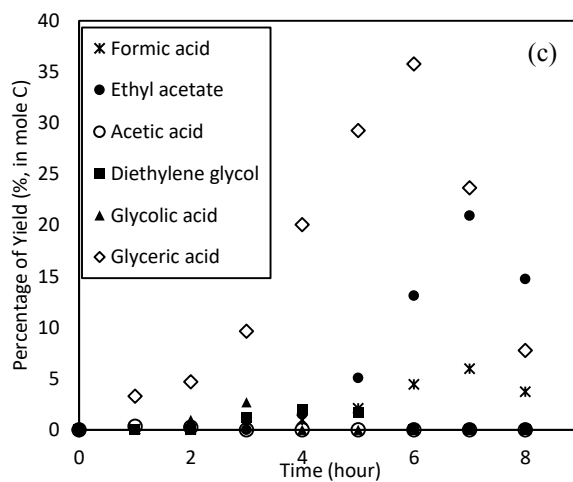
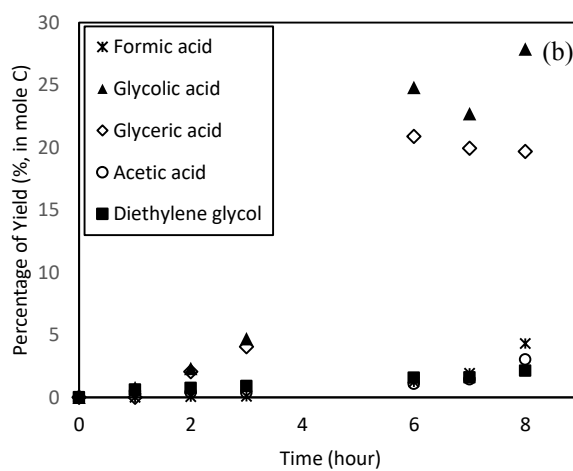
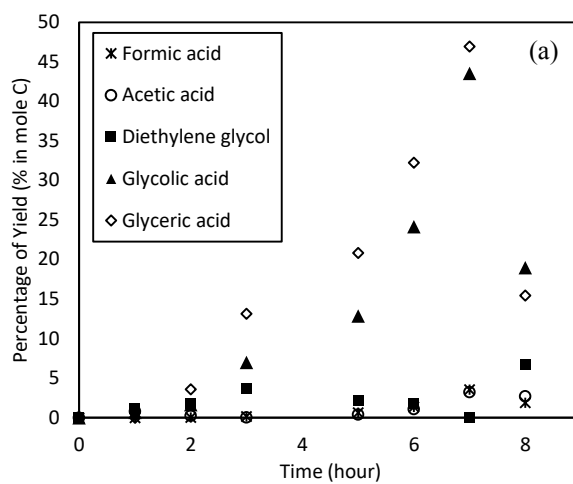


**Figure 4.60:** Product distribution from the electro-oxidation of glycerol in the presence of 9.6% w/v Amberlyst-15 at 2.0 A constant current and 80 °C on Pt anode electrode versus (a) Pt, (b) ACC, and (c) CBD cathode electrodes.

The products obtained from the electro-oxidation region were separated by GC analysis, and the corresponding chromatogram is shown in Figure 4.61. Glycolic acid appeared in two molecular forms, either glycolic acid itself or the glycolic acid derivative, which is glycolaldehyde diethyl acetate. This compound was derived from the reaction of glycolic acid with the ethanol solvent used for GC analysis. The analysis indicated the presence of the following chemical compounds, namely, formic acid, glycolic acid, glyceric acid, and DEG.

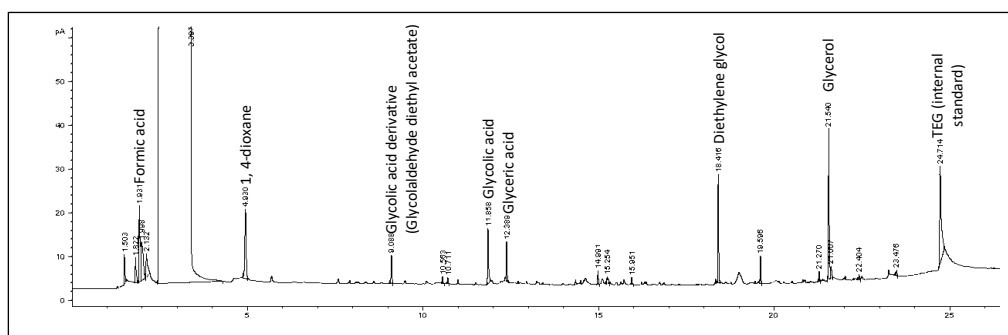
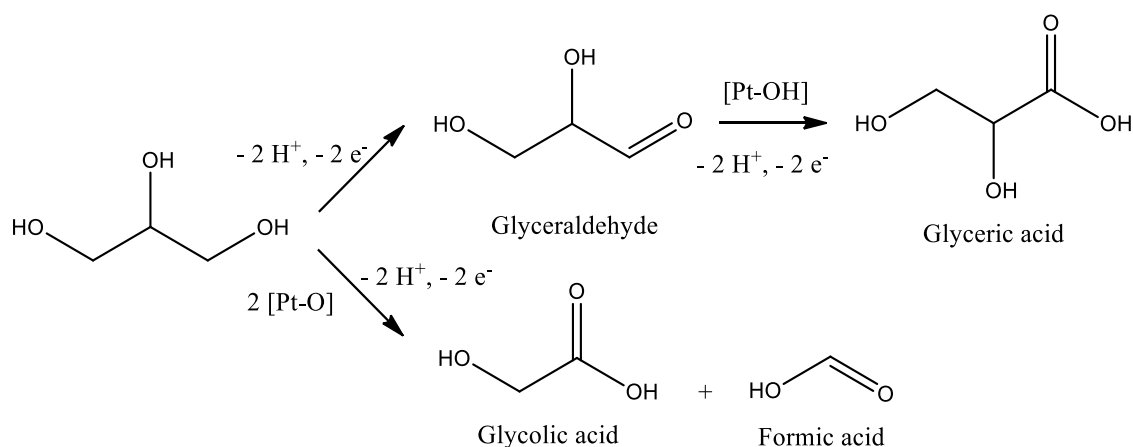


**Figure 4.61:** GC chromatogram of the products obtained from the electro-oxidation of glycerol in the presence of Amberlyst-15 on Pt anode electrodes at 80 °C and 2.0 A constant current.

During electro-oxidation, the glycerol primary OH group may be adsorbed on the Pt electrode surface and further oxidized to glyceraldehyde. The glyceraldehyde molecule would further interact with Pt–OH formed on the Pt electrode surface and may produce glyceric acid. When the reaction time increases, stable oxides are formed on the surface of the Pt electrode. These oxides could cause glycerol C–C bond cleavage and lead to the formation of glycolic and formic acids, as shown in Scheme 4.7.



**Scheme 4.7:** Proposed reaction mechanism for the electro-oxidation of glycerol.

In this study, the electroreduction and electro-oxidation of glycerol were successfully studied separately. At the cathodic region, 1,2-PDO was produced with a high selectivity. Although the three electrodes, namely, Pt, ACC, and CBD electrodes, exhibited a relatively similar yield for 1,2-PDO, ACC electrode was suggested for use in the future study because it is cheaper and can provide a larger active surface area with smaller geometrical surface.

At the anodic region, Pt electrode was used for the electro-oxidation study because Pt works well in acidic medium and is considered the only metal that can initiate the early stage of alcohol electro-oxidation (Kim *et al.*, 2008b). Although Pt was used as anode electrode for all the experiments in this case study, the conversion rate and yield varied according to the cathode electrode applied. Moreover, electrical conductivity was affected when both electrodes were different, thereby leading to different product yield selectivities and conversion rates. Glycolic and glyceric acids were the main compounds obtained from glycerol via the electro-oxidation on the Pt electrode.

## CHAPTER 5: CONCLUSION AND RECOMMENDATION FOR FUTURE RESEARCH

### 5.1 Conclusion

The electrochemical studies of glycerol with the solid acid catalyst, namely, Amberlyst-15, as reaction medium were carried out in a one-pot electrochemical cell. Three types of cathode materials including Pt, ACC, and CBD were investigated. Glycerol electrochemical conversion was also performed in a two-compartment electrochemical cell. The electro-oxidation and electroreduction were studied independently.

In the first objective, the electrochemical studies were carried out on Pt electrode in the presence of Amberlyst-15. Glycerol was successfully converted, mainly into glycolic and glyceric acids. At high reaction temperature of 80 °C and low electric current of 1.0 A, the optimum glycerol conversion was 97.2%. The maximum product yield for glycolic and glyceric acids was 44.7% and 27.2%, respectively. Amberlyst-15 displayed an added advantage because it can work as a redox catalyst during the electrosynthesis process.

Subsequently, two cathode materials (ACC and CBD) were evaluated, and results were compared with those obtained over Pt electrode. Product distribution considerably depended on the working electrode used. In the electrosynthesis study on Pt cathode electrode versus Pt anode electrode, glycerol was oxidized to glycolic and glyceric acids. Furthermore, in the study on ACC and CBD cathode electrodes versus Pt anode electrode, these electrodes, in addition to the oxidation compound (glycolic acid), reduced the reaction intermediates to some other high added-value compounds, such as lactic acid, 1,2-PDO, and 1,3-PDO. The reduction process was favored on high porous

surface. Other valuable intermediate compounds, such as acetol, acetaldehyde, ethylene glycol, and glyceraldehyde, were also obtained.

In the third objective, optimization of electrochemical studies were carried out on ACC and CBD electrodes. The effects of catalyst amount, reaction temperature, and electric current were investigated. According to the results obtained in both optimization studies, the reaction was favorable at high temperature (80 °C), medium electric current (2.0 A), and with 9.6% w/v Amberlyst-15. The highest glycerol conversions obtained were around 99%. The glycolic acid yield obtained for ACC and CBD electrodes was 66.1% and 58.1%, respectively. Maximum lactic acid yields were obtained on ACC and CBD electrodes at 25.9% and 21.4%, respectively.

Finally, the electrochemical studies of glycerol in a two-compartment reactor were investigated over three cathode materials, i.e., Pt, ACC, and CBD. Electro-oxidation and electroreduction were studied separately. The electroreduction of glycerol was also successfully examined. Glycerol was reduced into 1,2-PDO in the three cathode materials, given with selectivity of 85% on ACC cathode electrode. To the best of our knowledge, this study reported the direct electroreduction of glycerol for the first time. These findings successfully provided a new approach for the electroreduction study of glycerol.

In the anodic compartment, glycerol was generally converted to glycolic and glyceric acids on Pt anode electrode, given the maximum yield of 43.5% and 47.0%, respectively, together with a 100% glycerol conversion. When the electro-oxidation operation was isolated from the electroreduction process in a two-compartment reactor, lactic acid was not observed. Therefore, lactic acid could be a compound obtained from further reduction of intermediate in the oxidation region.

## 5.2 Suggestions for future studies

Glycolic acid, lactic acid, glyceric acid, and 1,2-PDO produced from this study exhibit high commercial value. Currently, they are widely applied in pharmaceutical, food, and cosmetic industries. In addition, these compounds can perform as a platform molecule to form polymer used to make fibers, plastics, and food packaging.

On the basis of the promising results obtained in this work, we suggest to use ACC in future electrochemical studies (either for the electro-oxidation or reduction process). This raw material (activated carbon) used for electrode preparation is more environmentally friendly, cheaper, and readily obtained compared with the expensive metal electrode. Furthermore, this material has no limitation on the electrode shape and can provide a large active surface area with small geometrical surface.

The electroreduction of glycerol can be further improved by varying the acidic medium (e.g., type of acid: sulfuric and methane sulfonic acids) and other operation parameters, such as electric current, reaction temperature, cathode size, and ratio of activated carbon to carbon black. A continuous system with electrode stack can be established to optimize the reaction process. Moreover, the energy cost can be reduced by replacing the direct electricity supply with solar energy supply.

Nevertheless, the main challenge for this work lies on separation and purification studies. Column or ion-exchange chromatography and membrane filtration are suggested for future product purification.

In conclusion, further improvement can be performed for product selectivity, scaling up of production, and separation process.



## REFERENCES

- Abdullah, M. O., Tan, I. A. W., & Lim, L. S. (2011). Automobile adsorption air-conditioning system using oil palm biomass-based activated carbon: A review. *Renewable and Sustainable Energy Reviews*, *15*(4): 2061-2072.
- Ajeel, M. A., Aroua, M. K., & Daud, W. M. A. W. (2015a). Anodic Degradation of 2-Chlorophenol by Carbon Black Diamond and Activated Carbon Composite Electrodes. *Electrochimica Acta*, *180*: 22-28.
- Ajeel, M. A., Aroua, M. K., & Daud, W. M. A. W. (2015b). p-Benzoquinone Anodic Degradation by Carbon Black Diamond Composite Electrodes. *Electrochimica Acta*, *169*: 46-51.
- Ajeel, M. A., Aroua, M. K., & Daud, W. M. A. W. (2015c). Preparation and characterization of carbon black diamond composite electrodes for anodic degradation of phenol. *Electrochimica Acta*, *153*: 379-384.
- Ajeel, M. A., Taeib Aroua, M. K., & AshriWan Daud, W. M. (2016). Reactivity of carbon black diamond electrode during the electro-oxidation of Remazol Brilliant Blue R. *RSC Advances*, *6*(5): 3690-3699.
- Alfaro, M. A. Q., Ferro, S., Martínez-Huitle, C. A., & Vong, Y. M. (2006). Boron doped diamond electrode for the wastewater treatment. *Journal of the Brazilian Chemical Society*, *17*: 227-236.
- Amada, Y., Shinmi, Y., Koso, S., Kubota, T., Nakagawa, Y., & Tomishige, K. (2011). Reaction mechanism of the glycerol hydrogenolysis to 1,3-propanediol over Ir-ReOx/SiO<sub>2</sub> catalyst. *Applied Catalysis B-Environmental*, *105*(1-2): 117-127.
- Anand, P., & Saxena, R. K. (2012). A comparative study of solvent-assisted pretreatment of biodiesel derived crude glycerol on growth and 1,3-propanediol production from *Citrobacter freundii*. *New Biotechnology*, *29*(2): 199-205.
- Anastas, P. T., & Breen, J. J. (1997). Design for the environment and Green Chemistry: The heart and soul of industrial ecology. *Journal of Cleaner Production*, *5*(1), 97-102.
- Ania, C. O., & Béguin, F. (2007). Mechanism of adsorption and electrosorption of bentazone on activated carbon cloth in aqueous solutions. *Water Research*, *41*(15): 3372-3380.
- Arcanjo, M. R. A., Silva Jr, I. J., Rodríguez-Castellón, E., Infantes-Molina, A., & Vieira, R. S. (2016). Conversion of glycerol into lactic acid using Pd or Pt supported on carbon as catalyst. *Catalysis Today*. (In Press, Corrected Proof)
- Avramov-Ivic, M., Léger, J. M., Beden, B., Hahn, F., & Lamy, C. (1993). Adsorption of glycerol on platinum in alkaline medium: effect of the electrode structure. *Journal of Electroanalytical Chemistry*, *351*(1-2): 285-297.
- Avramov-Ivić, M. L., Leger, J. M., Lamy, C., Jović, V. D., & Petrović, S. D. (1991). The electro-oxidation of glycerol on the gold(100)-oriented single-crystal

surface and poly crystalline surface in 0.1 M NaOH. *Journal of Electroanalytical Chemistry and Interfacial Electrochemistry*, 308(1-2): 309-317.

Bagheri, S., Julkapli, N. M., & Yehye, W. A. (2015). Catalytic conversion of biodiesel derived raw glycerol to value added products. *Renewable and Sustainable Energy Reviews*, 41: 113-127.

Bambagioni, V., Bianchini, C., Marchionni, A., Filippi, J., Vizza, F., Teddy, J., Serp, P., & Zhiani, M. (2009). Pd and Pt–Ru anode electrocatalysts supported on multi-walled carbon nanotubes and their use in passive and active direct alcohol fuel cells with an anion-exchange membrane (alcohol = methanol, ethanol, glycerol). *Journal of Power Sources*, 190(2): 241-251.

Beden, B., Çetin, I., Kahyaoglu, A., Takky, D., & Lamy, C. (1987). Electrocatalytic oxidation of saturated oxygenated compounds on gold electrodes. *Journal of Catalysis*, 104(1): 37-46.

Bełtowska-Brzezinska, M., Łuczak, T., & Holze, R. (1997). Electrocatalytic oxidation of mono- and polyhydric alcohols on gold and platinum. *Journal of Applied Electrochemistry*, 27(9): 999-1011.

Bianchini, C., & Shen, P. K. (2009). Palladium-Based Electrocatalysts for Alcohol Oxidation in Half Cells and in Direct Alcohol Fuel Cells. *Chemical Reviews*, 109(9): 4183-4206.

Biebl, H., & Cathrin, S. (2002). Taxonomy of the Glycerol Fermenting Clostridia and Description of *Clostridium diolis* sp. nov. *Systematic and Applied Microbiology*, 25(4): 491-497.

Biebl, H., Menzel, K., Zeng, A. P., & Deckwer, W. D. (1999). Microbial production of 1,3-propanediol. *Applied Microbiology and Biotechnology*, 52(3): 289-297.

Bo, X., & Guo, L. (2013). Simple synthesis of macroporous carbon–graphene composites and their use as a support for Pt electrocatalysts. *Electrochimica Acta*, 90: 283-290.

Bon Saint Côme, Y., Lalo, H., Wang, Z., Etienne, M., Gajdzik, J., Kohring, G.-W., Walcarius, A., Hempelmann, R., & Kuhn, A. (2011). Multiscale-Tailored Bioelectrode Surfaces for Optimized Catalytic Conversion Efficiency. *Langmuir*, 27(20): 12737-12744.

Boniardi, N., Rota, R., Nano, G., & Mazza, B. (1996). Analysis of the sodium lactate concentration process by electrodialysis. *Separations Technology*, 6(1), 43-54.

Boontawan, P., Kanchanathawe, S., & Boontawan, A. (2011). Extractive fermentation of l-(+)-lactic acid by *Pediococcus pentosaceus* using electrodeionization (EDI) technique. *Biochemical Engineering Journal*, 54(3), 192-199.

Bozell, J. J. (2010). Connecting Biomass and Petroleum Processing with a Chemical Bridge. *Science*, 329(5991): 522-523.

- Bühler, W., Dinjus, E., Ederer, H. J., Kruse, A., & Mas, C. (2002). Ionic reactions and pyrolysis of glycerol as competing reaction pathways in near- and supercritical water. *The Journal of Supercritical Fluids*, 22(1): 37-53.
- Brown, M. (2012). Advance BioFuels. Retrieved 20 September 2016, from <http://www.slideshare.net/chicagocleane/ccea-jan-19-final>
- Card, J. C., Valentin, G., & Storck, A. (1990). The Activated Carbon Electrode: A New, Experimentally - Verified Mathematical Model for the Potential Distribution. *Journal of The Electrochemical Society*, 137(9): 2736-2745.
- Cardona, C., Posada, J., & Montoya, M. (2007). *Use of glycerol from biodiesel production: Conversion to added value products*. Paper presented at the European Congress of Chemical Engineering (ECCE-6), Copenhagen, 16-20 September 2007.
- Carrettin, S., McMorn, P., Johnston, P., Griffin, K., Kiely, C. J., & Hutchings, G. J. (2003). Oxidation of glycerol using supported Pt, Pd and Au catalysts. *Physical Chemistry Chemical Physics*, 5(6): 1329-1336.
- Castillo Martinez, F. A., Balciunas, E. M., Salgado, J. M., Domínguez González, J. M., Converti, A., & Oliveira, R. P. d. S. (2013). Lactic acid properties, applications and production: A review. *Trends in Food Science & Technology*, 30(1): 70-83.
- Chaminand, J., Djakovitch, L. a., Gallezot, P., Marion, P., Pinel, C., & Rosier, C. (2004). Glycerol hydrogenolysis on heterogeneous catalysts. *Green Chemistry*, 6(8): 359-361.
- Che, T. M. (1985). C. Corporation.
- Chen, X., Zhang, D. J., Qi, W. T., Gao, S. J., Xiu, Z. L., & Xu, P. (2003). Microbial fed-batch production of 1,3-propanediol by *Klebsiella pneumoniae*; under micro-aerobic conditions. *Applied Microbiology and Biotechnology*, 63(2): 143-146.
- Childress, A. E., & Elimelech, M. (2000). Relating Nanofiltration Membrane Performance to Membrane Charge (Electrokinetic) Characteristics. *Environmental Science & Technology*, 34(17), 3710-3716.
- Clippel, F., Dusselier, M., Van Rompaey, R., Vanelderren, P., Dijkmans, J., Makshina, E., Giebeler, L., Oswald, S., Baron, G. V., Denayer, J. F. M., Pescarmona, P. P., Jacobs, P. A., & Sels, B. F. (2012). Fast and Selective Sugar Conversion to Alkyl Lactate and Lactic Acid with Bifunctional Carbon-Silica Catalysts. *Journal of the American Chemical Society*, 134(24): 10089-10101.
- Clomburg, J. M., & Gonzalez, R. (2011). Metabolic engineering of *Escherichia coli* for the production of 1,2-propanediol from glycerol. *Biotechnology and Bioengineering*, 108(4): 867-879.
- Costentin, C., Drouet, S., Robert, M., & Savéant, J.-M. (2012). Turnover Numbers, Turnover Frequencies, and Overpotential in Molecular Catalysis of Electrochemical Reactions. Cyclic Voltammetry and Preparative-Scale Electrolysis. *Journal of the American Chemical Society*, 134(27): 11235-11242.

- D'Hondt, E., Van de Vyver, S., Sels, B. F., & Jacobs, P. A. (2008). Catalytic glycerol conversion into 1,2-propanediol in absence of added hydrogen. *Chemical Communications*, (45): 6011-6012.
- Dabrock, B., Bahl, H., & Gottschalk, G. (1992). Parameters affecting solvent production by *Clostridium pasteurianum*. *Applied and environmental microbiology*, 58(4): 1233-1239.
- Danner, H., Madzingaidzo, L., Holzer, M., Mayrhuber, L., & Braun, R. (2000). Extraction and purification of lactic acid from silages. *Bioresource Technology*, 75(3), 181-187.
- Dasari, M. A., Kiatsimkul, P.-P., Sutterlin, W. R., & Suppes, G. J. (2005). Low-pressure hydrogenolysis of glycerol to propylene glycol. *Applied Catalysis A: General*, 281(1-2): 225-231.
- Datta, R., & Henry, M. (2006). Lactic acid: recent advances in products, processes and technologies — a review. *Journal of Chemical Technology & Biotechnology*, 81(7): 1119-1129.
- Daud, W. M. A. W., & Ali, W. S. W. (2004). Comparison on pore development of activated carbon produced from palm shell and coconut shell. *Bioresource Technology*, 93(1): 63-69.
- Demirel-Gülen, S., Lucas, M., & Claus, P. (2005). Liquid phase oxidation of glycerol over carbon supported gold catalysts. *Catalysis Today*, 102–103: 166-172.
- Dieuzeide, M. L., Jobbagy, M., & Amadeo, N. (2016). Vapor-Phase Hydrogenolysis of Glycerol to 1,2-Propanediol over Cu/Al<sub>2</sub>O<sub>3</sub> Catalyst at Ambient Hydrogen Pressure. *Industrial & Engineering Chemistry Research*, 55(9): 2527-2533.
- Dimitratos, N., Lopez-Sanchez, J. A., Lennon, D., Porta, F., Prati, L., & Villa, A. (2006). Effect of Particle Size on Monometallic and Bimetallic (Au,Pd)/C on the Liquid Phase Oxidation of Glycerol. *Catalysis Letters*, 108(3): 147-153.
- Drent, E., & Jager, W. W. (1998). S. O. Company.
- Dusselier, M., Van Wouwe, P., Dewaele, A., Makshina, E., & Sels, B. F. (2013). Lactic acid as a platform chemical in the biobased economy: the role of chemocatalysis. *Energy & Environmental Science*, 6(5): 1415-1442.
- Elmouwahidi, A., Zapata-Benabithé, Z., Carrasco-Marín, F., & Moreno-Castilla, C. (2012). Activated carbons from KOH-activation of argan (*Argania spinosa*) seed shells as supercapacitor electrodes. *Bioresource Technology*, 111: 185-190.
- Elisseeva, T. V., Shaposhnik, V. A., & Luschik, I. G. (2002). Demineralization and separation of amino acids by electro dialysis with ion-exchange membranes. *Desalination*, 149(1), 405-409.
- Everett, D. H. (1972). Manual of symbols and terminology for physicochemical quantities and units, Appendix II: definitions, terminology and symbols in colloid and surface chemistry. *Pure and Applied Chemistry* 31(4): 577-638.

- Fang, Y., Wang, T., Miao, R., Tang, L., & Wang, X. (2010). Modification of Nafion membranes with ternary composite materials for direct methanol fuel cells. *Electrochimica Acta*, 55(7): 2404-2408.
- Fardel, R., Griesbach, U., Pütter, H., & Comminellis, C. (2006). Electrosynthesis of trimethylorthoformate on BDD electrodes. *Journal of Applied Electrochemistry*, 36(2): 249-253.
- Farma, R., Deraman, M., Awitdrus, A., Talib, I. A., Taer, E., Basri, N. H., Manjunatha, J. G., Ishak, M. M., Dollah, B. N. M., & Hashmi, S. A. (2013). Preparation of highly porous binderless activated carbon electrodes from fibres of oil palm empty fruit bunches for application in supercapacitors. *Bioresource Technology*, 132: 254-261.
- Farnetti, E., Monte, R. D., & Kašpar, J. (2009). Homogeneous and Heterogeneous Catalysis In I. Bertini (Ed.), *Inorganic and Bio-Inorganic Chemistry*, Vol. 2: pp. 50-86. United Kingdom: Eolss Publishers Co. Ltd. .
- Farrell, J., Martin, F. J., Martin, H. B., O'Grady, W. E., & Natishan, P. (2005). Anodically Generated Short-Lived Species on Boron-Doped Diamond Film Electrodes. *Journal of The Electrochemical Society*, 152(1): E14-E17.
- Fashedemi, O. O., Miller, H. A., Marchionni, A., Vizza, F., & Ozoemena, K. I. (2015). Electro-oxidation of ethylene glycol and glycerol at palladium-decorated FeCo@Fe core-shell nanocatalysts for alkaline direct alcohol fuel cells: functionalized MWCNT supports and impact on product selectivity. *Journal of Materials Chemistry A*, 3(13): 7145-7156.
- Feng, J., Xiong, W., Xu, B., Jiang, W., Wang, J., & Chen, H. (2014). Basic oxide-supported Ru catalysts for liquid phase glycerol hydrogenolysis in an additive-free system. *Catalysis Communications*, 46: 98-102.
- Fidaleo, M., & Moresi, M. (2006). Assessment of the main engineering parameters controlling the electrodialytic recovery of sodium propionate from aqueous solutions. *Journal of Food Engineering*, 76(2), 218-231.
- Foo, K. Y., & Hameed, B. H. (2011). Utilization of rice husks as a feedstock for preparation of activated carbon by microwave induced KOH and K<sub>2</sub>CO<sub>3</sub> activation. *Bioresource Technology*, 102(20): 9814-9817.
- Foo, K. Y., & Hameed, B. H. (2013). Utilization of oil palm biodiesel solid residue as renewable sources for preparation of granular activated carbon by microwave induced KOH activation. *Bioresource Technology*, 130: 696-702.
- Fordham, P., Besson, M. I., & Gallezot, P. (1995). Selective catalytic oxidation of glyceric acid to tartronic and hydroxypyruvic acids. *Applied Catalysis A: General*, 133(2): L179-L184.
- Forsberg, C. W. (1987). Production of 1,3-propanediol from glycerol by *Clostridium acetobutylicum* and other *Clostridium* species. *Applied and environmental microbiology*, 53(4): 639-643.

- Francke, R., & Little, R. D. (2014). Redox catalysis in organic electrosynthesis: basic principles and recent developments. *Chemical Society Reviews*, 43(8): 2492-2521.
- Frija, L. M. T., & Afonso, C. A. M. (2012). Amberlyst-15: a reusable heterogeneous catalyst for the dehydration of tertiary alcohols. *Tetrahedron*, 68(36): 7414-7421.
- Frontana-Uribe, B. A., Little, R. D., Ibanez, J. G., Palma, A., & Vasquez-Medrano, R. (2010). Organic electrosynthesis: a promising green methodology in organic chemistry. *Green Chemistry*, 12(12): 2099-2119.
- Frusteri, F., Arena, F., Bonura, G., Cannilla, C., Spadaro, L., & Di Blasi, O. (2009). Catalytic etherification of glycerol by tert-butyl alcohol to produce oxygenated additives for diesel fuel. *Applied Catalysis A: General*, 367(1-2): 77-83.
- Future\_Market\_Insights. (2016, 2016). Biobased Propylene Glycol Market: Global Industry Analysis and Opportunity Assessment 2014 - 2020. Retrieved 14 July 2016, 2016, from <http://www.futuremarketinsights.com/reports/global-biobased-propylene-glycol-market>
- Garcia, R., Besson, M., & Gallezot, P. (1995). Chemoselective catalytic oxidation of glycerol with air on platinum metals. *Applied Catalysis A: General*, 127(1): 165-176.
- Gergova, K., Petrov, N., & Eser, S. (1994). Adsorption properties and microstructure of activated carbons produced from agricultural by-products by steam pyrolysis. *Carbon*, 32(4): 693-702.
- Ghaffar, T., Irshad, M., Anwar, Z., Aqil, T., Zulifqar, Z., Tariq, A., Kamran, M., Ehsan, N., & Mehmood, S. (2014). Recent trends in lactic acid biotechnology: A brief review on production to purification. *Journal of Radiation Research and Applied Sciences*, 7(2): 222-229.
- Gil, S., Cuenca, N., Romero, A., Valverde, J. L., & Sánchez-Silva, L. (2014). Optimization of the synthesis procedure of microparticles containing gold for the selective oxidation of glycerol. *Applied Catalysis A: General*, 472: 11-20.
- Gomes, J. F., Gasparotto, L. H. S., & Tremiliosi-Filho, G. (2013). Glycerol electro-oxidation over glassy-carbon-supported Au nanoparticles: direct influence of the carbon support on the electrode catalytic activity. *Physical Chemistry Chemical Physics*, 15(25): 10339-10349.
- Gomes, J. F., Martins, C., Giz, M. J., Tremiliosi-Filho, G., & Camara, G. A. (2013). Insights into the adsorption and electro-oxidation of glycerol: Self-inhibition and concentration effects. *Journal of Catalysis*, 301: 154-161.
- Gong, L., Lu, Y., Ding, Y., Lin, R., Li, J., Dong, W., Wang, T., & Chen, W. (2010). Selective hydrogenolysis of glycerol to 1,3-propanediol over a Pt/WO<sub>3</sub>/TiO<sub>2</sub>/SiO<sub>2</sub> catalyst in aqueous media. *Applied Catalysis A: General*, 390(1-2): 119-126.

- González, M. I., Alvarez, S., Riera, F. A., & Álvarez, R. (2008). Lactic acid recovery from whey ultrafiltrate fermentation broths and artificial solutions by nanofiltration. *Desalination*, 228(1), 84-96.
- Grand\_View\_Research, I. (2016). Global glycolic acid market by application (personal care, household cleaning, industrial) is expected to reach USD 277.8 million by 2020. Retrieved 14 July 2016, 2016, from <https://www.grandviewresearch.com/press-release/global-glycolic-acid-market>
- Griesbach, U., Zollinger, D., Pütter, H., & Comninellis, C. (2005). Evaluation of boron doped diamond electrodes for organic electrosynthesis on a preparative scale. *Journal of Applied Electrochemistry*, 35(12): 1265-1270.
- Gupta, O. P., Chauhan, M., & Loomba, R. (1984). Study of the variation in the cathode potential with temperature in Ni-Cd alloy plating from a sulphate bath. *Surface Technology*, 21(2): 155-160.
- Hábová, V., Melzoch, K., Rychtera, M., & Sekavová, B. (2004). Electrodialysis as a useful technique for lactic acid separation from a model solution and a fermentation broth. *Desalination*, 162, 361-372.
- Hazimah, A. H., Ooi, T. L., & Salmiah, A. (2003). Recovery of glycerol and diglycerol from glycerol pitch. *Journal of Oil Palm Research* 15(1): 1-5.
- He, X., Ling, P., Qiu, J., Yu, M., Zhang, X., Yu, C., & Zheng, M. (2013). Efficient preparation of biomass-based mesoporous carbons for supercapacitors with both high energy density and high power density. *Journal of Power Sources*, 240: 109-113.
- Heming, M. (2012). Glycerine Market Report *Glycerine Market Report* (N<sup>099</sup>), 3-25.
- Heyndrickx, M., Devos, P., Vancanneyt, M., & Deley, J. (1991). The fermentation of glycerol by *Clostridium butyricum* Lmg-1212T2 and Lmg-1213T1 and *C pasteurianum* Lmg-3285. *Applied Microbiology and Biotechnology*, 34(5): 637-642.
- Holade, Y., Morais, C., Servat, K., Napporn, T. W., & Kokoh, K. B. (2013). Toward the Electrochemical Valorization of Glycerol: Fourier Transform Infrared Spectroscopic and Chromatographic Studies. *ACS Catalysis*, 3(10): 2403-2411.
- Holm, M. S., Saravanamurugan, S., & Taarning, E. (2010). Conversion of Sugars to Lactic Acid Derivatives Using Heterogeneous Zeotype Catalysts. *Science*, 328(5978): 602-605.
- Honda, K., Yamaguchi, Y., Yamanaka, Y., Yoshimatsu, M., Fukuda, Y., & Fujishima, A. (2005). Hydroxyl radical-related electrogenerated chemiluminescence reaction for a ruthenium tris(2,2')bipyridyl/co-reactants system at boron-doped diamond electrodes. *Electrochimica Acta*, 51(4): 588-597.
- Huang, C., Xu, T., Zhang, Y., Xue, Y., & Chen, G. (2007). Application of electrodialysis to the production of organic acids: State-of-the-art and recent developments. *Journal of Membrane Science*, 288(1-2), 1-12.

- Huang, L., Zhu, Y., Zheng, H., Ding, G., & Li, Y. (2009). Direct Conversion of Glycerol into 1,3-Propanediol over Cu-H<sub>4</sub>SiW<sub>12</sub>O<sub>40</sub>/SiO<sub>2</sub> in Vapor Phase. *Catalysis Letters*, 131(1-2): 312-320.
- Hunsom, M., & Saila, P. (2013). Product distribution of electrochemical conversion of glycerol via Pt electrode: effect of initial pH. *International Journal of Electrochemical Science*, 8(9): 11288-11300.
- Hunsom, M., & Saila, P. (2015). Electrochemical conversion of enriched crude glycerol: Effect of operating parameters. *Renewable Energy*, 74: 227-236.
- Ishiyama, K., Kosaka, F., Shimada, I., Oshima, Y., & Otomo, J. (2013). Glycerol electro-oxidation on a carbon-supported platinum catalyst at intermediate temperatures. *Journal of Power Sources*, 225: 141-149.
- Jung, J. Y., Choi, E. S., & Oh, M. K. (2008). Enhanced production of 1,2-propanediol by *tpi1* deletion in *Saccharomyces cerevisiae*. *Journal of Microbiology and Biotechnology*, 18(11): 1797-1802.
- Jung, J. Y., Yun, H. S., Lee, J., & Oh, M. K. (2011). Production of 1,2-propanediol from glycerol in *Saccharomyces cerevisiae*. *J Microbiol Biotechnol*, 21(8): 846-853.
- Kadirgan, F., Beden, B., & Lamy, C. (1982). Electrocatalytic oxidation of ethylene-glycol. *Journal of Electroanalytical Chemistry and Interfacial Electrochemistry*, 136(1): 119-138.
- Kadirgan, F., Beden, B., & Lamy, C. (1983). Electrocatalytic oxidation of ethylene-glycol. *Journal of Electroanalytical Chemistry and Interfacial Electrochemistry*, 143(1): 135-152.
- Kalderis, D., Bethanis, S., Paraskeva, P., & Diamadopoulos, E. (2008). Production of activated carbon from bagasse and rice husk by a single-stage chemical activation method at low retention times. *Bioresource Technology*, 99(15): 6809-6816.
- Kishimoto, K. (2008). WO2008143146 A2. WO Patent.
- Katrlík, J., Voštiar, I., Šefčovičová, J., Tkáč, J., Mastihuba, V., Valach, M., Štefuca, V., & Gemeiner, P. (2007). A novel microbial biosensor based on cells of *Gluconobacter oxydans*; for the selective determination of 1,3-propanediol in the presence of glycerol and its application to bioprocess monitoring. *Analytical and Bioanalytical Chemistry*, 388(1): 287-295.
- Katryniok, B., Kimura, H., Skrzynska, E., Girardon, J.-S., Fongarland, P., Capron, M., Ducoulombier, R., Mimura, N., Paul, S., & Dumeignil, F. (2011). Selective catalytic oxidation of glycerol: perspectives for high value chemicals. *Green Chemistry*, 13(8): 1960-1979.
- Kenkel, P., & Holcomb, R. (2008). Feasibility of on-farm or small scale oilseed processing and biodiesel production. In B. C. English, R. J. Menard & K. Jensen



(Eds.), *Intergratopm of Agricultural and Energy Systems. Proceeding of a conference February 12-13, 2008, in Atlanta, Georgia* Farm Foundation

- Kim, J. H., Choi, S. M., Nam, S. H., Seo, M. H., Choi, S. H., & Kim, W. B. (2008a). Influence of Sn content on PtSn/C catalysts for electrooxidation of C1-3 alcohols: Synthesis, characterization, and electrocatalytic activity. *Applied Catalysis B: Environmental*, 82(1-2): 89-102.
- Kim, J. H., Choi, S. M., Nam, S. H., Seo, M. H., Choi, S. H., & Kim, W. B. (2008b). Influence of Sn content on PtSn/C catalysts for electrooxidation of C1-C3 alcohols: Synthesis, characterization, and electrocatalytic activity. *Applied Catalysis B: Environmental*, 82(1-2): 89-102.
- Kishida, H., Jin, F., Zhou, Z., Moriya, T., & Enomoto, H. (2005). Conversion of Glycerin into Lactic Acid by Alkaline Hydrothermal Reaction. *Chemistry Letters*, 34(11): 1560-1561.
- Kivistö, A., Santala, V., & Karp, M. (2012). 1,3-Propanediol production and tolerance of a halophilic fermentative bacterium, *Halanaerobium saccharolyticum* subsp. *saccharolyticum*. *Journal of Biotechnology*, 158(4): 242-247.
- Klepáčová, K., Mravec, D., & Bajus, M. (2005). tert-Butylation of glycerol catalysed by ion-exchange resins. *Applied Catalysis A: General*, 294(2): 141-147.
- Koivistoinen, O. M., Kuivanen, J., Barth, D., Turkia, H., Pitkänen, J.-P., Penttilä, M., & Richard, P. (2013). Glycolic acid production in the engineered yeasts *Saccharomyces cerevisiae* and *Kluyveromyces lactis*. *Microbial cell factories*, 12: 82.
- Kokoh, K. B., Parpot, P., Belgsir, E. M., Léger, J. M., Beden, B., & Lamy, C. (1993). Selective oxidation of D-gluconic acid on platinum and lead adatoms modified platinum electrodes in alkaline medium. *Electrochimica Acta*, 38(10): 1359-1365.
- Kongjao, S., Damronglerd, S., & Hunsom, M. (2011). Electrochemical reforming of an acidic aqueous glycerol solution on Pt electrodes. *Journal of Applied Electrochemistry*, 41(2): 215-222.
- Kraft, A. (2007). Doped Diamond: A Compact Review on a New, Versatile Electrode Material. *International Journal of Electrochemical Science*. (2): 355-385
- Kraus, G. A. (2008). Synthetic methods for the preparation of 1,3-propanediol. *Clean-Soil Air Water*, 36(8): 648-651.
- Kumar, K. S., Haridoss, P., & Seshadri, S. K. (2008). Synthesis and characterization of electrodeposited Ni-Pd alloy electrodes for methanol oxidation. *Surface and Coatings Technology*, 202(9): 1764-1770.
- Kurosaka, T., Maruyama, H., Naribayashi, I., & Sasaki, Y. (2008). Production of 1,3-propanediol by hydrogenolysis of glycerol catalyzed by Pt/WO<sub>3</sub>/ZrO<sub>2</sub>. *Catalysis Communications*, 9(6): 1360-1363.

- Kusunoki, Y., Miyazawa, T., Kunimori, K., & Tomishige, K. (2005). Highly active metal-acid bifunctional catalyst system for hydrogenolysis of glycerol under mild reaction conditions. *Catalysis Communications*, 6(10): 645-649.
- Kwon, Y., Birdja, Y., Spanos, I., Rodriguez, P., & Koper, M. T. M. (2012). Highly Selective Electro-Oxidation of Glycerol to Dihydroxyacetone on Platinum in the Presence of Bismuth. *ACS Catalysis*, 2(5): 759-764.
- Kwon, Y., Hersbach, T. P., & Koper, M. M. (2014). Electro-Oxidation of Glycerol on Platinum Modified by Adatoms: Activity and Selectivity Effects. *Topics in Catalysis*, 57(14-16): 1272-1276.
- Kwon, Y., Schouten, K. J. P., & Koper, M. T. M. (2011). Mechanism of the Catalytic Oxidation of Glycerol on Polycrystalline Gold and Platinum Electrodes. *ChemCatChem*, 3(7): 1176-1185.
- Lakshmanan, P., Upare, P. P., Le, N.-T., Hwang, Y. K., Hwang, D. W., Lee, U. H., Kim, H. R., & Chang, J.-S. (2013). Facile synthesis of CeO<sub>2</sub>-supported gold nanoparticle catalysts for selective oxidation of glycerol into lactic acid. *Applied Catalysis A: General*, 468: 260-268.
- Lee, C. S., Aroua, M. K., Daud, W. M. A. W., Cognet, P., Pérès-Lucchese, Y., Fabre, P. L., Reynes, O., & Latapie, L. (2015). A review: Conversion of bioglycerol into 1,3-propanediol via biological and chemical method. *Renewable and Sustainable Energy Reviews*, 42: 963-972.
- Lee, C. S., Ong, Y. L., Aroua, M. K., & Daud, W. M. A. W. (2013). Impregnation of palm shell-based activated carbon with sterically hindered amines for CO<sub>2</sub> adsorption. *Chemical Engineering Journal*, 219: 558-564.
- Lee, J. W., Kang, H., Kim, J. Y., & Kim, J. (2011). Electrode for electrochemical water treatment, method of manufacturing the same, method of treating water using the electrode, and device including the electrode for electrochemical water treatment: US Patent: US 20110198238 A1.
- Linares, N., Silvestre-Albero, A. M., Serrano, E., Silvestre-Albero, J., & Garcia-Martinez, J. (2014). Mesoporous materials for clean energy technologies. *Chemical Society Reviews*, 43(22): 7681-7717.
- Liu, H.-J., Zhang, D.-J., Xu, Y.-H., Mu, Y., Sun, Y.-Q., & Xiu, Z.-L. (2007). Microbial production of 1,3-propanediol from glycerol by *Klebsiella pneumoniae*; under micro-aerobic conditions up to a pilot scale. *Biotechnology Letters*, 29(8): 1281-1285.
- Liu, H., Liang, S., Jiang, T., Han, B., & Zhou, Y. (2012). Hydrogenolysis of Glycerol to 1,2-Propanediol over Ru–Cu Bimetals Supported on Different Supports. *CLEAN – Soil, Air, Water*, 40(3): 318-324.
- Liu, L., Ye, X. P., & Bozell, J. J. (2012). A Comparative Review of Petroleum-Based and Bio-Based Acrolein Production. *ChemSusChem*, 5(7): 1162-1180.

- Luo, G. S., Pan, S., & Liu, J. G. (2002). Use of the electro dialysis process to concentrate a formic acid solution. *Desalination*, 150(3), 227-234.
- Lux, S., Stehring, P., & Siebenhofer, M. (2010). Lactic acid production as a new approach for exploitation of glycerol. *Separation Science and Technology*, 45: 1921-1927.
- Madzingaidzo, L., Danner, H., & Braun, R. (2002). Process development and optimisation of lactic acid purification using electro dialysis. *Journal of Biotechnology*, 96(3), 223-239.
- Malkowsky, I. M., Griesbach, U., Pütter, H., & Waldvogel, S. R. (2006). Unexpected Highly Chemoselective Anodic ortho-Coupling Reaction of 2,4-Dimethylphenol on Boron-Doped Diamond Electrodes. *European Journal of Organic Chemistry*, 2006(20): 4569-4572.
- Mallat, T., & Baiker, A. (1994). Oxidation of alcohols with molecular oxygen on platinum metal catalysts in aqueous solutions. *Catalysis Today*, 19(2): 247-283.
- Maris, E. P., & Davis, R. J. (2007). Hydrogenolysis of glycerol over carbon-supported Ru and Pt catalysts. *Journal of Catalysis*, 249(2): 328-337.
- Markets\_and\_Markets. (2016a). 1,3-Propanediol market worth \$621.2 million by 2021. Retrieved 14 July 2016, 2016, from <http://www.marketsandmarkets.com/PressReleases/1-3-propanediol-pdo.asp>
- Markets\_and\_Markets. (2016b, 2016). Propylene Glycol Market worth \$4.2 Billion by 2019. Retrieved 14 July 2016, 2016, from <http://www.marketsandmarkets.com/PressReleases/propylene-glycol.asp>
- Marselli, B., Garcia-Gomez, J., Michaud, P.-A., Rodrigo, M. A., & Comninellis, C. (2003). Electrogeneration of Hydroxyl Radicals on Boron-Doped Diamond Electrodes. *Journal of The Electrochemical Society*, 150(3): D79-D83.
- Martin, C., Huser, H., Servat, K., & Kokoh, K. B. (2005). Electrosynthesis of lactic acid on copper and lead cathodes in aqueous media. *Electrochimica Acta*, 51(1): 111-117.
- Martin, C., Huser, H., Servat, K., & Kokoh, K. B. (2006). Electrosynthesis of lactic acid and 2,3-dimethyltartaric acid from pyruvic acid on lead cathode in aqueous medium. *Tetrahedron Letters*, 47(20): 3459-3462.
- Matsumoto, M., & Nishimura, Y. (2007). Hydrogen production by fermentation using acetic acid and lactic acid. *Journal of Bioscience and Bioengineering*, 103(3): 236-241.
- McDougall, G. J. (1991). The physical nature and manufacture of activated carbon. *Journal of the South African Institute of Mining and Metallurgy*, 91(4): 109-120.
- McMorn, P., Roberts, G., & Hutchings, G. J. (1999). Oxidation of glycerol with hydrogen peroxide using silicalite and aluminophosphate catalysts. *Catalysis Letters*, 63(3): 193-197.

- Menzel, K., Zeng, A. P., & Deckwer, W. D. (1997). High concentration and productivity of 1,3-propanediol from continuous fermentation of glycerol by *Klebsiella pneumoniae*. *Enzyme and Microbial Technology*, 20(2): 82-86.
- Metsoviti, M., Paramithiotis, S., Drosinos, E. H., Galiotou-Panayotou, M., Nychas, G. J. E., Zeng, A. P., & Papanikolaou, S. (2012). Screening of bacterial strains capable of converting biodiesel-derived raw glycerol into 1,3-propanediol, 2,3-butanediol and ethanol. *Engineering in Life Sciences*, 12(1): 57-68.
- Moon, P. J., Parulekar, S. J., & Tsai, S.-P. (1998). Competitive anion transport in desalting of mixtures of organic acids by batch electrodialysis. *Journal of Membrane Science*, 141(1), 75-89.
- Murayama, T., & Yamanaka, I. (2011). Electrosynthesis of Neutral H<sub>2</sub>O<sub>2</sub> Solution from O<sub>2</sub> and Water at a Mixed Carbon Cathode Using an Exposed Solid-Polymer-Electrolyte Electrolysis Cell. *The Journal of Physical Chemistry C*, 115(13): 5792-5799.
- Myszka, K., Leja, K., Olejnik-Schmidt, A. K., & Czaczyk, K. (2012). Isolation process of industrially useful *Clostridium bifermentans* from natural samples. *Journal of Bioscience and Bioengineering*, 113(5): 631-633.
- Nakagawa, Y., & Tomishige, K. (2011). Heterogeneous catalysis of the glycerol hydrogenolysis. *Catalysis Science & Technology*, 1(2): 179-190.
- Neher, A., Haas, T., Arntz, D., Klenk, H., & Girke, W. (1995). Process for the production of acrolein: US Patents: US 5387720 A
- Ng, E. (2015). Southeast Asian glycerin prices rise on PME plant shutdowns. Retrieved 5th July 2016, from <http://www.platts.com/latest-news/agriculture/singapore/southeast-asian-glycerin-prices-rise-on-pme-plant-26986662>
- Oh, J., Dash, S., & Lee, H. (2011). Selective conversion of glycerol to 1,3-propanediol using Pt-sulfated zirconia. *Green Chemistry*, 13(8): 2004-2007.
- Okada, K. (2013). *Electrochemical oxidation of glycerol in proton-exchange-membrane reactor* (Doctor of Philosophy), University of Michigan United States.
- Oliveira, V. L., Morais, C., Servat, K., Napporn, T. W., Tremiliosi-Filho, G., & Kokoh, K. B. (2014). Studies of the reaction products resulted from glycerol electrooxidation on Ni-based materials in alkaline medium. *Electrochimica Acta*, 117: 255-262.
- Omar, S., Girgis, B., & Taha, F. (2003). Carbonaceous materials from seed hulls for bleaching of vegetable oils. *Food Research International*, 36(1): 11-17.
- Ott, L., Bicker, M., & Vogel, H. (2006). Catalytic dehydration of glycerol in sub- and supercritical water: a new chemical process for acrolein production. *Green Chemistry*, 8(2): 214-220.

- Pagliaro, M., Ciriminna, R., Kimura, H., Rossi, M., & Della Pina, C. (2007). From Glycerol to Value-Added Products. *Angewandte Chemie International Edition*, 46(24): 4434-4440.
- Pal, R., Sarkar, T., & Khasnobis, S. (2012). Amberlyst-15 in organic synthesis *Archive for Organic Chemistry* 2012(1): 570-609.
- Pandhare, N. N., Pudi, S. M., Biswas, P., & Sinha, S. (2016). Selective Hydrogenolysis of Glycerol to 1,2-Propanediol over Highly Active and Stable Cu/MgO Catalyst in the Vapor Phase. *Organic Process Research & Development*, 20(6): 1059-1067.
- Panizza, M., & Cerisola, G. (2005). Application of diamond electrodes to electrochemical processes. *Electrochimica Acta*, 51(2): 191-199.
- Panizza, M., Siné, G., Duo, I., Ouattara, L., & Comninellis, C. (2003). Electrochemical Polishing of Boron-Doped Diamond in Organic Media. *Electrochemical and Solid-State Letters*, 6(12): D17-D19.
- Paula, J. d., Nascimento, D., & Linares, J. J. (2014). Electrochemical reforming of glycerol in alkaline PBI-Based PEM reactor for hydrogen production. *Chemical Engineering Transactions* 41: 205-210.
- Pazhavelikkakath Purushothaman, R. K., van Haveren, J., Melián-Cabrera, I., van Eck, E. R. H., & Heeres, H. J. (2014). Base-Free, One-Pot Chemocatalytic Conversion of Glycerol to Methyl Lactate using Supported Gold Catalysts. *ChemSusChem*, 7(4): 1140-1147.
- Pico, M. P., Rosas, J. M., Rodríguez, S., Santos, A., & Romero, A. (2013). Glycerol etherification over acid ion exchange resins: effect of catalyst concentration and reusability. *Journal of Chemical Technology & Biotechnology*, 88(11): 2027-2038.
- Prentice, G. A. (1991). *Electrochemical engineering principles*. Singapore: Prentice Hall.
- Prieto, J. C. B., Slavík, R., & Kolomazník, K. (2013a). *Effect of platinum electrode on partial oxidation of glycerol and optimization by central composite design*. Paper presented at the 6th international conference on urban rehabilitation and sustainability (URES'13), Greece.
- Prieto, J. C. B., Slavík, R., & Kolomazník, K. (2013b). Optimization of Electrochemical Oxidation of Glycerol for Glyceric Acid Production. *International journal of energy and environment*, 7(5): 229-235.
- Prieto, J. C. B., Slavík, R., Kolomazník, K., & Pecha, J. (2014). Evaluation of Kinetics and Reaction Mechanism of Partial Oxidation of Glycerol. *International Journal of Automation and Power Engineering*, 3(1): 72-74.
- Puetter, H., & Merk, C. (2002). Electrochemical regeneration and recycling of mediators used in a wide variety of oxidation and reduction reactions is effected by contact with a diamond electrode: German Patents: DE 10045664 A1.

- Purushothaman, R. K. P., van Haveren, J., van Es, D. S., Melián-Cabrera, I., Meeldijk, J. D., & Heeres, H. J. (2014). An efficient one pot conversion of glycerol to lactic acid using bimetallic gold-platinum catalysts on a nanocrystalline CeO<sub>2</sub> support. *Applied Catalysis B: Environmental*, *147*: 92-100.
- Qi, J., Xin, L., Chadderdon, D. J., Qiu, Y., Jiang, Y., Benipal, N., Liang, C., & Li, W. (2014a). Electrocatalytic selective oxidation of glycerol to tartronate on Au/C anode catalysts in anion exchange membrane fuel cells with electricity cogeneration. *Applied Catalysis B: Environmental*, *154-155*: 360-368.
- Qi, J., Xin, L., Chadderdon, D. J., Qiu, Y., Jiang, Y., Benipal, N., Liang, C., & Li, W. (2014b). Electrocatalytic selective oxidation of glycerol to tartronate on Au/C anode catalysts in anion exchange membrane fuel cells with electricity cogeneration. *Applied Catalysis B-Environmental*, *154*: 360-368.
- Qin, L.-Z., Song, M.-J., & Chen, C.-L. (2010). Aqueous-phase deoxygenation of glycerol to 1,3-propanediol over Pt/WO<sub>3</sub>/ZrO<sub>2</sub> catalysts in a fixed-bed reactor. *Green Chemistry*, *12*(8): 1466-1472.
- Qu, D. (2007). Investigation of oxygen reduction on activated carbon electrodes in alkaline solution. *Carbon*, *45*(6): 1296-1301.
- Research\_and\_Markets. (2015). Lactic acid market by application (biodegradable polymer, food & beverage, personal care & pharmaceutical) & polylactic acid market by application, & by geography - global trends & forecasts to 2020. Retrieved 14 July 2016, 2016, from [http://www.researchandmarkets.com/reports/3505450/lactic-acid-market-by-application-biodegradable?gclid=CI\\_58sSV7M0CFS8z0wodAj4Iqw](http://www.researchandmarkets.com/reports/3505450/lactic-acid-market-by-application-biodegradable?gclid=CI_58sSV7M0CFS8z0wodAj4Iqw)
- Rezayat, M., & Ghaziaskar, H. S. (2009). Continuous synthesis of glycerol acetates in supercritical carbon dioxide using Amberlyst-15. *Green Chemistry*, *11*(5): 710-715.
- Robertson, G. L. (2016). Edible, biobased and biodegradable food packaging material *Food Packaging: Principles and Practice* (3rd ed.): pp. 73. United States: CRC Press.
- Rode, C. V., Ghalwadkar, A. A., Mane, R. B., Hengne, A. M., Jadkar, S. T., & Biradar, N. S. (2010). Selective Hydrogenolysis of Glycerol to 1,2-Propanediol: Comparison of Batch and Continuous Process Operations. *Organic Process Research & Development*, *14*(6): 1385-1392.
- Rodrigues, E. G., Pereira, M. F. R., Chen, X., Delgado, J. J., & Órfão, J. J. M. (2013). Selective Oxidation of Glycerol over Platinum-Based Catalysts Supported on Carbon Nanotubes. *Industrial & Engineering Chemistry Research*, *52*(49): 17390-17398.
- Rodríguez-Reinoso, F., & Molina-Sabio, M. (1992). Activated carbons from lignocellulosic materials by chemical and/or physical activation: an overview. *Carbon*, *30*(7): 1111-1118.

- Roquet, L., Belgsir, E. M., Léger, J. M., & Lamy, C. (1994). Kinetics and mechanisms of the electrocatalytic oxidation of glycerol as investigated by chromatographic analysis of the reaction products: Potential and pH effects. *Electrochimica Acta*, 39(16): 2387-2394.
- Rousseau, S., Coutanceau, C., Lamy, C., & Léger, J. M. (2006). Direct ethanol fuel cell (DEFC): Electrical performances and reaction products distribution under operating conditions with different platinum-based anodes. *Journal of Power Sources*, 158(1): 18-24.
- Saila, P., & Hunsom, M. (2015). Effect of additives on one-pot electrochemical conversion of enriched crude glycerol. *Korean Journal of Chemical Engineering*, 32: 2412.
- Saxena, R. K., Anand, P., Saran, S., & Isar, J. (2009). Microbial production of 1,3-propanediol: Recent developments and emerging opportunities. *Biotechnology Advances*, 27(6): 895-913.
- Schäfer Hans, J., Harenbrock, M., Klocke, E., Plate, M., & Weiper-Idelmann, A. (2007). Electrolysis for the benign conversion of renewable feedstocks *Pure and Applied Chemistry* Vol. 79: pp. 2047.
- Schlaf, M., Ghosh, P., Fagan, P. J., Hauptman, E., & Bullock, R. M. (2001). Metal-Catalyzed Selective Deoxygenation of Diols to Alcohols. *Angewandte Chemie International Edition*, 40(20): 3887-3890.
- Semmelhack, M. F., Chou, C. S., & Cortes, D. A. (1983). Nitroxyl-mediated electrooxidation of alcohols to aldehydes and ketones. *Journal of the American Chemical Society*, 105(13): 4492-4494.
- Sharma, S., & Pollet, B. G. (2012). Support materials for PEMFC and DMFC electrocatalysts—A review. *Journal of Power Sources*, 208: 96-119.
- Sharninghausen, L. S., Campos, J., Manas, M. G., & Crabtree, R. H. (2014). Efficient selective and atom economic catalytic conversion of glycerol to lactic acid. *Nat Commun*, 5(5084): 1-9
- Shen, Y., Zhang, S., Li, H., Ren, Y., & Liu, H. (2010). Efficient Synthesis of Lactic Acid by Aerobic Oxidation of Glycerol on Au–Pt/TiO<sub>2</sub> Catalysts. *Chemistry – A European Journal*, 16(25): 7368-7371.
- Shen, Z., Jin, F., Zhang, Y., Wu, B., Kishita, A., Tohji, K., & Kishida, H. (2009). Effect of Alkaline Catalysts on Hydrothermal Conversion of Glycerin into Lactic Acid. *Industrial & Engineering Chemistry Research*, 48(19): 8920-8925.
- Shinmi, Y., Koso, S., Kubota, T., Nakagawa, Y., & Tomishige, K. (2010). Modification of Rh/SiO<sub>2</sub> catalyst for the hydrogenolysis of glycerol in water. *Applied Catalysis B: Environmental*, 94(3-4): 318-326.
- Sigma\_Aldrich Retrieved 1 July 2016, 2016, from <http://www.sigmaaldrich.com/>

- Simões, M., Baranton, S., & Coutanceau, C. (2010). Electro-oxidation of glycerol at Pd based nano-catalysts for an application in alkaline fuel cells for chemicals and energy cogeneration. *Applied Catalysis B: Environmental*, 93(3-4): 354-362.
- Simões, M., Baranton, S., & Coutanceau, C. (2011). Enhancement of catalytic properties for glycerol electrooxidation on Pt and Pd nanoparticles induced by Bi surface modification. *Applied Catalysis B: Environmental*, 110: 40-49.
- Simões, M., Baranton, S., & Coutanceau, C. (2012). Electrochemical Valorisation of Glycerol. *ChemSusChem*, 5(11): 2106-2124.
- Singh, R. N., Singh, A., & Anindita. (2009). Electrocatalytic activity of binary and ternary composite films of Pd, MWCNT and Ni, Part II: Methanol electrooxidation in 1 M KOH. *International Journal of Hydrogen Energy*, 34(4): 2052-2057.
- Steckhan, E. (1986). Indirect Electroorganic Syntheses—A Modern Chapter of Organic Electrochemistry [New Synthetic Methods (59)]. *Angewandte Chemie International Edition in English*, 25(8): 683-701.
- Tang, J., Wang, T., Sun, X., Hu, Y., Xie, Q., Guo, Y., Xue, H., & He, J. (2013). Novel synthesis of reduced graphene oxide-ordered mesoporous carbon composites and their application in electrocatalysis. *Electrochimica Acta*, 90: 53-62.
- Tanninen, J., & Nyström, M. (2002). Separation of ions in acidic conditions using NF. *Desalination*, 147(1), 295-299.
- Thornton, J., Besemer, A., & Schraven, B. (2002). A recovery method: Patents: WO 2002059064 A1
- Valencia, R., Tirado, J. A., Sotelo, R., Trejo, F., & Lartundo, L. (2015). Synthesis of 1,2-propanediol through glycerol hydrogenolysis on Cu–Al mixed oxides. *Reaction Kinetics, Mechanisms and Catalysis*, 116(1): 205-222.
- Van de Vyver, S., Odermatt, C., Romero, K., Prasomsri, T., & Román-Leshkov, Y. (2015). Solid Lewis Acids Catalyze the Carbon-Carbon Coupling between Carbohydrates and Formaldehyde. *ACS Catalysis*, 5(2): 972-977.
- Vasiliadou, E. S., & Lemonidou, A. A. (2011). Parameters Affecting the Formation of 1,2-Propanediol from Glycerol over Ru/SiO<sub>2</sub> Catalyst. *Organic Process Research & Development*, 15(4): 925-931.
- Vinke, P., Wit, D. d., de Goede, A. T. J. W., & Bekkum, H. v. (1992). Noble Metal Catalyzed Oxidation of Carbohydrates and Carbohydrate Derivatives. In P. Ruiz & B. Delmon (Eds.), *Studies in Surface Science and Catalysis*, Vol. 72: pp. 1-20.
- Wang, F., Shao, S., Liu, C.-L., Xu, C.-L., Yang, R.-Z., & Dong, W.-S. (2015). Selective oxidation of glycerol over Pt supported on mesoporous carbon nitride in base-free aqueous solution. *Chemical Engineering Journal*, 264: 336-343.



- Wang, S., & Liu, H. (2014). Selective hydrogenolysis of glycerol to propylene glycol on hydroxycarbonate-derived Cu-ZnO-Al<sub>2</sub>O<sub>3</sub> catalysts. *Chinese Journal of Catalysis*, 35(5): 631-643.
- Wilkens, E., Ringel, A. K., Hortig, D., Willke, T., & Vorlop, K. D. (2012). High-level production of 1,3-propanediol from crude glycerol by *Clostridium butyricum* AKR102a. *Applied Microbiology and Biotechnology*, 93(3): 1057-1063.
- Wołosiak-Hnat, A., Milchert, E., & Lewandowski, G. (2013). Optimization of Hydrogenolysis of Glycerol to 1,2-Propanediol. *Organic Process Research & Development*, 17(4): 701-713.
- Xia, S., Yuan, Z., Wang, L., Chen, P., & Hou, Z. (2012). Catalytic production of 1,2-propanediol from glycerol in bio-ethanol solvent. *Bioresource Technology*, 104: 814-817.
- Xia, S., Zheng, L., Wang, L., Chen, P., & Hou, Z. (2013). Hydrogen-free synthesis of 1,2-propanediol from glycerol over Cu-Mg-Al catalysts. *RSC Advances*, 3(37): 16569-16576.
- Xu, Y., Zondlo, J. W., Finklea, H. O., & Brennsteiner, A. (2000). Electrosorption of uranium on carbon fibers as a means of environmental remediation. *Fuel Processing Technology*, 68(3): 189-208.
- Xu, T. (2005). Ion exchange membranes: State of their development and perspective. *Journal of Membrane Science*, 263(1-2), 1-29.
- Yadav, G. D., Chandan, P. A., & Tekale, D. P. (2012). Hydrogenolysis of Glycerol to 1,2-Propanediol over Nano-Fibrous Ag-OMS-2 Catalysts. *Industrial & Engineering Chemistry Research*, 51(4): 1549-1562.
- Yang, F., Hanna, M., & Sun, R. (2012). Value-added uses for crude glycerol--a byproduct of biodiesel production. *Biotechnology for Biofuels*, 5(1): 13.
- Yang, G., Tian, J., & Li, J. (2007). Fermentation of 1,3-propanediol by a lactate deficient mutant of *Klebsiella oxytoca* under microaerobic conditions. *Applied Microbiology and Biotechnology*, 73(5): 1017-1024.
- Yang, X., Tang, S., Lu, T., Chen, C., Zhou, L., Su, Y., & Xu, J. (2013). Sulfonic Acid Resin-Catalyzed Oxidation of Aldehydes to Carboxylic Acids by Hydrogen Peroxide. *Synthetic Communications*, 43(7), 979-985.
- Yildiz, G., & Kadirgan, F. (1994). Electrocatalytic Oxidation of Glycerol: I. Behavior of Palladium Electrode in Alkaline Medium. *Journal of The Electrochemical Society*, 141(3): 725-730.
- Yuan, Z., Wang, J., Wang, L., Xie, W., Chen, P., Hou, Z., & Zheng, X. (2010). Biodiesel derived glycerol hydrogenolysis to 1,2-propanediol on Cu/MgO catalysts. *Bioresource Technology*, 101(18): 7088-7092.
- Zalineeva, A., Serov, A., Padilla, M., Martinez, U., Artyushkova, K., Baranton, S., Coutanceau, C., & Atanassov, P. B. (2014). Self-Supported PdxBi Catalysts for

the Electrooxidation of Glycerol in Alkaline Media. *Journal of the American Chemical Society*, 136(10): 3937-3945.

- Zelić, B., & Vasić-Rački, Đ. (2005). Process development and modeling of pyruvate recovery from a model solution and fermentation broth. *Desalination*, 174(3), 267-276.
- Zeng, A.-P., & Biebl, H. (2002). Bulk Chemicals from Biotechnology: The Case of 1,3-Propanediol Production and the New Trends *Tools and Applications of Biochemical Engineering Science*, Vol. 74: pp. 239-259.
- Zhang, C., Wang, T., Liu, X., & Ding, Y. (2016). Selective oxidation of glycerol to lactic acid over activated carbon supported Pt catalyst in alkaline solution. *Chinese Journal of Catalysis*, 37(4): 502-509.
- Zhang, G., Ma, B., Xu, X., Li, C., & Wang, L. (2007). Fast conversion of glycerol to 1,3-propanediol by a new strain of *Klebsiella pneumoniae*. *Biochemical Engineering Journal*, 37(3): 256-260.
- Zhang, M., Nie, R., Wang, L., Shi, J., Du, W., & Hou, Z. (2015). Selective oxidation of glycerol over carbon nanofibers supported Pt catalysts in a base-free aqueous solution. *Catalysis Communications*, 59: 5-9.
- Zhang, Z., Xin, L., & Li, W. (2012a). Electrocatalytic oxidation of glycerol on Pt/C in anion-exchange membrane fuel cell: Cogeneration of electricity and valuable chemicals. *Applied Catalysis B: Environmental*, 119-120: 40-48.
- Zhang, Z., Xin, L., & Li, W. (2012b). Supported gold nanoparticles as anode catalyst for anion-exchange membrane-direct glycerol fuel cell (AEM-DGFC). *International Journal of Hydrogen Energy*, 37(11): 9393-9401.
- Zhang, Z., Xin, L., Qi, J., Chadderdon, D. J., Sun, K., Warsko, K. M., & Li, W. (2014). Selective electro-oxidation of glycerol to tartronate or mesoxalate on Au nanoparticle catalyst via electrode potential tuning in anion-exchange membrane electro-catalytic flow reactor. *Applied Catalysis B: Environmental*, 147: 871-878.
- Zhou, C., Beltramini, J. N., Fan, Y.-X., & Lu, G. Q. (2008). Chemoselective catalytic conversion of glycerol as a biorenewable source to valuable commodity chemicals. *Chemical Society Reviews*, 37(3): 527-549.
- Zhou, L., Nguyen, T.-H., & Adesina, A. A. (2012). The acetylation of glycerol over amberlyst-15: Kinetic and product distribution. *Fuel Processing Technology*, 104: 310-318.
- Zhu, S., Gao, X., Zhu, Y., Zhu, Y., Xiang, X., Hu, C., & Li, Y. (2013). Alkaline metals modified Pt-H<sub>4</sub>SiW<sub>12</sub>O<sub>40</sub>/ZrO<sub>2</sub> catalysts for the selective hydrogenolysis of glycerol to 1,3-propanediol. *Applied Catalysis B: Environmental*, 140-141: 60-67.

- Zhu, S., Zhu, Y., Hao, S., Chen, L., Zhang, B., & Li, Y. (2012). Aqueous-Phase Hydrogenolysis of Glycerol to 1,3-propanediol Over Pt-H<sub>4</sub>SiW<sub>12</sub>O<sub>40</sub>/SiO<sub>2</sub>. *Catalysis Letters*, 142(2): 267-274.
- Zope, B. N., & Davis, R. J. (2011). Inhibition of gold and platinum catalysts by reactive intermediates produced in the selective oxidation of alcohols in liquid water. *Green Chemistry*, 13(12): 3484-3491.
- Zope, B. N., Hibbitts, D. D., Neurock, M., & Davis, R. J. (2010). Reactivity of the Gold/Water Interface During Selective Oxidation Catalysis. *Science*, 330(6000): 74-78.
- Zou, L., Morris, G., & Qi, D. (2008). Using activated carbon electrode in electrosorptive deionisation of brackish water. *Desalination*, 225(1-3): 329-340.

## LIST OF PUBLICATIONS AND PAPERS PRESENTED

No.	Manuscript Title	Status
1	Lee CS, Aroua MK, Daud WMAW, Cognet P, Pérès-Lucchese Y, Fabre P-L, Reynes O, Latapie L. A review: Conversion of bioglycerol into 1,3-propanediol via biological and chemical method. <i>Renewable and Sustainable Energy Review</i> (2015), 963-972 <a href="http://dx.doi.org/10.1016/j.rser.2014.10.033">http://dx.doi.org/10.1016/j.rser.2014.10.033</a> (ISI Q1 ranking journal, impact factor: 5.901)	Published
2	Lee CS, Aroua MK, Daud WMAW, Cognet P, Pérès-Lucchese Y, Al-Ajeel M, Reynes O, Latapie L. Electrosynthesis of glyceric and glycolic acids from glycerol in presence of Amberlyst-15. <i>Arabian Journal of Chemistry</i> (2016). (ISI Q1 ranking journal, impact factor: 3.597)	Under review
3	Lee CS, Aroua MK, Daud WMAW, Cognet P, Pérès-Lucchese Y, Al-Ajeel M, Reynes O, Latapie L. Electro-reduction of glycerol to 1,2-propaediol by activated carbon composite electrode. <i>RSC Advances</i> (2016). (ISI Q1 ranking journal, impact factor: 3.289)	In preparation

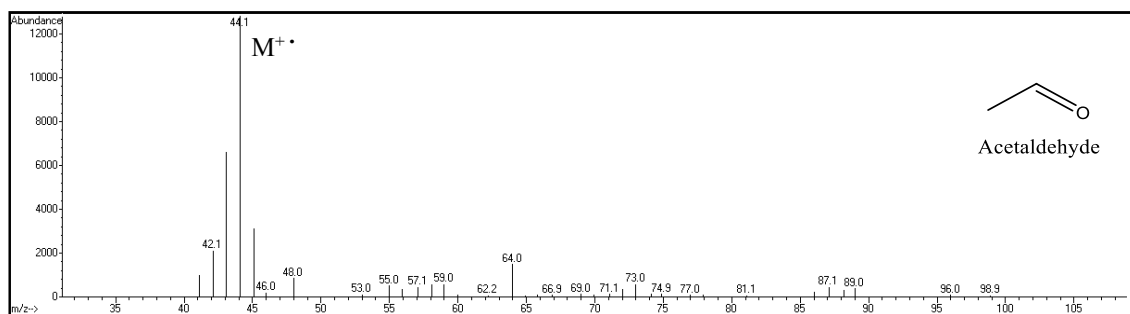
### Conference or Proceeding Paper

- 1) Lee CS, Aroua MK, Daud WMAW, Cognet P, Pérès-Lucchese Y, Fabre P-L, Reynes O, Latapie L. Electrochemical valorization of glycerol: Dehydration of glycerol over sulfuric acid medium. The 4th International Congress on Green Process Engineering. 7 – 10 April 2014. Sevilla, Spain. (Poster Presentation)
- 2) Lee CS, Aroua MK, Daud WMAW, Cognet P, Pérès-Lucchese Y, Fabre P-L, Reynes O, Latapie L. Studies of product formation from electrochemical conversion of glycerol. The 3rd International Symposium on Green Chemistry. 3-7 May 2015. La Rochelle, France. (Oral Presentation)
- 3) Lee CS, Aroua MK, Daud WMAW, Cognet P, Pérès-Lucchese. Production of lactic acid and glycolic acid in one-pot electrochemical cell. 19-24 June 2016. Mont Tremblant, Quebec, Canada. (Oral and Poster Presentation)

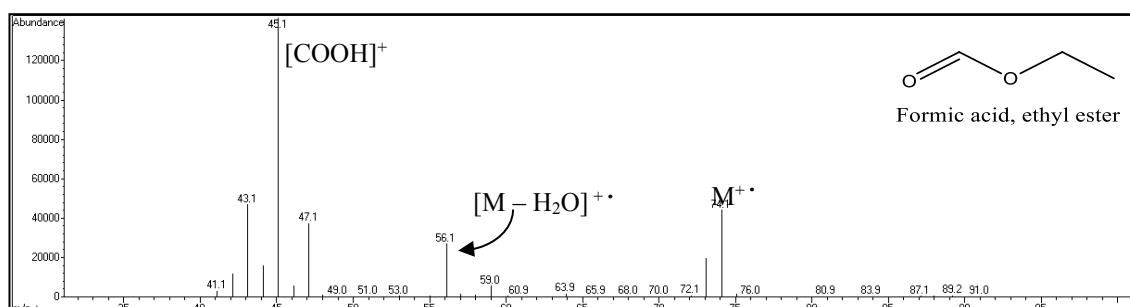
## APPENDICES

### Appendix 1: GC mass spectra for compounds obtained from the electrolysis

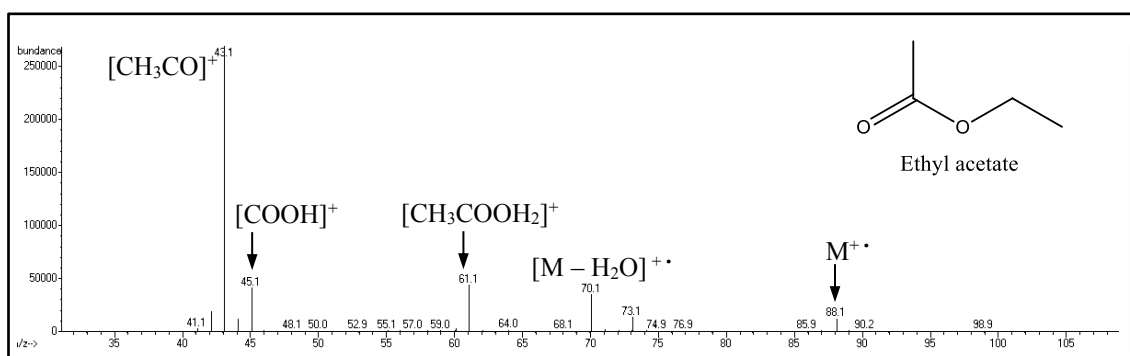
#### a) Acetaldehyde ( $R_t = 1.26$ min):



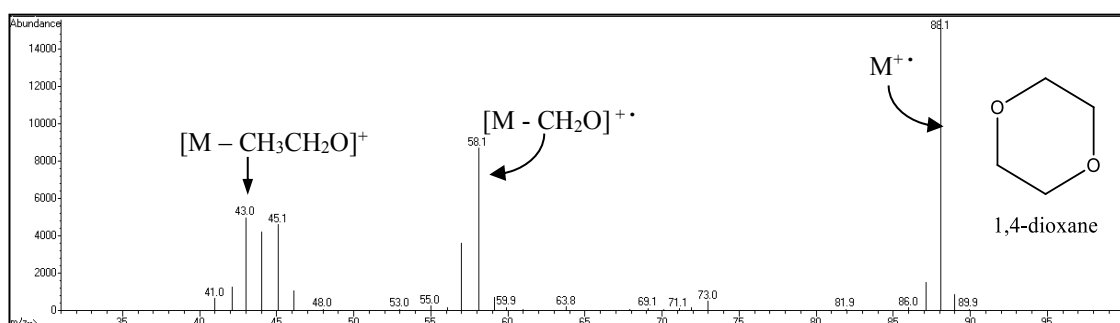
#### b) Formic acid, ethyl ester ( $R_t = 1.57$ min):



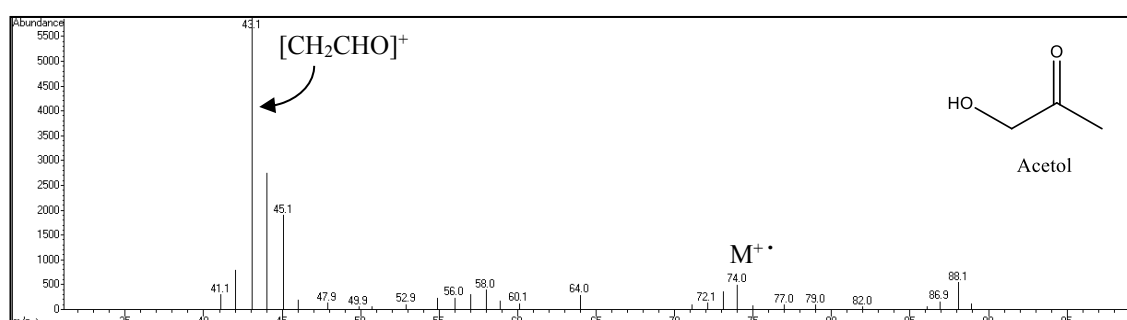
#### c) Ethyl acetate ( $R_t = 1.88$ min):



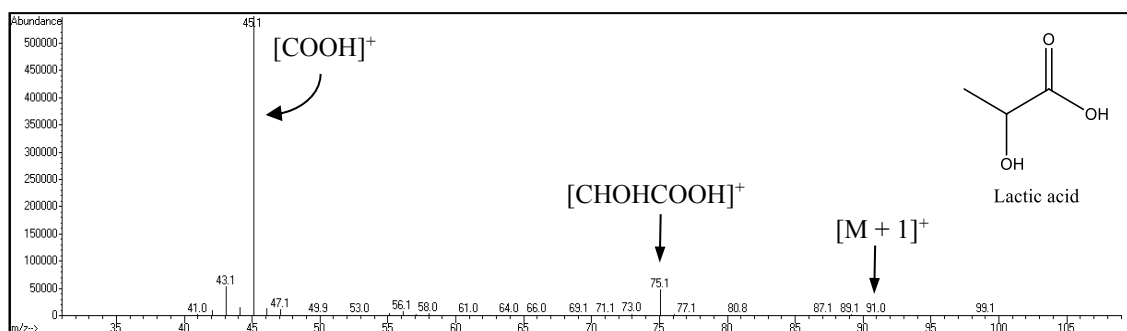
**d) 1,4-dioxane ( $R_t = 4.16$  min):**



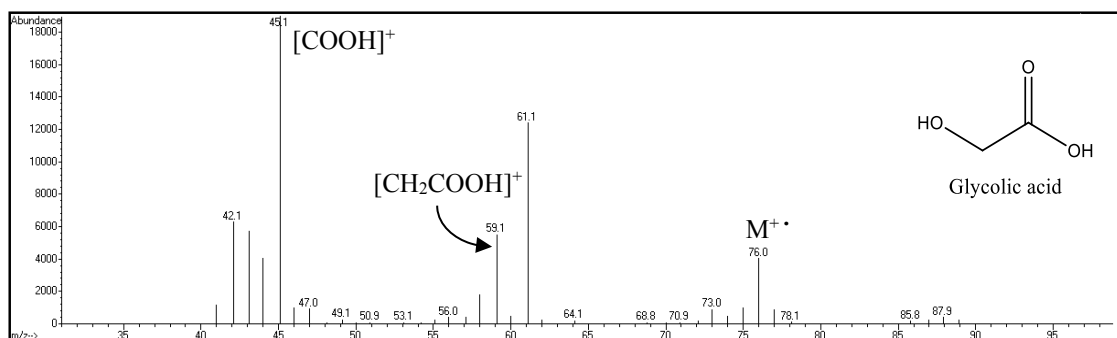
**e) Acetol ( $R_t = 9.61$  min):**



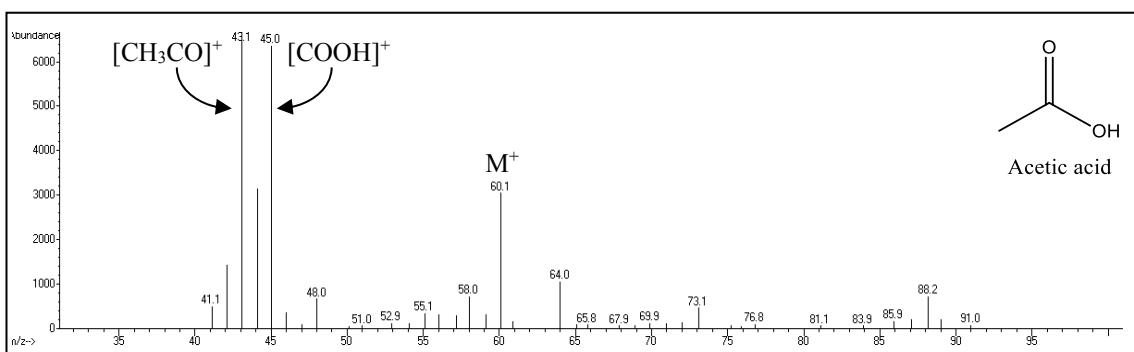
**f) Lactic acid ( $R_t = 10.40$  min):**



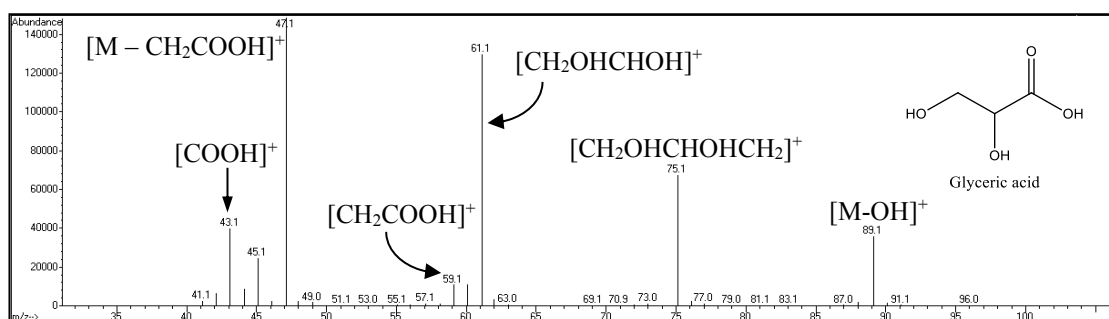
**g) Glycolic acid ( $R_t = 11.56$  min):**



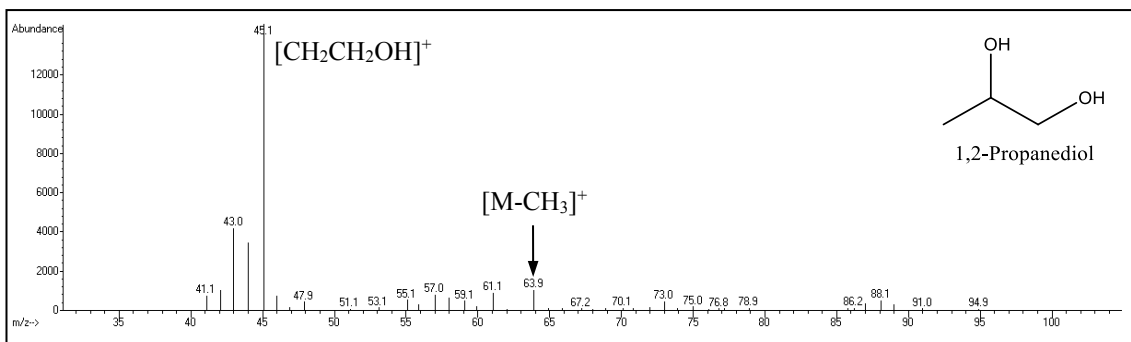
**h) Acetic acid ( $R_t = 12.04$  min):**



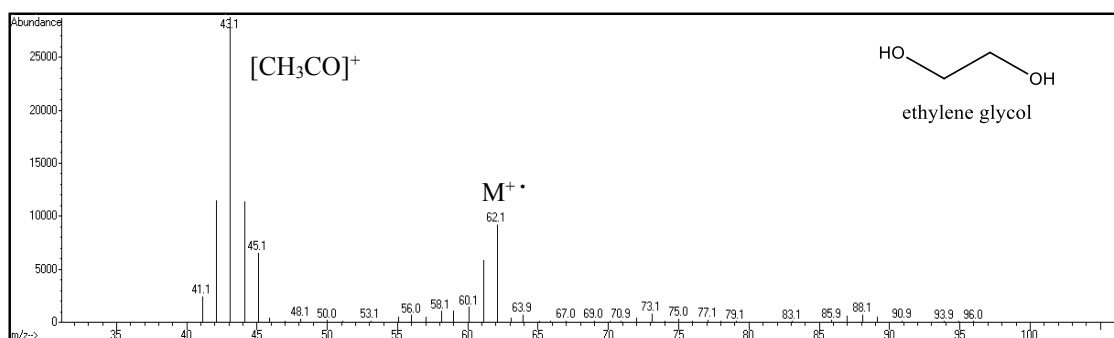
**i) Glyceric acid ( $R_t = 12.18$  min):**



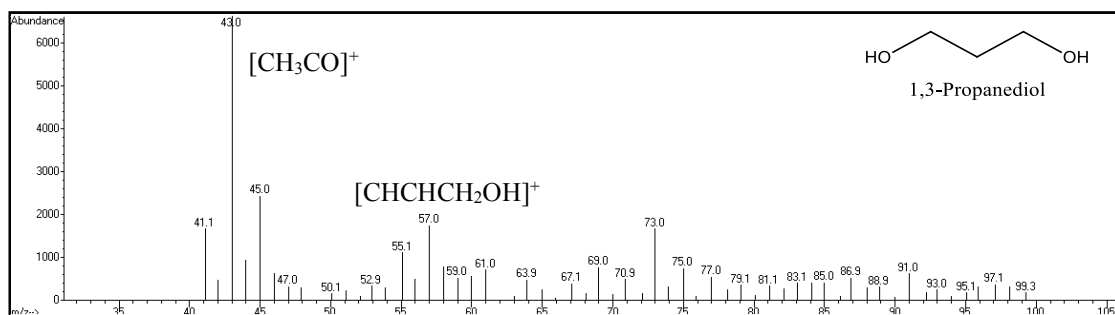
**j) 1,2-Propanediol ( $R_t = 13.87$  min):**



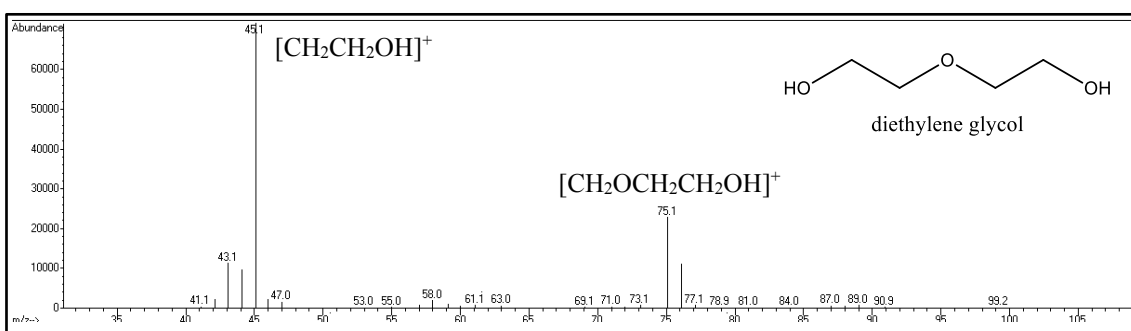
**k) Ethylene glycol ( $R_t = 14.27$  min):**



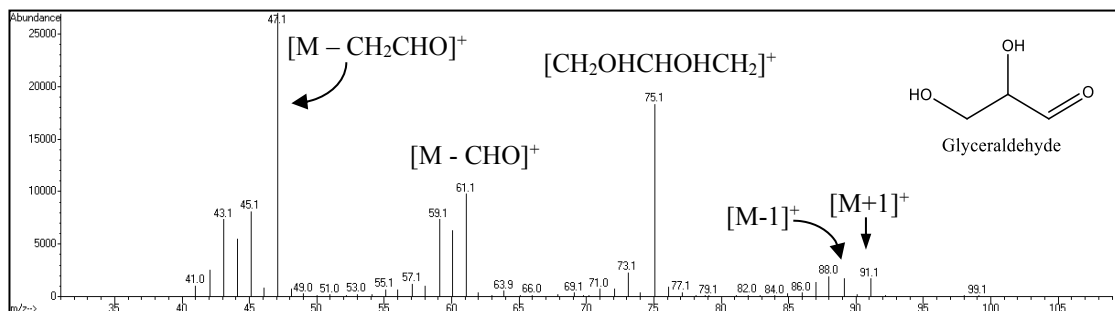
**l) 1,3-Propanediol ( $R_t = 16.12$  min):**



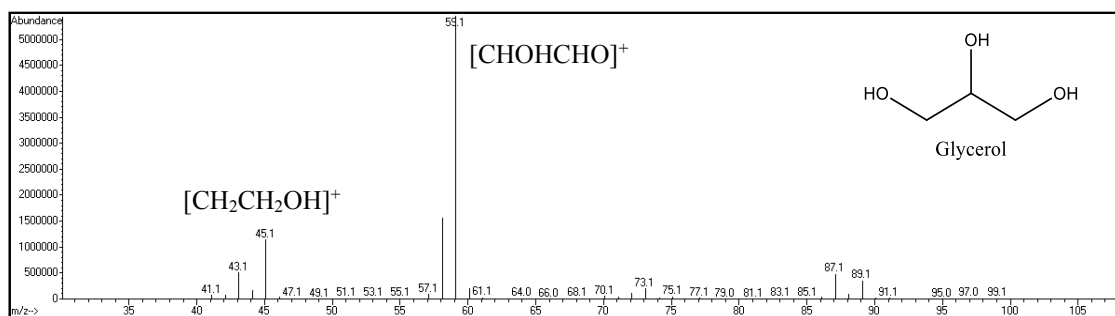
**m) Diethylene glycol ( $R_t = 18.06$  min):**



**n) Glyceraldehyde ( $R_t = 21.07$  min):**

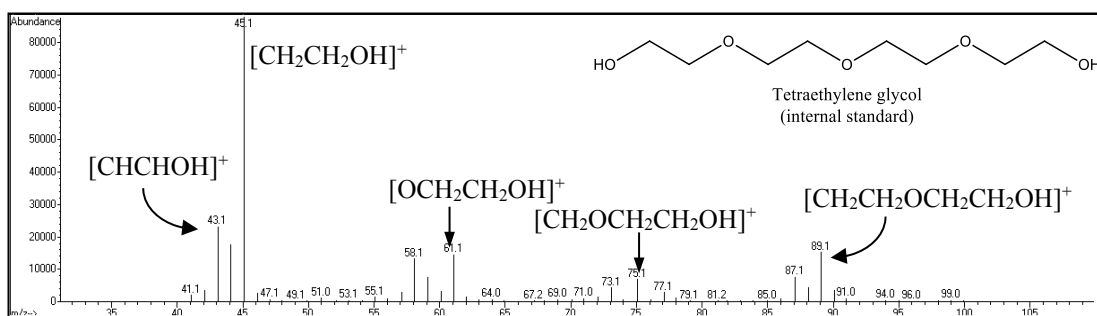


**o) Glycerol ( $R_t = 21.32$  min)**



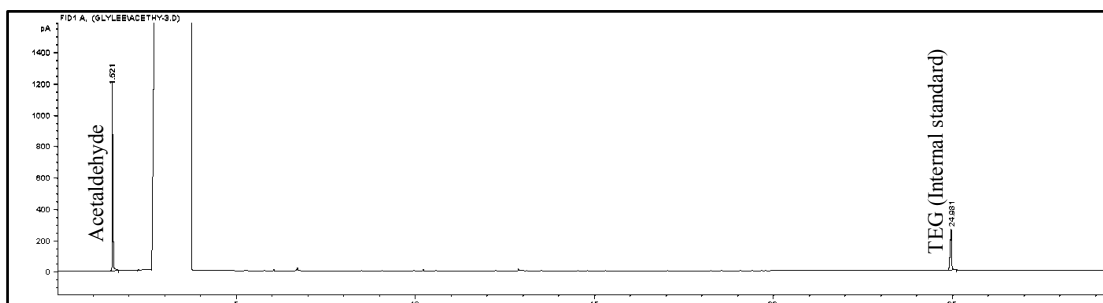


p) Tetraethylene glycol ( $R_t = 24.59$  min)

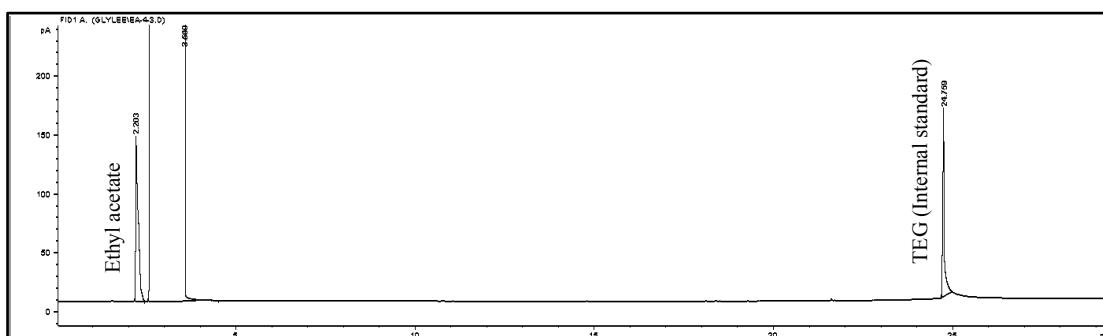


## Appendix 2: GC chromatograms for the standards

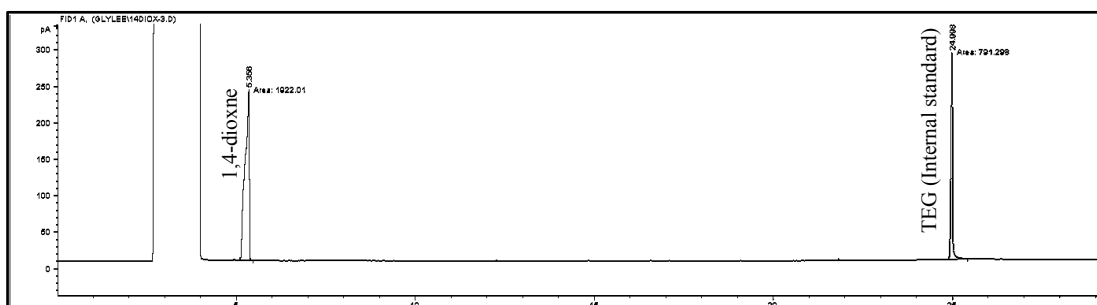
### a) Acetaldehyde ( $R_t = 1.52$ min)



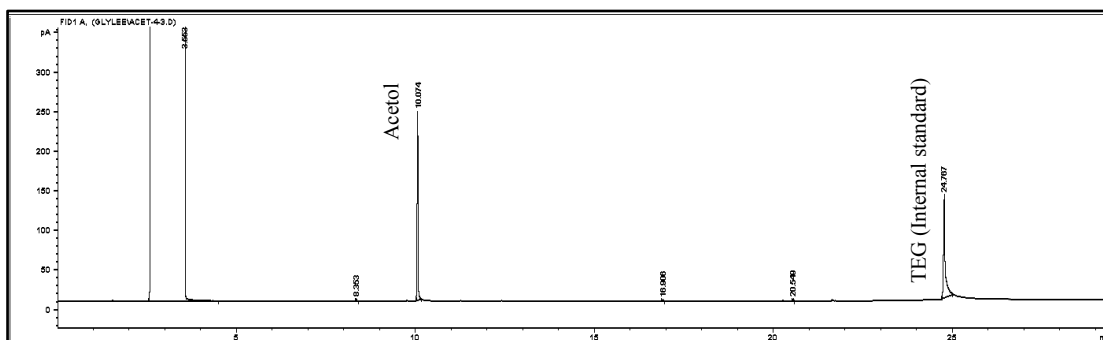
### b) Ethyl acetate ( $R_t = 1.89$ min)



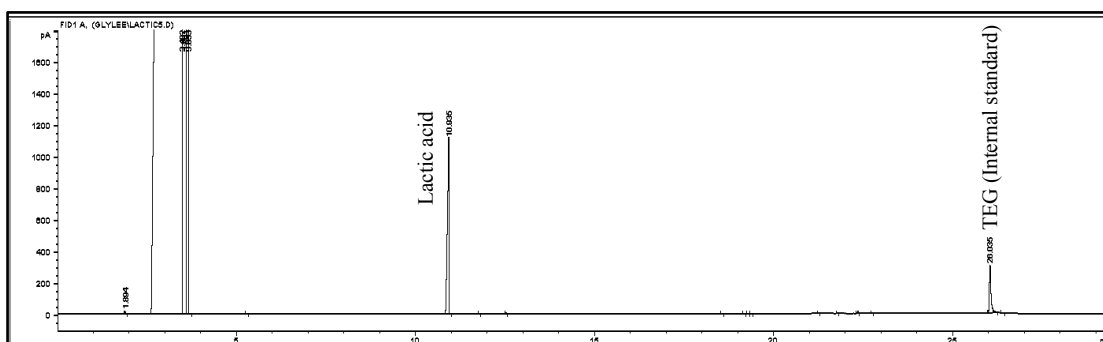
### c) 1,4-dioxane ( $R_t = 4.16$ min)



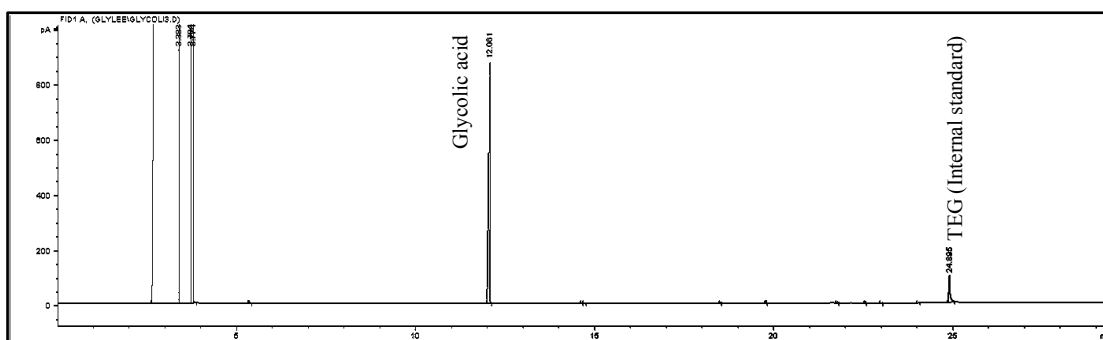
**d) Acetol ( $R_t = 10.31$  min)**



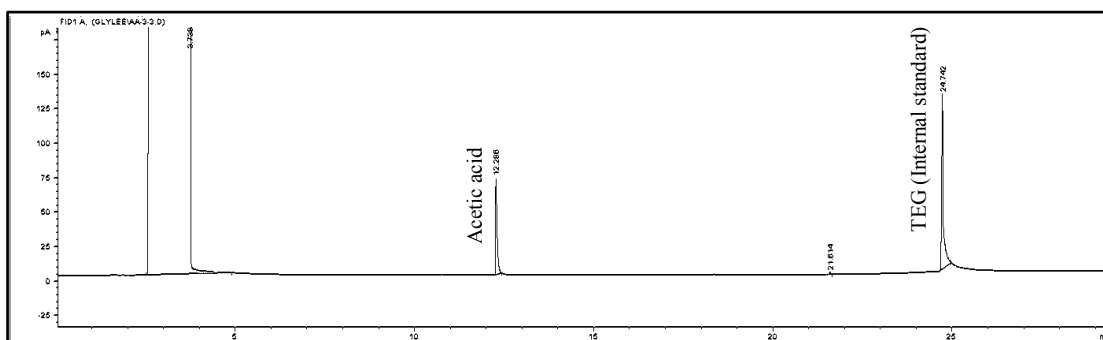
**e) Lactic acid ( $R_t = 10.94$  min)**



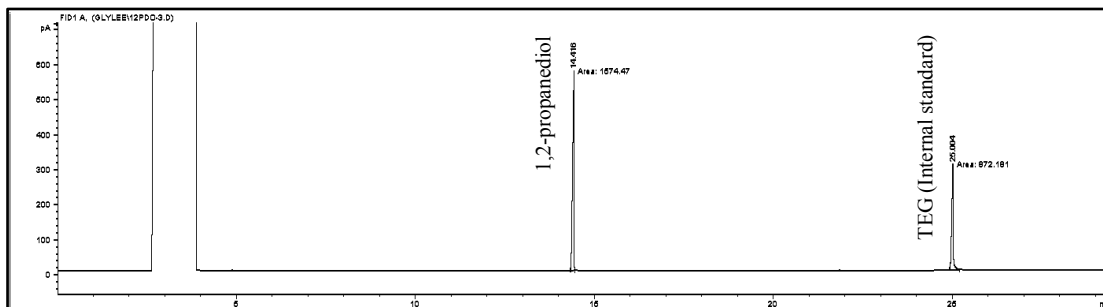
**f) Glycolic acid ( $R_t = 12.06$  min)**



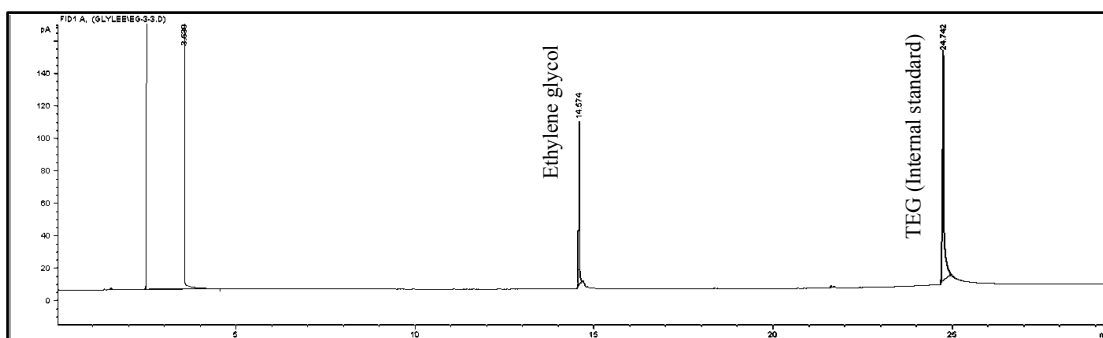
**g) Acetic acid ( $R_t = 12.26$  min)**



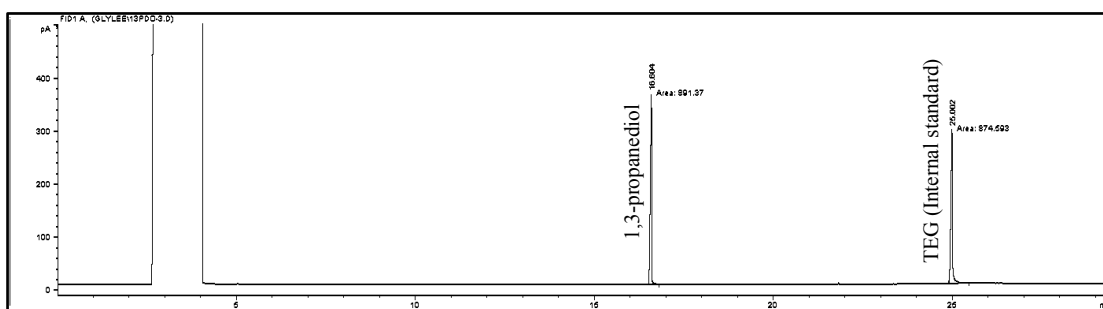
**h) 1,2-Propanediol ( $R_t = 14.42$  min)**



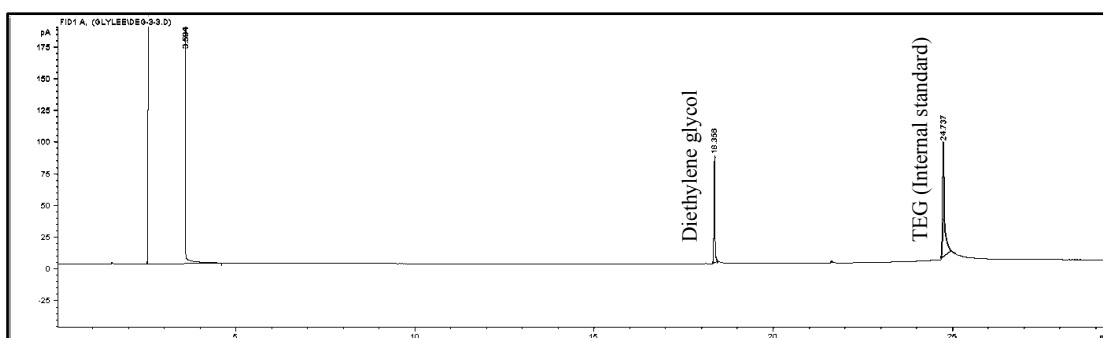
**i) Ethylene glycol ( $R_t = 14.60$  min)**



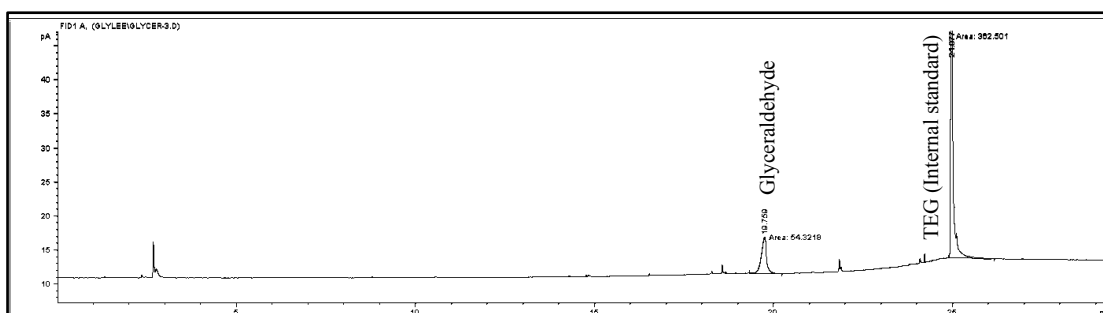
**j) 1,3-Propanediol ( $R_t = 16.60$  min)**



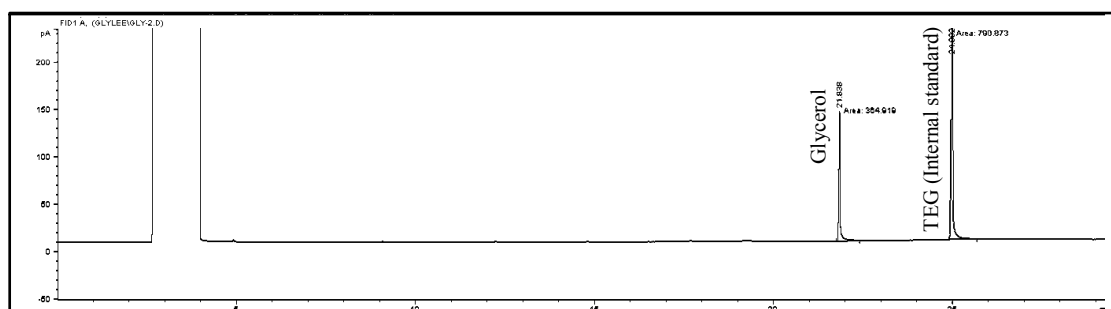
**k) Diethylene glycol ( $R_t = 18.61$  min)**



**l) Glyceraldehyde ( $R_t = 19.76$  min)**



**m) Glycerol ( $R_t = 21.84$  min)**



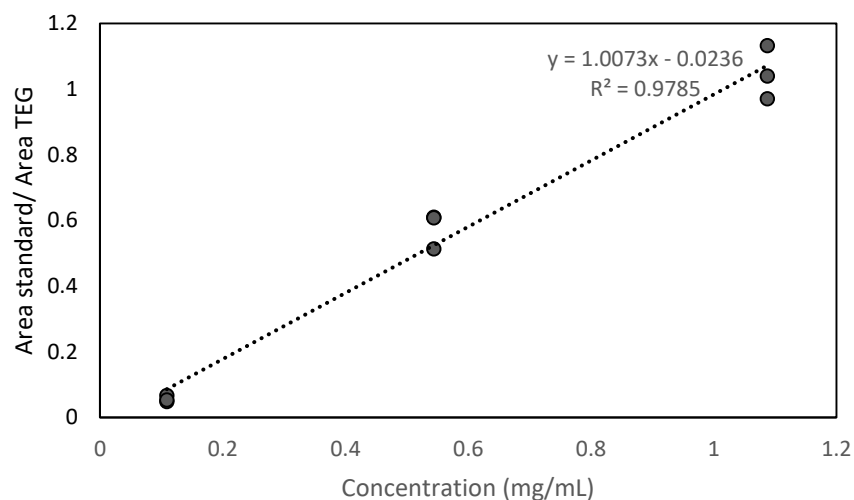
### Appendix 3: Standards calibration curve

#### a) Calibration of 1,2-Propanediol (1,2-PDO)

<b>Preparation of mother solution:</b>						
Amount of 1,2-PDO standard (mg)		: 108.77				
Volumetric flask (mL)		: 10				
Mother solution (mg/mL)	Volume taken from mother solution (µL)	Theoretical concentration (mg/mL)	Actual concentration (mg/mL) **	Area of 1,2-PDO (GC)	Area of TEG (GC)	Area 1,2-PDO/ Area TEG
10.8770 ± 0.0157	100	0.1	0.1088	28.9	595.2	0.0486
10.8770 ± 0.0157	100	0.1	0.1088	41.2	615.9	0.0669
10.8770 ± 0.0157	100	0.1	0.1088	36.8	684.1	0.0538
10.8770 ± 0.0157	500	0.5	0.5439	382.9	627.5	0.6102
10.8770 ± 0.0157	500	0.5	0.5439	348.3	572.8	0.6081
10.8770 ± 0.0157	500	0.5	0.5439	337	656.1	0.5136
10.8770 ± 0.0157	1000	1	1.0877	616.5	634.6	0.9715
10.8770 ± 0.0157	1000	1	1.0877	607	583.4	1.0405
10.8770 ± 0.0157	1000	1	1.0877	704.2	621.4	1.1332

Note: \*\*Dilution in 10 mL

1,2-PDO Calibration Curve

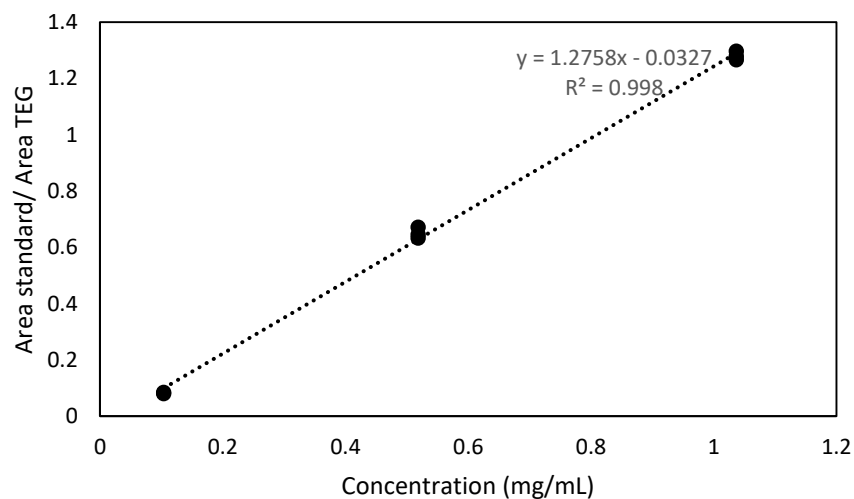


## b) Calibration of 1,3-Propanediol (1,3-PDO)

<b>Preparation of mother solution:</b>						
Amount of 1,3-PDO standard : 259.19 (mg)						
Volumetric flask (mL) : 25						
Mother solution (mg/mL)	Volume taken from mother solution (μL)	Theoretical concentration (mg/mL)	Actual concentration (mg/mL) **	Area of 1,3-PDO (GC)	Area of TEG (GC)	Area 1,3-PDO/ Area TEG
10.3676 ± 0.0060	100	0.1	0.1037	45.3	536.9	0.0844
10.3676 ± 0.0060	100	0.1	0.1037	41.7	525.7	0.0793
10.3676 ± 0.0060	500	0.5	0.5184	319.6	495.3	0.6453
10.3676 ± 0.0060	500	0.5	0.5184	299.2	472.9	0.6327
10.3676 ± 0.0060	500	0.5	0.5184	360.3	536.4	0.6717
10.3676 ± 0.0060	1000	1	1.0368	647.4	499	1.2974
10.3676 ± 0.0060	1000	1	1.0368	563	440.3	1.2787
10.3676 ± 0.0060	1000	1	1.0368	680.3	537.5	1.2657

Note: \*\*Dilution in 10 mL

1,3-PDO Calibration Curve

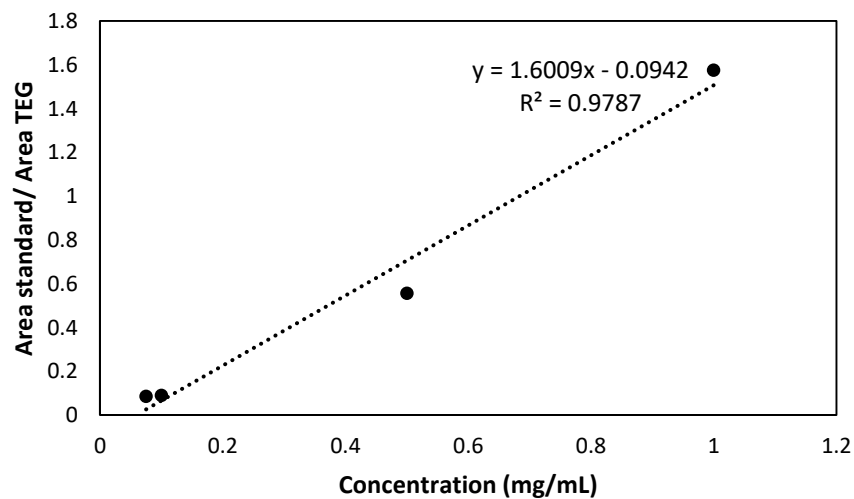


### c) Calibration of acetaldehyde

<b>Preparation of mother solution:</b>						
Amount of acetaldehyde standard (mg)		: 100.88				
Volumetric flask (mL)		: 10				
<b>Mother solution (mg/mL)</b>	<b>Volume taken from mother solution (μL)</b>	<b>Actual concentration (mg/mL) **</b>	<b>Theoretical concentration (mg/mL)</b>	<b>Area of acetaldehyde (GC)</b>	<b>Area of TEG (GC)</b>	<b>Area acetaldehyde / Area TEG</b>
10.0880 ± 0.0146	75	0.0757	0.075	31.8	376.2	0.0845
10.0880 ± 0.0146	100	0.1009	0.1	40.7	455.4	0.0894
10.0880 ± 0.0146	500	0.5044	0.5	268.7	483.7	0.5555
10.0880 ± 0.0146	1000	1.0088	1	536.1	340.3	1.5754

Note: \*\*Dilution in 10 mL

Acetaldehyde Calibration Curve



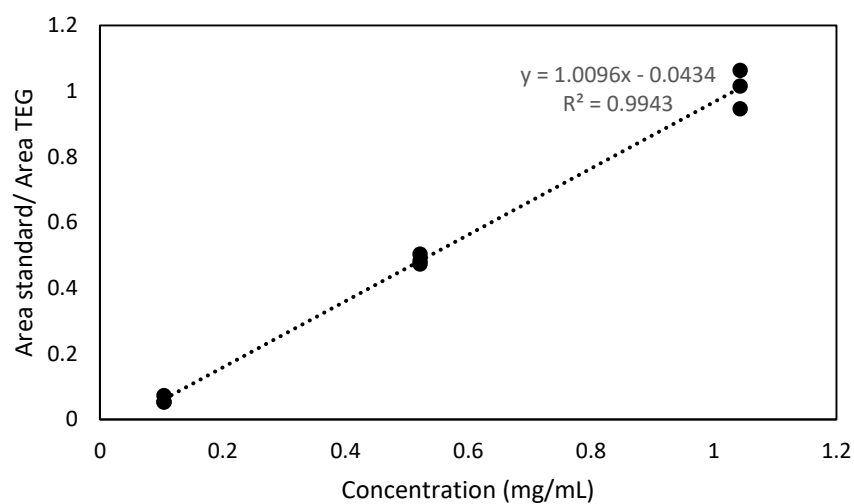


#### d) Calibration of acetic acid (AA)

<b>Preparation of mother solution:</b>						
Amount of AA standard (mg)		: 104.33				
Volumetric flask (mL)		: 10				
Mother solution (mg/mL)	Volume taken from mother solution (μL)	Actual concentration (mg/mL) **	Theoretical concentration (mg/mL)	Area of AA (GC)	Area of TEG (GC)	Area AA/ Area TEG
10.4330 ± 0.0151	100	0.1043	0.1	22	301.3	0.0730
10.4330 ± 0.0151	100	0.1043	0.1	19.1	358.3	0.0533
10.4330 ± 0.0151	100	0.1043	0.1	12.8	237.1	0.0540
10.4330 ± 0.0151	500	0.5217	0.5	177.7	352.7	0.5038
10.4330 ± 0.0151	500	0.5217	0.5	167.7	354.3	0.4733
10.4330 ± 0.0151	500	0.5217	0.5	196.8	407.8	0.4826
10.4330 ± 0.0151	1000	1.0433	1	365	343.3	1.0632
10.4330 ± 0.0151	1000	1.0433	1	374.2	368.3	1.0160
10.4330 ± 0.0151	1000	1.0433	1	305.9	323.3	0.9462

Note: \*\*Dilution in 10 mL

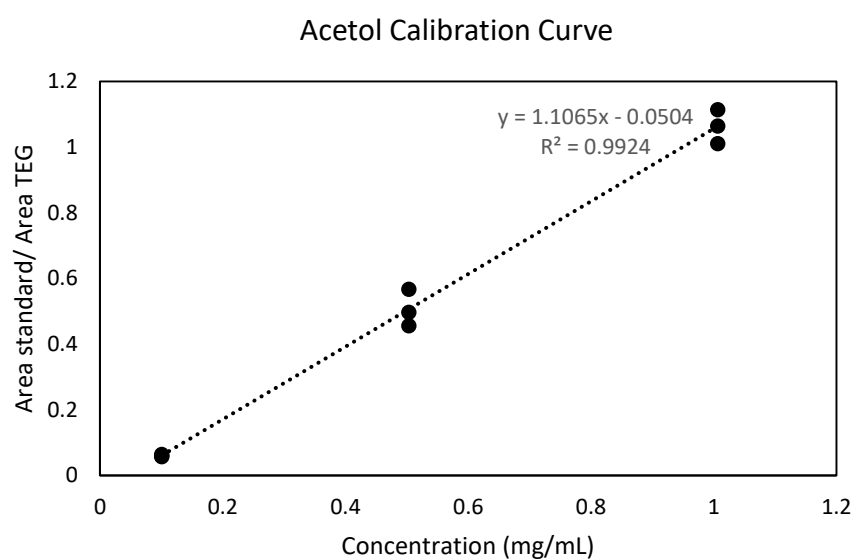
Acetic Acid Calibration Curve



### e) Calibration of acetol

<b>Preparation of mother solution:</b>						
Amount of acetol standard (mg)		: 100.66				
Volumetric flask (mL)		: 10				
<b>Mother solution (mg/mL)</b>	<b>Volume taken from mother solution (µL)</b>	<b>Actual concentration (mg/mL) **</b>	<b>Theoretical concentration (mg/mL)</b>	<b>Area of acetol (GC)</b>	<b>Area of TEG (GC)</b>	<b>Area acetol/ Area TEG</b>
10.0660 ± 0.0145	100	0.1007	0.1	30.2	467.1	0.0647
10.0660 ± 0.0145	100	0.1007	0.1	28.7	498.2	0.0576
10.0660 ± 0.0145	100	0.1007	0.1	26.1	439	0.0595
10.0660 ± 0.0145	500	0.5033	0.5	259.4	457.1	0.5675
10.0660 ± 0.0145	500	0.5033	0.5	241.7	486	0.4973
10.0660 ± 0.0145	500	0.5033	0.5	231.8	507.6	0.4567
10.0660 ± 0.0145	1000	1.0066	1	476.2	427.5	1.1139
10.0660 ± 0.0145	1000	1.0066	1	562.5	528.3	1.0647
10.0660 ± 0.0145	1000	1.0066	1	437.1	432.5	1.0106

Note: \*\*Dilution in 10 mL

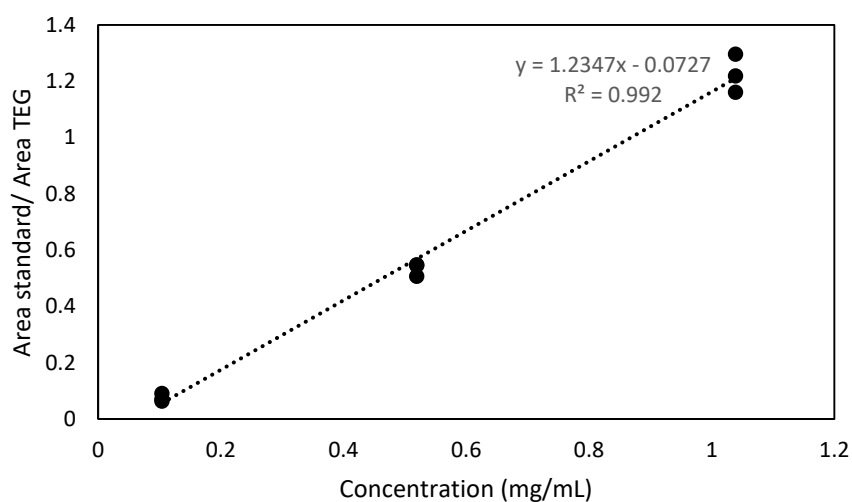


## f) Calibration of diethylene glycol (DEG)

<b>Preparation of mother solution:</b>						
Amount of DEG standard (mg)		: 103.87				
Volumetric flask (mL)		: 10				
<b>Mother solution (mg/mL)</b>	<b>Volume taken from mother solution (µL)</b>	<b>Actual concentration (mg/mL) **</b>	<b>Theoretical concentration (mg/mL)</b>	<b>Area of DEG (GC)</b>	<b>Area of TEG (GC)</b>	<b>Area DEG/ Area TEG</b>
10.3870 ± 0.0150	100	0.10387	0.1	22.8	325.4	0.0701
10.3870 ± 0.0150	100	0.10387	0.1	15.7	246.4	0.0637
10.3870 ± 0.0150	100	0.10387	0.1	23.3	255.2	0.0913
10.3870 ± 0.0150	500	0.51935	0.5	157.3	287.1	0.5479
10.3870 ± 0.0150	500	0.51935	0.5	168.7	309	0.5460
10.3870 ± 0.0150	500	0.51935	0.5	130.3	257.2	0.5066
10.3870 ± 0.0150	1000	1.0387	1	351.1	270.9	1.2961
10.3870 ± 0.0150	1000	1.0387	1	307.1	252	1.2187
10.3870 ± 0.0150	1000	1.0387	1	379.9	327.1	1.1614

Note: \*\*Dilution in 10 mL

DEG Calibration Curve

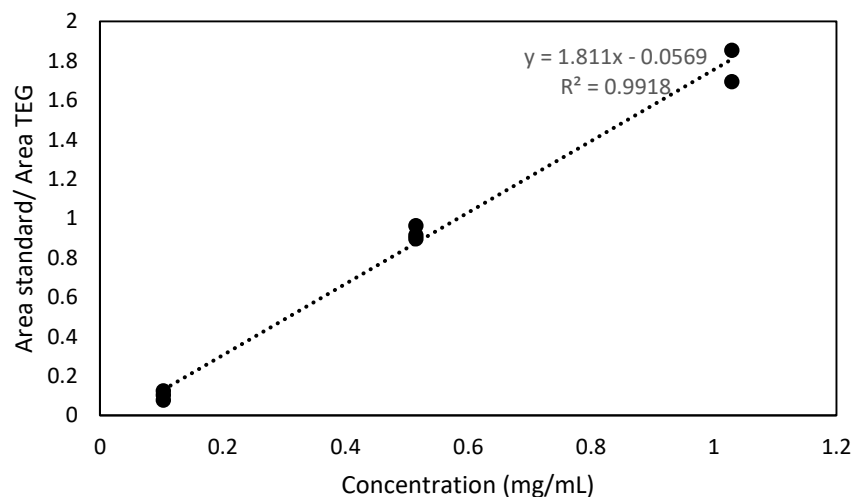


g) Calibration of ethyl acetate (EA)

<b>Preparation of mother solution:</b>						
Amount of EA standard (mg)		: 102.94				
Volumetric flask (mL)		: 10				
<b>Mother solution (mg/mL)</b>	<b>Volume taken from mother solution (µL)</b>	<b>Actual concentration (mg/mL) **</b>	<b>Theoretical concentration (mg/mL)</b>	<b>Area of EA (GC)</b>	<b>Area of TEG (GC)</b>	<b>Area EA/ Area TEG</b>
10.2940 ± 0.0149	100	0.1029	0.1	39.6	513.7	0.0771
10.2940 ± 0.0149	100	0.1029	0.1	48.8	470.5	0.1037
10.2940 ± 0.0149	100	0.1029	0.1	55.5	444.2	0.1249
10.2940 ± 0.0149	500	0.5147	0.5	484.1	502.5	0.9634
10.2940 ± 0.0149	500	0.5147	0.5	437.5	478	0.9153
10.2940 ± 0.0149	500	0.5147	0.5	455.5	508.2	0.8963
10.2940 ± 0.0149	1000	1.0294	1	822.4	485.2	1.6950
10.2940 ± 0.0149	1000	1.0294	1	823.7	444.4	1.8535

Note: \*\*Dilution in 10 mL

Ethyl Acetate Calibration Curve

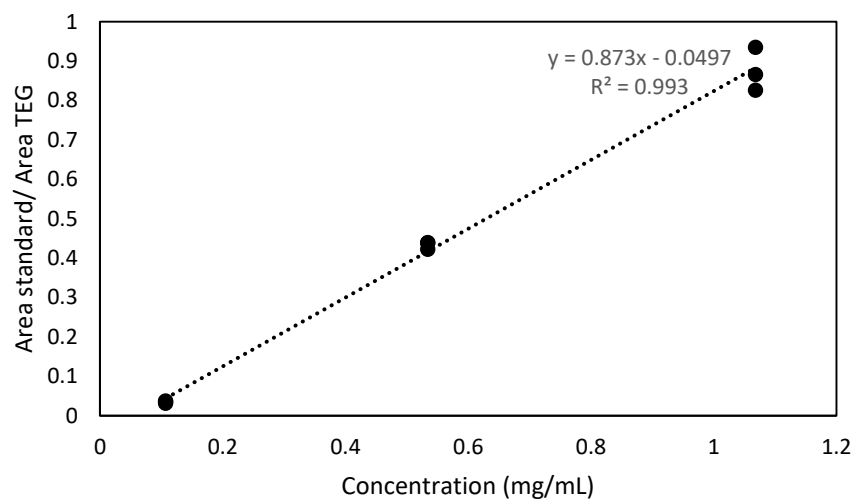


## h) Calibration of ethylene glycol (EG)

<b>Preparation of mother solution:</b>						
Amount of EG standard (mg)		: 106.84				
Volumetric flask (mL)		: 10				
<b>Mother solution (mg/mL)</b>	<b>Volume taken from mother solution (µL)</b>	<b>Actual concentration (mg/mL) **</b>	<b>Theoretical concentration (mg/mL)</b>	<b>Area of EG (GC)</b>	<b>Area of TEG (GC)</b>	<b>Area EG/ Area TEG</b>
10.6840 ± 0.0154	100	0.1068	0.1	15.7	446.4	0.0352
10.6840 ± 0.0154	100	0.1068	0.1	13.2	425.1	0.0311
10.6840 ± 0.0154	100	0.1068	0.1	17.6	473.6	0.0372
10.6840 ± 0.0154	500	0.5342	0.5	208.1	474.5	0.4386
10.6840 ± 0.0154	500	0.5342	0.5	225.9	514.5	0.4391
10.6840 ± 0.0154	500	0.5342	0.5	179.7	425.8	0.4220
10.6840 ± 0.0154	1000	1.0684	1	487	520.9	0.9349
10.6840 ± 0.0154	1000	1.0684	1	430.2	520.6	0.8264
10.6840 ± 0.0154	1000	1.0684	1	418.4	483.1	0.8661

Note: \*\*Dilution in 10 mL

Ethylene Glycol Calibration Curve

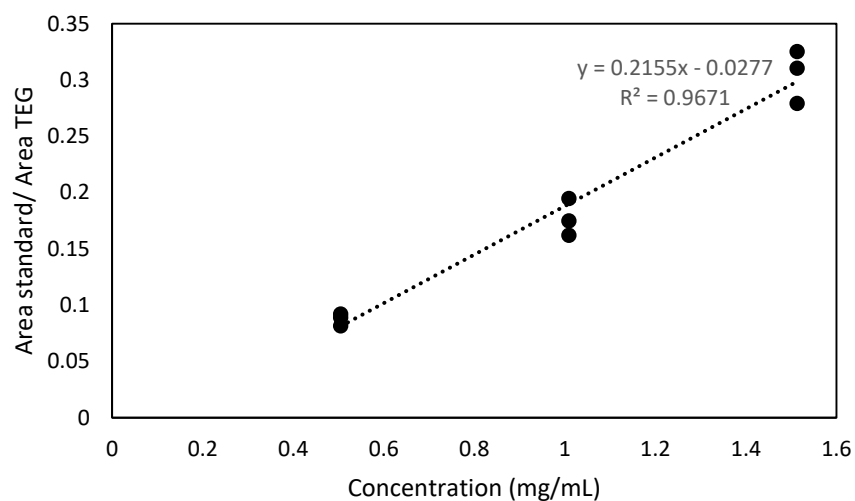


i) Calibration of lactic acid (LA)

<b>Preparation of mother solution:</b>						
Amount of LA standard (mg)		: 100.88				
Volumetric flask (mL)		: 10				
<b>Mother solution (mg/mL)</b>	<b>Volume taken from mother solution (µL)</b>	<b>Actual concentration (mg/mL) **</b>	<b>Theoretical concentration (mg/mL)</b>	<b>Area of LA (GC)</b>	<b>Area of TEG (GC)</b>	<b>Area LA/ Area TEG</b>
10.0880 ± 0.0146	500	0.5044	0.5	44.6	502.1	0.0888
10.0880 ± 0.0146	500	0.5044	0.5	33.2	408	0.0814
10.0880 ± 0.0146	500	0.5044	0.5	46.2	502.6	0.0919
10.0880 ± 0.0146	1000	1.0088	1	83.4	477.1	0.1748
10.0880 ± 0.0146	1000	1.0088	1	97.8	502.7	0.1945
10.0880 ± 0.0146	1000	1.0088	1	70.3	433.7	0.1621
10.0880 ± 0.0146	1500	1.5132	1.5	190.6	683	0.2791
10.0880 ± 0.0146	1500	1.5132	1.5	167.4	539.5	0.3103
10.0880 ± 0.0146	1500	1.5132	1.5	180.2	554.3	0.3251

Note: \*\*Dilution in 10 mL

Lactic acid Calibration Curve



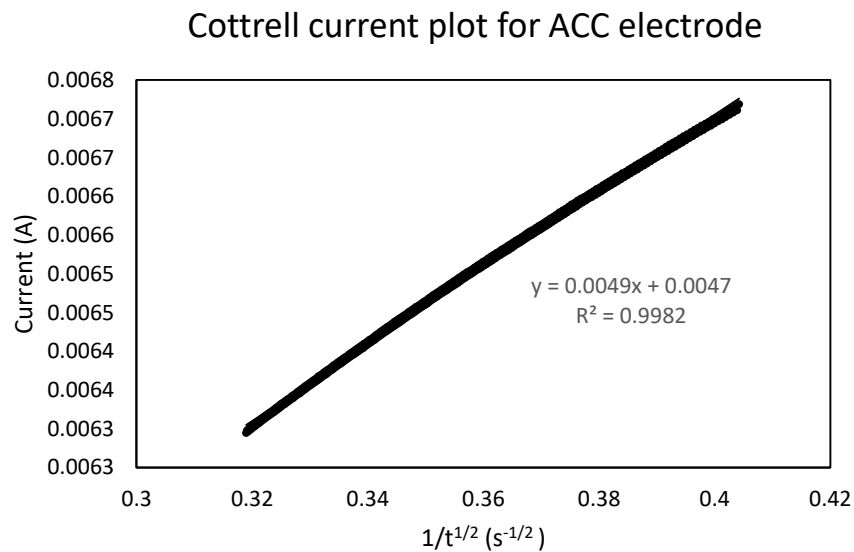
#### Appendix 4: Calculation for active surface area of an electrode by chronoamperometry analysis

The active surface area of the activated carbon composite (ACC), carbon black diamond (CBD) and platinum (Pt) electrodes were obtained using the Cottrell equation:

$$I = \frac{nFAD^{1/2}C_0}{\pi^{1/2}t^{1/2}} \text{ ----- (E. 1)}$$

where  $I$  is the current (A),  $n$  is the number of electrons,  $A$  is the active surface areas of the electrode ( $\text{cm}^2$ ),  $D$  is the diffusion coefficient ( $6.20 \times 10^{-6} \text{ cm}^2/\text{s}$ ) and  $C_0$  is the bulk concentration of  $\text{K}_4\text{Fe}(\text{CN})_6$  ( $5 \times 10^{-6} \text{ mol}/\text{cm}^3$ ),  $F$  is the Faraday constant 96487 (C/mol) and  $t$  is the time (s) (Ajeel *et al.*, 2015a).

##### a) Activated carbon composite electrode:



Based on the linear Cottrell curve above,

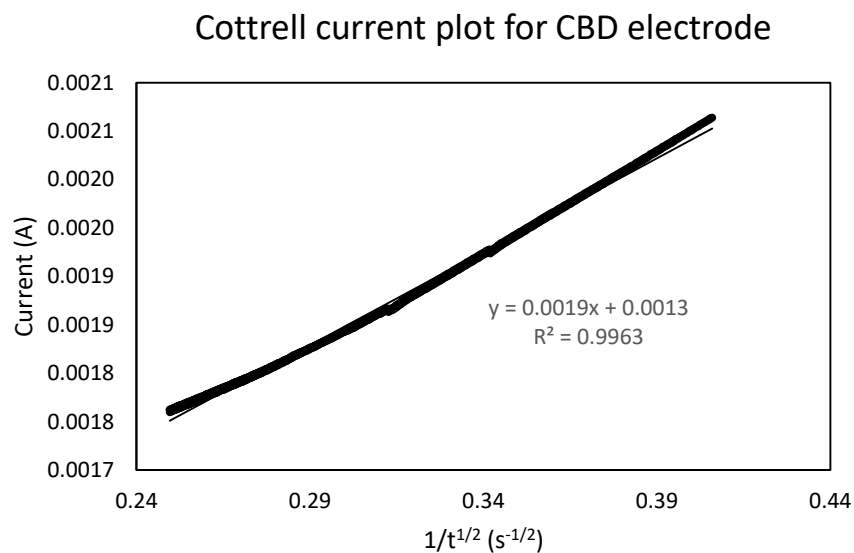
$$\text{Slope} = \frac{nFAD^{1/2}C_0}{\pi^{1/2}} \text{----- (E. 2)}$$

By replacing the constant value into this equation (E.2), the active surface area (A) for the ACC electrode (with geometrical surface area of 0.45 cm<sup>2</sup>) can be calculated as below:

$$0.0049 \text{ A s}^{1/2} = \frac{1 \times 96487 \text{ C mol}^{-1} \times A \times (6.2 \times 10^{-6} \text{ cm}^2 \text{ s}^{-1})^{1/2} \times 5 \times 10^{-6} \text{ mol cm}^{-3}}{3.142^{1/2}}$$

$$A_{\text{ACC}} = 7.22 \text{ cm}^2$$

**b) Carbon black diamond electrode:**



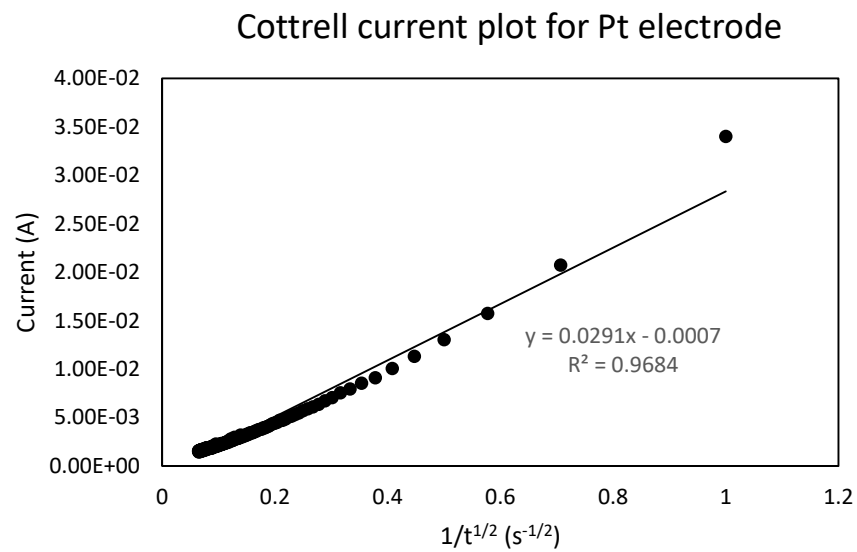
By replacing the constant value into the equation (E.2), the active surface area (A) for the CBD electrode (with geometrical surface area of 0.45 cm<sup>2</sup>) can be calculated as below:



$$0.0019 A s^{1/2} = \frac{1 \times 96487 \text{ C mol}^{-1} \times A \times (6.2 \times 10^{-6} \text{ cm}^2 \text{ s}^{-1})^{1/2} \times 5 \times 10^{-6} \text{ mol cm}^{-3}}{3.142^{1/2}}$$

$$A_{\text{CBD}} = 2.80 \text{ cm}^2$$

**c) Platinum electrode:**



Similar to the previous two calculations for ACC and CBD electrodes, by replacing the constant value into the equation (E.2), the active surface area (A) for Pt electrode (with geometrical surface area of 33 cm<sup>2</sup>) can be calculated as below:

$$0.029 A s^{1/2} = \frac{1 \times 96487 \text{ C mol}^{-1} \times A \times (6.2 \times 10^{-6} \text{ cm}^2 \text{ s}^{-1})^{1/2} \times 5 \times 10^{-6} \text{ mol cm}^{-3}}{3.142^{1/2}}$$

$$A_{\text{Pt}} = 42.79 \text{ cm}^2$$

**Titre :**

Étude de la conversion électrochimique du glycérol en différents composés à haute valeur ajoutée

---

**Résumé :**

Cette étude porte sur la valorisation électrochimique du glycérol. Elle rapporte pour la première fois l'utilisation de la résine Amberlyst-15 comme catalyseur d'oxydo-réduction pour la conversion électrochimique du glycérol. La performance électrochimique du système composé par la résine Amberlyst-15 et l'électrode au platine (Pt), a été comparée à celle utilisant un milieu électrolytique conventionnel acide ( $H_2SO_4$ ) ou alcalin (NaOH). Dans les conditions expérimentales optimales, ce nouveau procédé électrocatalytique permet de convertir le glycérol, soit en acide glycolique, avec un rendement de 45% et une sélectivité élevée de 65%, soit en acide glycérique, avec un rendement de 27% et une sélectivité de 38%.

D'autre part, deux autres électrodes ont été préparées et testées dans la réaction de transformation du glycérol : une électrode au charbon actif (ACC) et une électrode composite au noir de carbone et diamant (CBD). Dans les conditions expérimentales optimales, la sélectivité en acide glycolique peut atteindre jusqu'à 68% et 72% (avec un rendement de 58% et 66%) en utilisant respectivement l'électrode CBD et l'électrode ACC. L'acide lactique a aussi été obtenu avec une sélectivité de 16% et un rendement de 15% en utilisant l'électrode ACC et une sélectivité de 27% pour un rendement de 21% dans le cas de l'électrode CBD.

Enfin, l'électro-oxydation et l'électro-réduction du glycérol ont été effectuées dans une cellule à deux compartiments. L'étude s'est focalisée sur l'électro-réduction. Trois cathodes (Pt, ACC et CBD) ont été évaluées. C'est l'électrode ACC qui a démontré les meilleures performances puisqu'elle a permis de réduire le glycérol en 1,2-PDO avec une sélectivité élevée de 85%.

**Mots clés :**

Glycérol; Electro-oxydation; Electro-réduction; Amberlyst-15; Électrode composite de charbon actif ; Électrode composite de diamant

**Nom et adresse du ou des laboratoires :**

Laboratoire de Génie Chimique de Toulouse (Labège)

INP-ENSIACET

4 allée Emile Monso, 31432 Toulouse cedex 4, France

---

**Summary :**

This study reports for the first time the use of Amberlyst-15 as a redox catalyst for the electrochemical conversion of glycerol in one-pot electrochemical cell. The performance of Amberlyst-15 was compared with that of the conventional acidic ( $H_2SO_4$ ) and alkaline (NaOH) media on platinum electrode. Later, two types of cathode electrodes were evaluated: activated carbon composite electrode (ACC) and carbon black diamond electrode (CBD). Glycolic acid, glyceric acid and lactic acid were obtained from this study. Other parameters such as reaction temperature, the catalyst amount and electric current were also examined. Finally, the electro-oxidation and electro-reduction of glycerol was carried out in a two-compartment cell. The glycerol was successfully converted to 1,2-propanediol with a high selectivity.

**Keywords :**

Glycerol ; Electro-oxidation ; Electro-reduction ; Amberlyst-15 ; Activated carbon composite electrode ; Carbon black diamond electrode.

---